Characterisation and Regulation of the Tooth-Bone Interface during Tooth Development

Alfaqeeh, Sarah Ahmad A

Characterisation and Regulation of the Tooth-Bone Interface during Tooth Development

Sarah Ahmad Alfaqeeh

A thesis submitted for the degree of Doctor of Philosophy at the University of London

2014

Department of Craniofacial Development & Stem Cell Biology

and

Department of Orthodontics

Dental Institute

King's College London

Table of Figures

Table of Tables

Dedication

To

my sun, my father Mr Ahmad Alfaqeeh,

my moon, my mother Mrs Zahwah Althawaib

and

my two stars, my sisters

Dr Ghadah Alfaqeeh and Dr Aljoharah Alfaqeeh.

From Sarah with love

Declaration

I declare that this thesis has been collated and the work described in it performed by the candidate, Sarah Alfaqeeh. It has not been submitted for another degree either at this or another university. All sources of information have been acknowledged.

The copyright of this thesis rests with the author and no quotation or information derived from it may be published without prior consent of the author.

Acknowledgements

When I started this journey I did not understand the weight of gratitude that I would owe to others who have made the destination possible. My deepest appreciation goes to my supervisor Dr Abigail Tucker. As our working relationship developed I came to understand and value your teaching methods and direction. I am thankful that you were the one to introduce me to the field of molecular and developmental biology. You have been a tremendous mentor for me. You were always enthusiastic, optimistic and friendly which made the various challenges of the PhD more bearable.

I am grateful to Professor Fraser McDonald for introducing me to Dr Abigail Tucker, for reviewing my chapters, and providing the necessary research infrastructure. Professor Agi Grigoriadis for his instruction on the TRAP staining protocol and the provision of *c-Fos* mutants which has formed a key methodology throughout the thesis. Without your input my thesis would look very different. I would like to also thank Professor Tim Newton for always being available to lend a listening ear, I will always remember your concern for my welfare and regular support. A special thank you also to Dr Christopher Healy for his technical advice and support, Ms Angela Gates for her nurturing personality and many kindnesses towards me, Mrs Rebecca Whiltshire for putting up with my many printing requests and the 'Tucker Laboratory Team' for all their valuable suggestions and technical help.

I would like to use this opportunity to thank the Custodian of the Two Holy Mosques, His Royal Majesty King Abdullah bin Abdulaziz Al Saud for giving Saudi women opportunities to persue PhD study as part of his External Scholarship Programme, His Royal Highness Prince Mohammed bin Nawwaf bin Abdulaziz Al Saud, the Ambassador of the Custodian of the Two Holy Mosques to the United Kingdom and Ireland, for all his advice and support settling into a different cultural and educational context and overcoming the related obstacles and my sponsor The Ministry of Higher Education of the

Abstract

The tooth is closely related to the periodontium in which it sits, with a soft tissue interface forming between the alveolar bone and hard tissues of the tooth. This is known as the tooth-bone interface (TBI). In functional teeth, the TBI houses the periodontal ligament, while during development the TBI creates a space into which the tooth can grow. This project aims to provide an understanding of how the formation of the tooth and bone are coordinated during development and characterise the underlying factors and mechanisms that prevent bone formation and invasion at the interface between the tooth and bone.

Using murine mandibular first molar (M1) TRAP stained histological sections, osteoclasts were found to be closely associated with the border of the developing bone, lining the TBI, but not within the TBI itself. Slice culture was used to follow tooth development in explant culture as it provided an excellent opportunity for manipulation and lineage tracing. DiI labelling experiments showed the contribution of two sources of cells in the formation of alveolar bone namely, dental follicle cells from around the tooth and, bone cells from the margins of the dentary. Isolation experiments were used to investigate the impact of the tooth on the bone and bone on the tooth. Isolation of E14.5 mandibular first molar (M1) tooth germ from the surrounding mesenchyme and alveolar bone resulted in tooth germ expansion while removing the tooth epithelium did not change the normal layout of osteoclasts at E14.5. The effect of manipulating the BMP signalling pathway on the differentiation of cells in the TBI during tooth development was studied. A local reduction in the TBI was observed next to the BMP-4 beads whereas a local widening in the TBI was observed when Noggin beads were implanted. The effect of manipulating the RANK-RANKL signalling pathway was investigated next. *In situ* hybridisation revealed the presence of OPG, RANK, and RANKL in the alveolar bone but OPG and RANKL only in the dental epithelium. Addition of exogenous RANKL to tooth explants in culture resulted in a statistically significant increase in osteoclast numbers and a widening of the TBI. On the other hand, the results obtained after

exogenous OPG addition were regarded as inconsistent due to high variability. However, correlation of the difference in bone growth within a cultured tooth germ with the presence of osteoclasts showed absence of osteoclasts in areas of bone encroachment and the opposite, presence of osteoclasts, in areas devoid of bone. The TBI then was analysed in *c-Fos* mutants, a knockout mouse known to have a defect in osteoclastogenesis, resulting in lack of osteoclast production. Genotyping showed that the *c-Fos* mutant embryos were displaying the expected Mendelian ratio, but almost all the homozygotes died after birth, and the heterozygotes viability was found to be compromised. Micro-CT analysis of a 3 week old *c-Fos* homozygote showed a strong osteopetrotic phenotype. Defects in the midline diastema, tooth impaction, and lack of roots were also observed. The TBI showed signs of bone invasion, encroaching on the M1. TRAP assay revealed few positive-stained mononucleated cells, which were probably macrophages.

In conclusion this thesis demonstrates that the formation and maintenance of the TBI appears to be a finely regulated two-pronged process with control of osteoclast differentiation used to remove the bone (osteoclastogenesis), combined with inhibition of bone induction (osteogenesis). Together these two processes create a bone-free zone around the tooth. By changing either of these processes the TBI is disrupted and tooth development is altered.

1 <u>General Introduction</u>

1.1 Study of the interaction between the tooth and bone

Mammalian tooth formation is a complex process. The development of a tooth, an epithelial appendage, involves two different kinds of cells: the oral ectodermal cells and the cranial-neural crest derived mesenchymal cells. These cells gradually reorganise, differentiate and coordinate with the alveolar bone to form 'the tooth-alveolar bone complex'; this includes the periodontal tissues which facilitate the attachment of the tooth in the jaw (Thesleff and Tummers, 2008). A thorough understanding of the process of formation of 'the tooth-periodontium-alveolar bone complex' and the structures associated in the process is essential for providing clinicians with a better model for fabricating dentures, performing implant procedures and for future biomedical applications such as bio-tooth development (Fleischmannova *et al.*, 2010). In this work we aim to provide an improved understanding of the innate relationship between the tooth and the alveolar bone, and the molecular mechanisms associated with the same.

1.1.1 The Tooth

A definitive tooth is comprised of two main regions: a crown that visibly protrudes from the gingiva and a root that holds the tooth in the gingival socket. Mammalian teeth are composed of four tissues: an outermost layer of mineralized enamel, underlaid by the dentin, mineralized connective tissue with an organic matrix of collagenous proteins, and calcified cementum, which covers the root of the tooth and provides support for the periodontal ligaments (PDL) that hold the tooth in the socket and attaches it to the alveolar bone. The innermost layer is a soft connective tissue of dental pulp, which supplies the tooth with blood vessels and nerve fibres (Nguyen and Martin, 2008) (Figure 1.1).
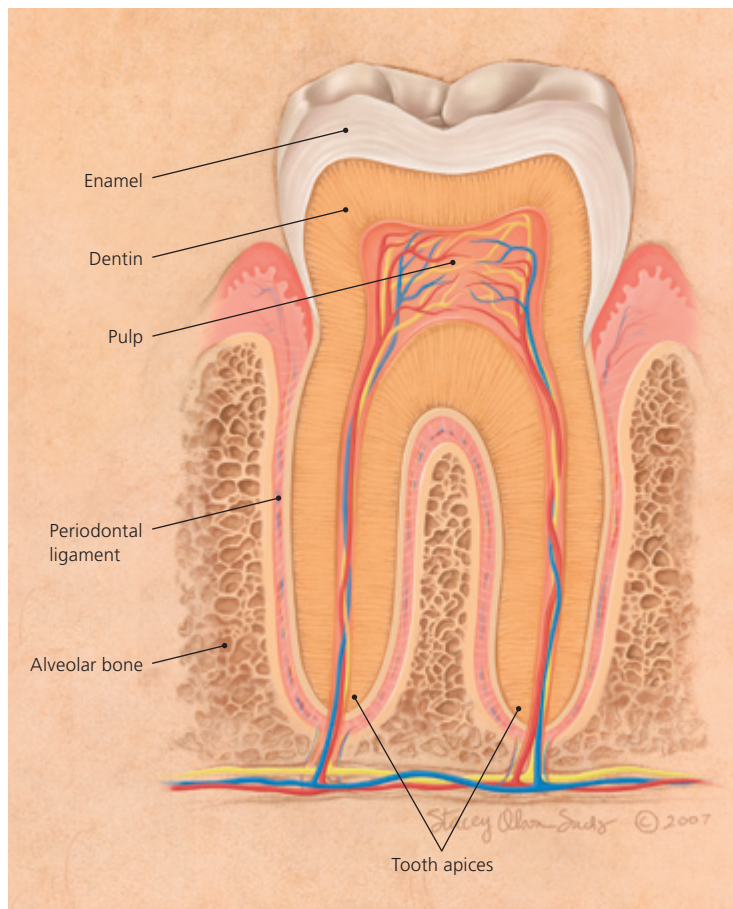
Figure 1.1 Structure of the tooth-periodontium-alveolar bone complex.

The tooth is embedded in the jaw bone; the outermost enamel, middle dentin, cementum and innermost pulp are accordingly labelled. *Adapted from Nguyen and Martin (2008)*.

1.1.2   The Alveolar Bone

The alveolar bone develops as an extension of the mandibular and maxillary jaw bones. The alveolar process supports the tooth in the socket and contributes towards the positioning of the teeth through the growth and development of the jaw bones. Furthermore, the biomechanical response of the alveolar bone and the adaptability of the periodontal tissues accompanied by occlusal strains facilitate the positional accommodation of the tooth during an orthodontic procedure or orthodontic tooth movements. Therefore, understanding the molecular basis of bone remodelling and periodontal flexibility is significantly important in

developing rational modes of treatments for various structural and functional orthodontic deformities (Sodek and McKee, 2000).

From a clinical perspective, the relationship between the tooth and the alveolar bone is crucial. It can provide a better understanding of the subsequent patterns of resorption of the alveolar ridges after tooth extraction by clinicians and critically contributes to the successful fabrication of implant prostheses (Winkler, 2002; Fleischmannova *et al.*, 2010). A detailed explanation of the tooth-alveolar bone development stages and the genetic and molecular factors that influence the development and maintenance of 'the tooth-periodontium-bone complex' will be discussed in the following section.

1.2   Bone and tooth development

1.2.1   General bone development

Bone development in mammals occurs in the late embryonic stages as the last step in the development of the skeleton. It occurs via two distinct mechanisms:

a) Intramembranous bone development, which involves the direct differentiation of the mesenchymal condensation cells into osteoblasts. For example parts of the skull and the clavicles of mouse are prefigured during development (Hall and Miyake, 1992; Huang *et al.*, 1997).

b) Endochondral bone development involves the formation of bone on a pre-existing mineralised cartilage scaffold. Differentiation of the mesenchymal cells into chondrocytes leads to the formation of the 'cartilage anlagen', which contributes to the rudimentary formation of future bones. The perichondrial cells present in the periphery of the anlage differentiate into osteoblasts with hypertrophic changes in peripheral regions of the anlage. Furthermore, calcification of the matrix around the hypertrophic chondrocytes is followed by movement of osteoblasts into the calcified cartilage mediated by the supply of blood vessels in the area (Horton, 1993; Erlebacher *et al.*, 1995). These events that lead to bone formation characterise the stages of endochondral ossification (Karsenty, 1999).

1.2.2 Odontogenesis

The formation of both dental and periodontal structures is known as Odontogenesis. The alveolar bone, the periodontal ligament (PDL), and cementum together constitute the periodontium (Cho and Garant, 2000; Diep *et al.*, 2009).

1.2.2.1 Development of the tooth

Teeth develop from the ectodermal surface of the first branchial (pharyngeal) arch and the frontonasal prominence, followed by the formation of a solid epithelial band and the dental lamina, particularly at the sites of the future dental arches of the maxilla and the mandible (Thesleff, 2006).

Four stages of tooth development are shown in Figure 1.2:

1. Formation of the dental lamina and the bud stage (initiation), in which the invagination of the thickened oral ectoderm into the underlying neural-crest-derived mesenchyme forms a tooth bud. A shift of odontogenic potential to the dental mesenchyme triggers the epithelial signalling centre, which regulates the transitions from the bud-to-cap stage, known as the primary enamel knot (Jernvall *et al.*, 1998).

2. Formation of the cap; the cap stage (proliferation) commences the process of histological differentiation to form the enamel, dental papilla, and dental follicle, which differentiates to form the cementoblasts, osteoblasts, and fibroblasts. Osteoblasts form the alveolar bone, which surrounds the roots of the teeth, and fibroblasts, which give rise to the PDL that attach the teeth to the alveolar bone through the cementum, formed from the cementoblasts (Somerman *et al.*, 1999; Cho and Garant, 2000; Mizuno *et al.*, 2005; Kim *et al.*, 2007; Fleischmannova *et al.*, 2010).

Figure 1.3 shows the osteogenic differentiation that leads to formation of the bone, cementum, and PDL, respectively.

3. The early bell stage: differentiation of the mesenchymal cells attached to the dental epithelial cells occurs to form the odontoblasts, and the epithelial cells of the inner enamel differentiate into enamel-producing ameloblasts. This stage completes histodifferentiation and morphodifferentiation in the tooth. In the late

bell stage, the dental follicle subdivides into three separate layers: an inner investing layer that merges with the lower region of the dental papilla and the outer enamel, the intermediate layer and the outer layer next to the developing alveolar bone, known as the perifollicular layer (Palmer and Lumsden, 1987; Cho and Garant, 2000).

4. The crown stage: cytodifferentiation occurs at this stage with the formation of enamel (mineralisation) and dentin matrices.
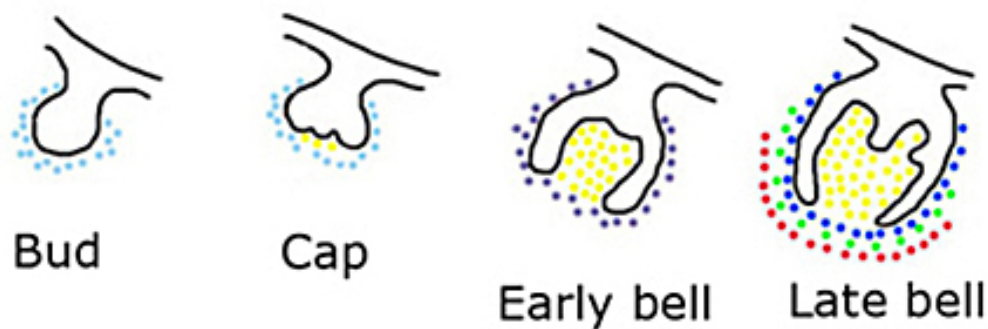
Figure 1.2 Schematic representation of the three key stages of tooth development.

In the bud and cap stages: condensing mesenchyme is shown as light blue spots. In the early bell stage: the dental follicle is shown as purple spots. In the late bell stage, the follicle is divided into the investing layer (dark blue), the intermediate layer (green), and the outer layer (red). The developing dental papilla in the cap-bell stage is shown as yellow spots. *Adapted and modified from Diep et al. (2009).*

Various molecular mechanisms and genetic factors control the above stages of tooth development. Around 300 genes have been identified as having regulatory affects on the pattern generation, morphogenesis, and differentiation of teeth (Thesleff, 2006).

A graphical database created by Pekka Nieminen at the University of Helsinki (http://bite-it.helsinki.fi) reports the schematic expression pattern of genes and the mutations that can lead to major dental deformities (Thesleff and Pirinen, 2003; Thesleff, 2006).

1.2.2.2 Development of the supporting structures of the tooth

Development of the supporting structures of the tooth, that is, the alveolar bone and periodontium, are an integral part of the process of odontogenesis.

1.2.2.2.1 Development of the alveolar bone

As mentioned earlier, the alveolar bone arises from the osteoblasts differentiating from the dental follicle and as such is a membranous bone. The development of the mandibular and maxillary jaw bones, which extend to form the alveolar bone, is controlled by the homeobox genes, which control the formation of the skeletal pattern (Erlebacher *et al.*, 1995). In addition, molecular signals, such as cytokines, chemokines and growth factors, might locally control the mesenchymal condensations at the onset of organogenesis, and affect the development of the alveolar bone (Sodek and McKee, 2000). The alveolar bone is the primary structure that supports the roots of the teeth and encapsulates them to provide the functions of adaptation, rapid tooth remodelling during tooth eruption, and mastication. The alveolar bone accommodates anchoring of the tooth germ into its base, which is evident from the bell stage of tooth development (Radlanski *et al.*, 1998). The anatomical structure of the bone (Saffar *et al.*, 1997) can be summarised as follows:

1. Alveolar bone proper consists of the bundle bone (Schroeder, 1992). The bundle bone is present in layers in the direction of the tooth, that is, penetrated by Sharpey's fibres, which are continuous with the principle fibres of the PDL.

2. Supporting bone comprises the remainder of the alveolar bone that is attached to the alveolar bone proper. It consists of the thick outer cortical plates and the spongy supporting bone sandwiched between the cortical plates and the alveolar bone proper. Numerous marrow channels fill the cancellous bone with smaller endosteal spaces, which are strewn in the cortical bone and can merge with the PDL (Sodek and McKee, 2000).

1.2.2.2.1.1 Osteoblasts and osteocytes

Osteoblasts are cells originating from the mesenchyme and are responsible for bone formation and regeneration. Osteoblasts are mononuclear, cuboidal cells that are not terminally differentiated. In the active state, their cytoplasmic content shows the presence of abundant rough endoplasmic reticulum and large Golgi apparatus with secretory granules, microtubules, endosomal organelles, and cytoskeleton (Scherft and Groot, 1990; McKee and A., 1993). Collagen type I and various noncollagenous bone proteins and plasma proteins constitute the organic matrix in the osteoblasts (Heinegard *et al.*, 1989; Delmas and Malaval, 1993; Sodek and McKee, 2000). These cells have tight junctions and acquire an ability to secrete bone matrix as they differentiate. Otherwise, they continue to remain as bone lining cells. In the innermost layer of the tooth alveolus, the alveolar bone osteoblast cells align to form a continuous perforated sheet that accommodates the embedded segments of Sharpey's fibres of the PDL (Kurihara and Enlow, 1980; Johnson *et al.*, 1997; Sodek and McKee, 2000). Morphologically, osteoblasts are indistinguishable from fibroblasts and most genes expressed in fibroblasts are also expressed in osteoblasts. The osteoblasts on maturation are trapped in their own bone matrix to form osteocytes while some undergo apoptosis (Capulli *et al.*, 2014).

Osteocytes lie in lacunae (spaces) in bone, either in mineralised bone or in the osteoid matrix (Marotti, 1977; Bonucci, 1990; Sodek and McKee, 2000). Osteocytes are very numerous and long-lived cells with an estimated life span of up to 25 years (Capulli *et al.*, 2014). Osteocytes have a different morphology to osteoblasts, having a smaller cell size, and a larger nucleus (Marotti, 1977) and less synthetic and secretory organelles. Each osteocyte has up to 50 long cellular processes. These processes extend throughout the bone matrix and make a network of interconnecting canaliculi (Capulli *et al.*, 2014). Osteocytes in the bone tend to communicate with each other, osteoblasts and bone-lining cells (on the surface) through these cellular extensions of their plasma membranes and through gap junctions (Palumbo, 1986; Palumbo *et al.*, 1990; Sodek and McKee,

2000). It is thought that this network of osteocytes is essential for producing a coordinated response of bone to mechanical and other signals (Knothe Tate *et al.*, 2008). Dentine matrix protein 1 (DMP1) and Sclerostin (Sost) are highly expressed in osteocytes, while the osteoblast markers, such as collagen type I, osteocalcin, Bone sialoprotein (BSPII) and Alkaline phosphatase (ALP) are downregulated (Capulli *et al.*, 2014).

1.2.2.2.2   Development of the periodontal ligament

The PDL forms a flexible vascular and cellular connection between the tooth and alveolar bone. The PDL is composed of connective tissues that act as a supportive structure to anchor the tooth cementum to the bone; it also has additional sensory functions. The PDL consists of osteoblasts and osteoclasts on the alveolar bone side. The solid body of the PDL is comprised of fibroblasts, epithelial cells, macrophages, undifferentiated mesenchymal cells, neural elements, and endothelial cells, whereas the root surface consist of cementoblasts. The gel-like matrix, which impregnates the PDL, comprises incompressible collagen fibres, glycosaminoglycans, glycoproteins, and glycolipids (Lekic and McCulloch, 1996). These provide the PDL with an innate and adaptable shock absorbing characteristic to facilitate rapid adjustment to the applied levels of force and hence accommodate renewal and repair of cells and tissues. These features allow the PDL to act as an anchor to attach the root of the tooth to the jaw bone as well as to dissipate the mechanical stress applied during the process of mastication, tooth eruption and development (Takano-Yamamoto *et al.*, 1994). The PDL arises from fibroblasts differentiated from the inner layer of the dental follicle (Ten Cate, 1994). Two mechanisms known to control the formation of the PDL are epithelial mesenchymal interactions and epithelial-hard teeth tissue interactions (Lekic and McCulloch, 1996). The signalling controls of PDL development and maintenance as observed in young quiescent cells are BMP3, MSX2, TWIST, and PLAP-1 (Periodontal ligament-associated protein-1/asporin), which prevent conditions such as ankylosis due to the nonphysiological mineralization of the PDL (Yoshizawa *et al.*, 2004; Komaki *et al.*, 2007; Yamada *et al.*, 2007). Other factors like BMP antagonists, such as NOGGIN, act to

modulate various BMP pathways and can further affect the pattern of the PDL development (Capdevila and Johnson, 1998; McMahon *et al.*, 1998; D'Souza and Patel, 1999; Schweitzer *et al.*, 2001; Holleville *et al.*, 2003; Jin *et al.*, 2003; Nakamura *et al.*, 2006; Kim *et al.*, 2007).

1.2.2.2.2.1 Fibroblasts and Cementoblasts

Fibroblasts are the principal cells of the PDL and provide flexibility, support and structural organization during the process of development, and movements of the tooth and its supporting structures (Ten Cate, 1994). Fibroblasts are involved in synthesising and remodelling repair, and in the regeneration of extracellular matrices, such as fibres of collagen, elastin and other larger complements of non-fibrillar glycoproteins. They act to provide contractility and motility to the tissue, which contributes to the structural organization as observed during the development of the PDL (Lekic and McCulloch, 1996). Fibroblasts are also involved in processes such as the phagocytosis of collagen, the production of cytokines for tissue destruction, and the stimulation of bone resorption by osteoclasts (Genco, 1992). They also prevent collagenolysis at physiological pH by secretion of tissue inhibitors for metalloproteinases (Overall and Sodek, 1990; Birkedal-Hansen, 1993). The fibroblast is an essential component of the tooth and contributes massively to the remodelling of periodontal tissues (Lekic and McCulloch, 1996).

The cementoblasts differentiate from the connective tissue of the dental follicle cells and are involved in cementogenesis, the formation of the cementum during periodontium formation. They primarily contribute to the function and physiology of the periodontal tissues (Beertsen *et al.*, 1997). The Cementum-derived Growth Factor (CGF), an Insulin-like growth factors I (IGF-I)-like molecule and a 14-kDa protein, appears to be unique to cementum. It is weakly mitogenic to fibroblasts and in the presence of epidermal growth factor (EGF), it reveals a synergistic potential (Ikezawa *et al.*, 1998). Cementoblasts are believed to move between the Hertwig's epithelial root sheath (HERS) cells during HERS fenestration. It was proposed that HERS cells might secrete initial cementum during cementum formation (Diekwisch, 2002; Fleischmannova *et al.*, 2010); it

was finally confirmed that cementoblasts can originate from HERS cells (Huang *et al.*, 2009). This was in line with the evidence that suggested that cementoblasts producing cellular intrinsic fibre cementum and acellular extrinsic fibre cementum have unique phenotypes, such as expression of unique markers, that are unrelated to osteoblasts (Bosshardt, 2005). Cementum produced by cementoblasts might be cellular or have a fibrillar collagenous matrix of collagen type 1, or might be acellular cementum composed of mineralized matrix without the fibrillar collagenous material (Saygin *et al.*, 2000; Diekwisch, 2001). It was suggested by Zeichner-David *et al.* (2003) that the acellular and cellular cementum regions are constituted by two different kinds of cells. The cementoblasts derived from the HERS cells produce the acellular cementum, whereas the cellular cementum is derived from the cells of the neural crest (Zeichner-David *et al.*, 2003). Cells known as cementocytes occur in the cellular cementum as a result of cementoblasts being embedded in lacunae (spaces in the cementum) (Bosshardt and Schroeder, 1996). One potential marker of cementoblastic differentiation is CP-23 (cementum protein 23) (Alvarez-Perez *et al.*, 2006). Differentiation of dental follicle cells to produce cementoblasts is controlled by numerous factors such as BMP2 and BMP7, as observed in both *in vitro* and *in vivo* experiments (Zhao *et al.*, 2003).

1.2.2.3   *Potential of follicle cells to differentiate into bone*

The osteogenic potential of dental mesenchymal cells originates from the early developmental stages (bud and cap). The mesenchymal cells of the neural crest condenses around the invaginated dental epithelium (Chai *et al.*, 2000), which, if isolated at the bud stage (E13.5), will develop into bone when cultured in a bone-supporting medium (Yamazaki *et al.*, 2007). Similarly, dental follicular cells in the cap stage tooth (E14.5) form bone when cultured under a kidney capsule for 2 weeks (Kim *et al.*, 2007). These phenomena are controlled by genes such as Runx2, Dlx5, Msx1, and Bmp4, which are co-expressed in the early and later stages of development of alveolar bone around the developing tooth at the bud and bell stages (Zhang *et al.*, 2003). Runt-related transcription factor 2 (Runx2) is also called core-binding factor alpha(1) (Cbfa1), but in this thesis it will be referred to as Runx2. Furthermore, bone formation and tooth development is

completely arrested in Runx2 knockout mice (Ducy *et al.*, 1997; D'Souza *et al.*, 1999; Diep *et al.*, 2009). However, culture assays of dental follicle cells at E14 show that early dental follicle cells, such as dental pulp cells, have an innate osteogenic potential to differentiate into hard tissue without being affected by environmental factors (Nakamura *et al.*, 1994). Furthermore, many studies emphasise the fact that dental follicular cells in the early developmental stages lack the potential to differentiate into a PDL-like structure, indicating that environmental factors must be responsible for controlling the formation of the PDL. Thus, in isolation, the tooth-bone interface (TBI) forms hard tissue rather than the soft tissues in the periodontal area (Kim *et al.*, 2007). A recent study by Diep *et al.* (2009) showed that mesenchymal cells that condense around the epithelia of the tooth bud eventually form the bone at the bell-stage. Studies conducted at more advanced developmental stages (i.e. postnatal day 6 (P6)) show that the alveolar bone forms from dental follicle cells, which indicates the contribution of the dental follicle layer in alveolar bone formation (Diekwisch, 2002; Diep *et al.*, 2009). Therefore some cells in the TBI at early stages do normally go on to form bone.

Interestingly, at early stages of differentiation, a TBI cell not only has the potential to differentiate into osteoblasts that form bone, but also can form two other cell types: cementoblasts that form cementum and fibroblasts that form periodontal ligaments, as illustrated in Figure 1.3. Osteoblasts, cementoblasts and fibroblasts therefore share a common lineage. In addition, cells of the developing TBI may stay in an undifferentiated state as stem cells (PDLSC), controlling homeostasis and repairing the periodontium (reviewed in Acharya *et al.* (2010)).

Cellular Differentiation in Periodontal Tissues
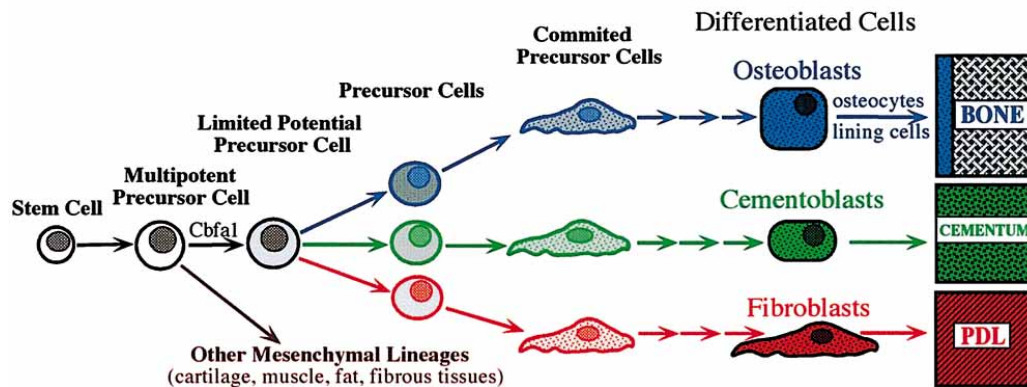
Figure 1.3 Osteogenic differentiation of the multipotent stem cell in the periodontium.

Several lineages can potentially be generated, including the osteogenic lineage. In each case, a decrease in proliferation potential occurs as differentiation progresses. Expression of the Runt-related transcription factor 2 (Runx2), the gene that triggers osteogenesis directs multipotent cells to differentiate into the osteoblast, cementoblast and PDL fibroblast cells. The physical environment as well as growth factors and cytokines that influence the progression along each lineage during the process of differentiation are shown. PDL: periodontal ligament. *Adapted from Sodek and McKee (2000).*

1.3   Bone remodelling

Bone is a mineralized connective tissue that forms the skeleton and has multiple mechanical and metabolic roles in constituting the endoskeleton of mammals. The bulk of the bone consists mainly of three different cell types: the osteoblasts, or bone-forming cells, the osteocytes (mature bone cells) and the osteoclasts, or bone-resorbing cells (Ducy *et al.*, 2000; Capulli *et al.*, 2014). Bone formation or osteogenesis in mammals begins during prenatal development and persists throughout life, accompanied by bone growth, bone mineralization, and bone remodelling (Ducy *et al.*, 2000). In the bone tissue, the osteoclasts are involved in the continuous break down of bone, otherwise known as bone resorption. This process is followed by the process of bone ossification, or new bone formation, where osteoclasts are replaced by osteoblasts. These two processes together constitute the physiologic process of bone remodelling (Frost, 1969; Ducy *et al.*,

2000). There are three phases of the bone remodelling process: resorption, during which osteoclasts destroy the existing bone; reversal, a process in which the mononuclear cells appear on the bone surface; and formation, when osteoblasts replace the old bone with the new bone until the resorbed bone is completely replaced (Hadjidakis and Androulakis, 2006) (Figure 1.4). The molecular control of the bone remodelling process is under investigation; however, few systemic regulators include parathyroid hormone (PTH), calcitriol, and other hormones such as growth hormone, glucocorticoids, thyroid hormones, and sex hormones. In addition, various factors such as insulin-like growth factors (IGFs), prostaglandins, transforming growth factor-beta (TGF-beta), bone morphogenetic proteins (BMP), and cytokines have been recently identified as controlling the activity of osteoclasts and osteoblasts and in turn provide a balance between bone formation and resorption. In many bone diseases, an imbalance in the process eventually leads to increased bone resorption, resulting in bone loss (Hadjidakis and Androulakis, 2006; Trouvin and Goeb, 2010).

Increasingly as role of osteocytes in bone remodelling has been suggested (Figure 1.6). Osteocytes can directly control the differentiation and activity of osteoblasts and osteoclasts (Capulli *et al.*, 2014). Osteocytes are able to respond to mechanical stimulation by regulating osteoblast differentiation controlled by Sclerostin (Sost). Sost, secreted by osteocytes, inhibits osteoblast differentitation, and is the main negative regulator of osteoblast differentiation (Capulli *et al.*, 2014). Osteocytes also can modulate osteoclast behaviour. In cases of bone damage, apoptosis (programmed cell death) of osteocytes leads to an influx of osteoclasts, with apoptotic osteoclasts expressing high levels of pro-osteoclast signaling molecules, such as RANKL (Capulli *et al.*, 2014).
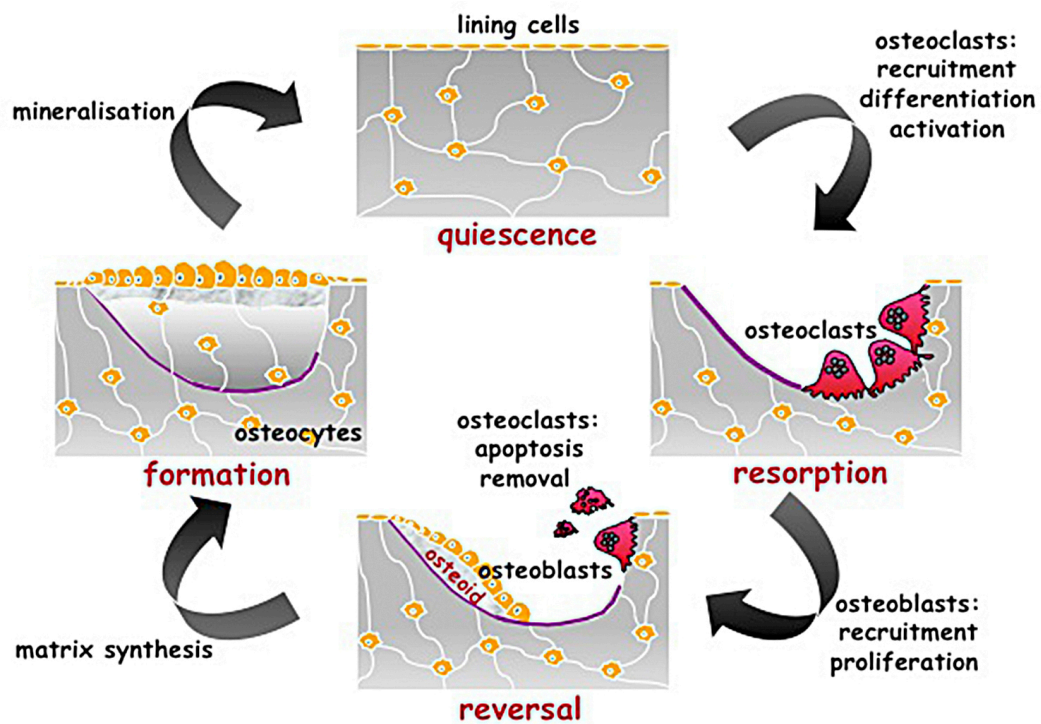
Figure 1.4 A schematic representation of the phases of the bone remodelling process.

The phases of activation, resorption, and bone formation are shown. *Adapted from Prof Agamemnon Grigoriadis lecture titled bone biology and skeletal development in 6BBYC302– Taught Course BSc Craniofacial Sciences.*

1.3.1   Osteoclasts

Bone resorption is an important phenomenon for many skeletal processes. The process is obligatory during bone growth, tooth eruption and fracture healing, and also contributes towards the maintenance of an appropriate level of blood calcium (Vaananen *et al.*, 2000). Osteoclasts, which are multinuclear cells derived from hematopoietic stem cells, are principally responsible for bone resorption, and hence play a central role in the process of bone formation and bone mass regulation (Teitelbaum, 2000). A promyeloid precursor can differentiate into an osteoclast, a macrophage or a dendritic cell depending on its exposure to specific molecular signalling factors. Receptor activator of NF-kB ligand (RANKL), leads to osteoclastogenesis (Vaananen *et al.*, 2000). RANKL is also called tumour necrosis factor-related activation-induced cytokine (TRANCE), osteoprotegerin ligand (OPGL) or osteoclast differentiation factor

(ODF), but in this thesis it will be referred to as RANKL. The role of macrophage colony-stimulating factor (M-CSF) in osteoclastogenesis is crucial as it binds to its receptor, c-Fms, which results in the formation of early osteoclast precursors, leading to survival and proliferation of the mature osteoclasts (Teitelbaum, 2000). Furthermore, studies have reported the presence of the surface-residing molecule RANKL, which is produced by the bone marrow stromal cells and osteoblast membrane that positively regulates osteoclastogenesis (Vaananen *et al.*, 2000). Osteoprotegerin (OPG) was identified by Simonet *et al.* (1997). OPG inhibited osteoclastogenesis, both *in vivo* and *in vitro* (Simonet *et al.*, 1997), competitively inhibiting the binding of RANKL to the receptor, RANK (Lacey *et al.*, 1998). Therefore, OPG-deficient animals show signs of accelerated osteoclastogenesis and develop severe osteoporosis (Simonet *et al.*, 1997). RANK is expressed on osteoclasts, and their precursors (Lacey *et al.*, 1998), and its ligand RANKL is present on stromal cells and is also expressed by activated T lymphocytes. Activated T lymphocytes can trigger osteoclastogenesis in joints, which might lead to bone destruction, as observed in rheumatoid arthritis (Kong *et al.*, 1999). A tuned expression of the stimulator, RANKL, and the inhibitor, OPG, can lead to a balanced bone resorption without bone loss (Hofbauer *et al.*, 1999a). Many osteoclastogenic agents like PTH and 1,25-dihydroxyvitamin D_3 act on the stromal cells and osteoblasts leading to enhanced RANKL expression, which in turn surpasses the levels of OPG expressed and thus leads to osteoclast differentiation (Kitazawa *et al.*, 1999; Lee and Lorenzo, 1999; Teitelbaum, 2000). Other than RANKL and RANK being members of the tumour necrosis factor (TNF) family, TNF is known as a potent osteoclastogenic agent that stimulates the expression of RANKL and M-CSF in osteoblastic cells, which in turn prompts macrophages to differentiate into osteoclasts. Furthermore, two TNF receptors, p55 TNF and p75 TNF with osteoclastogenic and anti-osteoclastogenic effects, respectively regulate the process of osteoclastogenesis (Kimble *et al.*, 1996; Hofbauer *et al.*, 1999b; Abu-Amer *et al.*, 2000). Various genetic factors that can affect the osteoclast differentiation in conditions like osteopetrosis are shown in Figure 1.5.
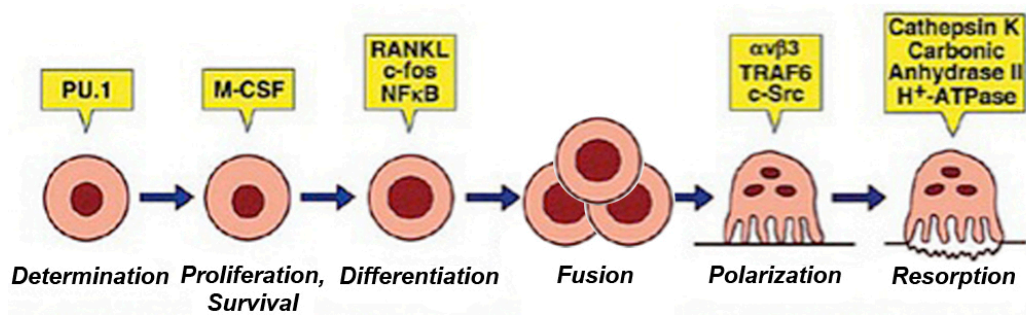
Figure 1.5 Molecular mechanisms of osteopetrosis and genetic factors controlling the condition.

Genetic mutants of osteopetrotic mice provide insights into the genes that regulate the phases of osteoclast differentiation and function. *Adapted and modified from Teitelbaum (2000).*

Basic of knowledge of genes that regulate the phases of osteoclast differentiation and function was obtained from the genetic mutants of osteopetrotic mice as portrayed in Figure 1.5. PU.1 mutant mice have no early macrophage precursors so its deficiency was considered essential for early macrophage formation. M-CSF mutant mice have reduced expression of macrophages and generate immature macrophages, indicating a slightly later requirement for this gene in the osteoclast lineage. Normal macrophage development was found in mutant mice that had deficient *c-Fos*, NF-kB, and RANKL gene, but these macophages did not commit to osteoclast differentiation. These pathways will be discussed in more detail in later chapters. Considerable numbers of osteoclasts were found in mice that lack $\alpha v \beta 3$ integrin, TRAF6, or c-Src genes, but these osteoclasts failed to adequately polarize, as seen from the absence of a normal ruffled membrane. Osteoclasts that are morphologically normal, yet without bone resorption ability were found in mutant mice that lack cathepsin K, carbonic anhydrase II, and H^+-ATPase. The carbonic anhydrase II or H^+-ATPase is essential for osteoclasts to acidify the resorptive microenvironment between themselves and bone, while the cathepsin K is needed to degrade the organic matrix of bone (Teitelbaum, 2000).

1.3.2   Alveolar bone remodelling

Continual and rapid alveolar bone remodelling is a fundamental phenomenon that occurs during the process of mastication and tooth eruption, and might exert

detrimental effects on the progression of certain periodontal diseases (Sodek and McKee, 2000). Continuous alveolar bone remodelling causes temporary detachments of PDL fibres attached to the surface of the alveolus. However, this is followed by formation of new periodontal fibres by fibroblasts and osteoblastic generation of new alveolar bone, that in due course allows for reattachment at the remodelled sites (Sodek and McKee, 2000). Alveolar remodelling contributes to the positional adaptation of the tooth and to the tooth's biomechanical functions. Moreover, it accommodates the physiological movement of teeth in the jaw that occurs in response to occlusive forces and orthodontic forces used for the clinical re-positioning of teeth in different orthodontic diseases and interventions. Orthodontic tooth movement is dependent on the efficient remodelling of the alveolar bone in the absence of an inflammatory response. Usually, periodontal tissues under pressure leads to osteoclastic activity and hence bone resorption, whereas periodontal tissue tension generates osteoblastic activity and triggers bone formation as a result of orthodontic tooth movements (Roberts-Harry and Sandy, 2004). Heavy or prolonged mechanical loading can also influence the tooth, leading to root resorption due to changes in mineralisation-related activity (Wan Hassan *et al.*, 2012).

The homeostasis of the alveolar bone is different from that of the endochondral bone, due to differences in their matrix composition and connections with the PDL (Fleischmannova *et al.*, 2010). The replacement of the primary dentition with successional teeth is accompanied by rapid and complete remodelling of the alveolar bone. Complete resorption of the old alveolar bone is followed by formation of a new bone that supports the newly formed tooth and prevents the tooth from drifting within the developing jaw bones (Sodek, 1977). In addition, alveolar bone prompts tissue regeneration during periodontal diseases and osseointegration of implants, which are primarily used in restorative dentistry.

The molecular mechanisms and signal transduction regulating the process are under investigation and several have been recently identified. Some involve hormones and autocrine and/or paracrine factors that in turn affect the differentiation, generation, and activity of different bone cells. The expression

and regulation of various development genes, transcription factors, and bone morphogenetic factors control the process of bone formation and resorption, which in turn affect the process of bone remodelling.

In mice with impaired osteoclast function, the alveolar bone starts to encroach into the tooth-bone interface, disrupting development of the growing tooth germ (Liu *et al.*, 2000; Ida-Yonemochi *et al.*, 2002; Kitahara *et al.*, 2002; Mekaapiruk *et al.*, 2002; Suzuki *et al.*, 2004; Helfrich, 2005). Regulation of osteoclastogenesis also has a critical role in facilitating dental eruption, clearing the bone away from the path of eruption (Wise and King, 2008). Accordingly, failure in osteoclast formation leads to primary failure of eruption in humans and rats (Helfrich, 2005; Frazier-Bowers *et al.*, 2010).

1.3.3 Signals controlling bone remodelling

Signals that control bone remodelling are primarily those that regulate the production and apoptosis of osteoclastic and osteoblastic cells. Various local (autocrine/paracrine), and endocrine factors regulate bone remodelling, like growth factors and hormones. The effect of different hormones on bone remodelling is shown in Table 1.1.

Table 1.1 Effects of hormones on bone remodelling and bone mass

Response to Hormones	Effects on Bone Remodelling	Effects on Bone Mass
Increased secretion of PTH (McSheehy and Chambers, 1986)	Increased bone resorption and decreased bone formation	Rapid loss of bone
Calcitonin (Azria *et al.*, 1995)	Inhibited differentiation of osteoclast precursors	Bone formation
Increased secretion of insulin (Delany *et al.*, 1994)	Stimulation of bone matrix formation and mineralization	Gradual bone formation
Decreased secretion of hormones involved in pregnancy (Sun *et al.*, 2006)	Increased bone resorption due to loss of estrogen	Loss of bone
Glucocorticoid stimulate osteoclastogenesis (Weinstein *et al.*, 2002)	Increased bone resorption	Rapid loss of bone
Thyroid hormone (Baran and Braverman, 1991)	Stimulation of normal growth and development of bones	Increased bone mass
Calcium absorption impaired due to decreased 1,25 D_3 (DeLuca, 1980; Tsoukas *et al.*, 1984; Roodman *et al.*, 1985)	Increased bone resorption through synthesis of osteocalcin and osteopontin by osteoblastic cells while suppressing collagen production	Loss of bone
Estrogen (Jilka *et al.*, 1992)	Suppression of the production of bone-resorbing cytokines, such as IL-1, IL-6, and prevention of formation of mature osteoclasts	Increased bone mass

The process of bone remodelling is mainly influenced by factors, such as BMPs, which work in coordination with other growth factors and hormones to control the bone formation-resorption dynamics. BMPs can be metalloproteinase (such as BMP1) or proteins belonging to the transforming growth factor-β (TGF-β) family (BMP2, 3, 4, 5, 6 and 7). BMP2, 4 and 7 have been shown to induce chondrogenic and osteogenic differentiation in undifferentiated mesenchymal cells, leading to bone formation or destruction (Wozney, 1992). More about BMPs will be covered in chapter 4, The mutual relationship between the developing tooth and bone: impact of mechanical forces and signalling pathways. The effects of signalling molecules on the process of bone remodelling is summarised in Figure 1.6. All pro-inflammatory cytokines appear to act through the OPG/RANK/RANKL regulatory pathway (Franzoso *et al.*, 1997; Martin *et al.*, 1998) affecting osteoclast generation and activity (Figure 1.6).
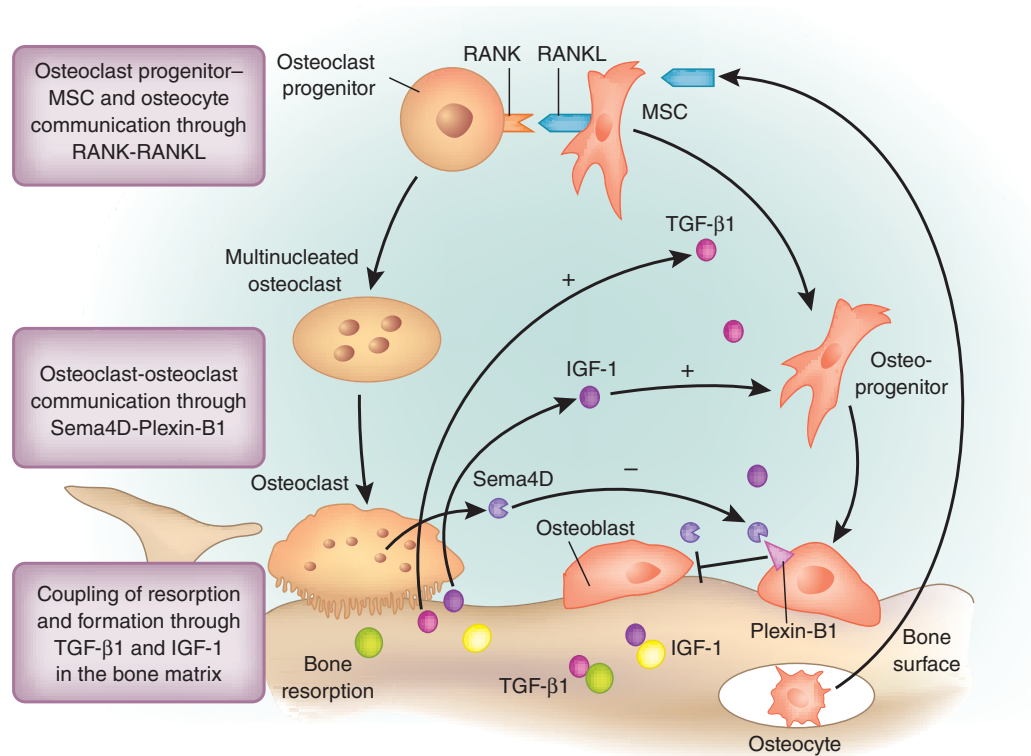
Figure 1.6 The signalling molecules involved in regulating bone remodelling in mammalian cells.

The factors that modulate the differentiation and functions of osteoblasts and osteoclasts are shown. *Adapted from Cao (2011)*.

Figure 1.6 shows the factors that modulate the differentiation and functions of osteoblasts and osteoclasts together with mechanisms of coupling between bone resorption and formation. In each cycle of bone remodeling, new bone formation occurs at bone resorption sites to maintain the microarchitecture required for bone's mechanical properties, which occurs through different levels of cellular communication. TGF-β1, and probably IGF-1 in bone matrix act as the primary coupling factors and are released in response to osteoclastic bone resorption. These factors induce the migration of osteoblastic cells so that the new bone formation is spatiotemporally coupled with resorption. It was recently revealed that Sema4D secreted from osteoclasts regulates osteoblast differentiation (Negishi-Koga *et al.*, 2011); Sema4D activates downstream of RhoA by binding to Plexin-B. The actions of both TGF-β1 and IGF-1 are also mediated by RhoA. Furthermore, Sema4D–Plexin-B1–mediated osteoclast-osteoblast communication through RhoA is integrated with the matricellular signaling of

TGF-β1 and IGF-1. The differentiation of osteoclast progenitors is mediated through the RANK-RANKL communication. Increased osteoblastic RANKL stimulates Sema4D production by osteoclasts. Sema4D balances the supply of osteoclasts and osteoblasts by inhibiting the differentiation of osteoblasts, hence, functioning in a negative-feedback loop (Cao, 2011). Osteocytes trapped in the bone signal to osteoclasts via RANKL when undergoing apoptosis.

1.4 Rationale for the study

In this study, we aim to provide an understanding of the developmental biology and molecular mechanisms surrounding the tooth-bone interface. This involves investigating the factors that regulate the homeostatic balance between the formation and survival of osteoclasts and osteoblasts, which in turn controls the formation of the tooth-bone interface. Furthermore, we intend to acquire an understanding of the RANK-RANKL pathway and the factors, both molecular and genetic, that may modulate the cascade and the physiological outcomes of the same. We aim to explore the interactive nature of the tooth and bone in the creation of a coordinated system by manipulating normal development using an explant culture approach. Finally, we will monitor the process of growth and development of bone in a mouse model known to have osteopetrosis. Together, these approaches will allow an understanding of the nature of ankylosis, as ankylosis in different conditions may have similar underlying mechanisms. It is hoped that this knowledge could contribute to the field of tooth tissue engineering and might provide better understanding of the relative relationship between the epithelium, dental papilla, and alveolar bone, and facilitate the recreation of a tooth *in vitro*. Furthermore, this study will provide improved understanding of bone development in clinical cases of oligodontia (missing teeth) and socket formation defects. It could also contribute to research in craniofacial genetics through identification of genetic and molecular markers that regulate the process of tooth development and alveolar bone formation and resorption (Sodek and McKee, 2000).

1.5   Hypothesis and Aims

In this study, we hypothesize that one or more cellular mechanisms may be responsible for the prevention of bone formation at the tooth-bone interface. The lack of bone immediately surrounding the tooth is important as it creates a space for the developing tooth to grow and forms a gap between the tooth and bone in which the soft tissues of the periodontium can develop. When cultured in isolation, the tissue around the developing tooth forms bone, indicating its osteogenic potential. We propose that signalling factors produced by the tooth may be instrumental in preventing the cells within the tooth-bone interface from differentiating into osteoblasts, while osteoclasts play a role in preventing encroachment of the alveolar bone into the space around the tooth. In this work, we aim to identify and characterise the underlying factors and mechanisms that prevent bone formation and invasion in the interface between the tooth and bone. This area of research is being investigated using embryonic mice as models. Detailed aims of the present study are:

1. To investigate the relationship between the tooth and bone *in vivo* using histological study.

2. To identify the location of osteoclasts in the tooth-bone interface during development using the TRAP stain assay, *in vivo*.

3. To monitor the growth and development of the alveolar bone in explant culture.

4. To identify the origin of the alveolar bone cells using DiI labelling in explant culture.

5. To investigate the impact of the alveolar bone on the tooth and that of the tooth on the alveolar bone. This will be achieved by studying the effects of removal of the surrounding tissues, mainly the alveolar bone, on the tooth, and the effects of removal of the epithelium of the tooth on the alveolar bone.

6. To modulate the BMP signalling pathway using factors such as BMP-4 and Noggin and investigate its effect on osteogenesis.

7. To identify and characterise the expression of genes thought to control osteoclast formation, such as OPG, RANK, and RANKL in the RANK-

RANKL signalling cascade during alveolar bone development, using *in situ* hybridization.

8. To modulate the RANK-RANKL signalling pathway using factors such as OPG and RANKL and to investigate its effect on osteoclastogenesis.

9. To study and characterize the tooth-bone interface in a knockout mouse known to have a defect in osteoclastogenesis, the *c-Fos* mutant.

10. To describe the condition of osteoclasts, if any, in the *c-Fos* mutants.

11. To monitor the progress of bone invasion into the tooth-bone interface in *c-Fos* mutants in explant culture.

2 <u>Materials and Methods</u>

This project employed basic histology methods, organ culture and manipulation techniques, *in situ* hybridization and micro computerized tomography (Micro-CT). All methods and aspects of the study were ethically approved by the Animal Care and Use Committee of King's College London and were performed in accordance with institutional policy and guidelines governing the humane treatment of vertebrate animals.

2.1 Reagents and Solutions

2.1.1 Organ Culture and Manipulation

Dulbecco's Modified Eagle Medium (DMEM)/F12	Gibco®, 12634-010
Penicillin-Streptomycin solution	Sigma®, P0781
GlutaMAX™	Life Technologies/Invitrogen® 35050061
Organ Culture Dish (Center-Well Organ Culture Dish)	Falcon®, 353037
Cell Culture Insert (0.4 μm pore size, PET track-etched membrane, 6 well format)	BD Falcon™, 353090
Stainless Steel - AISI 304 - Mesh (Fe/Cr18/Ni10)	Goodfellow®, FE228710
Recombinant Mouse Osteoprotegerin/TNFRSF11B Fc Chimera	R&D System®, 459-MO-100
Recombinant Mouse TRANCE/RANKL/TNFSF11	R&D System®, 462-TEC-010
Affi-Gel agarose beads	Bio-Rad, Inc. 153-7301
Recombinant Mouse BMP-4	R&D System®, 5020-BP-010
Bovine Serum Albumin	Sigma®, A2058
Recombinant Mouse Noggin	R&D System®, 1967-NG- 025
Alizarin red stain	BDH Prolabo®, 343152T
Dispase	Gibco®, 17105-041
Dulbecco's Phosphate Buffered Saline (Modified, without calcium chloride and magnesium chloride)	Sigma®, D8537
Millipore Express® PLUS Membrane Filters (0.22μm)	Merck Millipore®, GPWP14250

2.1.2 Tissue Processing

Di-ethyl-pyro-carbonate (DEPC)	Sigma®, D5758
Paraformaldehyde	Sigma®, P6148
(4% Stock solution in Nuclease-free 1XPBS)	
Ethylene-diamine-tetra-acetic acid (EDTA)	VWR®, 20302.293
Methanol (Absolute - Acetone free)	Sigma-Aldrich®, M1775
Ethanol	VWR®, 101077Y
Histoclear	National Diagnostics, Inc., HS-202
Isopropanol	Acros Organics®, AC39698
1,2,3,4-Tetra-hydro-naphthalene	Sigma®, 429325
Ultraplast Poly-iso-butylene Histological Wax	Solmedia®, WAX060

2.1.3 Analysis Methods

Naphthol AS-TR	Sigma®, N6125
(phosphate disodium salt ≥99% (HPLC))	
Sodium acetate	Sigma-Aldrich®, S 2889
N,N-Dimethylformamide anhydrous, 99.8%	Sigma-Aldrich®, 227056
Sodium Tartrate	Sigma®, S-8640
Fast Red TR Salt	Sigma®, F-2768
(hemi (zinc chloride) salt)	
Aquatex™	Merck Millipore®, 108562
Liquid Blocker (Super Pap Pen)	Pelco®, 22309
Industrial Methylated Spirit	Solemedia®, IMS025
Alcian Blue	Sigma-Aldrich®, 05500 Fluka
Acetic acid (Analytical Reagent, ≥96%)	Sigma-Aldrich®, 33206
Erhlich's Haematoxylin	Solemedia®, HST003
Phosphomolybdic acid	Sigma-Aldrich®, 79560 Fluka
Sirius Red	Sigma-Aldrich®, 43665 Fluka
Picric acid	Sigma-Aldrich®, 80452 Fluka
Xylene	Solemedia®, XYL025
DPX	BDH Prolabo®, 360294H
Hydrochloric acid (Analytical Reagent)	Sigma-Aldrich®, 38283 Fluka
Eosin, aqueous solution (0.5% Eosin Y in disilled H_2O)	Sigma-Aldrich®, 32617 Riedel-de Haën

2.1.4 Molecular Biology Techniques

Agarose™	Amresco®, 0710
Ethidium bromide	Fisher Scientific®, BP1302-10
Quickload® 1 kb ladder	Biolabs, Inc., N0468L
Blue/Orange Loading Dye, 6X	Promega®, G1881
Luria-Bertani (LB) broth	
1% Tryptone	Oxoid Limited, LP0042
1% NaCl	BDH, Inc., 102415K
0.5% Yeast	Oxoid Limited, LP0021

Luria-Bertani (LB) agar
    1%   Tryptone   Oxoid Limited, LP0042
    1%   NaCl   BDH, Inc., 102415K
    0.5% Yeast   Oxoid Limited, LP0021
Agar Bacteriological (Agar No.1)   Oxoid Limited, LP0011
Ampicillin Sodium Salts (50 mg/ml)   Sigma®, A9518
Subcloning Efficiency™ DH5α™ Invitrogen®, 18265-017
Competent cells
QIAprep Spin Miniprep Kit   Qiagen®, 27104
Sodium dodecyl sulfate (SDS)   Severn Biotech Limited, 30-33-50
(10% stock solution in Nuclease-free H_2O)
QIAquick® Gel Extraction Kit   Qiagen®, 28706
Restriction enzymes and buffers   obtained from Promega®

2.1.5 *In-Situ* Hybridization

DTT, Molecular Grade (DL-Dithiothreitol) Promega®, P1171
Polymerase enzymes   obtained from Promega®
Riboprobe® System Buffers   Promega®, P1121
DIG RNA Labeling Mix   Roche®, 11277073910
Formamide   Merck Millipore®, 344205
Tween-20   Sigma®, P7949
(10% stock solutions in Nuclease-free H_2O)
tRNA (RNA from yeast)   Roche®, 109223
(10 mg/ml stock solution in Nuclease-free H_2O)
Proteinase K   Sigma®, P2308
(10 mg/ml stock solution in Nuclease-free H_2O)
Goat serum   Invitrogen®, 16210
Blocking Reagent   Roche®, 11096176001
(10% stock solution in 1x MAB)
Maleic acid   Sigma-Aldrich®, M0375
NBT 4-(Nitro blue tetrazolium) chloride, Roche®, 11383213001
solution
Anti-Digoxigenin-AP Fab fragments
Super PAP Pen   Invitrogen®, 00-8899
BCIP (5-Bromo-4-chloro-3-indolyl- Roche®, 11383221001
phosphate)
^{35}S isotope   Perkin Elmer®, 800-762- 4000
Scintillation fluid, Ultima Gold™ LLT Perkin Elmer®, 6013371
Glycine   Sigma®, G7403
Triethanolamine (TEA)   BDH, Inc., 103704U
Acetic anhydride   BDH, Inc., 100022M
Dextran Sulfate 50% Solution   Merck Millipore®, S4031
50 X Denhardt's
    1% (w/v) Ficoll 400   Sigma®, F4375
    1% (w/v) Polyvinylpyrrolidone BDH, Inc., 436032C
    1% (w/v) Bovine Serum   Sigma®, A9647
    Albumin
GBX developer/replenisher   Sigma®, P7042
GBX fixer/replenisher   Sigma®, P7167
K5 emulsion   Ilford Scientific Product, 1355136

Kodak D-19 developer	Kodak[®], 1464593
Kodak Unifix	Kodak[®], 5211412
Malachite Green oxalate salt	Sigma[®], M9015

2.2   Obtaining Embryonic and Neonatal Mouse Tissues

For obtaining embryonic and neonatal mouse tissues, CD-1 male and female mice were first mated overnight to obtain wild type animals, while tests for vaginal plug were carried out from the following day. To establish the embryonic stage following the mating, the day on which the vaginal plug was discovered was designated as embryonic day 0.5 (E0.5). Following this, the collection of embryonic and neonatal tissue was carried out according to the Home Office schedule one specification.

Pregnant females carrying embryos of the desired developmental stage were identified and sacrificed using cervical dislocation. The procedure was carried out at specific time points to obtain embryos at different developmental stages. Embryos were harvested using caesarean section and were collected in an ice-cold culture medium consisting of DMEM/F12 (Dulbecco Modified Eagle Medium, nutrient mix F-12, GIBCO[®], Invitrogen) supplemented with 1% penicillin/streptomycin and 1% GlutaMAX™. The gestation period lasted typically for 18 days with birth on the 19th day (P0).

2.2.1   Organ Culture and Manipulation

Dissection instruments were sharpened (using a sharpening stone lubricated with mineral oil) and sterilized prior to use for organ culture. Dissections were performed in a laminar-flow hood to minimize contamination. Dissection needles were sharpened using electrolysis in 2M sodium hydroxide using a 12V supply.

A complete culture medium was prepared for dissection and culture of embryonic organs. The prepared culture consisted of Advanced Dulbecco's Modified Eagle Medium F12 (DMEM F12) (Invitrogen™) supplemented with 1% Glutamax™ (Invitrogen™) and 1% penicillin-streptomycin. Dissection tools

were periodically cleaned during the dissection process using a 70% ethanol spray and dry-heat sterilization in a Geminator500™.

For dissecting the mandibles from the head, a cut was performed in the oral cavity using the scalpel and blade and tissue slices containing the region of interest were obtained.

2.2.2 Slice culture method

Tissue slices containing molar tooth germs were prepared from the mandibles of mice using a standard table McIlwain tissue chopper (Ted Pella, Inc.). Mandibles at the desired stages of development were arranged in frontal orientation over the cutting table and 250 μm thick slices were prepared. Tissue slices containing the first molars (M1) representing the correspondent developmental stage were carefully selected under a stereomicroscope (Figure 2.1).

Figure 2.1 Obtaining embryonic tissue slices containing the mandibular first molars.

An E14.5 embryo is shown for illustration purposes. (**A**) The axes along which the mandible extraction was performed. (**B**) The cut mandible after brain removal. (**C**) The mandible on the cutting plate of the chopper ready for slicing. (**D**) A tissue slice chosen for transfer into an organ culture dish. T = tongue, RT M1 = right mandibular first molar, Lt M1 = left mandibular first molar.

The tissue slices explants were transferred using a Pasteur pipette to be cultured at the medium-gas interface in an organ culture dish (Falcon®, Center-Well Organ Culture Dish). Explants were mounted on membranes cut to the correct size (BD Falcon™ cell culture inserts, pore size 0.4 μm) supported by metal grids and floated over ≈1 ml culture medium in a humidified atmosphere of 5% CO_2 at 37 ºC i.e. incubator (Nuaire™ DH Autoflow) for an average of 6 days. The

explants were cultured in the previously illustrated medium and the culture medium solution was changed every 48 hours unless otherwise stated.
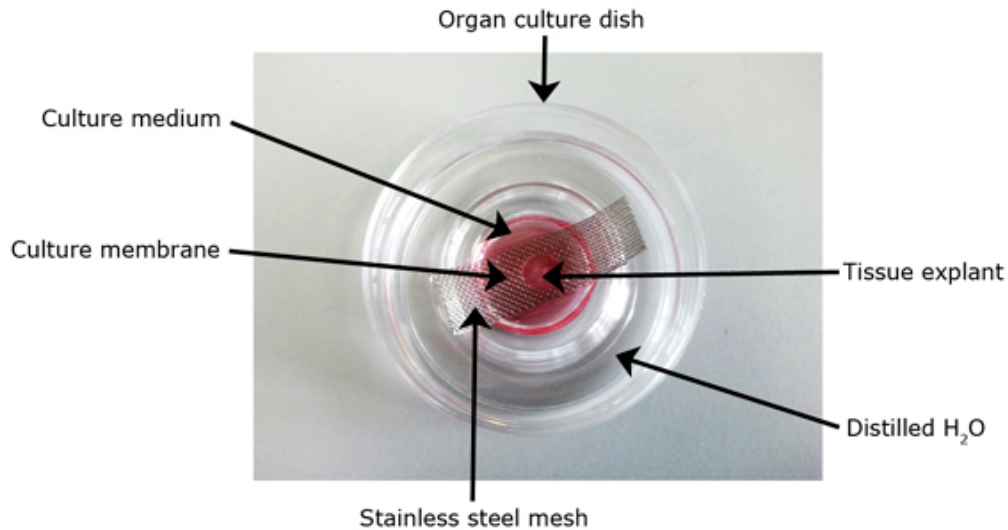
Figure 2.2 The culture of embryonic mouse mandibles using an organ culture dish (classical) method.

2.3 Tissue Processing

2.3.1 Fixation, decalcification and dehydration

Di-ethyl-pyro-carbonate (DEPC) treatment is carried out to deactivate RNases. This involves preparing a 0.1% concentration solution of di-ethyl-pyro-carbonate (DEPC), leaving it in the fume hood overnight and then inactivating the DEPC by autoclaving at 100°C for 15 minutes.

Tissues were fixed by incubating in 4 % Paraformaldehyde (PFA) (Sigma®) in DEPC treated PBS in a glass or plastic tube (BD Falcon™) at 4 ºC. Tissues were kept fixed for a duration of between 18 and 22 hours (generally the time of fixation depends on the temperature and size of the tissue). After fixation, calcified postnatal tissues were decalcified using 1% PFA and 25% 0.5M Ethylene-diamine-tetra-acetic acid (EDTA) (VMR®) pH8 solution in PBS. The decalcification process lasted up to 2 months and was carried out at room temperature (time of decalcification depends on the size of specimen and its age (degree of hard tissue)). The solution was gently agitated and regularly changed

47

during the process. The decalcified sample was visually compared with a non-decalcified adult mouse head using an x-ray machine (Faxitron® MX-20) to ensure that desired level of decalcification had occurred.

This was followed by the dehydration of fixed tissues. The dehydration process began with the rinsing of tissue samples in PBS (or DEPC treated PBS for samples intended to be used for *in situ* hybridization). The tissue samples were then dehydrated in a series of methanol solutions of increasing concentration (please refer to Table 2.1 of solution composition). Variable incubation time was used for each dehydration stage depending on size and developmental stage of tissue (please refer to Table 2.2 for incubation times). The samples were stored overnight at 4 ºC or -20 ºC according to level of dehydration and gently agitated during the dehydration process. Once completely dehydrated, the samples were stored at -20 ºC in 100% methanol (Sigma-Aldrich®) until use. Cultured tissues were dehydrated using ethanol (VWR®).

Table 2.1 Ethanol/Methanol dehydration series.

Dehydration step	Solution composition	Storage temperature (°C)
PBS	PBS only	Not Applicable
30%	30% ethanol/methanol, 70% PBS	4
50%	50% ethanol/methanol, 50% PBS	4
70%	70% ethanol/methanol, 30% PBS	4
85%	85% ethanol/methanol, 15% dH$_2$O	4
90%	90% ethanol/methanol, 10% dH$_2$O	-20
95%	95% ethanol/methanol, 5% dH$_2$O	-20
100%	100% ethanol/methanol	-20

NB: Methanol solutions were diluted in DEPC treated PBS/dH$_2$O if tissues were to be processed for *in situ* hybridization.

Table 2.2 Ethanol/Methanol dehydration conditions.

Tissue stage/size	Time per wash	# of washes per step	# of histoclear washes
E11.5 head, slices or tooth germ explants	30 minutes	1	2
E12.5 head	40 minutes	1	2
E13.5 head	50 minutes	1	2
E14.5 head	60 minutes	1	3
E15.5 head	90 minutes	2	5
E16.5 head	100 minutes	2	5
E17.5 head	150 minutes	2	8
E18.5 head	180 minutes	2	9
Postnatal heads	Full day or overnight	2	Not applicable

NB: All samples were washed 3 times in 100% ethanol/methanol prior to long term storage.

2.3.2   Clearing and wax embedding

The dehydrated samples to be wax embedded were first brought to room temperature and transferred to a glass vial. Samples dehydrated using ethanol were washed a number of times (as stated in Table 2.2) in 100% histoclear (National Diagnostics, Inc.) with each wash lasting 20 minutes. The samples were further incubated for 15 minutes at about 65 ºC in histoclear and then moved to Leica™ EG1150H wax embedding station for further processing.

Samples dehydrated using methanol were washed twice in 100% isopropanol (Acros Organics®) before being cleared using incubation in 1,2,3,4-tetra-hydro-naphthalene (THN) (Sigma®). Incubation was carried out until the sample was completely clear, that is, transparent.

In both cases, molten poly-iso-butylene histological wax (Ultraplast, Solmedia®) was used. Samples were incubated for 30 minutes at 65 ºC in wax, and changes of wax repeated 6 times for 1 hour. Some larger samples were incubated once overnight in wax at 65º C. E16.5 heads and older samples underwent incubation at 65 ºC in a vacuum embedder (Hearson) for the same duration as their respective methanol washes.

Following wax incubation, the samples were positioned in the fresh molten wax-filled molds kept on a hot plate, which was maintained at 65 ºC before being transferred to a 4 ºC cold stage. The sample was held in place manually until the wax solidified sufficiently to immobilize the sample. Before solidification of the wax, a labeled plastic embedding cassette (VWR® International) was quickly pushed into the warm wax. The wax blocks were further solidified for 30 minutes before being removed and stored at 4 ºC until required.

2.3.3 Sectioning and mounting

Excess wax around the embedded tissues was removed using a razor blade and the edges were aligned to form a straight wax ribbon. 8 µm thick sections were cut using microtome (Leica™ RM2245 or Reichert-Jung®) and these sections were immediately mounted on glass slides (Superfrost plus™, VWR® International). Slides were moistened with dH_2O to prevent premature adhesion and slices were carefully placed on moistened slides using a razor blade and forceps. All the slides were carefully labeled with a pencil as other labels may get removed during alcohol incubation. Some serial sections were mounted on alternate slides so as to make comparative tests on comparable tissue areas. The sections were mounted so that each section was touching the next section so to ensure that the sections did not get separated during the water-bath incubation step.

After the mounting procedure was complete, the sections were incubated in a water-bath (electro-thermal, Grant®) for 10 minutes at 42 ºC to remove any creases in the wax. Following incubation, sections were mounted back to the center of the slides before being dried at 42 ºC on a slide drying bench (Thermo Scientific®) overnight. The samples which required quick drying were dried at 65 ºC for 30 minutes. After drying the slides were either immediately used or stored at 4 ºC until required.

2.4   Analysis Methods

2.4.1   Tartrate-resistant acid phosphatase (TRAP) staining

Burstone's (1979) technique was adopted for staining. Paraffin sections were de-waxed and rehydrated using histoclear and ethanol. The slides were placed within the staining solution in a coplin jar and incubated at 37 °C for 30-40 minutes.

For the staining solution, 1 mg Naphthol-AS-TR-phosphate (Sigma®) was added per ml Acetate buffer (pH5.2). Acetate buffer (10.5 ml Glacial Acetic acid: 0.2 M + 39.5 ml Sodium Acetate (Sigma-Aldrich®): 0.2 M brought to 100 ml with H_2O). 1 µl N-N-Dimethylformamide, 23 mg Sodium Tartrate (Sigma®), and 1 mg Fast Red TR Salt (Sigma®) are added per ml of staining solution.

Slides were then washed in H_2O, counterstained for ≈3 minutes in methyl green, and sections were outlined with a liquid blocker (Super pan pen, Pelco®) and mounted in aqueous conditions (Microscopy Aquatex™, Merck Millipore®).

2.4.1.1   *Numeric analysis of TRAP positive cells in the TBI*

The number of TRAP stained cells was counted on the microscopic images of all the TRAP stained sections obtained from any first molar explant culture. The magnification power was standardized for all images being 10x/0.25, and all multinucleated red stained cells within the field were counted. The count was performed with the aid of the count tool in the Fiji program. The cell count from all sections was then averaged for each sample and considered for use in all further forms of statistical analysis. In the present study, the error of the method was determined by repeating the TRAP cells count, which was obtained from five M1 explant cultures at one-week intervals. All measurements were made by the same operator.

2.4.2   Trichrome staining (Sirius red, Alcian blue and Haemotoxylin)

The slides were de-paraffinized using histoclear in preparation for rehydration through an ethanol series in dH$_2$O. Staining of sections was carried out using the Trichrome method with Sirius Red in picric acid, Alcian Blue and Haematoxylin.

Alcian Blue is useful in staining acid and neutral mucopolysaccharides (Mowry, 1956), Sirius Red is useful in staining and visualizing bone and connective tissue, while haemotoxylin is useful in counterstaining cell nuclei.

Before staining, slides were first de-waxed being incubated twice in Histoclear II™ for 10 minutes each. Following this, the slides were rehydrated in decreasing concentrations of Industrial Methylated Spirit (IMS) (Solmedia®) with each rehydration cycle (for each concentration) lasting 2 minutes. The slides were then incubated in deionized H$_2$O for 2 minutes. The staining process began with incubation in 1% Alcian Blue (Sigma-Aldrich®) dissolved in 3% acetic acid (Analytical Reagents, Sigma-Aldrich®) pH2.5 for 10 minutes followed by a rinse under running water for 10 minutes and under deionized H$_2$O for a short time.

The next stage of staining began with incubation in Ehrlich's haematoxylin (Solemedia®) for 2 minutes, followed again by a 10 minute rinse under running water and a brief rinse in deionized H$_2$O. To differentiate staining, slides were incubated in 2.5% phosphomolybdic acid (Sigma-Aldrich®) for 10 minutes and rinsed in deionized H$_2$O.

Following this, sections were first stained in 0.5% Sirius Red (Sigma-Aldrich®) in saturated picric acid (Sigma-Aldrich®) for 20 minutes followed by rinsing in 0.5% acetic acid. The samples were then dried using blotting paper and washed three times in 100% IMS for 2 minutes each. The slides were dipped in Xylene (Solmedia®) before cover slipping immediately with DPX (BDH Prolabo®) mounting medium.

2.4.3   Haematoxylin and eosin staining

Haematoxylin and eosin (H&E) staining techniques have been in use for over a century to distinguish between cell nuclei (stained purple/black by haemotoxylin) and cytoplasm (stained pale pink by eosin) (Fischer *et al.*, 2008). H&E staining was used to ensure that sections contained appropriate anatomical structures for carrying out radioactive *in situ* hybridization.

H&E staining was carried out at room temperature. The process began with de-waxing of slides by incubating them twice for 10 minutes, each time in Histoclear II™. Following de-waxing, the slides were rehydrated in decreasing concentrations of IMS for 2 minutes at each concentration followed by incubation in deionized H_2O for 2 minutes. Sections were incubated in Ehrlich's haematoxylin for 10 minutes, followed by a wash under running water for 10 minutes before being rinsed briefly in deionized H_2O. Haematoxylin staining was differentiated in 1% hydrochloric acid (Analytical Reagent, Sigma-Aldrich®) in 95% IMS for 15 seconds, before washing again under running water for 10 minutes and rinsing in deionized H_2O. Following Haematoxylin staining, Eosin staining was carried out by staining the sections in 0.5% aqueous Eosin (Sigma-Aldrich®) for 1-5 minutes duration depending on the depth of stain required. Sections were then rinsed twice in deionized H_2O and dehydrated in an IMS series. Following this, the sections were air dried and cover-slipped (Menzel-Glaser, Inc. coverslips 25 x 60 mm #1) using DPX mounting medium.

2.4.4   Eosin counterstaining

Eosin counterstaining was carried out following the *in situ* hybridization (please refer to 5.2.2.1.4 Post-hybridization washes and signal detection). The process began with dehydration of slides by washing in graded series of 90% ethanol for 2 minutes per wash. Following the dehydration, the sections were counterstained in a solution of 25% eosin, diluted in 90% ethanol for around 3 minutes. The actual duration of counterstaining depended on the desired depth of counterstain.

The slides were then dehydrated by washing in 95% ethanol for 2 minutes, and twice in 100% ethanol for 2 minutes each. The slides were then air dried and cover slipped with DPX mounting medium.

2.5   Micro Computerized Tomography (Micro-CT) Analysis

Fixed mouse heads washed in PBS were used for scanning. Mouse heads were then immobilized using ultrasound gel and cotton before being scanned in 14 μm voxel size volumes using a GE Locus SP microCT scanner. The scanned image was visually analyzed using the Explore Microview software programme (GE). The software was used to generate 3-D reconstructions and 3-D isosurfaces of mouse teeth, maxillas and mandibles.

2.6   Microscopy, photography and imaging processing

A Nikon Eclipse 80i microscope was used to view the slides. All sections except the radioactive *in situ* hybridized sections were viewed under brightfield. Photographs of tissue sections were taken using a Nikon Digital Sight Camera.

Live organ cultures were routinely prepared and viewed under a Leica MZFLIII dissecting microscope, and photographed with a Leica DFC300 FX camera.

Brightness and contrast were altered using Photoshop CS5.1, applying identical settings to images used for comparison within experiments.

3   Development and fate mapping of the alveolar bone during formation of the tooth-bone interface

3.1   Introduction

The region between the alveolar bone and the dental cementum of the tooth can be defined as the tooth-bone interface (TBI) (Fleischmannova *et al.*, 2010). In functional teeth, the TBI houses the soft tissues of the periodontal ligament, a mainly neural-crest-derived structure that anchors the tooth and jawbone together (Kaku *et al.*, 2012). The TBI accommodates the shock-absorbing function of the periodontal ligament and distributes the mechanical stress generated during mastication, tooth movement, and bone remodeling (Lekic and McCulloch, 1996; Sodek and McKee, 2000). During tooth crown development, a TBI is found between the tooth germ and the surrounding alveolar bone (Figure 3.1) and creates a space for the developing tooth to grow, while during root development it forms a soft-tissue space in which the periodontal ligament can develop.
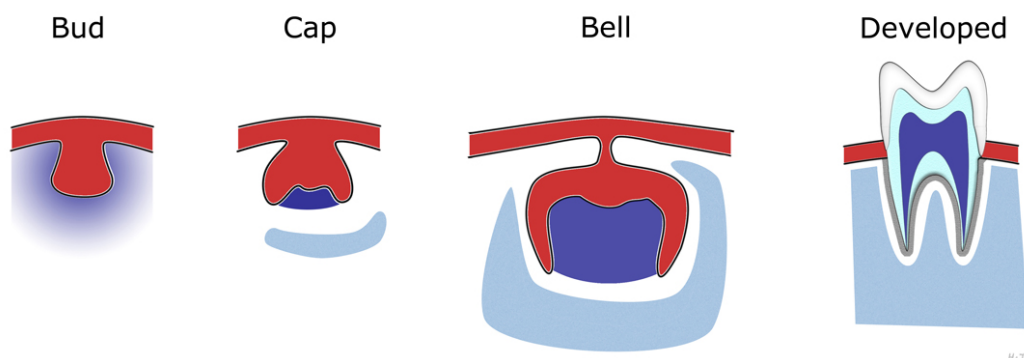
Figure 3.1 Diagrammatic representation of the TBI formation during the various tooth-alveolar bone development stages.

The TBI is first shown forming at the cap stage as a gap between the dental epithelium and the alveolar bone. This gap persists in all the subsequent developmental stages until it is located between the dental cementum of the root and the alveolar bone in the fully developed tooth. Epithelium is displayed in red, mesenchyme in blue, alveolar bone in light blue, enamel in white, dentin in turquoise, and cementum in grey. *Scheme obtained from Dr Hannah Thompson, Department of Craniofacial Development and Stem Cell Biology, and Department of Orthodontics, King's College London, Guy's Hospital, London Bridge, London, United Kingdom.*

3.1.1 Tooth-bone interface

In an adult tooth, the region between the alveolar bone and the dental cementum of the tooth can be defined as the tooth-bone interface (TBI) and houses the periodontal ligament (Figure 3.2). This region mainly accommodates the shock-absorbing function of the periodontal ligament and maintains the developmental and tissue homeostasis of the tooth with its surrounding alveolar bone. This region is clearly defined when the tooth is viewed by histology.
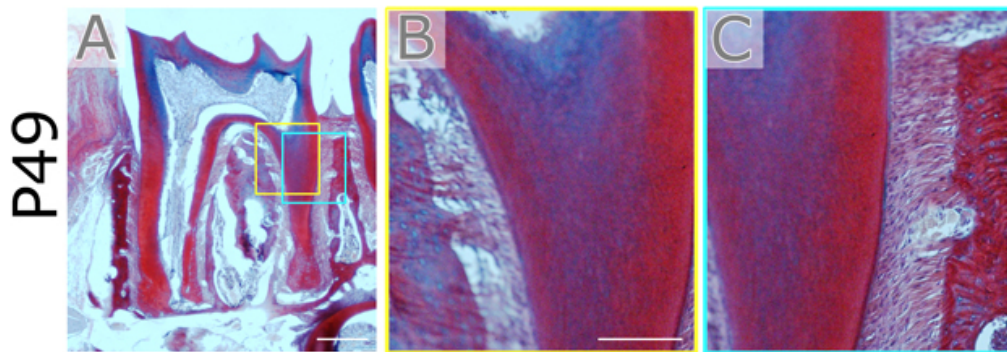
Figure 3.2 Histology of an adult's (7 weeks old) TBI.

(**A**) Sagittally viewed CD1 wild-type mandibular first molar morphology after Trichrome staining at P49. (**B**) High power view of the yellow boxed area in (**A**) showing the TBI from the inner side of the tooth root. (**C**) High power view of the turquoise boxed area in (**A**) showing the TBI from the outer side of the tooth root. From both sides (**B** and **C**), the root of the mandibular first molar was seen to lie at a distinct distance from its surroundings. This distance was uniform on (**A**) and represents the TBI. It is a bone-free region as it did not pick the sirius red stain of the tri-chrome. Scale bar in **A** = 300 μm. Scale bar in **B** = 100 μm (same scale in **C**).

Within the TBI are found various cytokine producing cells and activated fibroblasts (Figure 3.3).
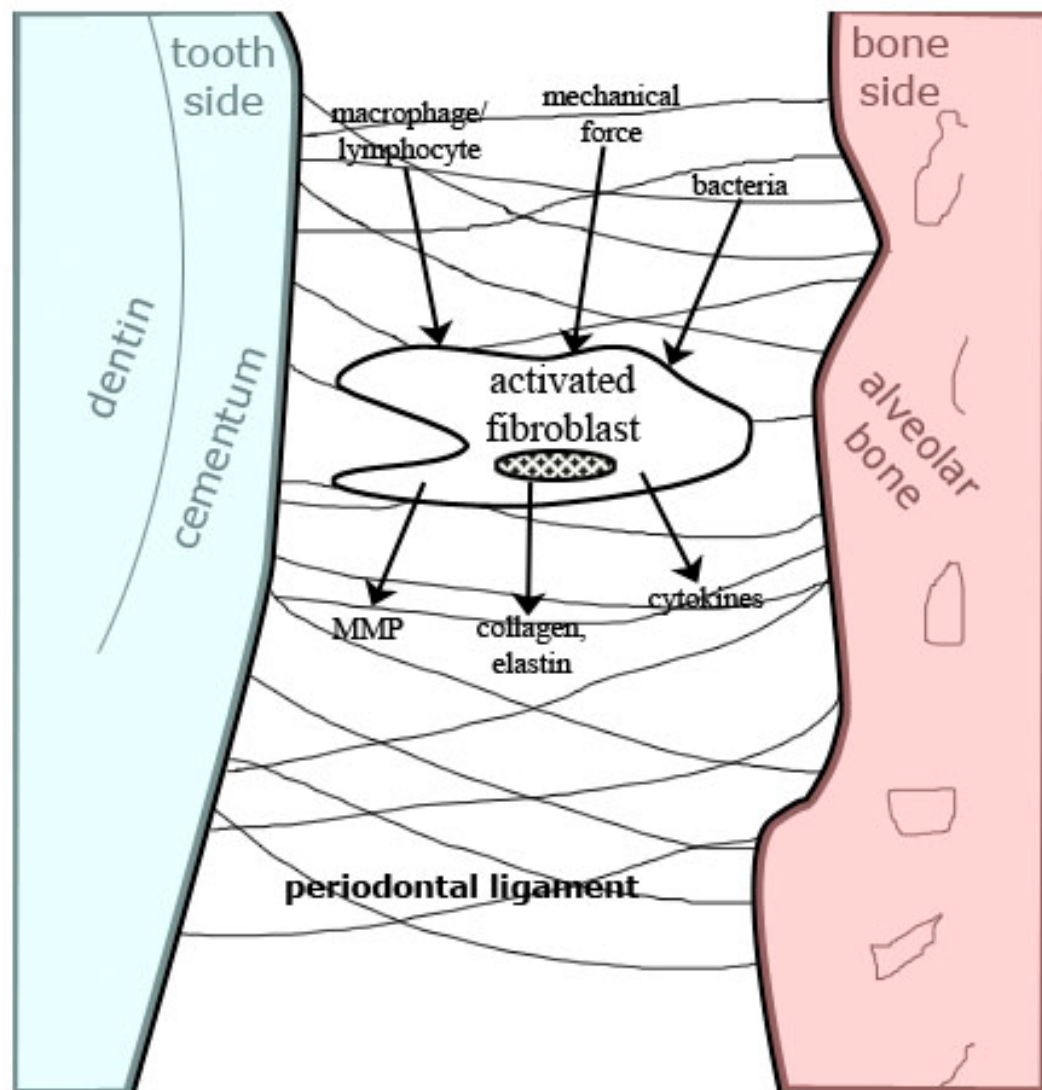
Figure 3.3 Representation of the TBI.

The TBI is formed between the dental cementum and the alveolar bone. It consists of the periodontal ligament and activated fibroblasts that produce matrix metalloproteinase (MMP) and cytokines, induced by specific stimuli from macrophages, lymphocytes, mechanical force, and bacteria. The fibroblast can also be induced to produce collagens and elastin. *Adapted and modified from Lekic and McCulloch (1996).*

The TBI can also be clearly viewed as a gap between the tooth and the bone on Micro-CT sections (Figure 3.4).
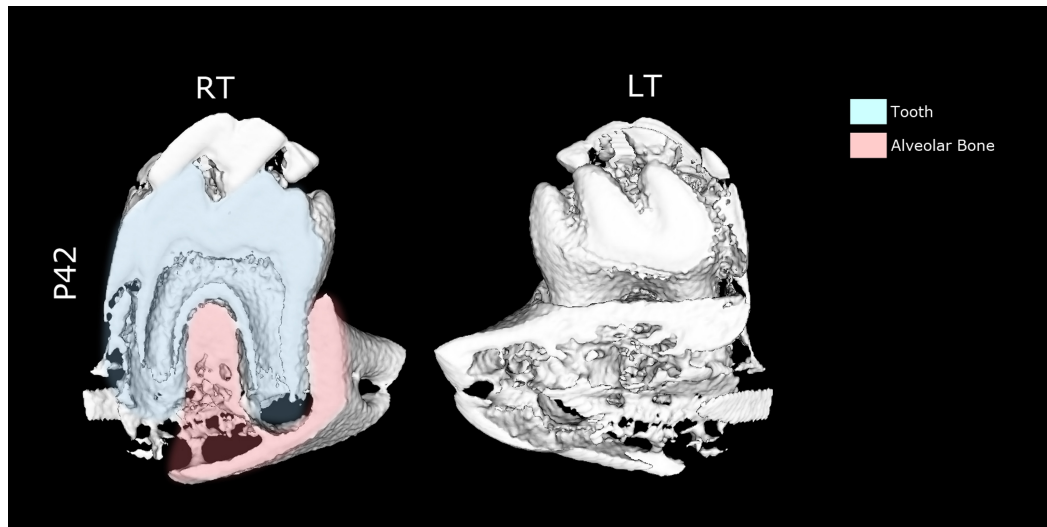
Figure 3.4 Micro-CT of an adult's TBI.

The mandibular first molar of a CD1 wild-type mouse at the age of 6 weeks old. A buccal view of the tooth is shown on the left while a mid-sagittal view of the same is shown on the right. In the mid-sagittal view, the dental tissues, crown and root have been coloured in light blue while the surrounding tissues are in light red. The dental and surrounding tissues after colouring were seen separated with a distinct region, the TBI, in between.

3.1.2   Significance of tooth-bone interface

The TBI performs certain functions that are related to the structures that surround the region. In the functional tooth, the TBI accommodates the shock-absorbing properties of the periodontal ligament that anchor the tooth root to the jaw bone and in turn works to distribute the mechanical stress generated during mastication, tooth movement and during rapid remodelling of teeth during periodontal diseases or tooth regeneration (Takano-Yamamoto *et al.*, 1994; Lekic and McCulloch, 1996; Sodek and McKee, 2000).

From a clinical perspective, the relationship and interactions between the tooth and the alveolar bone are crucial. They can provide a better understanding of the subsequent patterns of resorption of the alveolar ridges after tooth extraction by clinicians, which would contribute to the successful fabrication of implant prostheses (Winkler, 2002; Fleischmannova *et al.*, 2010). Together, this

knowledge could also contribute in the field of dental tissue engineering and might provide a better understanding of the relative relationship between the epithelium, dental papilla, and alveolar bone, to facilitate the recreation of a tooth *in vitro*. Furthermore, the study can provide improved understanding of clinical cases like ankylosis, failure of eruption (unerupted/impacted), and socket formation defects (Diep *et al.*, 2009). It could also help in formulating a better treatment plan when placing implants for cases of oligodontia (missing teeth).

When the tooth-bone interface is compromised, the bone can fuse with the tooth, resulting in ankylosis (Albers, 1986). The prevalence of ankylosed teeth can reach up to 40% depending on the population (Helpin and Duncan, 1986). For ankylosis to be avoided, it is essential that the tooth-bone interface remains free from mineralization.

3.1.3   Relationship of tooth and alveolar bone

3.1.3.1   *Evidence that they form from the same population*

Reports from labelling experiments have physically linked the development of the tooth to its supporting structures; the alveolar bone, the periodontal ligament, and cementum as labelled cells from the tooth bud mesenchyme were found to take part in the formation of the dental follicle, showing the tooth organ as an entity comprising of both the dental and periodontal tissue (Diep *et al.*, 2009).

Prior to that, contributions made by the follicle layer of the dental follicle in forming the alveolar bone were reported as labelled cells from the dental follicle have formed the alveolar bone at a late developmental stage - postnatal day 6 (Diekwisch, 2002).

Culturing experiments reported the development of the tooth along with its supporting structures intact when a tooth germ was dissected out and cultured

subcutaneously, or within the eye or kidney capsule of an adult host which, furthermore, pointed out the presence of all the periodontium forming cells within the tooth germ itself (Ten Cate *et al.*, 1971; Ten Cate and Mills, 1972; Yoshikawa and Kollar, 1981; Palmer and Lumsden, 1987; Kratochwil *et al.*, 1996).

Tissue culturing experiments have shown the osteogenic potential of dental mesenchymal cells from early developmental stages (the bud and cap stages). Yamazaki *et al.* (2007) showed that isolation of the condensing dental mesenchyme at E13.5 (the bud stage), followed by culturing in a bone supporting medium, can form bone. In a comparable study, Kim *et al.* (2007), showed that isolation of dental follicle cells at E14.5 (the cap stage) formed bone when cultured under a kidney capsule for 2 weeks. The expression of numerous genes that are associated with bone development, namely, *Runx2*, *Dlx5*, *Msx1*, and *Bmp4* are also expressed at early stages of tooth development and could explain the potential of the tooth germ to develop when isolated unto bone (Zhang *et al.*, 2003).

In this chapter, we report the results of our study in which we examine the spatial relationship between the bone and tooth during embryonic development, concentrating on the first lower molar (M1). This chapter provides a framework for further characterization of the underlying factors and mechanisms that prevent bone formation and invasion at the interface between the tooth and bone investigated in other chapters. We used histochemistry, explant culture, and lineage labelling to understand the close relationship between the bone and tooth.

Aims

- To describe the relationship of the tooth and bone during development.
- To identify the location of osteoclasts in the tooth-bone interface during development *in vivo*.
- To visualise the formation of the tooth-bone interface in explant culture using slice culture method.

- To determine the source of cells forming the alveolar bone using fate mapping experiments.

3.2   Materials and Methods

3.2.1   Whole-mount Alizarin red staining

Alizarin red stain was one of the methods tried to stain bone in the tissue slices. In the culture dishes containing the samples, the tissue slices were first washed with distilled water followed by introduction of 0.2% Alizarin red stain (BDH Prolabo®). Samples were maintained overnight followed by washing out of the dye using distilled water dye and washing of samples.

Finally the images of the samples were captured using a light microscope and Leica™ image analyzing software.

3.2.2   DiI labelling

1, 1'-Dioctadecyl-3, 3, 3', 3'-Tetramethylindocarbocyanine perchlorate (DiI) is a lipophilic dye that intercalates in the cell membrane, marking groups of cells. DiI (Cell tracker CM-DiI, C-7000, Molecular Probes, Eugene, OR, USA) was dissolved in 100% EtOH. Before culture, small amounts of DiI were injected into the slices by means of a mouth aspirator (Diep *et al.*, 2009). The position of the DiI was recorded with a fluorescence Leica dissecting microscope (Leica Microsystems Ltd, Milton Keynes, UK) every 24 hours (N = 20).

3.2.2.1   Lineage tracing in steps (Alfaqeeh and Tucker, 2013)

1. Pull glass capillary needles using a needle puller.
2. Break the tip of the needle using forceps and place tip down into the dye solution. Leave for a few minutes while the dye fills the tip by capillary action.

3. Place the filled needle into a holder and attach via tubing to an injector or mouth pipette.

4. Position the tip of the needle in the culture medium touching the area of the slice due to be labelled. Apply air pressure to displace a small amount of dye out of the needle and onto the tissue.

5. Remove needle and check for labelling under fluorescence.

6. Successfully labelled slices can be transferred to filters and cultured as described in the slice culture technique (see 2.2.2 Slice culture method).

3.3   Results

3.3.1   Formation of the TBI during development

The relationship between the mouse mandibular first molar and alveolar bone was reviewed on histological sections from E14.5 up to P0 (from initiation of the alveolar bone to complete enclosure of the developing tooth at birth). At E13.5 when the tooth is at the bud stage, no alveolar bone was observed (Figure 3.6, A). By the cap stage, however, at E13.5, the alveolar bone, connected to the dentary bone (also known as the mandibular bone), was observed forming adjacent to the buccal side of the tooth (Figure 3.5, A). As the tooth developed from the late cap to the bell stage, the alveolar bone reached around the buccal side of the tooth and started to form on the lingual side (Figure 3.5, B and C). By the late-bell stage, the bone was observed on both sides of the tooth, reaching up toward the oral epithelium (3.5, D and E). Figure 3.5 shows that the developing tooth germ formed with a cellular gap separating the developing alveolar bone from the outer enamel epithelium of the tooth. Although this gap reduced over time, the developing tooth remained at a distance separated from the alveolar bone (Figure 3.5, E).
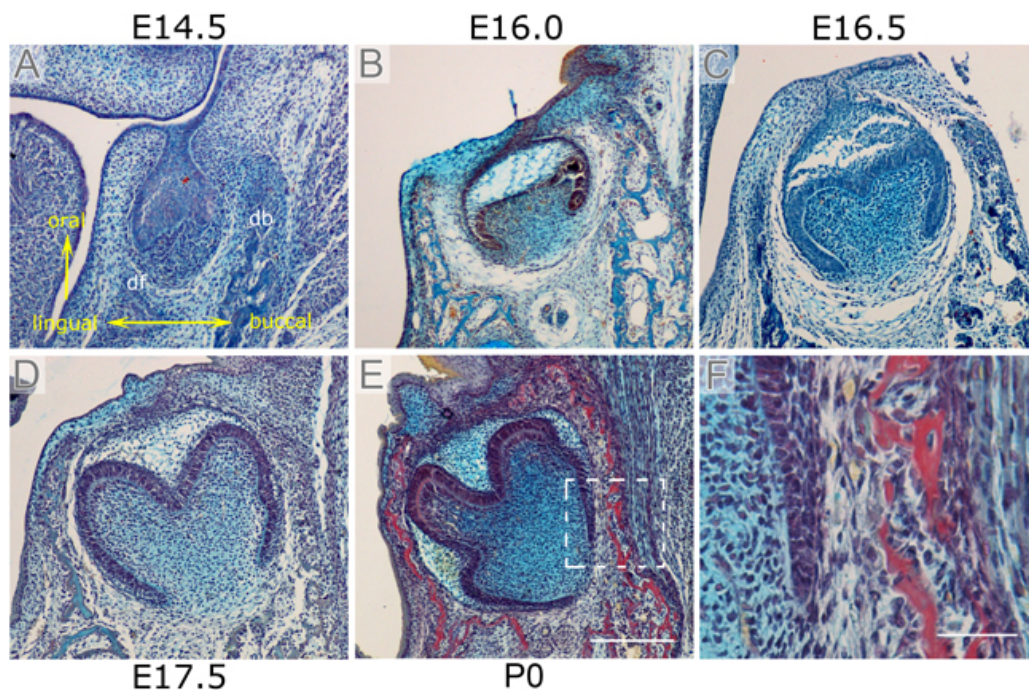
Figure 3.5 Histological study of the mouse mandibular first molars.

Histological sections of the mouse mandibular first molar. Morphology after Trichrome staining at E14.5 (**A**), E16.0 (**B**), E16.5 (**C**), E17.5 (**D**), P0 (**E**), and the magnifed view of the area (dotted lines) at P0 (**F**). df = dental follicle, db = dentary bone. Scale bar in **E** = 200 μm (same scale in **A**, **B**, **C**, and **D**). Scale bar in **F** = 50 μm.

To investigate whether the unossified gap between the bone and tooth was regulated by osteoclasts, we compared the location of timing of osteoclasts to the development of the TBI. Osteoclasts were followed by the TRAP assay which labels cells from the macrophage/osteoclast lineage in addition to dendritic cells (Hayman *et al.*, 2000). Although TRAP is a good indicator of an osteoclast, it can not be used to definitively say that a cell is an osteoclast. We therefore used it as a potential marker of putative osteoclasts.

3.3.1.1 Location of osteoclasts in relation to bone
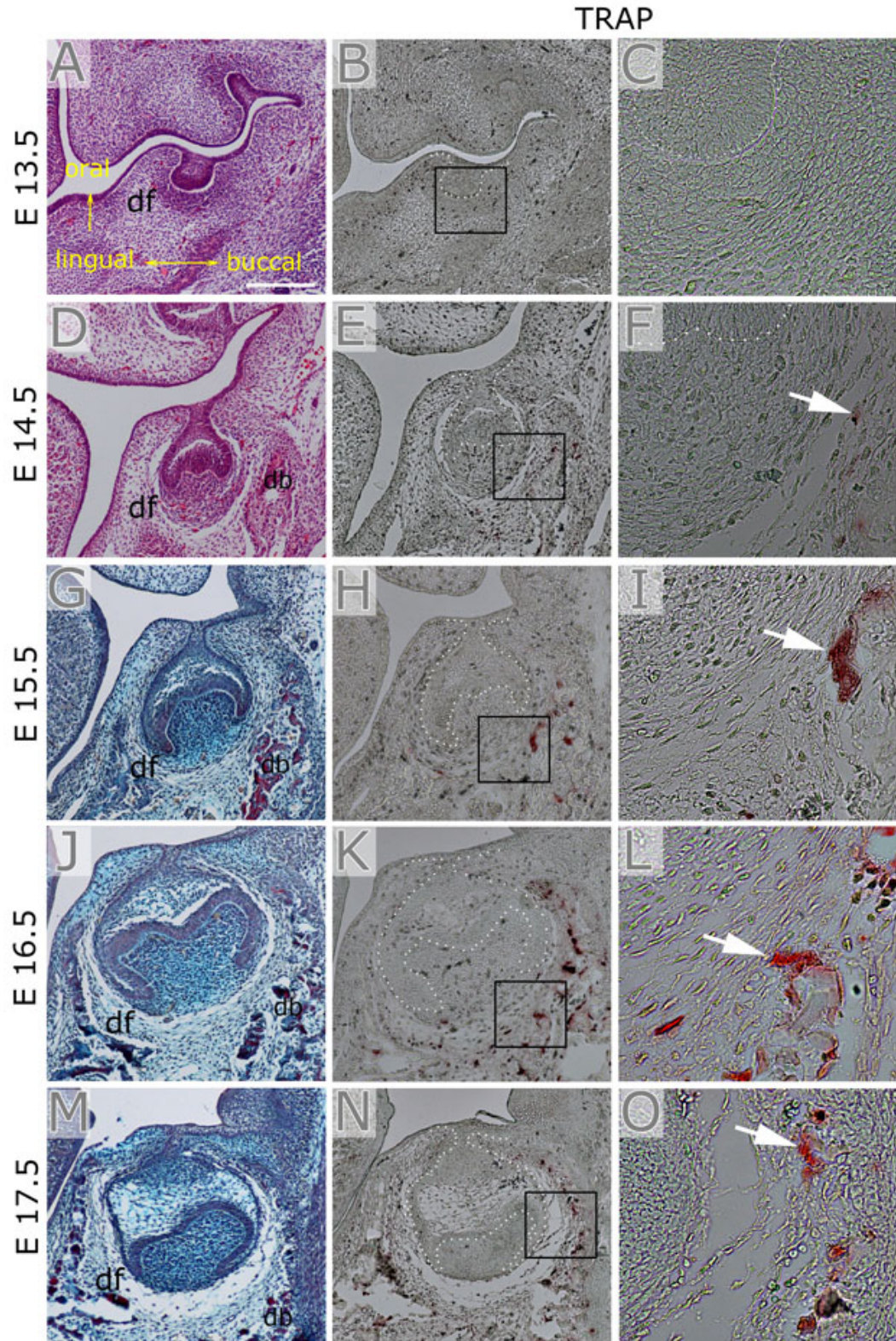
Figure 3.6 Initiation of the alveolar bone and osteoclastogenesis.

Figure 3.6 Initiation of the alveolar bone and osteoclastogenesis.

(**A** and **D**) H&E-stained developing tooth germs, frontal section. (**G**, **J**, and **M**) Trichrome stain of developing tooth germs, frontal section. (**B**, **E**, **H**, **K**, and **N**) Alternate sections stained for TRAP (red stain). (**C**, **F**, **I**, **L**, and **O**) High-power view of area boxed in (**B**, **E**, **H**, **K**, and **N**). (**A-C**) E13.5, at the tooth bud stage of development, no TRAP-positive cells were evident. (**D-F**) By the cap stage, E14.5, small patches of alveolar bone were evident on the buccal side of the tooth, with a few TRAP-positive cells lining the tooth-bone interface (TBI) (arrow). (**G-I**) At E15.5, alveolar bone was obvious on the buccal side, again associated with TRAP-positive cells lining the TBI (arrow). (**J-L**) By the bell stage (E16.5), alveolar bone was clearly also seen on the lingual side of the tooth, with TRAP cells lining the TBI (arrow). (**M-O**) By the late bell stage (E17.5), the alveolar bone had extended up toward the oral epithelium on both sides of the tooth, with TRAP cells lining the TBI (arrow). df = dental follicle, db = dentary bone. Scale bar in **A** = 300 μm (same scale in **B**, **D**, **E**, **G**, **H**, **J**, **K**, **M**, and **N**).

At E13.5, when the tooth had reached the bud stage, no TRAP-positive cells were evident (Figure 3.6, A-C). By the cap stage, however, at E14.5, a few TRAP-positive cells were located on the buccal side of the tooth lining the bone facing the tooth-bone interface (Figure 3.6, D-F). As the tooth developed from the late cap to the bell stage, a greater number of TRAP positive cells were detected buccally, lining the bone facing the tooth-bone interface. In addition, a few TRAP positive cells were located on the lingual side of the tooth lining the bone facing the tooth-bone interface (Figure 3.6, G-L). By the late-bell stage, a greater number of TRAP positive cells were located lining the bone facing the tooth-bone interface, on both the buccal and lingual sides of the tooth (Figure 3.6, M-O). At all these stages, a distinct non-mineralized TBI was evident, with TRAP-positive cells lining the bone side.

3.3.2   Identification of the differentiating bone cells using Alizarin red stain

In order to follow the differentiating bone cells, the cultures at day 5-6 were stained with the bone stain Alizarin red. The Alizarin staining results were fairly variable (Figure 5.5); hence to obtain a strong indication of the level of bone development, histological sections of the cultures were used instead to determine the level of differentiation of the bone cells.
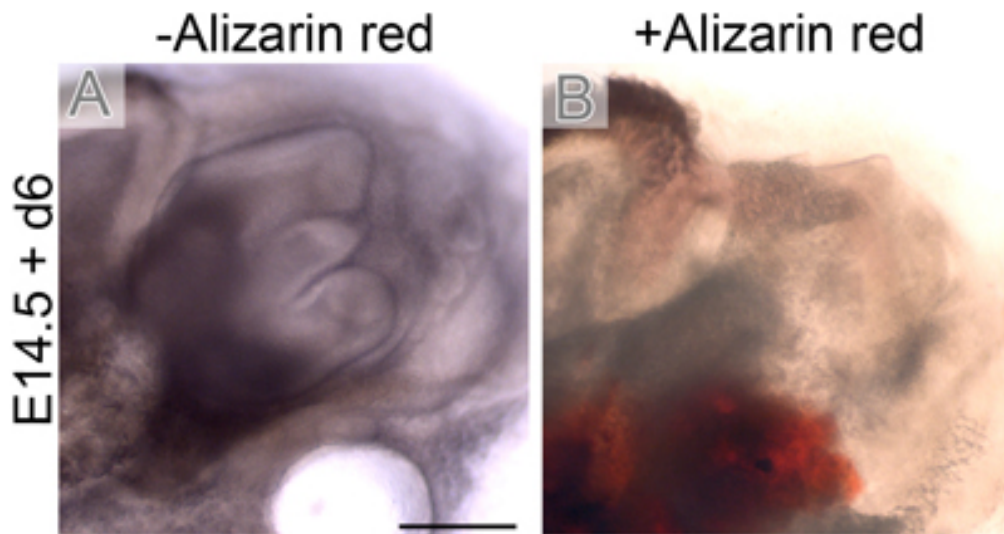
Figure 3.7 Alizarin red stain histochemistry.

(**A**) The M1 culture explant before staining on day 6 and (**B**) the M1 culture explant on uptake of Alizarin red stain. Scale bar in **A** = 300 μm (same scale in **B**).

3.3.3 Understanding the relationship between the bone and tooth

3.3.3.1 *Monitoring the development using M1 explant culture*

In order to visualize the interactions of tooth and bone during embryonic development, frontal mandible slices were cultured from E14.5. This stage was chosen, as the appearance of the first signs of alveolar bone was observed *in vivo* at this stage. Slice cultures have also been used to culture the mandibles of 28 day old rats (Smith *et al.*, 2010). The thin slices cut using a diamond wafer saw created 1.5mm thick slices, allowing good nutrient and gas exchange in these more mature tissues.
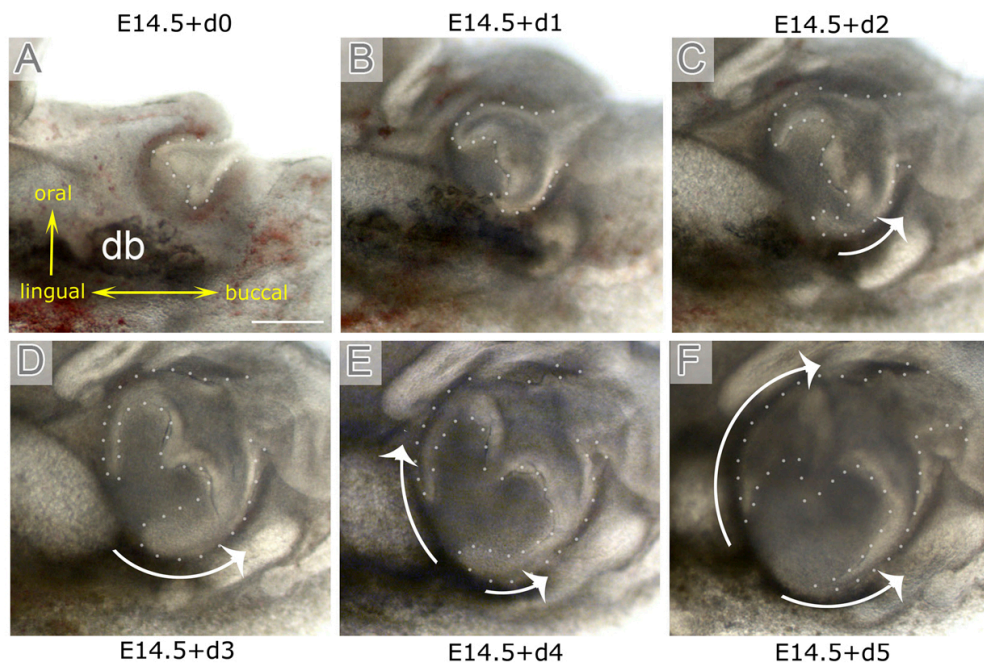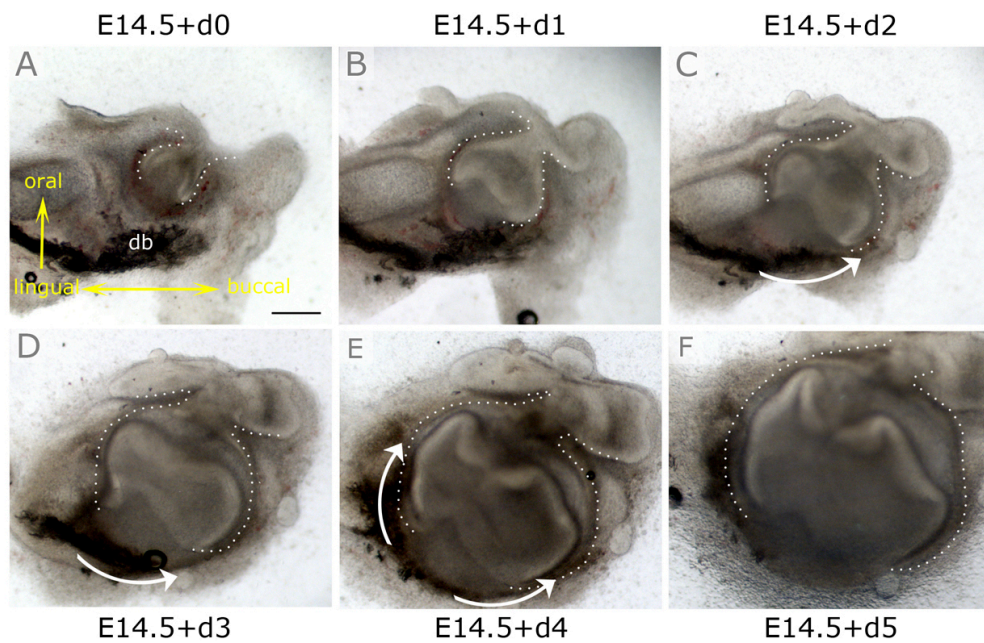
Example 1

Example 2

Figure 3.8 Following the developing mandibular first molar and alveolar bone in slice culture.

Figure 3.8 Following the developing mandibular first molar and alveolar bone in slice culture.

Two examples, 1 and 2, showing the development of a cap-stage mandibular first molar tooth germ (E14.5) over 5 days in explant culture. Day 0 (**A**), day 1 (**B**), day 2 (**C**), day 3 (**D**), day 4 (**E**), and day 5 (**F**). The bone appeared dark under transmission light. Initially, the bone was at a distance from the tooth (**A**) and then started to appear on the buccal side of the tooth (arrow in **C**), followed by the lingual side (arrow in **E**). White arrows indicate alveolar bone. db, dentary bone. Epithelium of the tooth germ is outlined with white dots. Example 1, Scale bar in **A** = 200 μm (same scale bar in **B**, **C**, **D**, **E**, and **F**). Example 2, Scale bar in **A** = 200 μm (same scale bar in **B**, **C**, **D**, **E**, and **F**).

Cultures of lower first molar explants developed well, with the cap-staged M1 tooth germ successfully reaching the late bell stage as depicted in Figure 3.8.

In slice cultures, the bone was evident as a darkly stained region that appeared to extend out from the dentary bone of the jaw, wrapping itself around the tooth during the culture period (Figure 3.8, A-F). As observed from histology, the bone first progressed around the buccal side of the tooth (Figure 3.8, C and D) and then was seen around the lingual side, reaching up toward the oral epithelium (Figure 3.8, E and F) mimicking the process observed *in vivo*.

This pattern of development has been suggested to be generated by the osteogenic cells migrating around the tooth extending out from the dentary bone (Ramaesh and Bard, 2003). Alternatively, it could represent a wave of differentiation of the mesenchyme around the tooth forming bone as suggested by previous lineage labelling experiments (Diekwisch, 2002; Diep *et al.*, 2009). To distinguish between these 2 possibilities, we labelled the cells next to the dentary bone with the fluorescent label DiI.

3.3.3.2 Development of the alveolar bone
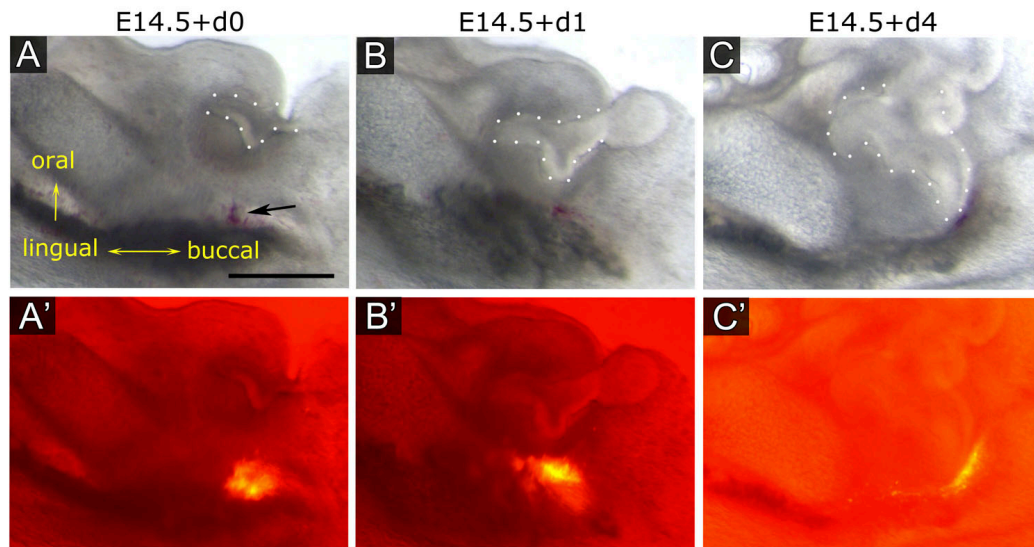
Figure 3.9 DiI labelling to follow the cells at the margin of the dentary bone.

(**A-C**) Bright field of developing tooth germ in culture. (**A'-C'**) images in merged bright and dark field. (**A**, **A'**) Day 0, a DiI dot is placed at the margin of the dentary bone (arrow). (**B**, **B'**) Day 1, no movement of the DiI-labelled cells was observed, but the tooth germ had grown towards the injection site. (**C**, **C'**) Day 4, the tooth had grown toward the dentary bone, and labelled cells were observed around the buccal side of the tooth germ in the developing alveolar bone. Epithelium of the tooth germ outlined with white dots. Scale bar in **A** = 500 μm (same scale in **A'**, **B**, **B'**, **C**, and **C'**).

Initially, the DiI-labelled cells remained in position next to the border of the dentary bone as the tooth grew (Figure 3.9, A, A', B, and B'). After 4 days in culture, the tooth germ had grown considerably, meeting the original site of injection, and labelled cells were observed in an arc along the outer enamel epithelium on the buccal side (Figure 3.9, C and C'). The labelled cells therefore were recruited into the alveolar bone.

We also labelled cells of the dental follicle (Figure 3.10). The DiI-labelled cells, which are much closer to the tooth germ, were shown to move together with the tooth as it grew (Figure 3.10, B, C, and D). After 7 days in culture, the DiI label was found near the forming tooth-bone interface and alveolar bone in a similar

position to the DiI when cells from much further away were labelled (compare Figure 3.9, C and 3.10, D).
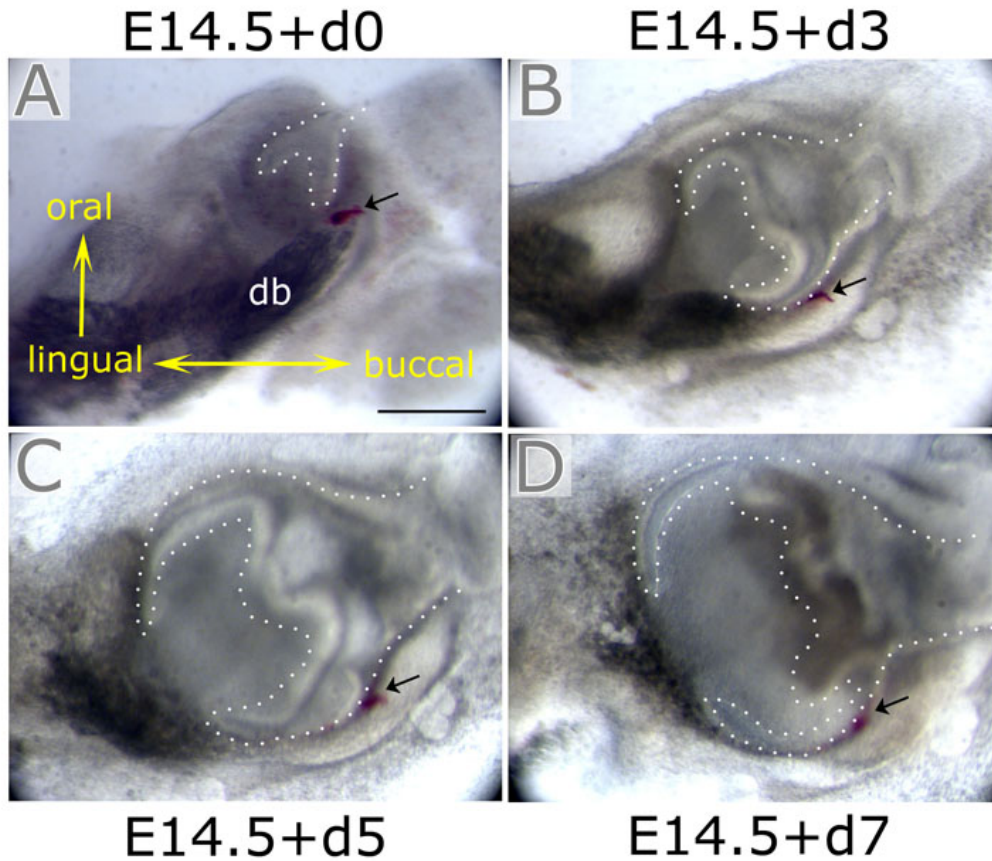
Figure 3.10 DiI labelling to follow the cells of the dental follicle.

(**A-D**) Bright field of developing tooth germ in culture. (**A**) Day 0, a DiI dot is placed within the dental follicle (darker region of condensed mesenchyme) (arrow). (**B**) Day 3, the tooth germ had grown, and the DiI labelled cells had moved concomitantly with the tooth germ growth that occurred. (**C**) Day 5 and (**D**) day 7, the tooth had grown toward the dentary bone, and the labelled cells were observed around the buccal side of the tooth germ in the area of the developing alveolar bone. Epithelium of the tooth germ outlined with white dots. Scale bar in **A** = 500 μm (same scale in **B**, **C**, and **D**).

3.4   Discussion

This chapter identified both novel information about how the TBI normally forms and the origin of the alveolar bone. Osteoclasts were found to be closely associated with the border of the developing bone, lining the TBI, but not within the TBI itself. The DiI labelling experiments showed the contribution of two sources of cells to the formation of alveolar bone namely, dental follicle cells from around the tooth and, bone cells from the margins of the dentary. Importantly, the slice culture method provided an excellent opportunity for following the development of the tooth and allowing lineage tracing. This method was documented and published as a video article.

In the first part of this project, the relationship of the tooth and bone during development was assessed from E13.5 using a histological study, TRAP staining and mandible slice culture to help understand how the TBI is preserved as the tooth and bone grow.

It is proposed that the gap that surrounds the developing tooth germ actually protects the tooth from invasion by alveolar bone and is reserved for development of the soft tissues of the periodontium.

It has previously been proposed that osteoclasts play a role in protecting the tooth germ from invasion by bone. Interestingly, TRAP positive cells were first observed at E14.5, coinciding with the first signs of bone. The positive cells were closely associated with the border of the developing bone, lining the TBI, but were initially not found within the TBI itself. Presence of the TRAP-positive cells was found to follow the pattern of alveolar bone development, first on the buccal side of the tooth (cap stage) and after on the lingual side (early and late bell stages). As these TRAP positive cells were multinucleated and were positioned in close association with the bone, it makes it highly likely that these positive cells are indeed osteoclasts. However, as a definitive test of osteoclasts it

would be necessary to look for structures under the confocal microscope, such as the ruffled border and actin ring, and expression of markers such as cathepsin K (Teitelbaum, 2000). It is possible that osteoclasts prevent the alveolar bone encroaching on the TBI and therefore spare this space for the periodontium and at the same time provide the space needed for the tooth to develop.

The results of following the differentiating bone in cultures using Alizarin red stain were not reproducible. However, Alizarin is a useful dye in terms of simplicity of administration, provides ready visibility, and is persistent in its effect.

The organ culture of mouse mandibular explants, including dental follicle and alveolar bone, is an excellent tool to examine the complex process of tooth-germ development, however the mechanisms by which the alveolar bone accommodates the developing tooth germ are not yet clear (Tabata *et al.*, 1996; Liu *et al.*, 1998; Liu *et al.*, 2000; Abe *et al.*, 2002; Mekaapiruk *et al.*, 2002; Tabata *et al.*, 2002).

Recently, we visually demonstrated the slice culture as a method for following tooth germ development in explant culture, which allows unique access to the tooth during development, providing an excellent opportunity for manipulation and lineage tracing, not available using more traditional culture methods (Alfaqeeh and Tucker, 2013). We adopted this method to monitor the development of the mandibular first molar and its supporting structures, hence, the tooth-bone interface, and for the lineage tracing experiments of this chapter.

Our results illustrate the close relationship of the tooth and bone during development. *In vivo* and in culture, the alveolar bone appears to form as an extension of the dentary bone. In our DiI labelling experiments, we show that cells at the margin of the dentary bone do indeed end up surrounding the tooth as part of the developing alveolar bone. This movement appears aided by the down growth of the tooth germ towards the dentary bone. Such movement and bone

developmental behaviour had been also reported during the process of suture growth when bone precursor cells migrated upwards, from the outer ring of the eyeball towards the skull vault, their final destination (Yoshida *et al.*, 2008). We show that the extension of bone cells from the dentary bone up towards tooth germ to form the alveolar bone happens in quite a similar manner. This agreed with the findings of a previous study that showed the alveolar bone develops as a result of localized vertical growth of the superior border of the mandible and extension of the bone proximal and distal to the tooth bud (Ramaesh and Bard, 2003). In our DiI labelling experiments, we also show that cells close to the tooth from the dental follicle form the tooth-bone interface and alveolar bone itself. These dental follicle cells move with the tooth germ as it grows towards the dentary bone and end up within the surrounding structures of the tooth as part of the developing alveolar bone. This agrees with previous labelling experiments that have shown cells within the dental follicle can contribute to the developing alveolar bone (Diekwisch, 2002; Diep *et al.*, 2009). Having labelled two distinct regions initially and ended up with the same final labelling, it would appear, therefore, that two distinct mechanisms form the alveolar bone: both a differentiation of dental follicle cells around the tooth and, concurrently, a recruitment of bone cells from the margins of the dentary bone.

4 The mutual relationship between the developing tooth and bone: impact of mechanical forces and signalling pathways

4.1 Introduction

In the last chapter the close relationship between the developing tooth and alveolar bone was described. In this chapter the impact of the tooth on the bone and bone on the tooth will be addressed. From 3D reconstructions of the developing mandible, it has been suggested that spatial impediment by the developing bone might be a factor in controlling the morphogenesis of the developing tooth from the bell stage onwards (Radlanski *et al.*, 1998). In this way, the rigid bone would cause a mechanical constraint on the shape of the tooth. In addition, inhibitory signals in the mesenchyme surrounding the tooth have been proposed to control the number of tooth germs that develop, as trimmed incisor explants develop supernumerary incisors (Munne *et al.*, 2009). This indicates that the tissue surrounding the tooth can impact on how many teeth develop from a placode. The tissue surrounding the tooth during its development can therefore influence the tooth by exerting a mechanical force and by acting as a source of signalling factors. Whether the bone and surrounding mesenchyme influences the shape and size of developing molar teeth was therefore investigated by manipulating the forming tooth and bone in culture.

It has previously been proposed that osteoclasts play a role in protecting the tooth germ from invasion by bone. In the first results chapter of this thesis we showed that osteoclasts line the bone along the tooth-bone interface (TBI) from the very earliest stages of tooth development, as soon as bone is deposited. We know that mammalian tooth formation is a complex process, involving epithelial-mesenchymal interactions between the ectoderm and neural crest-derived mesenchyme (Chai *et al.*, 2000; Rothova *et al.*, 2012). This pattern of TRAP

positive cells suggests that a signal from the tooth might be responsible for controlling the layout of osteoclasts, thereby controlling the TBI. This idea was investigated in this chapter by removing the tooth epithelium in culture to investigate the impact on the pattern of TRAP positive cells.

Finally, tissue culture experiments have shown that the TBI possesses osteogenic potential, as isolated dental follicle at the cap stage (E14.5) can form bone when cultured under a kidney capsule for 3 weeks (Kim *et al.*, 2007). This indicates that, as well as preventing bone invading the TBI using osteoclasts, the TBI cells themselves must be prevented from undergoing differentiation into osteoblasts and forming bone. As the TBIs default state in isolation is to form bone, signalling from the surrounding tissue is likely to be responsible for inhibiting the osteoblast pathway. A well known pro-osteoblast signal is bone morphogenetic protein (BMP). We therefore investigated the effect of manipulating this pathway on the differentiation of cells in the TBI during tooth development.

4.1.1   Brief introduction of BMP signalling molecule

The bone morphogenetic proteins (BMPs) are constituents of the transforming growth factor-beta (TGF-β) superfamily of ligands, which play significant roles in a myriad of biological activities (Waite and Eng, 2003). They are factors that possess multiple functions during growth and powerfully participate in the regulation of the processes of cartilage and bone formation during embryonic development and post-natal life regeneration (Reddi, 2001). In the osteoblast progenitor cells and non-osteogenic lineage cells, such as fibroblasts and myoblasts, BMPs induce osteoblastic differentiation (Katagiri *et al.*, 1990; Katagiri *et al.*, 1994; Komaki *et al.*, 1996). BMPs also play roles in the development and repair of extra-skeletal tissues, such as the brain, kidneys, and nerves (Reddi, 1997).

4.1.1.1   *BMP pathway*

As depicted in Figure 4.1, the BMP pathway operates by the BMP ligand, binding to complexes of two BMP receptor-type I (BMPR-I) and two BMP receptor-type II (BMPR-II) receptors, and tempering the expression of target genes through a series of signal transduction pathways. The activated ligand-receptor complex could initiate signalling through a number of pathways; out of these, the SMAD proteins are the best characterized, followed by the mitogen-activated protein (MAP) kinase pathway (Nohe *et al.*, 2004). A number of inhibitors of this pathway have been identified. These include soluble antagonists, such as Noggin, that sequester the BMP ligands (Yanagita, 2005).
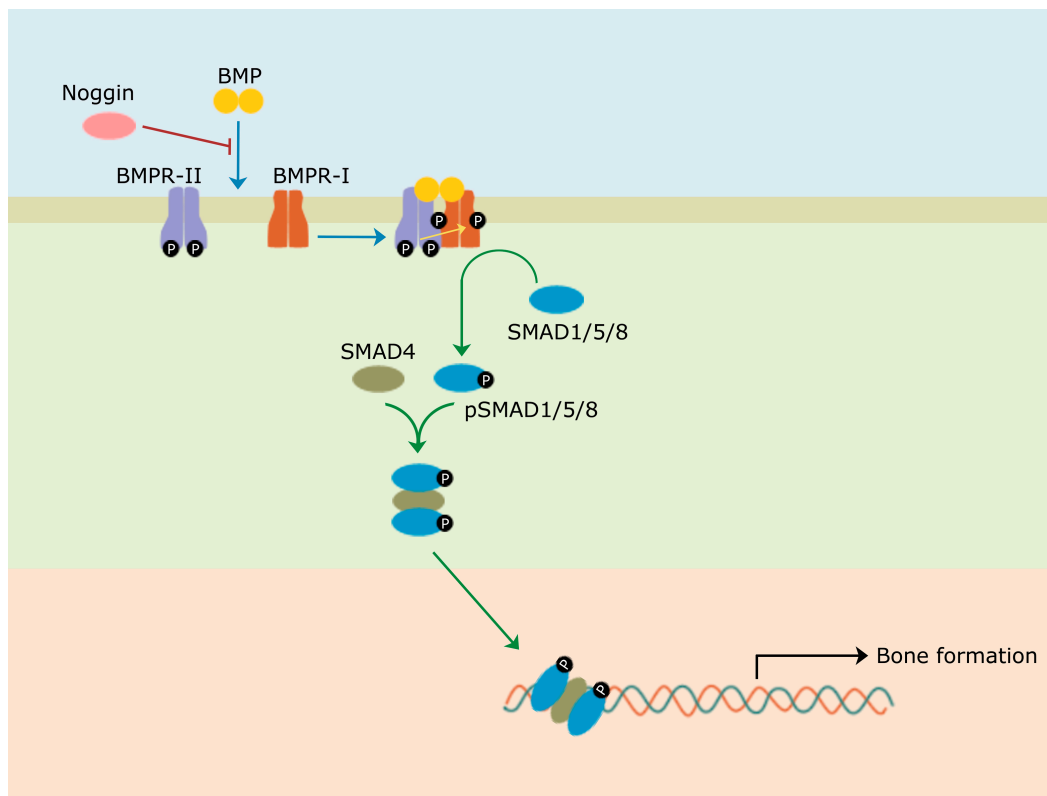
Figure 4.1 BMP-Noggin signalling pathway.

Figure 4.1 BMP-Noggin signalling pathway.

The constitutively active kinase domains of type II receptors phosphorylate type I receptors, and this in turn activates the SMAD signalling pathway through phosphorylation of receptor SMADs (SMAD1, SMAD5 and SMAD8). These associate with co-SMADs (SMAD4) to form a heteromeric complex that translocates to the nucleus and stimulates the expression of a wide range of target genes, including the gene encoding the process of bone formation. Many of the previously known inhibitors of BMP signalling (such as noggin) act upstream to sequester BMPs. *Adapted and modified from Anderson and Darshan (2008).*

4.1.1.2   Where is BMP expressed in relation to the TBI?

In the mandibular first molar in post-natal two day-old mice, Kim *et al.* (2007) have proposed a broad localization pattern of BMP4 expression in the soft tissue and hard tissue, specifically, the PDL- forming region, alveolar bone and tooth root-forming areas.

4.1.1.3   BMP role

BMPs have been proposed to have therapeutic potential for periodontal regeneration (Ripamonti *et al.*, 1994; Ripamonti *et al.*, 1996), and this potential is based on their powerful induction of osteogenesis and involvement in tooth root development (Thomadakis *et al.*, 1999; Yamashiro *et al.*, 2003). BMP-7 was reported to potently stimulate alveolar bone regeneration around teeth (Giannobile *et al.*, 1998), endosseous oral implants (Rutherford *et al.*, 1992), and in maxillary sinus floor augmentation procedures (van den Bergh *et al.*, 2000). Varying degrees of ankylosis have been observed with the use of BMPs for periodontal regeneration (Sigurdsson *et al.*, 1996).

Despite BMPs' remarkable and discriminatory features of *de novo* endochondral osteogenesis induction in ectopic sites (e.g., skin or muscle), BMP-7 did not perturb the mechanisms that regulate periodontal ligament width and maintained periodontal homeostasis, and so could not induce bone formation in PDL (Rajshankar *et al.*, 1998). However, BMP-2 has been shown to lead to mineralization of the PDL (Yamada *et al.*, 2007), and BMP-2 increased transient ankylosis in rats (King and Hughes, 1999), ankylosis being more apparent when combined with a lack of mechanical stress. In contrast, a recent study has shown that instead of inducing osteogenesis, application of BMP-2 to PDL cells may cause apoptosis (cell death), due to increased sensitivity of these cells to high levels of BMPs (Muthukuru, 2013). BMP-2, -6 and -7 have been shown to induce mineralization in human PDL stem cells (Hakki *et al.*, 2014), however

BMP-2 and -6 increased (ALP) activity but not mineralization in PDL cells (Khanna-Jain *et al.*, 2010). The link between BMPs and mineralization of periodontal ligament cells is therefore still unclear. In addition to their ability to induce new bone BMPs can also induce cementum in regenerating dental tissue *in vivo* (King *et al.*, 1998; Talwar *et al.*, 2001).

4.1.2   Brief introduction of Noggin signalling molecule

Noggin, a BMP ligand antagonist, initially identified in the Spemann organizer region of the *Xenopus* is known to modulate BMP activity, along with other proteins like chordin and follistatin. It is a secreted glycoprotein that binds to selected BMPs and blocks the binding of BMP-2, -4, and -7 to cell surface receptors. Noggin inhibits BMP-2–induced alkaline phosphatase activity in C2C12 cells *in vitro* and membranous ossification *in vivo* (Aspenberg *et al.*, 2001).

4.1.2.1   *Where is Noggin expressed?*

PDL-forming region cells express Noggin, indicating that expression of the BMP pathway in this tissue is necessary to inhibit osteogenic function. In the mandibular first molar in post-natal two day-old mice, Kim *et al.* (2007) detected strong Noggin immunostaining in the PDL-forming and bone-forming regions. Higher intensities of Noggin localization were found specifically in the lateral margins of the PDL-forming region, particularly next to the bone-forming area. The synchronization of that expression pattern with strong localization of PCNA-positive cells suggested that Noggin and cell proliferation were important for the maintenance of the TBI during postnatal development.

4.1.2.2   *Noggin role*

Unchecked BMP activity in the Noggin null mutant mice resulted in coarse and thickened bones, excess cartilage, and failure of the initiation of joint formation,

inferring an essential role of Noggin for proper skeletal development, and an inhibitory function in periosteal bone growth (Brunet *et al.*, 1998). The Noggin mice die at birth due to a number of skeletal defects.

BMPs and Noggin interactions have been reported to regulate tendon formation in earlier reports (Capdevila and Johnson, 1998; McMahon *et al.*, 1998; D'Souza and Patel, 1999; Schweitzer *et al.*, 2001). Others reported an important role for Noggin in ligament development (Jin *et al.*, 2003; Nakamura *et al.*, 2006). Holleville *et al.* (2003) reported another important role Noggin plays in the fusion of skull sutures. In titanium bone chambers, Noggin has been also shown to inhibit membranous ossification (Aspenberg *et al.*, 2001). In keeping with this, addition of Noggin to cultured murine mesenchymal stem cells significantly reduced osteoblast differentiation and bone nodule formation through inhibiting BMP-2 and 4 (Edgar *et al.*, 2007), while knockdown of Noggin using small interfering (si) RNA lead to enhanced osteogenesis in cultured C2C12 cells (Takayama *et al.*, 2009). In addition, Kim *et al.* (2007) indicated that Noggin together with higher cell proliferation inhibited mineralization of the PDL-forming region and prevented the fusion of the tooth root with surrounding alveolar bone. The addition of Noggin led to a widening of the TBI in postnatal stage mice. The addition of Noggin has also been shown to lead to an inhibition of cementogenesis (Jin *et al.*, 2004), indicating that endogenous BMPs are necessary for cementoblasts to effect mineral formation. BMPs therefore appear to contribute to normal function of mature cementoblast populations besides being a trigger for mesenchymal precursor cell differentiation into cementoblast or osteoblasts. Unpublished data mentioned by the same investigators, Jin *et al.* (2003), on upregulated Noggin activity in cultured PDL fibroblasts, suggested that Noggin might be the source of the PDL/tooth signal that prevents ankylosis and retains the PDL compartment.

Aims

- To investigate the impact of the bone on the tooth using isolation experiments.

- To examine the impact of the tooth epithelium on the pattern of osteoclasts and formation of the TBI.

- To study the effect of manipulating the BMP signalling pathway on the differentiation of cells in the TBI during tooth development.

A further understanding of the potential mechanical role of the alveolar bone and surrounding tissue on tooth development, combined with an understanding of the signals that lead to coordinated development of the tooth and bone will help us understand how defects, such as ankylosis, occur and can be avoided or treated more efficiently.

4.2   Materials and Methods

4.2.1   Isolation of M1 from surrounding tissues

For the comparison of isolated and encapsulated tooth germs, slices were divided into right and left, one side cultured as a whole slice, while the molar tooth germ was dissected out of the other side. The dissection was performed by means of a sharpened tungsten needle along the perifollicular layer described by Palmer and Lumsden (1987) and Cho and Garant (2000), which represents a line of weakness around the tooth and once it has been touched the epithelium naturally peels apart at that point. Both pieces (encapsulated and isolated tooth germ) were cultured on the same filter paper, so that the culture conditions would be as standard as possible.

4.2.1.1   Morphometric analysis of M1 cultures

To calculate the two-dimensional surface areas; an image of the explant was analysed using the computer software Fiji which employed ImageJ (version 1.46j), an open source Java based image processing program.
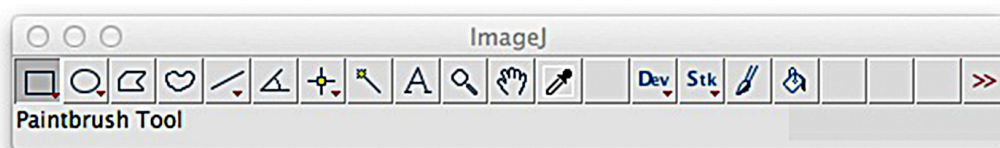
Figure 4.2 Toolbar of ImageJ program.

The area around the epithelial and mesenchymal portions of the first molar tooth germ in the slice culture was selected using the polygon tool in the ImageJ program and the selected area was converted from pixels to mm^2 using the scale

tool. The two dimensional surface area was recorded at different time intervals, t=0…x. These surface areas were then used to calculate ratio of growth in surface area at different time intervals, like the Spooner ratio which calculates salivary gland epithelial branching (Spooner *et al.*, 1989). The calculated ratios of treated and untreated explants from the same embryo were compared using the student t-test or ANOVA tests with a 95% confidence level.

All data was entered into Microsoft Excel 2011 spreadsheets. Statistical testing and construction of charts was performed in Graphpad Prism 5. All experiments were repeated 2-3 times and the mean ± standard deviation (SD) statistics were recorded.

Numbers for morphometric analysis: N= 20 encapsulated and N= 20 isolated tooth germs at three time points (2, 3 and 6 days in culture).

4.2.2   BrdU whole mount antibody staining

Bromodeoxyuridine (BrdU) uses nucleotide substitution to replace thymidine with uridine in the DNA structure of dividing cells both *in vitro* and *in vivo* (Gage, 2000). BrdU has been utilised in a number of *in vitro* and *in vivo* studies to label a variety of cellular sources, from human olfactory epithelium (Hahn *et al.*, 2005) and neural progenitors (Nieoullon *et al.*, 2005) to neural stem cells (Chu *et al.*, 2004).

A final concentration of 30 uM BrdU in medium was made by putting 1 ul BrdU from a frozen stock of 30 mM into 1 ml of medium. The molar slice cultures were incubated in BrdU medium for two hours at 37 °C in the incubator. After the first hour, the grid that was carrying the sample in the culture dish was removed so the filter holding the sample could drop to the base of the dish. Incubation was continued in this way during the second hour. After culture, the tissue was fixed in 4% PFA PBS for 2 - 3 hours at RT or ON at 4ºC with

shaking. After fixation samples could be stored for up to 2 weeks in PBS at 4°C if needed.

The BrdU protocol takes 3 days. Day 1 commenced with tissue permeabilization in PBSTr 0.5% (Triton 0.5% in PBS) 3x 30 minutes. Samples were shaken while being permeabilized. This was followed by sample incubation in Trypsin 1x in PBS on ice without shaking. Trypsin 1x is trypsin 0.25% in PBS (Gibco 15090-046-Invitrogen). The tissue was following washed by first rinsing in PBS then washing for 2x 10 minutes in PBS on ice. Tissues were denatured in the fume hood then by incubation in HCl 4M for 15 minutes without shaking. The tissue was then washed by first rinsing in PBSTr 0.5% and later washing for 3x 15 minutes in PBSTr 0.5% with shaking. Blocking in IB solution for 1-2 hours at RT followed (IB (immuno block): 10% goat serum, 1% DMSO, 0.5% Triton, in PBS). The tissue was placed in an IB solution to which a primary antibody had been added and left at 4°C ON with shaking (the primary antibody was BrdU anti rat 1:500 (Abcam)).

Day 2 began by first rinsing in PBSTr 0.5% then washing for 6x 30 minutes in PBSTr 0.5% with shaking. The secondary antibody was applied next, together with DAPI in PBSTr 0.5% and BSA 1% ON at 4°C with shaking, secondary antibody (1:500), DAPI (1:1000).

Numerous washes took place on day 3, first by rinsing in PBSTr 0.5% then washing for 6x 30 minutes in PBSTr 0.5% with shaking. Eventually, the tissues were put in PBS for 5 minutes.

4.2.2.1 *Confocal imaging and analysis*

Samples were then flattened and mounted with Vectashield® with DAPI mounting media for fluorescence. The samples were examined using a Leica SP5 laser scanning confocal microscope to take optical section images through the cultures.

4.2.3   Separation of epithelium and mesenchyme

Dispase (Gibco®) was employed for enzymatic separation of the epithelium and mesenchyme. For each separation task, a fresh digestion buffer of Dispase was prepared with 2U Dispase/ml in Dulbecco's Phosphate Buffered Saline (modified, without calcium chloride and magnesium chloride (Sigma®)). The dispase solution was sterile-filtered through a 0.22um filter (Merck Millipore®) (Millipore or equivalent).

The process began with brief rinsing of the tissue slices containing the first molar tooth germ explants in PBS to free them from any Ca^{2+} and Mg^{2+} present in the culture medium solution. The slices of tissues were then transferred to the freshly prepared Dispase solution. Tissue was incubated in the dispase at 37°C for 10 to 15 minutes. Digestion was considered complete when the epithelium began to show signs of wrinkles and was easily removable from the mesenchyme. At this stage, the tissue slices were transferred back to the culture medium to stop further digestion.

Epithelial and mesenchymal tissues were then microsurgically separated using Tungsten needles (in previously described culture medium) under a stereomicroscope (Vainio *et al.*, 1989). Explants were cultured in the previously described conditions with and without epithelium for 24 hours.

Numbers for separation of epithelium and mesenchyme slice culture: N= 6 control (with epithelium) and N= 8 experimental (without epithelium).

4.2.3.1   *Whole-placode culture analysis*

In whole-placode cultured samples, the epithelium was separated by means of dispase and control as well as minus epithelium placodes were cultured for 3

days. After culture, explants were fixed, embedded, sectioned, and stained for histology and Tartrate-Resistant Acid Phosphatase (TRAP) cell detection.

Numbers for separation of epithelium and mesenchyme whole-placode culture: N= 9 control (with epithelium) and N= 10 experimental (without epithelium).

4.2.4   Recombinant proteins and bead implantation assays

The effect of certain recombinant proteins on the development of the tooth-bone-interface (TBI) was tested on tissue slices containing first molar tooth germs. Some proteins believed to affect the epithelial-mesenchymal signalling process were added through coated beads directly placed at the region of interest, next to the tooth-bone interface. The bead process was utilized to produce a more localized effect compared to the dissolution process. The proteins and concentrations used for the process are given below.

4.2.4.1   *Addition of proteins to the tissue slices with beads*

Two proteins were used in the bead application process: Recombinant Mouse Bone Morphogenetic Protein 4 (BMP-4) and Noggin.

The type and preparation of the beads depends on the loaded molecules. Affi-Gel blue agarose beads (100-200 mesh, 75-150 µm diameter; Bio-Rad, Inc.) composed of cross-linked agarose mesh with covalently attached Ci- bacrome blue F3GA dye were used. Agarose beads had previously been used as carriers of peptides and as a source of slowly released growth factors (Schreiber *et al.*, 1986; Hayek *et al.*, 1987; Hayamizu *et al.*, 1991). Agarose Beads were washed once with PBS, pelleted and were manually counted under a stereomicroscope (100 beads/tube). Recombinant BMP-4 (R&D System®) was diluted in sterile PBS containing 1% Bovine serum albumin (BSA) and stored in a stock concentration 100 µg/ml (for BMP it is important to use siliconised tubes). Recombinant Noggin was diluted in sterile PBS containing 1% BSA and stored in a stock

concentration 100 µg/ml. Dried beads were then picked up on a needle and added to the recombinant protein dilute. The beads within the recombinant protein were then incubated at 37°C for 30 minutes.

The beads which were not treated immediately were stored at 4°C until used. Prolonged storage of the beads (up to 3 weeks) leads to some loss of the activity of BMP. Before use, loaded beads were rapidly washed in PBS and transferred individually in a small drop held between the curved tips of a watchmaker's forceps to be placed directly at the tooth-bone interface on the freshly chopped tissue slices and then cultured for 5 days. Control beads were treated identically using the same concentrations of bovine serum albumin (BSA, 1 µg/µl; Sigma[®]) in PBS.

Numbers for BMP signalling culture: N= 8 control (BSA), N = 11 BMP-4 and N = 13 Noggin beads.

4.3   Results

4.3.1   Effect of surrounding tissues on tooth size: isolated cultures (surface area, volume, proliferation)

4.3.1.1   Isolated M1s develop well

As the tooth germ develops, surrounded by a hard case of bone, the size of the tooth might be restricted by the presence of this hard tissue. To understand the impact of the surrounding tissues and alveolar bone on tooth development, tooth germs were cultured in isolation or within the surrounding tissue and bone.

In order to check first whether the mandibular first molar (M1) tooth germ can grow in isolation of all surrounding tissues, we used our slice method as before and then removed the first mandibular molar (M1) from its surrounding tissues (including the developing alveolar bone) at E14.5. Isolated tooth germs were then cultured over a period of seven days. The isolated first molar tooth germs developed well with the cap-staged tooth germ successfully reaching the expected late bell stage as depicted in Figure 4.3.

Having established that the tooth germs could develop when isolated, we then cultured tooth germs from one side of a slice in isolation while the tooth germs from the contralateral side were left intact (Figure 4.4, A and B). Using this method, tooth germs isolated from the surrounding tissue appeared to grow much larger than their reciprocal tooth germs surrounded by jaw tissue (Figure 4.4 I and J). When the increase in surface area of the tooth germs was calculated, the larger size of the isolated tooth germs was shown to be highly statistically significant (Figure 4.5).

To rule out the possibility that the isolated tooth germs simply being flattened during culture, encapsulated and isolated explants were fixed after culture and

their volume calculated on a confocal microscope (Alfaqeeh *et al.*, 2013). After two days in culture, the isolated tooth germs were already larger than the encapsulated tooth germs, this difference increasing after three days in culture (data not shown). The volume analysis was carried out in collaboration with a colleague for inclusion in the paper.

The surface area and the volume measurement both show that the isolated mandibular first molar (M1) tooth germ develops to a greater extent than the encapsulated.
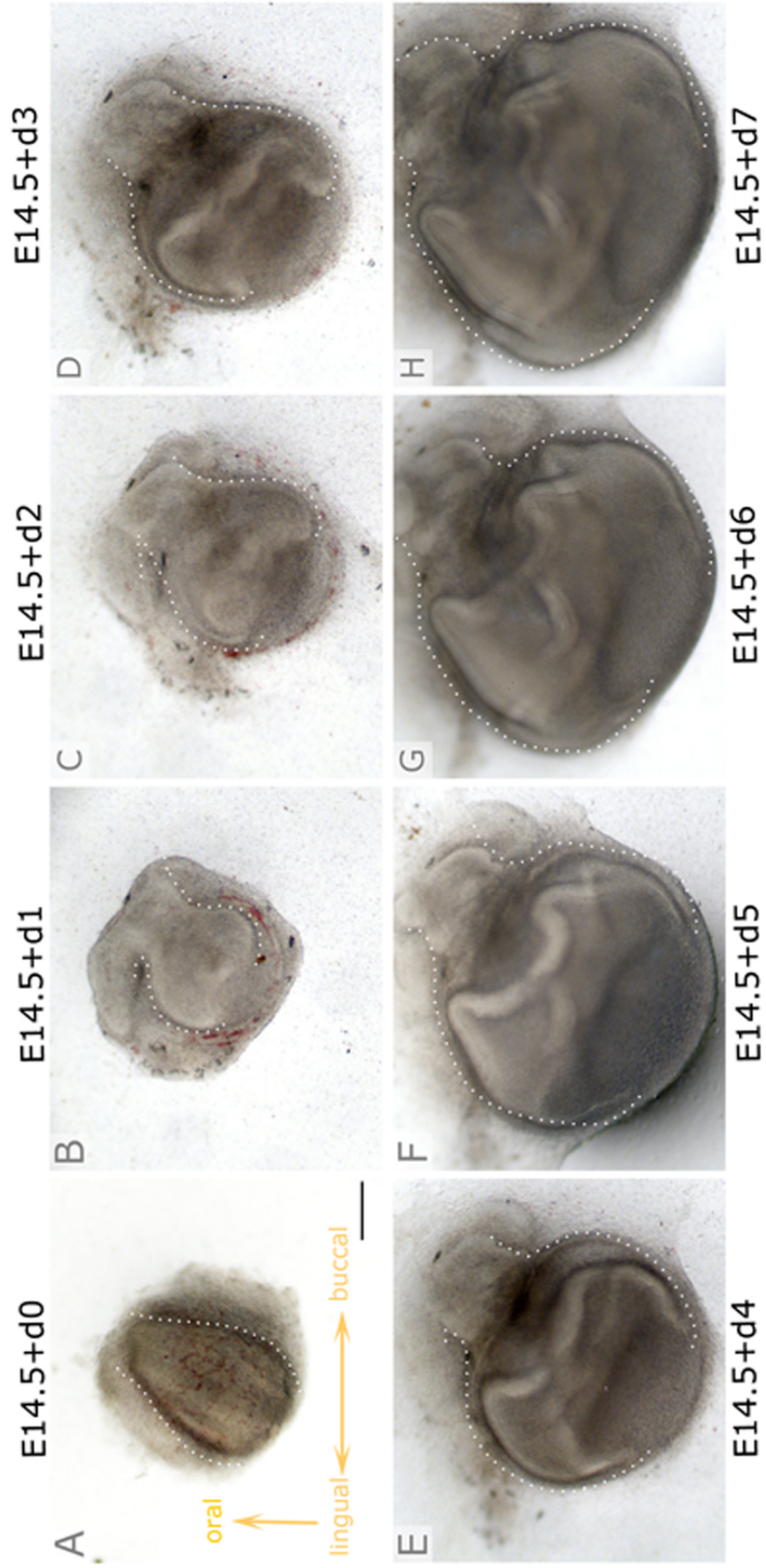
Figure 4.3 Following mandibular first molar (M1) development in isolation from the effect of the surrounding tissue.

94

Figure 4.3 Following mandibular first molar (M1) development in isolation from the effect of the surrounding tissue.

E14.5, a cap-stage, mandibular first molar tooth germ development after being dissected out from any surrounding tissue over 7 days in explant culture. Day 0 (**A**), day 1 (**B**), day 2 (**C**), day 3 (**D**), day 4 (**E**), day 5 (**F**), day 6 (**G**), and day 7 (**H**). White dots outline the epithelium outer border. Scale bar in **A** = 200 μm (same scale in **B**, **C**, **D**, **E**, **F**, **G**, and **H**).
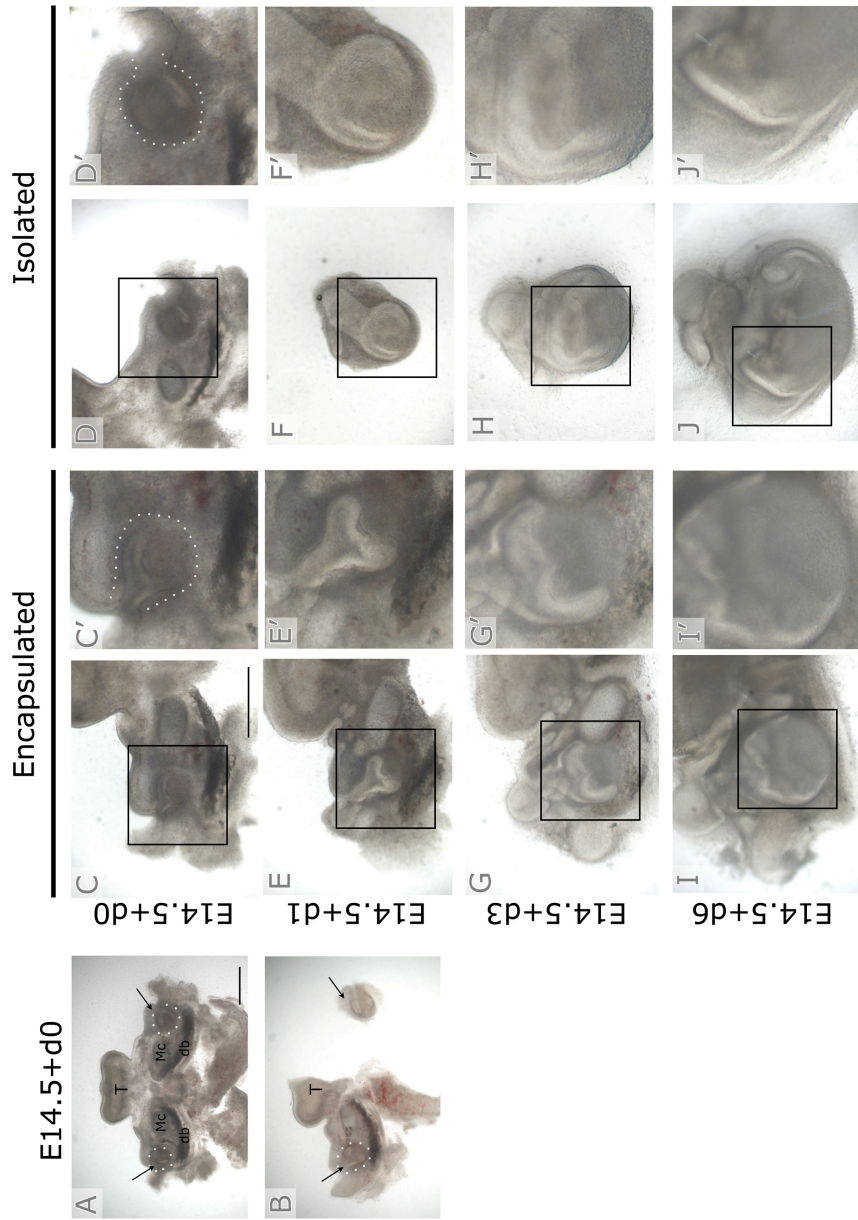
Figure 4.4 Increased size of isolated mandibular first molar (M1) germs in slice culture.

Figure 4.4 Increased size of isolated mandibular first molar (M1) germs in slice culture.

(**A** and **B**) E14.5 tooth slices day 0. (**A**) Intact representative slice. (**B**) Similar slice after isolation of the molar tooth germ on one side. Arrows indicate molar tooth germs, outlined by white dots. T = tongue, Mc = Meckel's cartilage, and db = dentary bone. (**C-J**) Cultured tooth germs in slice culture. (**C** and **D**) E14.5 tooth slices, day 0. The tooth germ (dotted line in **C'**) was left intact, while the tooth germ in **D** was dissected out of the surrounding tissue (along dotted lines in **D'**). (**E** and **F**) C and D slices after 1 day in culture. (**G** and **H**) C and D slices after 3 days in culture. (**I** and **J**) C and D slices after 6 days in culture. (**C'-J'**) High-power view of boxed regions in **C-J**. Scale bar in **A** = 500 μm (same scale in **B**). Scale bar in **C** = 500 μm (same scale in **C'**, **D**, **D'**, **E**, **E'**, **F**, **F'**, **G**, **G'**, **H**, **H'**, **I**, **I'**, **J**, and **J'**).

A

E14.5+ld   E14.5+h0

Surface area-ratio = Surface area/Surface area
h0 = hour 0
ld = last day

B

E14.5+6.75d
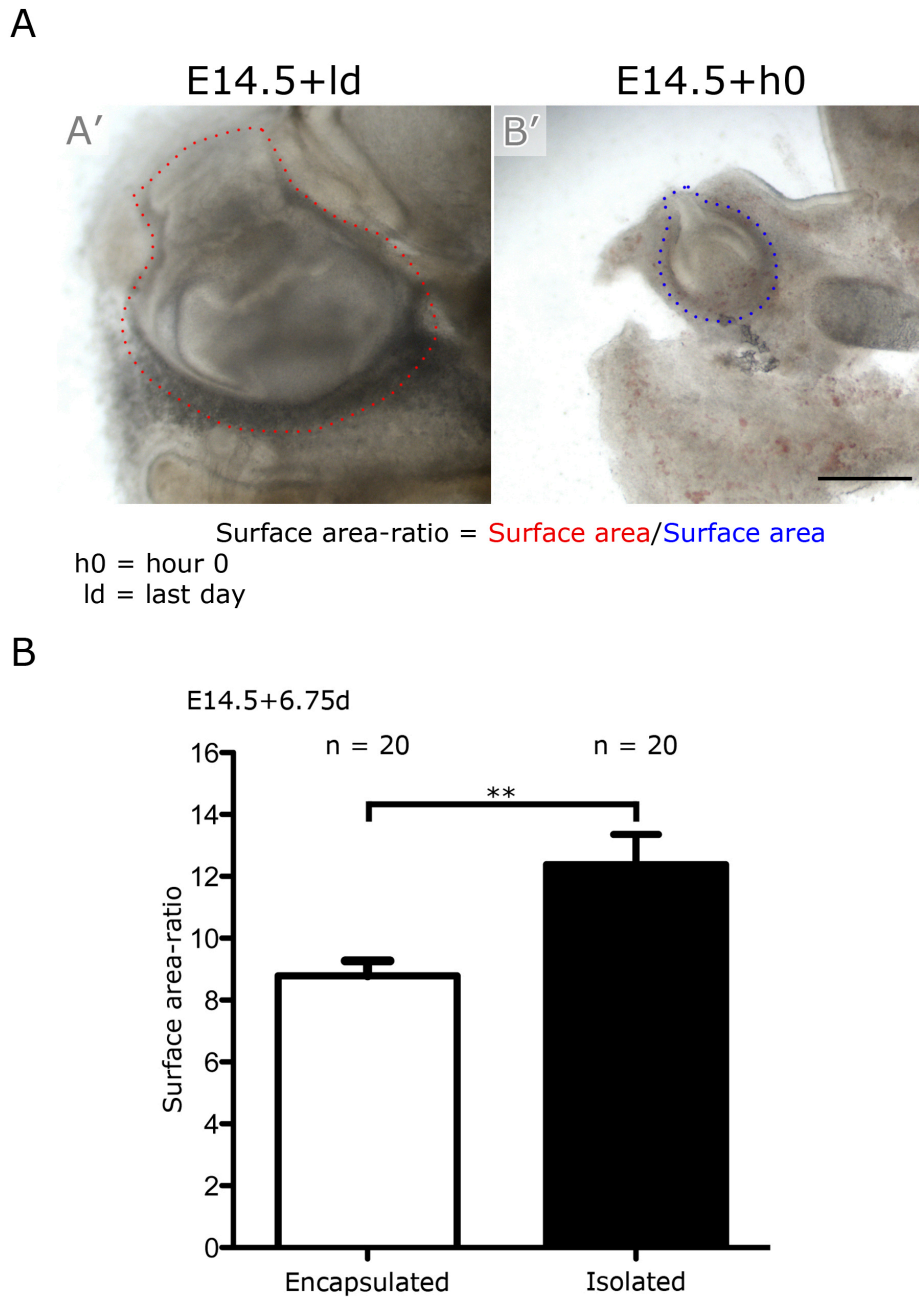
Figure 4.5 Morphometric analysis of the mandibular first molar (M1).

(**A**) Demonstrates how the two-dimensional surface areas of an E14.5 mandibular first molar (M1) at the start and end of the culturing process were used to calculate the ratio of the growth in surface area. (**B**) The graph shows a statistically significant difference in surface area ratio between tooth germs cultured with or without the surrounding tissue after ≈ 6 days in culture. Paired student's t-test. Scale bar in **B'** = 300 μm (same scale in **A'**).

4.3.1.2   Enhanced proliferation in isolated M1

To assess whether the size difference was due to enhanced proliferation in isolated tooth germs, we cultured the tissue prior to fixation in BrdU and then identified the proliferating cells in whole-mount. We aspired to count the number of BrdU-positively stained cells, cells proliferating in a common region, the cervical loop, (Figure 4.6, B). In each case, we aimed to calculate the mitotic index ratio by dividing the number of proliferating cells over the total number of cells, as identified by DAPI. This turned out to be problematic, most probably due to penetration problems as the BrdU could not reach all the proliferating cells, and was concentrated at the periphery of the culture. In addition, the DAPI did not stain the nucleus of every cell, indicating that the post-fixation treatment of the tooth germs might have disrupted the nucleus. The arrow in Figure 4.6, B exemplifies a cell in which both the nucleus and dividing DNA were stained while the arrowhead shows a BrdU-positively stained cell in which the nucleus was not stained by the DAPI.

Having a definite penetration problem with the BrdU administered in culture, we changed to the phosphohistone H3. Again this was carried out in collaboration with a colleague for the paper (Alfaqeeh *et al.*, 2013). After two days of culture, the mitotic index (calculated by counting the number of phosphohistone H3 positive cells versus total cell number) was significantly increased in the isolated tooth germs compared to the encapsulated contralateral side. In contrast, after three days of culture this difference was no longer evident, indicating that the increase in proliferation occurred during a limited time-window (data not shown).

The presence of surrounding tissue therefore appears to restrict the growth of developing tooth germs.
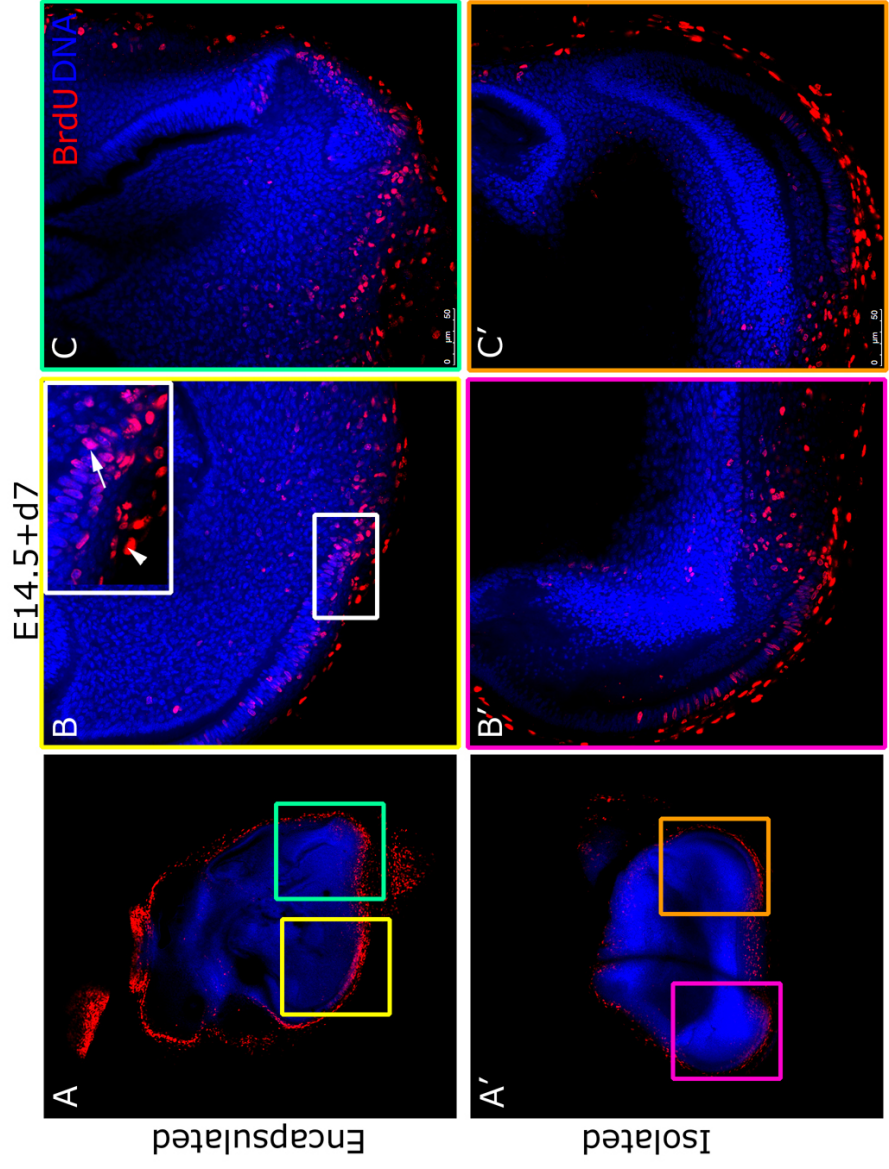
Figure 4.6 Encapsulated and isolated mandibular first molar (M1) proliferation assay using BrdU staining.

100

Figure 4.6 Encapsulated and isolated mandibular first molar (M1) proliferation assay using BrdU staining.

(**A** and **A'**) Confocal images of E14.5 7-day culture encapsulated and isolated mandibular first molar (M1) tooth germs, respectively, incubated with BrdU antibody to observe the DNA synthesis in a whole mount fashion. (**B** and **C**) High-power view of boxed regions in **A**, yellow and green respectively. (**B'** and **C'**) High-power view of boxed regions in **A'**, pink and orange respectively. The cervical loop region, the area chosen for studying the proliferation is white-boxed in **B** and a high power view of the same area is shown on the same image, **B**. BrdU positive cells are stained in red, nuclei with DAPI in blue; the arrow shows a BrdU and a DAPI-stained cell while the arrowhead shows only a BrdU stained cell in which the DAPI could not stain the nucleus.

4.3.2   Effect of epithelium on TBI and arrangement of TRAP +ve cell

To investigate how signals from the tooth might influence the surrounding tissues and in particular the arrangement of osteoclasts, we took away the epithelium of the tooth and looked at what happened to the surrounding tissues and the TBI.

In E14.5 mandibular first molar (M1) one-day slice culture TRAP staining revealed positive cells on the bone side of the tooth-bone interface area, while the TBI itself was TRAP-negative as expected (Figure 4.7, D). The aforementioned cells were arranged to take the form of a ring enclosing the bone-free zone adjacent to the dental follicle.

4.3.2.1   TRAP +ve cells maintain the same arrangement pattern after the epithelium is removed

The epithelium of the tooth was removed using dispase, and the slices then cultured. Initially, the slices were cultured just for one day. Interestingly, a comparable arrangement of TRAP positive cells was observed, with a negative TRAP region between the remaining mesenchymal tissues of the tooth and the developing bone (Figure 4.7, D'). Therefore, the pattern of the TRAP positive cells stayed equivalent in the tooth-bone interface region of the mandibular first molar (M1) when cultured in slice for one day with or without the epithelium. We wanted to investigate whether this pattern would change after longer culture but the dispase treated slices started to disintegrate after a longer culture period. We therefore adapted our culture method to use whole dental placodes instead of slices. These cultures were much more healthy over long-term culture compared to the slices.
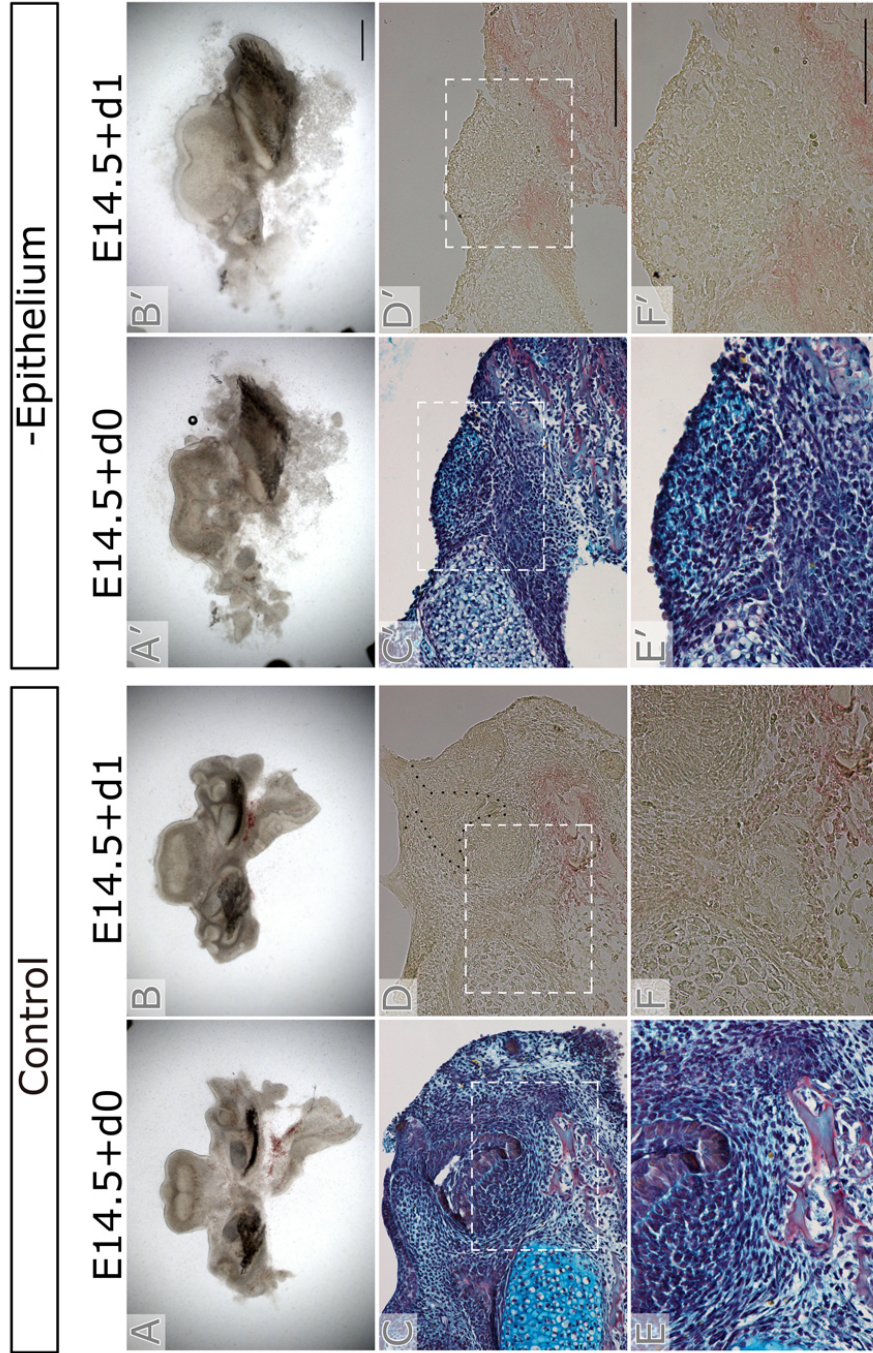
Figure 4.7 Mandibular first molar (M1) slice culture with epithelium (control) and without epithelium (mesenchyme only) (experimental).

103

Figure 4.7 Mandibular first molar (M1) slice culture with epithelium (control) and without epithelium (mesenchyme only) (experimental).

E14.5 mandibular first molar (M1) slice plus/minus epithelium one-day culture. (**A** and **A'**) Zero-day plus/minus epithelium, respectively. (**B** and **B'**) **A** and **A'**, respectively, after one day in culture. (**C** and **C'**) Histological sections of B and B', respectively, after Trichrome staining. (**D** and **D'**) Alternate sections of **C** and **C'**, respectively, after TRAP-staining. (**E**, **F**, **E'**, and **F'**) High-power views of dash-boxed areas in **C**, **D**, **C'**, and **D'** respectively. The pattern of the mandibular first molar (M1) TRAP positive cells in the tooth-bone interface region stays the same and is unaffected by the removal of the epithelium as seen in **D** and **D'**, plus and minus the epithelium, respectively; red stained ring observed at a distance environing the dental mesenchyme. Dotted line in **D** outlines the epithelium. Scale bar in **B'** = 500 μm (same scale in **A**, **B**, and **A'**). Scale bar in **D'** = 200 μm (same scale in **C**, **D**, and **C'**). Scale bar in **F'** = 100 μm (same scale in **E**, **F**, and **E'**).

After three days in culture, the E14.5 mandibular first molar (M1) tooth germ was visible adjacent to the bone (Figure 4.8, A, and C). TRAP positive cells were visible in an arc around the tooth and TBI (Figure 4.8, B and D), while the TBI and tooth were negative, agreeing with the previous findings (Figure 4.7, D). The dotted line in the figure outlines the tooth and highlights the TRAP negative zone that is surrounded by the TRAP positive cells.

TRAP staining of the tooth-bone interface area of E14.5 mandibular first molar (M1) placode cultured without the epithelium for three-days displayed the TRAP positive cells to be again arranged in a sort of arc surrounding a TRAP negative domain (Figure 4.8, D' and F'), agreeing again with the previous findings from the one day cultures (Figure 4.7, D'). In keeping with the location of the presumptive osteoclasts, the bone did not invade the space where the TBI and dental mesenchyme were located (Figure 4.8, C' and E').

The removal of the epithelium therefore does not affect the arrangement of TRAP positive cells along the tooth-bone interface region of the mandibular first molar (M1), and bone does not encroach into the TBI.
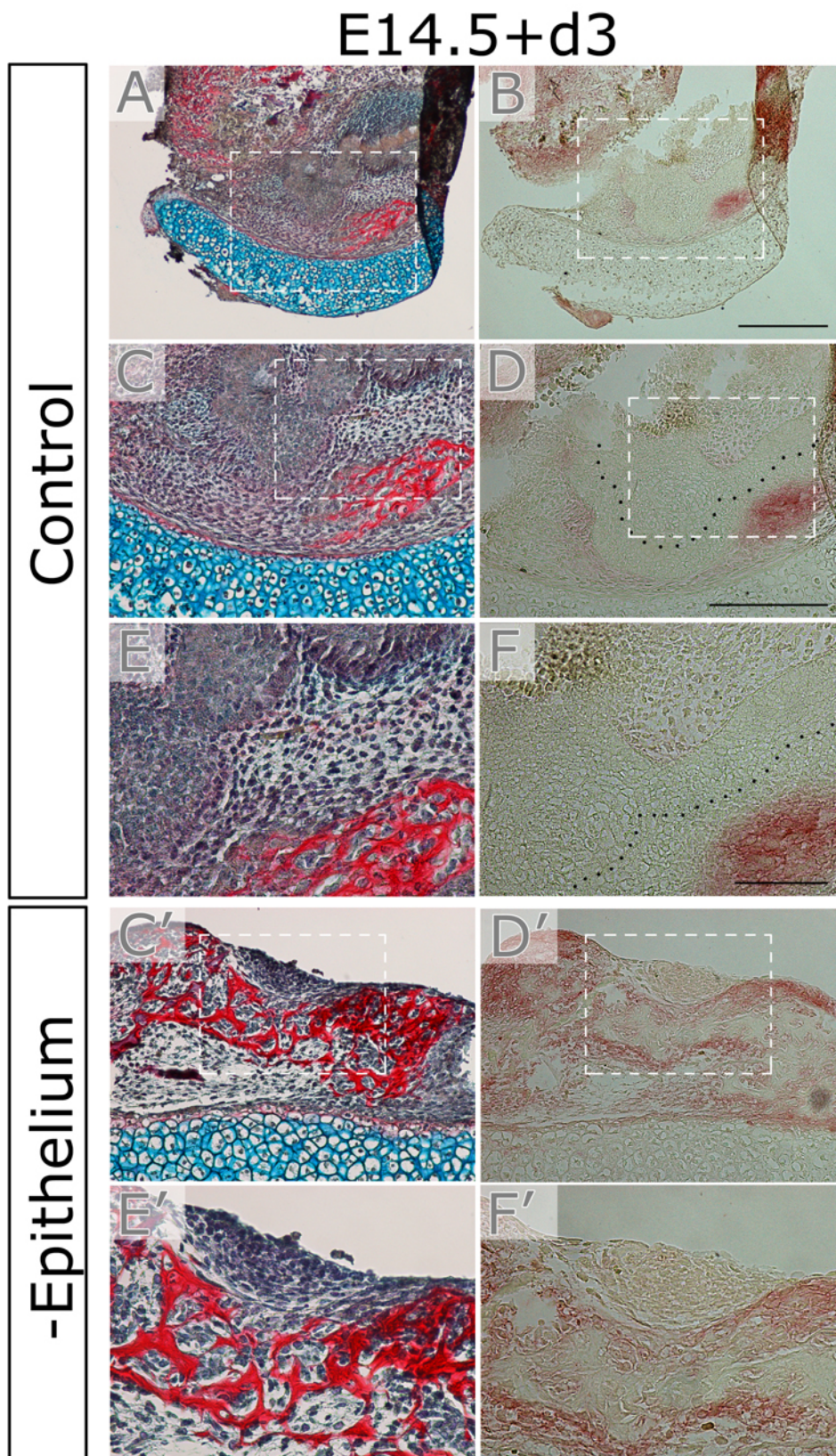
Figure 4.8 Mandibular first molar (M1) placode with epithelium (control) and without epithelium (mesenchyme only) (experimental).

Figure 4.8 Mandibular first molar (M1) placode with epithelium (control) and without epithelium (mesenchyme only) (experimental).

E14.5 mandibular first molar (M1) plus/minus epithelium placode three day culture. (**A**) Three-day control mandibular first molar placode histological section after Trichrome staining. (**B**) Alternate section of **A** after TRAP staining. (**C** and **D**) High-power view of boxed regions in **A** and **B**. (**D**) From top to bottom, the epithelium, the mesenchyme, the TRAP-negative cells zone, and finally the TRAP positive cells in a sort of arc shape. The dotted line separates the mesenchyme from the TRAP positive cell-free zone. (**C'** and **D'**) Comparable views of **C** and **D** but of experimental mandibular first molar placode. (**D'**) Similar pattern of TRAP positive cells arrangement to that seen in **D**. (**E**, **F**, **E'**, and **F'**) High-power view of boxed regions in **C**, **D**, **C'**, and **D'**, respectively. Scale bar in **B** = 300 μm (same scale in **A**). Scale bar in **D** = 200 μm (same scale in **C**, **C'**, and **D'**). Scale bar in **F** = 100 μm (same scale in **E**, **E'**, and **F'**).

4.3.3   Role of BMPs and Noggin in maintaining a bone free gap

As mentioned in the introduction, BMP signalling has an important role in regulating bone. To investigate the effect of altering BMP signalling on the development of the tooth-bone interface during embryonic development, we started with the local application of BMP-coated agarose beads to E14.5 mandibular first molar (M1) slice culture. At this stage the first signs of bone deposition are observed. Beads were placed within the emerging TBI and slices were cultured for 5 days to see the impact on this region (Figure 4.9 A, B, A', and B'). BMP-4 was used in our studies as it is known to be strongly expressed by the mesenchyme of the developing tooth (Aberg *et al.*, 1997; Kim *et al.*, 2007) and has previously been shown to be more potent than BMP-2 at stimulating osteoprogenitor cells in culture (Hughes *et al.*, 1995).

4.3.3.1   Manipulation of the BMP signalling alters osteogenesis

After five days of culture, the histological section, using a Trichrome stain, showed bone close to the tooth next to the BMP-4 bead and a resultant smaller tooth-bone interface (Figure 4.9, D') and (Figure 4.10, E and F), when compared to control slices with control BSA (Bovine Serum Albumin) beads (Figure 4.9, D) and (Figure 4.10, A-D). In some cases the TBI was completely lost and the ectopic bone started to encroach on the dental mesenchyme (Figure 4.10, E and F). The BMP-4 therefore, as predicted, led to an increase of bone in areas normally devoid of bone.

We then went to look at the effect of inhibiting the BMP signalling pathway by the use of Noggin loaded beads similarly placed in explants cultured for five days.

The local application of Noggin-coated agarose beads to E14.5 mandibular first molar (M1) slice culture had the opposite effect to that of the BMP beads on the

tooth-bone interface, with less bone close to the tooth immediately around the bead and locally a larger tooth-bone interface (Figure 4.10, I and J), when compared to control beads (Figure 4.10, A-D). These results therefore agree with the findings on the addition of Noggin in postnatal cultures (Kim *et al.*, 2007).

Chapter 4: Results 2
The mutual relationship between the developing tooth and bone: impact of
mechanical forces and signalling pathways
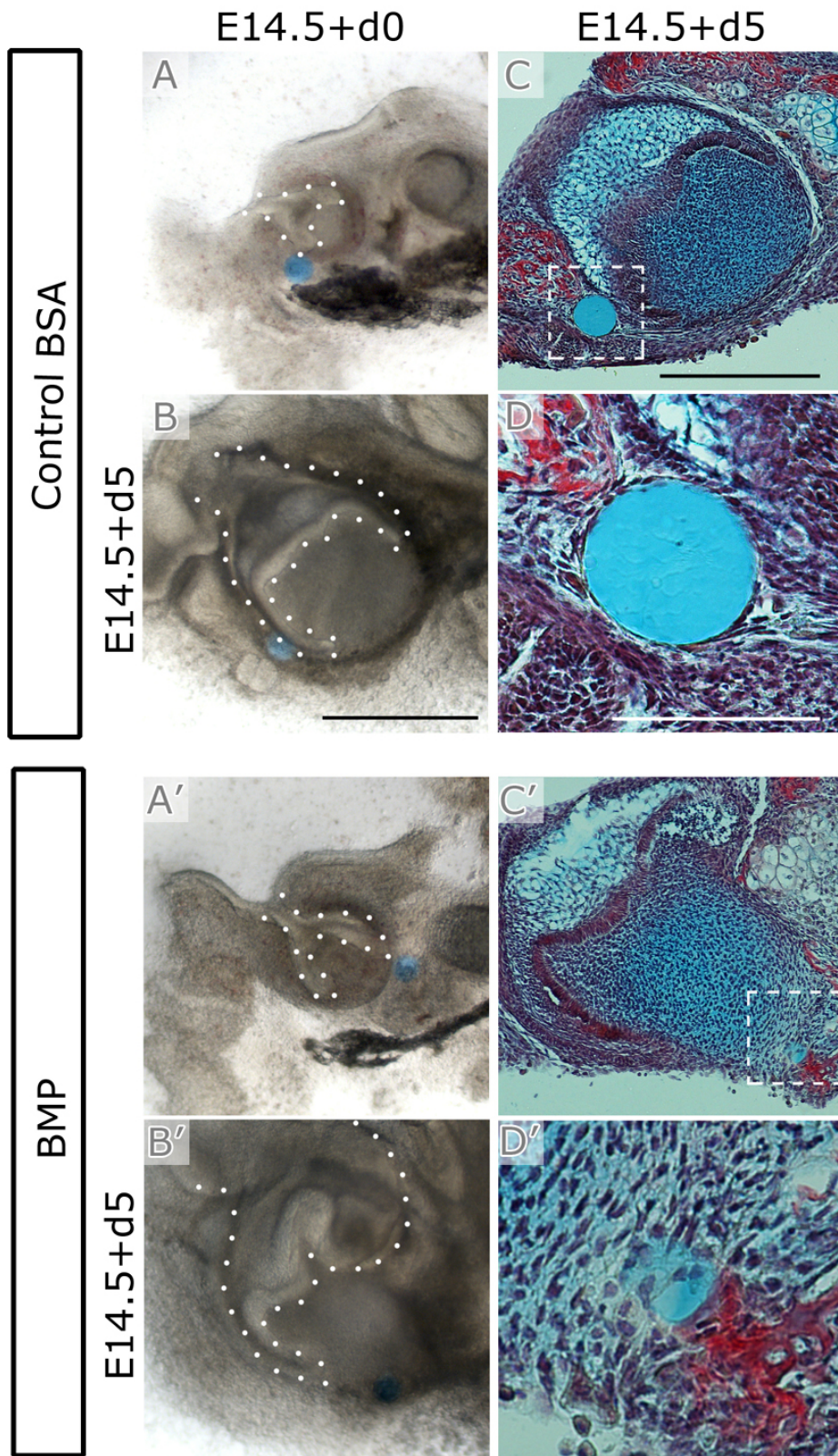
Figure 4.9 Local application of BMP to the developing tooth-bone interface (TBI) of E14.5 mandibular first molar (M1) in slice culture.

Figure 4.9 Local application of BMP to the developing tooth-bone interface (TBI) of E14.5 mandibular first molar (M1) in slice culture.

(**A**) Zero-day control culture. (**A'**) Zero-day BMP treated culture. (**B**) Five-day control culture. (**B'**) Five-day BMP treated culture. (**C**) Morphology after Trichrome staining of five-day control culture. (**C'**) Morphology after Trichrome staining of five-day BMP treated culture, enhanced formation of bone with a resultant smaller tooth-bone interface was seen. (**D** and **D'**) High-power view of areas dash-boxed in **C** and **C'** respectively. The agarose bead soaked in 100 µg/ml BMP-4 recombinant mouse protein. The control bead soaked in 1 µg/ml BSA, bovine saline albumin. The dotted line outlines tooth epithelium. Scale bar in **B** = 100 µm (same scale in **A**, **A'**, and **B'**). Scale bar in **C** = 300 µm (same scale in **C'**). Scale bar in **D** = 100 µm (same scale in **D'**).

Figure 4.10 Histological sections after local application of BMP and Noggin to the developing tooth–bone interface in the mandibular first molar (M1) slice culture.
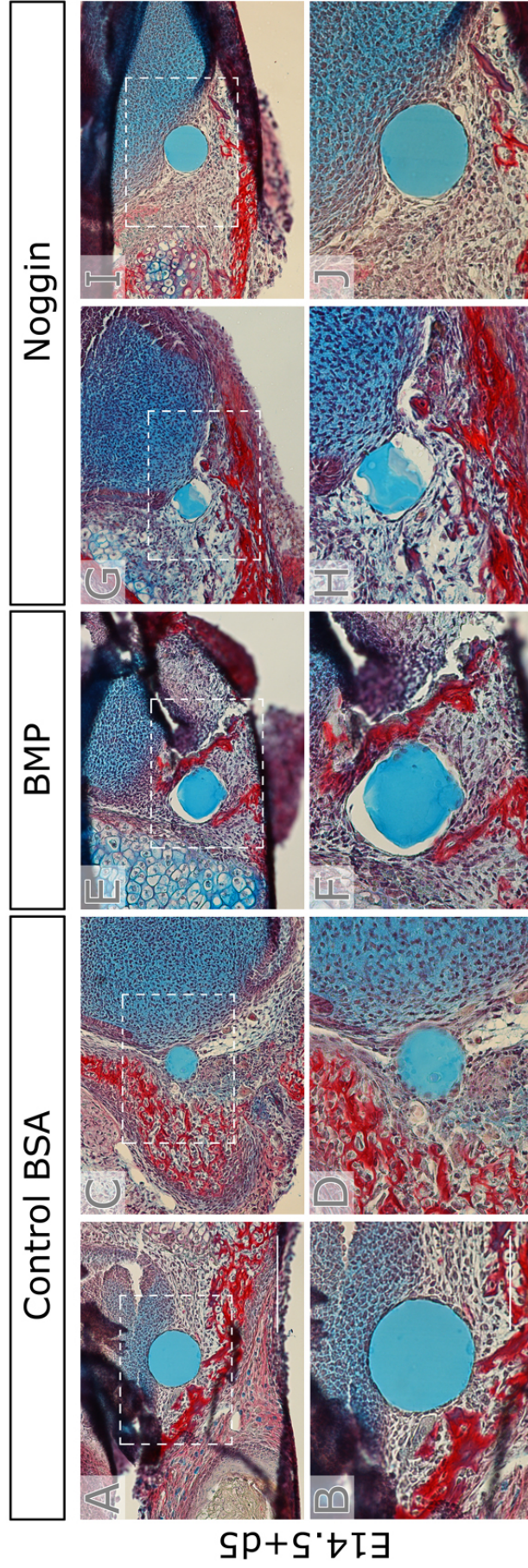
E14.5+d5

Figure 4.10 Histological sections after local application of BMP and Noggin to the developing tooth-bone interface in the mandibular first molar (M1) slice culture.

(**A** and **C**) Morphology after Trichrome staining of E14.5 five-day control culture. Bone lines the bone-free tooth-bone interface. (**E**) Morphology after Trichrome staining of E14.5 five-day BMP treated culture. Enhanced formation of bone with a resultant smaller tooth-bone interface. (**G** and **I**) Morphology after Trichrome staining of E14.5 five-day Noggin treated culture. Reduced formation of bone with a resultant larger tooth-bone interface. (**B**, **D**, **F**, **H**, and **J**) High-power view of areas dash-boxed in **A**, **C**, **E**, **G**, and **I** respectively. Agarose beads soaked in 100 µg/ml BMP-4 recombinant mouse protein and 100 µg/ml Noggin recombinant mouse protein. The control bead soaked in 1 µg/ml BSA, bovine saline albumin. Scale bar in **A** = 200 µm (same scale in **C**, **E**, **G**, and **I**). Scale bar in **B** = 100 µm (same scale in **D**, **F**, **H**, and **J**).

4.4   Discussion

This chapter revealed a number of unexpected findings. Isolation of the mandibular first molar (M1) tooth germ from the surrounding mesenchyme and alveolar bone led to an expansion of the tooth germ, therefore, the presence of the surrounding tissue appeared to restrict the growth of developing tooth germs. Such a mechanical role for the bone in shaping the tooth has not been previously shown. Interestingly, removal of the tooth epithelium in culture experiments did not affect the normal layout of osteoclasts, suggesting that this pattern is not controlled by the tooth, however further experiments are necessary to confirm this. Following local application of BMP-4 and Noggin on agarose coated beads in culture, a change in fate of the TBI was observed. We observed a local reduction in the TBI near to the BMP-4 bead with enhanced bone formation. In contrast, we observed a local widening in the TBI when Noggin beads were implanted with a loss of bone. Although these experiments agree with previous thoughts on the role of BMPs in bone formation, our methods allow this process to be visualised as the TBI develops.

Isolation of the mandibular first molar (M1) from the surrounding mesenchyme and alveolar bone led to an expansion of the tooth germ. This was shown in collaboration with a colleague to be due to increased proliferation in both the epithelium and mesenchyme in the isolated tooth germs. These isolation experiments indicate that the growth of the tooth germ is constrained by the surrounding tissues. This may represent a physical restriction by the enveloping alveolar bone, or equally it may indicate the presence of inhibitory signalling molecules in the surrounding tissue. It may be possible to work out which mechanism is in action by inhibiting bone formation in such cultures, without the physical removal of the surrounding tissue. That the environment constrains the tooth and controls its growth rate suggests that *in vivo* the size of the tooth is not determined at early stages. The size of the tooth therefore may be shaped by the size of the bony socket into which it forms. In primates, the tooth and jaw appear

ontogenetically and functionally coordinated by regional variations in corpus growth, which creates a space for the molars to grow (Boughner, 2011). This can therefore be directed by the tooth signalling to the osteoclasts to remove the nearby bone as the tooth germs expand, or by changes in bone deposition leading to an inhibition of tooth growth in a specific direction. Of particular relevance to our findings, it has recently been suggested that differences in alveolar bone underlie the differences in cusp pattern between vole and mouse molars (unpublished results, Elodie Renvoise and Jukka Jernwall). In this study, the more developed alveolar bone of the vole constrains the tooth in the lingual-labial direction, resulting in a narrowed tooth with cusps arranged in a zigzag pattern. If the bone is removed, the vole tooth in isolation forms a more rounded shape, reminiscent of the mouse molar, with the cusps developing in parallel. Mechanical constraints enforced by the bone therefore appear to play an important role not just in controlling the size of a tooth but also its shape and cusp pattern. Mechanical forces have also been shown to influence the number of osteoclasts in mandible slice cultures, with increased forces leading to increased numbers of osteoclasts in the periodontal ligament (Wan Hassan *et al.*, 2012).

In the first results chapter, the close relationship between the osteoclasts and TBI was assessed. By removing the epithelium in this chapter we examined whether the pattern of TRAP positive cells was controlled by signals from the tooth epithelium. At E14.5 the dental epithelium expresses a wealth of signalling factors including FGFs, SHH, BMPs, Wnt, and TGF-β (Caton and Tucker, 2009). These are known to signal to the surrounding tissues to control proliferation and gene expression in the dental mesenchyme. Whether they are involved specifically in signalling to the TBI is unknown, although the outer enamel epithelium is closely associated with the TBI. In our cultures without epithelium, the TBI appeared to be maintained with no encroachment of bone into the remaining dental mesenchyme and the layout of TRAP-positive cells appeared similar to the controls, with an area of TRAP-negative cells surrounded by an arc of TRAP-positive cells. This layout was observed in slices cultured for one day without epithelium but also in whole placode explants cultured for three days. These results indicate that the layout of TRAP-positive cells at E14.5 and

onwards is not controlled by a signal from the dental epithelium. The TRAP staining in our epithelium removal experiments was not as defined as shown in our previous results using TRAP stain on cultures, and a clear multi-nucleated form was not observed. It is therefore possible that the method is compromised by the dispase treatment. This is something we would like to test further. Our results do not exclude the possibility that a signal comes from the tooth, as the dental mesenchyme was left intact in our experiments. It would be therefore necessary to dissect the whole tooth primordium leaving the TBI intact in order to test for this, however this is very difficult to do in practice. The results could also be explained by a signal from the dental epithelium being important in setting up the layout of osteoclasts, but this signal might have occurred before our removal of the epithelium. For example, signals from the tooth at E13.5 might set up the initial pattern. It would therefore be good to repeat our experiments at earlier time points.

To investigate the role of BMP signalling in controlling the TBI, we moved to the use of protein loaded beads, with BMP-4 and Noggin. A change in the fate of the tooth-bone interface (TBI) was observed after altering the level of BMP signalling in culture, with bone induced around the beads, in some cases forming right up against the tissues of the tooth. This leads to local reduction in the TBI near to the bead. This confirms the potential of the cells of the TBI to form bone as indicated by the isolated experiments of Kim *et al.* (2007). Our results show the plastic nature of the TBI cells during development. Previous experiments with the addition of BMPs have had conflicting results about the ability of BMP to induce bone formation in PDL cells derived from adult tissue in mice and humans *in vitro*, perhaps indicating a shift in the potential of these cells over time. The early potential of the TBI to form bone would lead to ankylosis of the tooth and bone if the cells of the TBI were not inhibited from this pathway. Noggin is a likely candidate for repressing a bone fate. Similar to the findings of Kim *et al.* (2007) in postnatal mice, we show that in prenatal development application of Noggin leads to a loss of bone and a local widening of the TBI. Other BMP inhibitors may also be involved in this process, such as gremlin and

cerberus. If BMPs are to be used as therapeutic agents in regeneration of damaged dental tissue, it will be important to control the level of bone induction to avoid ankylosis. Ankylosis has been observed after BMP-2 treatment, with unwanted bone growth beyond the defect margin (King and Hughes, 1999). One possibility is to use a degradable matrix impregnated with BMPs to control the speed of delivery release (Talwar *et al.*, 2001).

By these manipulation experiments we have shown the interactive nature of the tooth and bone, providing both signalling molecules and mechanical cues to create a coordinated system.

5 <u>Impact of manipulation of the RANKL signalling pathway on formation of the tooth-bone interface</u>

5.1 Introduction

In the last chapter, the interaction between the developing tooth and bone was investigated. The BMP-4 and Noggin experiments highlight the importance of inhibiting osteoblast differentiation within the TBI. In addition to this inhibition of osteogenesis, encroachment of bone from the jaw into the TBI also needs to be prevented. From the close association between the TBI and the presence of TRAP positive cells shown in Chapter 3 this would be predicted to involve the action of osteoclasts, regulating bone resorption along the margin of the bone facing the TBI. In mice with impaired osteoclast function, the alveolar bone starts to encroach into the TBI, disrupting development of the growing tooth germ (Liu *et al.*, 2000; Ida-Yonemochi *et al.*, 2002; Kitahara *et al.*, 2002; Mekaapiruk *et al.*, 2002; Suzuki *et al.*, 2004; Helfrich, 2005). Regulation of osteoclastogenesis also has a critical role in facilitating dental eruption, clearing the bone away from the path of eruption (Wise and King, 2008). In keeping with this, failure in osteoclast formation leads to primary failure of eruption in humans and rats (Helfrich, 2005; Frazier-Bowers *et al.*, 2010). In order to further understand the role of these cells, presumably osteoclasts, we decided to look at the RANK-RANKL pathway, which has been shown to play an essential role in osteoclastogenesis.

5.1.1 RANK-RANKL signalling pathway

The RANK signalling pathway involves three components: OPG (Osetoprotegerin), RANK (Receptor Activator of Nuclear factor Kappa B), and RANKL (RANK ligand). The three are involved in a signalling cascade that has been implicated in various degenerative bone diseases such as osteoarthritis,

rheumatoid arthritis and psoriatic arthritis (Trouvin and Goeb, 2010). RANKL (human) is a 317-amino acid peptide whereas RANK (human), the receptor, is 616-amino acids and consists of a signal peptide, an N-terminal extracellular domain, a short transmembrane domain, and a large C-terminal cytoplasmic domain. RANKL binds to RANK to induce osteoclast differentiation, activation, and survival (Liu *et al.*, 2010). Loss of function mutations in RANK and RANKL lead to osteoclast-poor osteopetrosis (OMIM 612301, OMIM 259710) (Sobacchi *et al.*, 2007; Guerrini *et al.*, 2008). In contrast, gain of function mutations for RANK have been associated with familial expansile osteolysis (OMIM 174810) and early onset Paget's disease (OMIM 602080) (Hughes *et al.*, 1994; Nakatsuka *et al.*, 2003). These two disorders are characterized by an increase in osteoclasts with premature permanent tooth loss due to excessive bone remodelling (Mitchell *et al.*, 1990). OPG exists as a 380 residue soluble protein that acts as a decoy receptor and binds to RANKL to prevent osteoclastogenesis and bone resorption (Khosla, 2001). Mutations in OPG have been associated with Juvenile Paget's disease (OMIM 239000) (Whyte *et al.*, 2002). Therefore, a definitive balance of the RANKL, RANK and OPG is crucial to modulating osteoclastogenesis and bone remodelling (Trouvin and Goeb, 2010). The levels of RANKL pathway components is also influenced by the level of periodontitis, with different forms of periodontitis leading to variable upregulation of RANKL or loss of OPG (Bostanci *et al.*, 2007b). In general, however, enhanced RANKL and reduced OPG are found in periodontitis patients indicating a move towards higher stimulation of this pathway (Bostanci *et al.*, 2007a). The OPG/RANK/RANKL pathway and its downstream targets are shown in Figure 5.1.
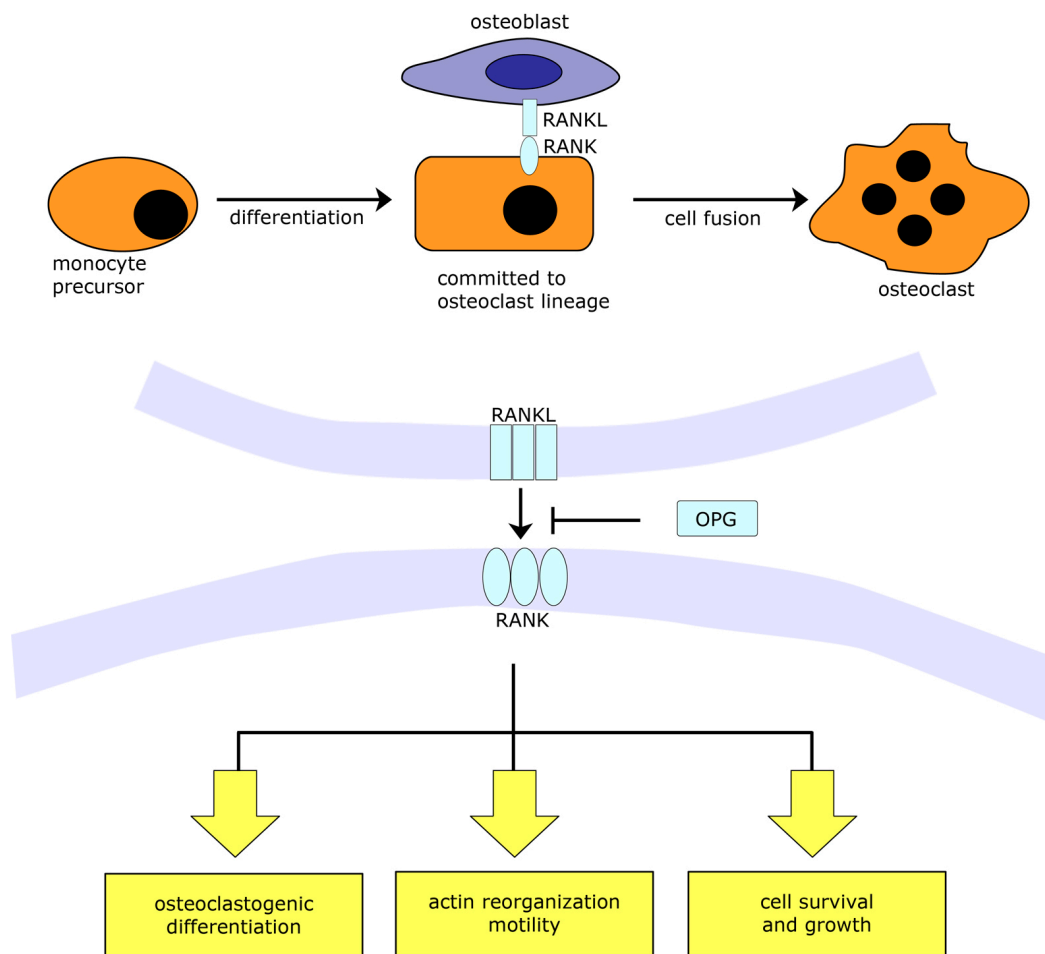
Figure 5.1 The OPG/RANK/RANKL pathway.

The osteoclastogenic differentiation and the resulting process of bone formation-resorption are modulated by the activation of the RANK on binding of RANKL (which is inhibited by OPG that binds to RANKL). This results in processes that in turn regulate cytoskeletal changes, differentiation of the osteoclast, and cell survival. *Adapted and modified from Aeschlimann and Evans (2004).*

A comprehensive expression pattern of the RANK, RANKL and OPG during tooth development in the mouse was shown by Ohazama *et al.* (2004). The receptor RANK was expressed in the tooth and surrounding mesenchyme at early stages, and then became focused in the developing alveolar bone from the late bell stage onwards. In contrast RANKL was only associated with the developing bone at all stages investigated. Another study charactering the expression of RANKL at the late bell stage showed expression in the developing TBI and bone

(Suzuki *et al.*, 2004). RANKL and OPG were also shown to be expressed in the occlusal pathway postnatally during tooth eruption (Heinrich *et al.*, 2005). Laser capture of the TBI region in postnatal rats also confirmed the expression of RANKL and OPG at P1 to P7, with both factors also being found in the surrounding alveolar bone (Yao *et al.*, 2004). RANKL and OPG have also been found to be expressed in human periodontal ligament cells, indicating a sustained role for this pathway throughout the life of the tooth (Kanzaki *et al.*, 2001). Figure 5.2 demonstrates the expression and contribution of the RANK, RANKL, and OPG proteins at different stages of tooth development in the mouse.
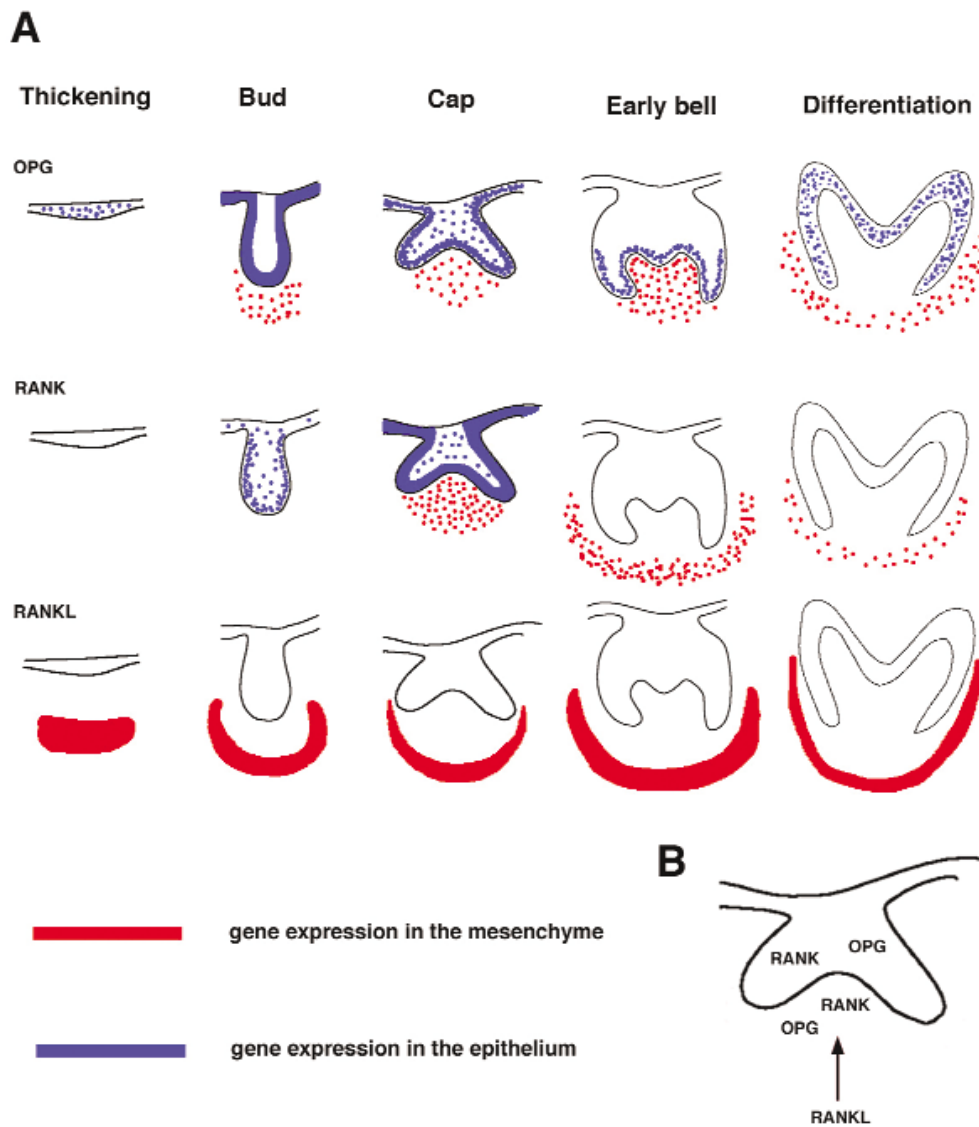
Figure 5.2 The expression of OPG, RANK, and RANKL during stages of early tooth development, and the proposed interaction between RANK and RANKL.

(**A**) Expression of OPG, RANK, and RANKL in epithelium shown in blue and in mesenchyme in red. (**B**) Relationship between RANKL in the mesenchymal cells and RANK and OPG in tooth germ at the cap stage is demonstrated. *Adapted from Ohazama et al. (2004).*

Various factors such as hormones, cytokines, growth factors, and vitamins interact and affect the OPG/RANK/RANKL pathway. Table 5.1 enumerates the factors and their effects on the pathway. The phenotypic effects seen in OPG/RANK/RANKL knockout mice compared to wild type are listed in Table 5.2.

Table 5.1 Factors affecting the OPG/RANK/RANKL pathway.

Factors affecting the OPG/RANK/RANKL pathway	Effects on the OPG/RANK/RANKL pathway
Estrogen	Stimulates OPG secretion and downregulates expression of RANKL (Khosla *et al.*, 2002; Bord *et al.*, 2003; Eghbali-Fatourechi *et al.*, 2003; Trouvin and Goeb, 2010).
Androgens	Upregulates OPG expression in cultured mice osteoblasts and decreased levels of mRNA for OPG in human cells. RANKL levels not affected (Hofbauer *et al.*, 2002; Chen *et al.*, 2004).
PTH	Proresorptive effects, lowers levels of mRNA of OPG and reciprocal effects on RANKL (Lee and Lorenzo, 1999).
IL-1, IL-17, and TNF-α	Upregulates RANKL, RANK, and negatively regulates OPG. Exerts proresorptive effects (Ponchel *et al.*, 2011).
IL-4, IL-13, and interferon-γ	Antiresorptive agents that suppress osteoclastogenesis (Kearns *et al.*, 2008; Trouvin and Goeb, 2010).
IGF-1	Negative effect on OPG-RANKL interaction and vice-versa on RANK-RANKL interaction. Stimulates RANKL and M-CSF expression in young animals and effect reduced with age (Zhao *et al.*, 2008).
Pigment epithelium-derived factor (PEDF)	Stimulates expression of OPG and suppresses RANKL expression (Akiyama *et al.*, 2010).

Various genetic variations, mutations, and polymorphism in the OPG/RANKL pathway contribute to the difference in bone mass density (BMD) in different populations. The contribution of single nucleotide polymorphism in the OPG, RANKL, and RANK genes has been associated with bone turnover and BMD (Roshandel *et al.*, 2010). However, these results are under investigation and are still to be confirmed in other populations (Trouvin and Goeb, 2010).

Table 5.2 The phenotypic effects observed in OPG/RANK/RANKL knockout mice.

OPG knockout mouse
Decreased mineralisation of alveolar bone and increased mineralisation of enamel and dentin compared to the wild type (WT) mouse (Sheng *et al.*, 2010). Severe osteoporosis due to enhanced osteoclastogenesis increasing with age (Bucay *et al.*, 1998; Mizuno *et al.*, 1998).
RANK knockout mouse
Absence of osteoclasts leading to severe osteopetrosis. A typical finding in osteopetrosis models is lack of functional teeth i.e. incisors and molars, which fail to erupt during development (Li *et al.*, 2000).
RANKL knockout mouse
Severe osteopetrosis with tooth eruption defects. Presence of osteoclasts was negligible. Defects in early differentiation of T and B cells were observed. Absence of lymph nodes, defects in thymic differentiation and defects in development of mammary glands. Death of newborns occurs due to inability to form lobulo-alveolar structures during pregnancy (Khosla, 2001).

5.1.2 Manipulation of the RANK pathway in culture

In addition to knocking out the RANK pathway, various experiments have tried to manipulate the pathway by addition of soluble factors. An example would be to use OPG to transiently inhibit signalling through RANK. The addition of exogenous OPG loaded into beads at the placode thickening stage of tooth development *in vitro* led to a retardation in growth, with the tooth germs only progressing to the bud stage after three days in culture, while control treated tooth germs had reached the cap stage (Ohazama *et al.*, 2004). When cultured in kidney capsules to achieve mineralization, these retarded tooth germs did form teeth but showed reduced mineralization and abnormal pulps. These experiments indicate an early role for the RANK pathway in tooth development. When OPG was added later in tooth development at the cap stage, the number of TRAP positive osteoclasts was reduced after culture for 10 days and the cultured tooth started to be invaded by the surrounding bone (Suzuki *et al.*, 2004). Reduction of osteoclasts was shown to be altered in a dose-dependent manner. In this case, the development of the tooth itself appeared normal, indicating that the retardation

observed by Ohazama *et al.* (2004) was due to loss of the pathway at an early stage.

Given the central importance of RANKL and OPG to regulating the osteoclastogenesis and recognizing the crucial role that osteoclasts appeared to play in controlling the TBI, we therefore tested the hypothesis that this signalling pathway is going to be important in the TBI during development. For this we studied the outcomes of manipulating this signalling pathway in culture on the process of osteoclastogenesis.

Aims

- To examine the expression of OPG, RANK, and RANKL genes involved in the pathway by *in situ* hybridization .
- To investigate the importance of the process of osteoclastogenesis in controlling the tooth-bone interface through manipulation of the RANK-RANKL signalling pathway.

5.2   Materials and Methods

5.2.1   Molecular Biology Techniques

5.2.1.1   *Agarose gel electrophoresis*

Gels containing 1% agarose (Amresco®) dissolved in Tris-acetate-EDTA (TAE) buffer (40 mM Tris-acetate, 1 mM EDTA, pH8.5) were used to visualise nucleic acid fragments. To dissolve the agarose in the buffer solution, the mixture was placed in a glass bottle and microwaved for a short durations (to prevent boiling over) untill the agarose gel was completely dissolved in the buffer solution. Different quantities of agarose gel were mixed to prepare solutions of different concentration.

After cooling the gel and just before solidification, ethidium bromide (Fisher Scientific®) was added (in proportion of 1 unit of ethidium bromide per 50 units of gel) for fluorescent labelling of nucleic acids. The mixture was then poured into a mould and a comb used to create separated wells where the gel was left to cool and solidify for 20 minutes.

Nucleic acid samples were loaded by placing the gels in an electrophoresis tank (Scie-Plas HU6 Mini) and covered with TAE buffer. A sample of DNA ladder (most commonly NEB Biolabs, Inc. Quickload® 1 kb ladder) was dispensed into the left-most well. Routinely, 1 µl of the nucleic acid sample for visualisation was mixed with 4 µl of H_2O and 1 µl of blue/orange loading dye (Promega®), pipetted up and down briefly to mix, and dispensed into a well to the right of the ladder. Nucleic acid fragments were migrated towards the anode by application of an electric field (usually 100 v for 20 minutes). Nucleic acid bands were visualised in a UV transilluminator (UVP), adjusting the zoom and exposure for

optimum visualisation. Images were captured and printed on a black and white video printer (Mitsubishi P91).

5.2.1.2   *Plasmid DNA transformation and growth*

Before starting the transformation process, Lysogeny Broth (LB) broth medium (1% NaCl, (BDH, Inc.,) 1% bacto-trypton (Oxoid Ltd.), 0.5% bacto-yeast extract (Oxoid Ltd.)), and Luria-Bertani (LB) agar (LB medium containing 2% Agar bacteriological No.1 (Oxoid Ltd.)) were prepared. The medium was autoclaved. LB agar was liquidized in a microwave and cooled sufficiently to prevent any deactivation of ampicillin. Ampicillin (Sigma®) was added to a final concentration of 250 µg/ml. 30 ml of LB agar was poured per 9 cm disposable Petri dishes (Sterilin, Fisher Scientific®). The dishes were labeled and the solution was left to solidify at room temperature. Afterwards, solidification plates were wrapped in Parafilm™ (Fluka Biochemika®) and stored at 4°C until needed.

Competent cell aliquots (Subcloning Efficiency™ DH5α™, Invitrogen®) were defrosted on ice for 30 minutes. For transformation of these competent cells with plasmid DNA, 10 ng of DNA was mixed with 30 µl of cells in a sterile 1.5 ml tube and the mixture incubated on ice for 40 minutes. A control tube was prepared in which plasmid DNA was replaced with an identical volume of autoclaved H_2O. Cells were then subjected to heat shock for 45 seconds in a 42°C water-bath, before being placed immediately onto ice for 1 minute.

Bacterial growth was initiated, 800 µl of LB medium was added to each tube and incubated at 37ºC for 1 hour. The tubes were vigorously shaken during incubation. After incubation, 200 µl of the transformed cells were spread evenly on an agar plate using a sterile L-shaped spreader (Greiner bio-one®) and left to dry at room temperature for 30 minutes. The plate was partially covered. To encourage formation of individual separated bacterial colonies the inoculated plates were turned over at the end of the day. The plates were stored in an oven

maintained at temperature of 37ºC. The maximum incubation period was 16 hours to prevent overgrowth of bacteria and merging of colonies.

The following day, checks were carried out for the presence of separated colonies and control plates were checked for the absence of microbes. A single colony of transformed bacteria was transferred to the 5 ml quantity of LB (containing 250 µg/ml ampicillin) medium using sterile pipette while the control tubes were inoculated with a sterile pipette tip free from transformed bacteria. Following this, the cells were incubated overnight at 37ºC with vigorous shaking for a maximum of 16 hours to prevent cell lysis and loss of ampicillin effectiveness.

The following day, cultures were visually checked for evidence of bacterial growth indicated by a cloudy medium, while control cultures were verified to be free of bacteria indicated by a clear medium. Bacterial cells were pelleted by centrifuging at 13,000 rpm for 1 minute and removing the supernatant.

5.2.1.3   *Mini-preparation of plasmid DNA*

Qiagen Miniprep kit (Qiagen®) was used for DNA extraction and purification. The process was undertaken as per the manufacturer's instructions. The cells were re-suspended by vortexing in TE buffer supplemented with RNase A to prevent RNA contamination of purified DNA (buffer P1). A 200 mM NaOH and 1% Sodium dodecyl sulfate (SDS, Severn Biotech Ltd.) (buffer P2) solution was used to lyse the cells which were then neutralized in a solution containing guanidine-HCl and KOAc (buffer N3). The solution was centrifuged at 13,000 rpm for 10 minutes to pelletize the cell debris.

Following this, the DNA-containing supernatant was applied to the silica gel membrane of a DNA-affinity column (Qiaprep spin column) and bonded to the membrane by centrifuging at 13,000 rpm for 1 minute and discarding the flow through. DNA was washed in a solution containing guanidine-HCl and ethanol

(buffer PB), and then in a solution of TE buffer and ethanol. At each wash the DNA was centrifuged at 13,000 rpm for 1 minute and flow through was discarded each time. DNA was extracted in 50 µl of 10 mM Tris-HCl pH8.5 (buffer EB) and its concentration was measured by electrophoresis using a DNA of known concentration compared to a DNA sample before storing the samples at -20ºC.

5.2.1.4 Plasmid DNA linearization

10 µg of plasmid DNA was linearized in a 1.5 ml tube using an appropriate reaction mixture containing the reagents shown in the table below. The volume of dH$_2$O was adjusted according to DNA concentration and all reagents were supplied by Promega$^®$.

Table 5.3 Reagents used for linearization of plasmid DNA (per reaction).

Reagents	Volume
10 X restriction endonuclease buffer	5 µl
10 mg/ml bovine serum albumin (BSA)	0.5 µl
Plasmid DNA	10 µg
Appropriate restriction endonuclease 10,000 U/ml	2 µl
dH$_2$O	make to 50 µl

Following linearlization, plasmid DNA was purified using a gel extraction kit (QIAquick$^®$ Gel Extraction, Qiagen$^®$). The purification process was carried out as per the manufacturer's instructions. 3:1 Solution of Binding buffer (buffer QG) and isopropanol were added to the linearlized plasmid DNA sample and mixed by inverting.

The sample was applied to a DNA-affinity column (QIAquick spin) and centrifuged for 1 minute at 13,000 rpm to bind DNA to the column membrane. After centrifugation, the flow-through was discarded. The DNA was washed with ethanol-containing buffer (buffer PE) and centrifuged for 1 minute. Flow through was discarded and the column was centrifuged for a further 1 minute at 13,000 rpm. After centrifugation, the upper aqueous phase containing the DNA

was transferred into a fresh tube. In order to precipitate the DNA, 30 µl of 10 mM Tris-HCl pH8.5 (buffer EB) was added directly to the column membrane and allowed to stand for 1 minute. The mixture was then centrifuged for 1 minute. After cleanup, DNA concentration was measured and eluted DNA was stored at -20ºC.

5.2.2   *In situ* hybridization

5.2.2.1   *Radioactive in situ hybridization*

A radioactive course was attended on safe handling of ^{35}S prior to performing radioactive *in situ* hybridization.

Radioactive section *in situ* hybridization with the use of ^{35}S-UTP radiolabelled riboprobes was carried out according to Wilkinson (1992), with modifications as described by Tucker *et al.* (1998).

The radioactive *in situ* hybridization method will be described in detail.

5.2.2.1.1 ^{35}S-labelled RNA probe preparation

Using 2 µg of linearised plasmid DNA in a 25 µl reaction volume, ^{35}S-labelled RNA probes were synthesised by adding the reagents outlined in table 5.4 below in sequential order to a 1.5 ml tube. The volume of DEPC treated H_2O was adjusted according to DNA concentration.

Table 5.4 Reagents used for transcription reaction (per reaction).

Reagents	Volume
5 X transcription buffer (200 mM Tris-HCl, 30 mM MgCl$_2$, 10 mM spermidine, 50 mM NaCl)	5 µl
1 M DTT	0. 5 µl
10 mM rGTP	1.2 µl
10 mM rATP	1.2 µl
10 mM rCTP	1.2 µl
50 µM rUTP	1 µl
RNase inhibitor (40 U/µl)	0.5 µl
[^{35}S] UTP	7 µl
Linearised plasmid DNA	2 µg
Appropriate RNA polymerase 10,000 U/mL	1 µl
DEPC treated H$_2$O	make to 25 µl

The reaction was first incubated at 37ºC for 2 hours followed by the removal of the DNA template by adding 0.5 µl of 40 µg/µl DNAseI, 1 µl of tRNA and 0.5 µl of 1M DTT to the reaction, and incubating at 37ºC for 10 minutes. RNA was precipitated by adding 160 µl of DEPC treated H$_2$O, 4 µl of 1M DTT, 4 µl of 5M NaCl of 3M NaOAc pH5.2 and 400 µl of absolute ethanol to the reaction and incubating overnight at -20ºC.

The next day, probes were centrifuged, washed in a solution of 10 mM DTT diluted in absolute ethanol, and re-suspended in 50 µl DEPC treated H$_2$O containing 50 mM DTT.

5.2.2.1.2 Hydrolysis of radioactive probes

Probes were hydrolysed to aid penetration of the probe into cells by adding 50 µl of hydrolysis buffer (80 mM NaHCO$_3$, 120 mM Na$_2$CO$_3$, pH10.2 and 10 mM DTT) and incubated at 60ºC to improve tissue penetration. Probes were hydrolysed to a length of 0.3 kb for a time interval which was determined using the following equation:

Hydrolysis time (minutes) = Original transcript length – Desired transcript length

0.11 X Original transcript length X Desired transcript length

Following hydrolysis, 50 µl of neutralising buffer (0.2M NaOAc, 1% glacial acetic acid, 10 mM DTT) was added to the reaction and mixed. The RNA was then precipitated, centrifuged, washed, and resuspended in 50 µl of DEPC treated H_2O.

To check probe radioactivity, a 1 µl sample of resuspended probe was mixed with 2 ml of scintillation fluid (Ultima Gold™ LLT, Packard) in a scintillation vial, and placed in a scintillation counter (Beckman LS60001C). Radioactivity of probes was recorded in counts per minute.

Table 5.5 gives details of all cDNA-containing plasmid vectors used for riboprobe generation in this thesis.

Table 5.5 List of probes.

Gene (mouse)	Vector	Restriction endonuclease used for antisense probe generation	RNA Polymerase used for antisense probe generation	Insert size
Opg	pBlueScript II SK(+)	SpeI	T7	545 bp
Rank	pBlueScript II SK(+)	HindIII	T7	2.1 kb
Rankl	pBlueScript II SK(+)	SpeI	T7	749 bp

5.2.2.1.3   Pre-treatment of tissue sections

Sections were dewaxed and rehydrated. Slides were then incubated in 2% HCl for 20 minutes, and 2 X SSC pH4.5 for 5 minutes, followed by Proteinase K treatment. Sections were then treated with 2 mg/ml glycine in DEPC treated PBS for 2 minutes, and washed in PBS for a further 2 minutes. Sections were then incubated for 10 minutes in 0.1M tris-acetate EDTA (TEA, BDH, Inc.) diluted in 0.25% acetic anhydride (BDH, Inc.) pH8, washed in PBS for 5 minutes and for 2 minutes in DEPC treated H_2O. Sections were dehydrated in a series of ascending ethanol concentrations and air dried under foil for 1 hour.

5.2.2.1.4   Hybridization and washes

Probes were diluted in a hybridization buffer containing 50% formamide, 10% dextran sulphate (Merck Millipore®), 50 mM DTT, 1% yeast RNA. 0.3 NaCl, 0.02 M Tris-HCl pH8, 5 mM EDTA and 1 X Denhardt's reagent. Probes were diluted to a concentration of $1X10^4$ counts. After dilutions, probes were vortexed, heated at 85ºC for 3 minutes and placed on ice. 100 µl of diluted probe was applied to each slide, and covered with a glass coverslip. Slides were hybridized overnight at 55ºC in a humidity chamber.

The following day, slides were briefly incubated at 55ºC in a solution containing 50% formamide, 2 X SSC pH4.5 and 10 mM DTT to remove coverslips. Slides were then washed twice for 20 minutes at 55ºC in the same solution, followed by a further wash at 65ºC for 20 minutes. Sections were incubated in RNase buffer (500 mM NaCl, 10 mM Tris-HCl pH8, 1 mM EDTA) twice for 15 minutes each at 37ºC, then in RNase buffer containing 40 µg/ml RNase A for 15 minutes at 37ºC, and then washed for further 15 minutes in RNase buffer only at 37ºC. Slides were then washed twice in a solution containing 50% formamide, 2 X SSC pH4.5 and 10 mM DDT for 20 minutes each at 65ºC, followed by two

further washes in 0.1 X SSC 10 mM DTT, first for 20 minutes at 65ºC, and then for 5 minutes at room temperature. Slides were incubated in 300 mM NH$_4$OAc in 70% ethanol for 2 minutes, for a further 2 minutes in 95% ethanol, and finally washed for 2 minutes in 100% ethanol. Slides were air dried for 1 hour, and exposed to a ^{35}S autoradiography film (Kodak Biomax) in a dark room (working under red light) overnight.

5.2.2.1.5 Autoradiography

The following day, the film was developed in a dark room (again under red light) by immersing in developer (GBX, Sigma®) for 5 minutes and rinsing in stop buffer (Kodak Indicator) for 30 minutes. The film was then immersed in fixative for 10 minutes (GBX Fixer, Sigma®), washed in running water for 10 minutes and air dried. The hybridization signal was assessed by the visibility of silver grain precipitation. If hybridization was successful, an emulsion solution was prepared by dissolving 25 ml of solid emulsion shreds (Ilford K5) in a 25 ml solution of 2% glycerol pre-warmed for 35 minutes to 45ºC. Slides were dipped briefly in emulsion, and dried in the dark for 2 hours. Slides were then placed in a box containing silica parcels and protected from light at 4ºC for a maximum of 2 weeks, the time depending on the density of silver grain precipitation visible on the autoradiography film.

5.2.2.1.6 Developing and staining

To visualize the signal, slides were brought to room temperature and submerged for 5 minutes in Kodak D19 developer solution in a dark room (working under yellow light). Slides were rinsed in dH$_2$O and incubated in fixative (Kodak Unifix) for 5 minutes. Slides were then washed under running water for 2 hours, before rinsing in dH$_2$O and counterstaining in 0.25% Malachite Green for 1 minute. Finally, the slides were rinsed in H$_2$O, air dried, and cover-slipped using a DPX mounting medium.

5.2.2.1.7 Photography

The mounted slides were cleaned to remove remaining emulsion on the back side and excess mounting agent before taking photographs. To observe the silver grains reflecting expression of the gene of interest, the sections were pictured with dark-field and light-field illumination using a microscope (Axioskop 2 plus, Zeiss®).

5.2.3   Recombinant proteins assays

The effect of certain recombinant proteins on the development of the TBI was tested on tissue slices containing first molar tooth germs. Some proteins believed to affect the epithelial-mesenchymal signalling process were added to the aforementioned culture medium. The proteins and concentrations used for this processes are given below.

5.2.3.1   *Global addition of proteins in the culture medium*

Recombinant mouse Osteoprotegerin (OPG) and Receptor activator of nuclear factor kappa-B ligand (RANKL) were tested through the dissolution in the culture medium. For OPG protein (R&D System®, Minneapolis, MN, USA) (diluted in sterile Phosphate buffered saline (PBS) and stored in a stock concentration 100 µg/ml) tested concentrations (in medium) were 50, 100, 150, 200 ng/ml while for RANKL protein (R&D System®, Minneapolis, MN, USA) (diluted in sterile PBS containing 1% BSA and stored in a stock concentration 10 µg/ml) tested concentrations (in medium) were 5, 25, 50 ng/ml. These proteins were added to the culture medium and results were compared to controls.

Numbers for RANK-RANKL signalling culture: N= 110 control, N= 34 RANKL 50 ng/ml, N= 22 RANKL 25 ng/ml, N= 37 RANKL 5 ng/ml, N= 36 OPG 100 ng/ml, and N= 22 OPG 200 ng/ml.

5.2.4   Cell death assay

Analysis of cell death after RANKL treatment was performed by the incubation of cultures for 30 min in LysoTracker® red (Invitrogen, Carlsbad, CA, USA). Lysotracker stains cells that are undergoing apoptosis and necrosis. Cultures were then fixed and incubated in Alexa Fluor® 488 Phalloidin (Invitrogen) 1:150 for 3 hrs at RT, washed in PBS+Triton (Tr), mounted in Vectashield® (Vector Labs, Burlingame, CA, USA), and scanned confocally.

5.3   Results

5.3.1   Investigating the expression pattern of OPG, RANK, and RANKL genes using *in situ* hybridization technique

As the RANK-RANKL signalling pathway is important in regulating osteoclasts differentiation; the expression patterns of RANK, RANKL, and OPG genes were investigated at postnatal day (P) 0 using *in situ* hybridization assay (Figure 5.3). This stage had previously been investigated by Ohazama *et al.* (2004) but the expression of RANK was very unclear. P0 was chosen because this is a period of intense bone remodelling in the alveolar bone. At this stage the TBI is well established and the bone has differentiated. We compared expression of RANK, RANKL and OPG in frontal head sections at the position of the first molar tooth.

Expression of OPG, RANK, and RANKL were observed overlapping in the region of the developing alveolar bone (Figure 5.3). In addition, RANKL and OPG but not RANK were expressed in the tooth, in the differentiating tissues, such as ameloblasts. The results for RANKL gene expression were slightly different to the findings of Ohazama *et al.* (2004), who reported no expression of RANKL in the pre-ameloblasts or pre-odontoblasts, however our findings for RANK and OPG were similar. Expression of RANK appeared at much lower levels than that of OPG or RANKL, which had much more robust expression patterns.
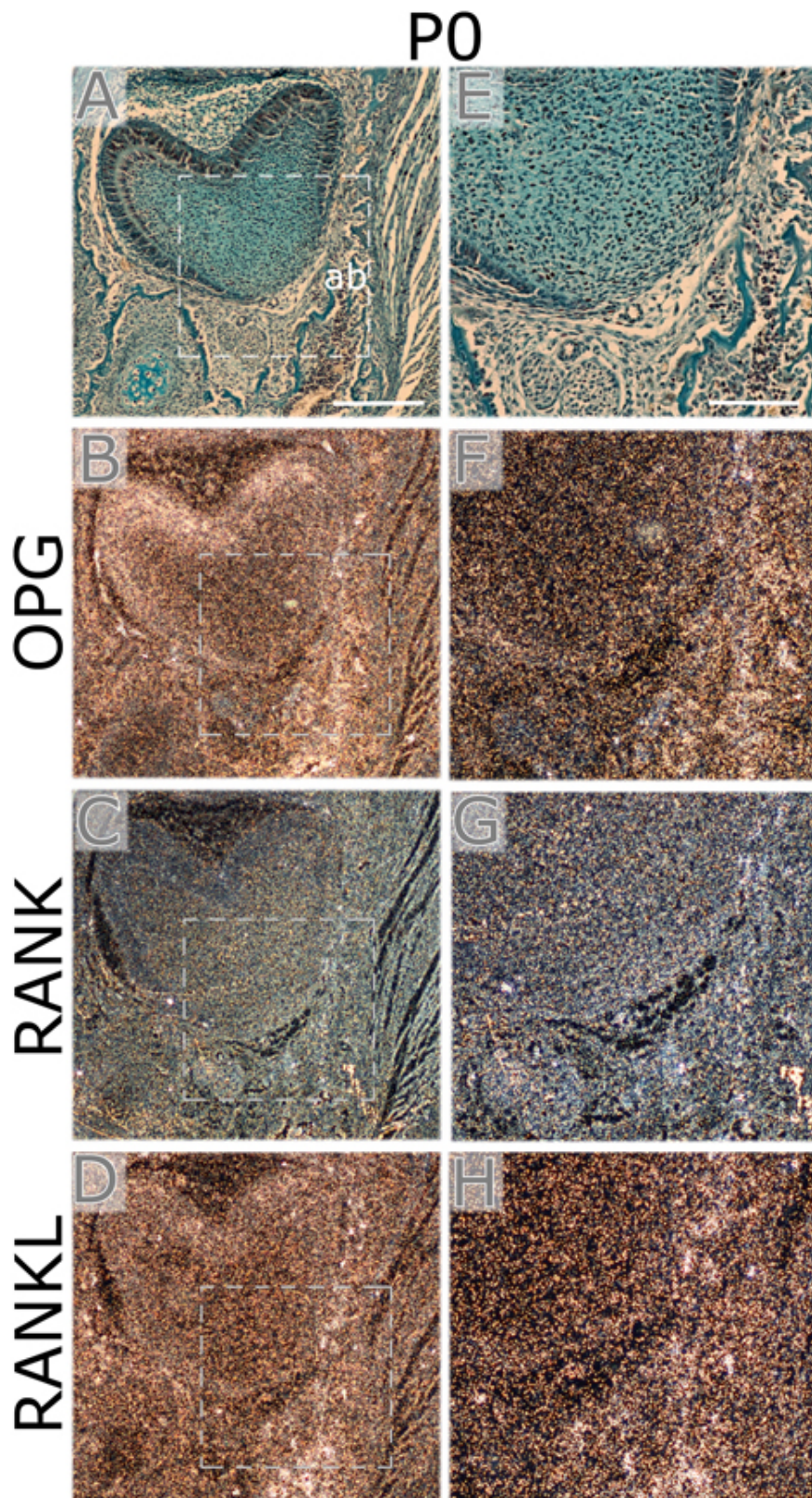
Figure 5.3 OPG, RANK, and RANKL expression detected by *in situ* hybridization.

Figure 5.3 OPG, RANK, and RANKL expression detected by *in situ* hybridization.

The expression of OPG, RANK, and RANKL genes were detected by *in situ* hybridization at P0. P0 morphology after Trichrome staining in (**A**) and dark field images of OPG expression in (**B**), RANK expression in (**C**), and RANKL expression in (**D**). (**E**, **F**, **G**, and **H**) High power views of the dashed boxes in **A**, **B**, **C**, and **D**. ab, alveolar bone. Scale bar in **A** = 200 μm (same scale in **B**, **C**, and **D**). Scale bar in **E** = 100 μm (same scale in **F**, **G**, and **H**).

5.3.2   Manipulation of the RANK-RANKL signalling pathway

Two methods were chosen to manipulate the RANK-RANKL signalling pathway in our culture system as illustrated in Figure 5.4, below:

A)   Addition of RANKL to enhance signalling through RANK.

B)   Addition of OPG to inhibit signalling through RANK.

RANK receptor activator of nuclear factor-kB
RANKL ligand of receptor activator of nuclear factor k-B
OPG osteoprotegerin
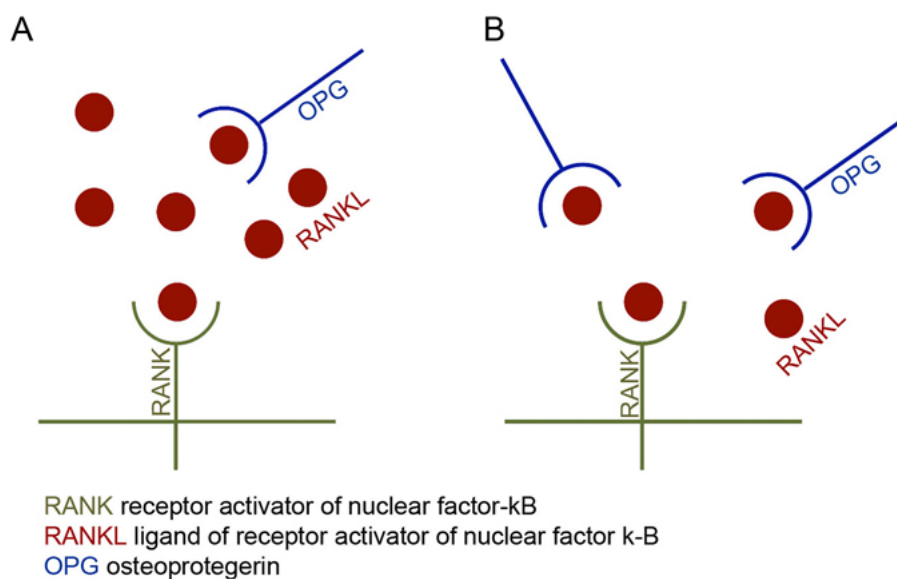
Figure 5.4 Schematic illustration of the manipulation of RANK-RANKL signalling pathway.

(**A**) Stimulation of the pathway by the addition of RANKL. (**B**) Inhibition of the pathway by the addition of OPG.

5.3.3   RANKL experiments

5.3.3.1   *Treatment of M1 culture explant with RANKL*

The RANK-RANKL signalling pathway was manipulated by the addition of RANKL to the medium. E14.5 was chosen for slice cultures at this stage as this is the point at which TRAP positive cells are first observed. The addition of

RANKL was predicted to have a stimulatory effect on osteoclastogenesis and hence promote bone resorption. In chondrocyte cell culture experiments the use of 10 ng/ml of recombinant RANKL was reported to affect the RANK-RANKL signalling pathway (Komuro *et al.*, 2001). For explant tissue cultures usually a higher concentration of protein is required for penetration through the tissue layers. We therefore started our experiments at 25 and 50 ng/ml and initially started with a relatively small number of samples as a pilot study.
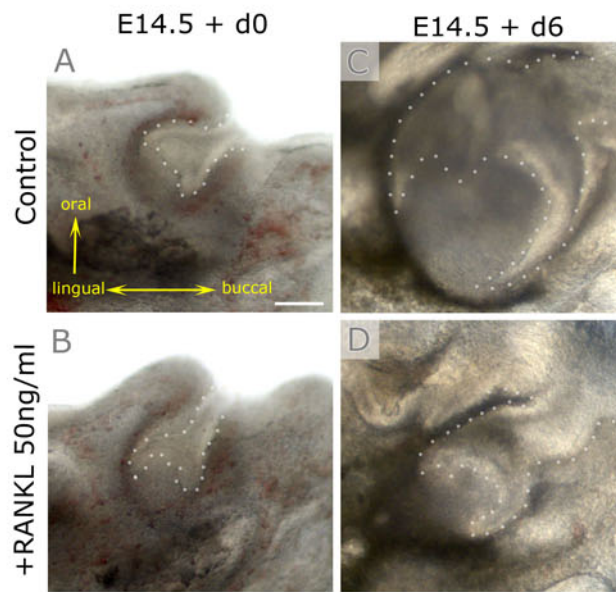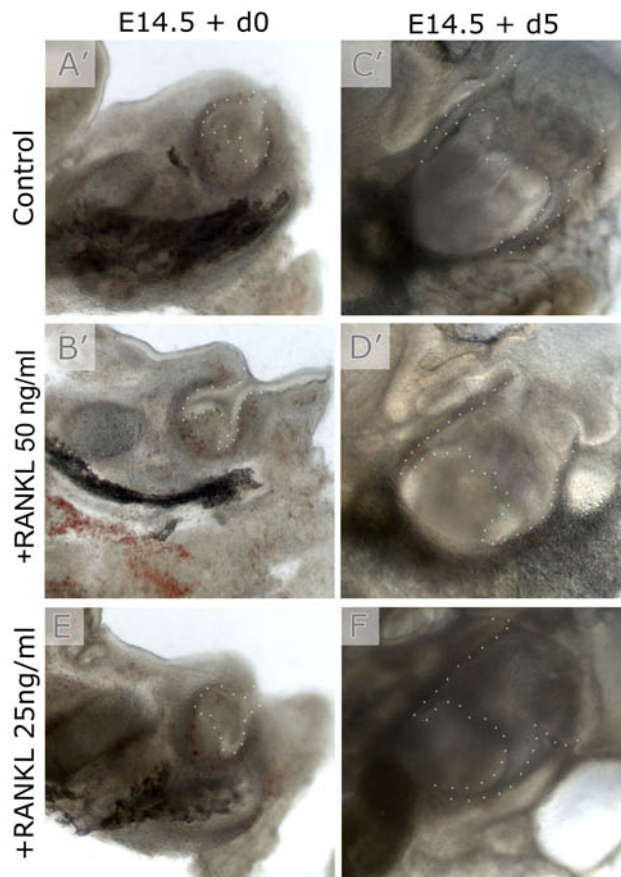
Figure 5.5 RANKL-treated M1 development in explant culture.

Figure 5.5 RANKL-treated M1 development in explant culture.

(**C** and **D**) Molar tooth after 6 days in culture. (**C**) Control medium. (**D**) RANKL, 50 ng/ml. (**C'**, **D'**, and **F**) Molar tooth after 5 days in culture. (**C'**) Control medium. (**D'**) RANKL, 50 ng/ml. (**F**) RANKL, 25 ng/ml. In **D** and **F**, RANKL- treated M1s developed to a shorter extent, attained smaller size than the untreated ones. In **D'**, RANKL-treated M1 evolved in a comparable manner to the control. Dental epithelium is outlined with white dots. Scale bar in **A** = 300 μm (same scale in **B**, **C**, **D**, **E**, **F**, **A'**, **B'**, **C'**, and **D'**).

In approximately 50% of RANKL-treated explants, the M1s were less developed in shape and size compared to the controls (Figure 5.5, A-D, E and F). However, in the rest of the RANKL-treated explants, the M1 developed in a normal manner with clear development of cusps (Figure 5.5, A'-D'), so the RANKL-treated M1 results were considered to be quite variable at these concentrations.
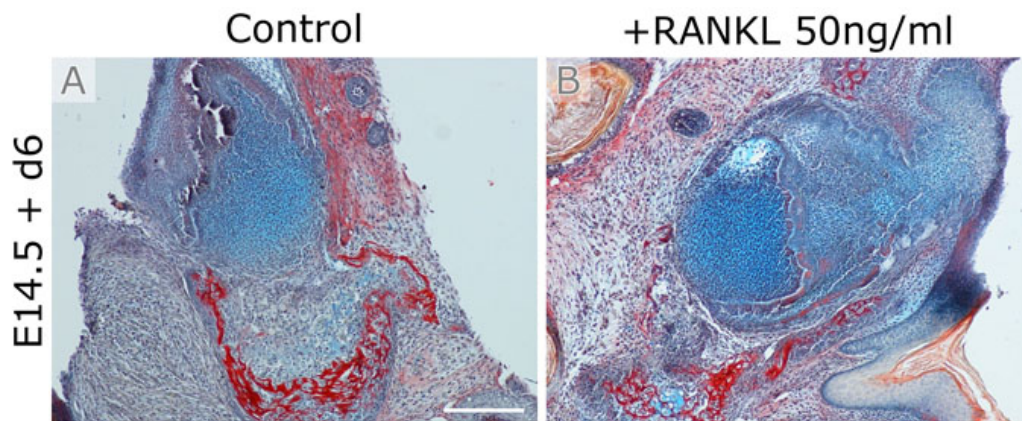
Figure 5.6 Histological sections of M1 RANKL-treated explant cultures.

(**A**) Untreated M1 morphology after Trichrome staining. (**B**) RANKL-treated M1 morphology after Trichrome staining. RANKL treatment was at a concentration of 50 ng/ml. Reduced bone was seen in RANKL-treated M1s compared to untreated ones invading the tooth wherever present. Scale bar in **A** = 200 μm (same scale in **B**).

Less bone was observed in many RANKL-treated M1s compared to untreated ones (Figure 5.6 B and A), respectively. However, where present the bone appeared to encroach the tooth at the apical margin (Figure 5.6, B). A large number of TRAP stained positive cells were observed in many RANKL-treated M1 explant cultures compared to the untreated ones, agreeing with the expected results of RANKL stimulating osteoclastogenesis (Figure 5.7, A and B). However, other cultures showed a loss of TRAP positive cells.

Figure 5.7 TRAP assay of RANKL-treated M1 explant.

(**A**) Untreated M1 TRAP assay. (**B**) RANKL-treated M1 TRAP assay. TRAP assay showed an increased number of TRAP stained positive cells aligned on the alveolar bone at the border of the TBI in RANKL-treated explants compared to untreated explants. RANKL treatment was at a concentration of 50 ng/ml. Dental epithelium is outlined with white dots. Scale bar in **A** = 200 μm (same scale in **B**).

5.3.3.2   *Dose response to RANKL (TRAP +ve numbers)*

To quantify the number of TRAP-stained positive cells, these were counted for three cultures. The graph (Figure 5.8) portrays the number of TRAP-stained positive cells counted in RANKL-treated M1 at concentration of 25 and 50 ng/ml. As we expected, the RANKL-treated M1s possessed more TRAP stained positive cells at a concentration of 25 ng/ml, however, the difference was not statistically significant. On the other hand, the TRAP stained positive cells count of the 50 ng/ml RANKL-treated M1s was surprisingly lower than the control and 25 ng/ml RANKL dose counts. This loss of TRAP-stained positive cells was highly statistically significant. The finding was considered to be surprising given the known role of RANKL and suggested that higher concentrations of RANKL could produce toxic effects on the cells.
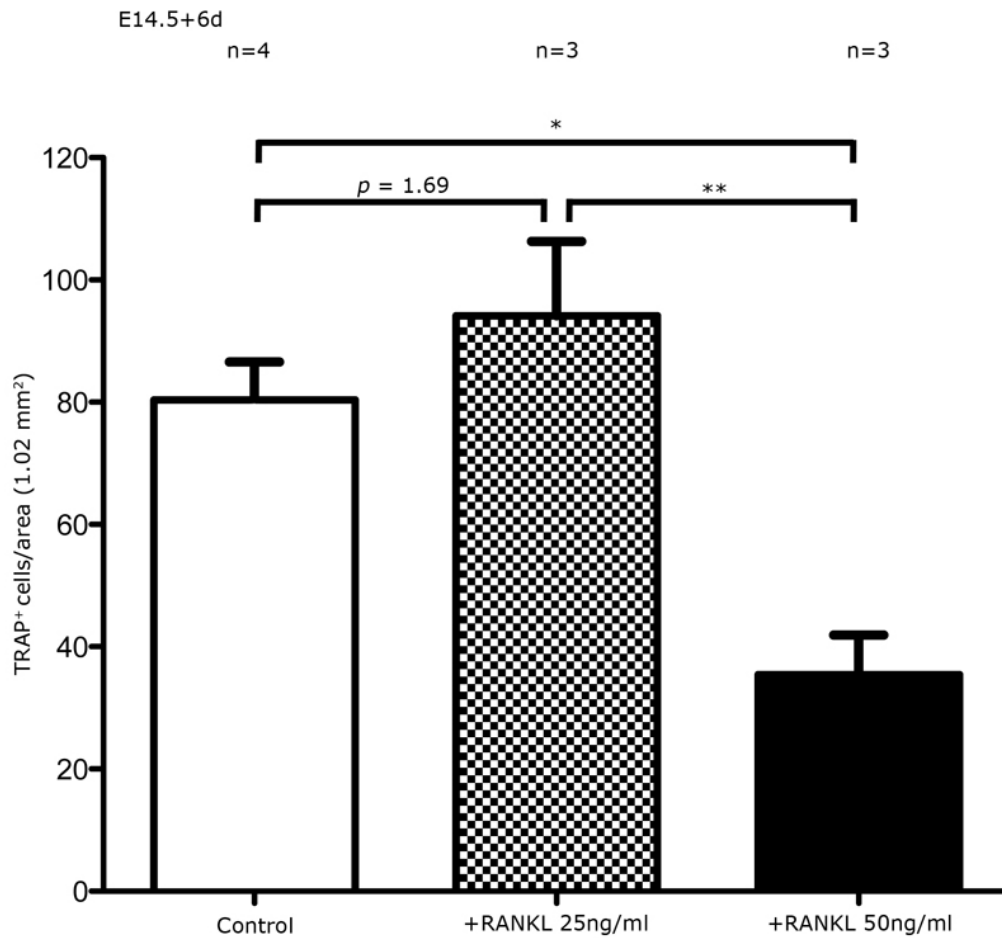
Figure 5.8 Graphical representation of the number of TRAP positive cells in the RANKL-treated and control cultures.

Two asterisks (**) correspond to $p \leq 0.01$. One asterisk (*) corresponds to $p \leq 0.05$. Dose response to rising concentrations of RANKL as indicated by the average number of TRAP-positive cells counted within a cultured tooth germ. High levels of RANKL, 50 ng/ml, have negative effects on enhancement of osteoclastogenesis compared with lower concentrations. ANOVA test.

5.3.3.3   *Assessing cell death at lower concentration of RANKL*

Given the variable results at 25 and 50 ng/ml, we then moved to 5 ng/ml and repeated our experiments. To rule out any toxic effects at this lower concentration, we assessed the level of apoptosis and necrosis using Lysotracker red, with phalloidin as a counter stain to outline the cells. M1 was again cultured as before and Lysotracker was then added to the medium before fixation. A

histogram analysis of the RANKL-treated M1s confocal scanned images following lysotracker red and phalloidin staining revealed no difference in the number of the Lysotracker stained positive cells over the untreated ones (Figure 5.9). If anything, in fact, less cell death was found in the RANKL-treated M1s with an average of 74 cells versus 92 cells in the untreated M1. Therefore, the nontoxic nature of RANKL treatment at that lowered concentration on the M1 explant cultures was confirmed.
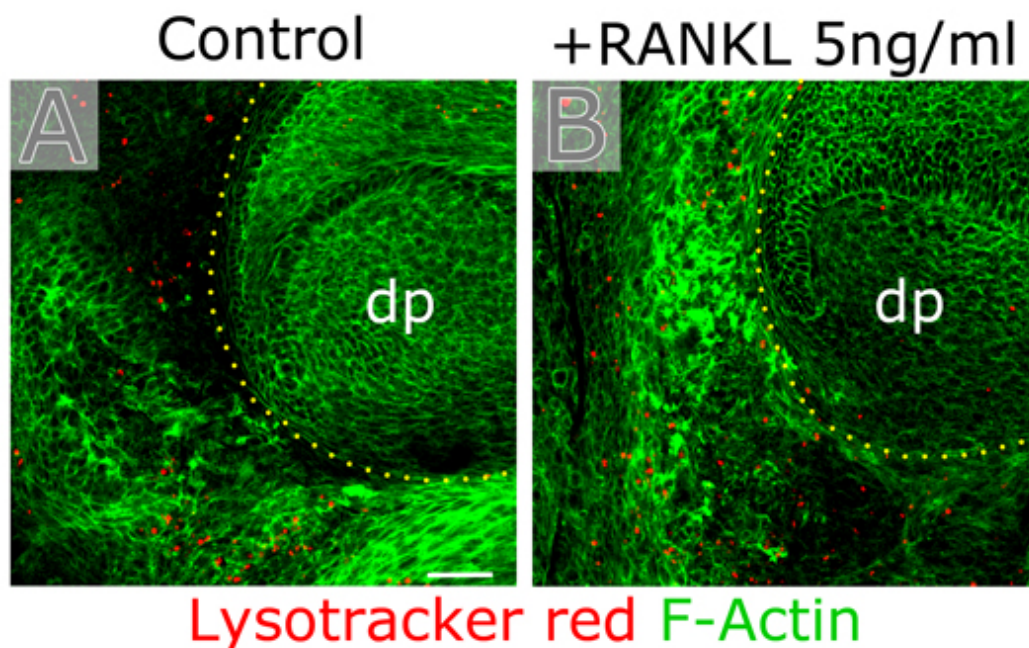
Figure 5.9 Increase in TRAP-positive cells only without cell death.

A 5 ng/ml quantity of RANKL leads to an increase in TRAP-positive cells in culture but does not induce cell death. (**A and B**) Confocal image of molar tooth cultures cultured for 2 days. Cell death (red spots); Phalloidin (green) outlines the cells to show morphology. (**A**) Control molar slice culture. (**B**) Slice treated with 5 ng/ml RANKL. Yellow dots outline tooth germ. dp = dental papilla. Apoptosis is low in the tooth germ but high in the surrounding tissue where bone remodelling is taking place in both sets of cultures (Matalova *et al.*, 2012). Scale bar in **A** = 50 μm (same scale in **B**).

Having established the non-toxic nature of using 5 ng/ml of RANKL, we then assessed whether this concentration had an effect on the morphology of the cultures and on the number of TRAP positive cells.

(Figure 5.10, D) shows that using lower concentrations of RANKL in explant cultures produced a molar tooth with good cuspal morphology, which was able to attain a larger size compared to the control (Figure 5.10, B), and to those teeth cultured in higher concentrations of RANKL (Figure 5.5, D and F).
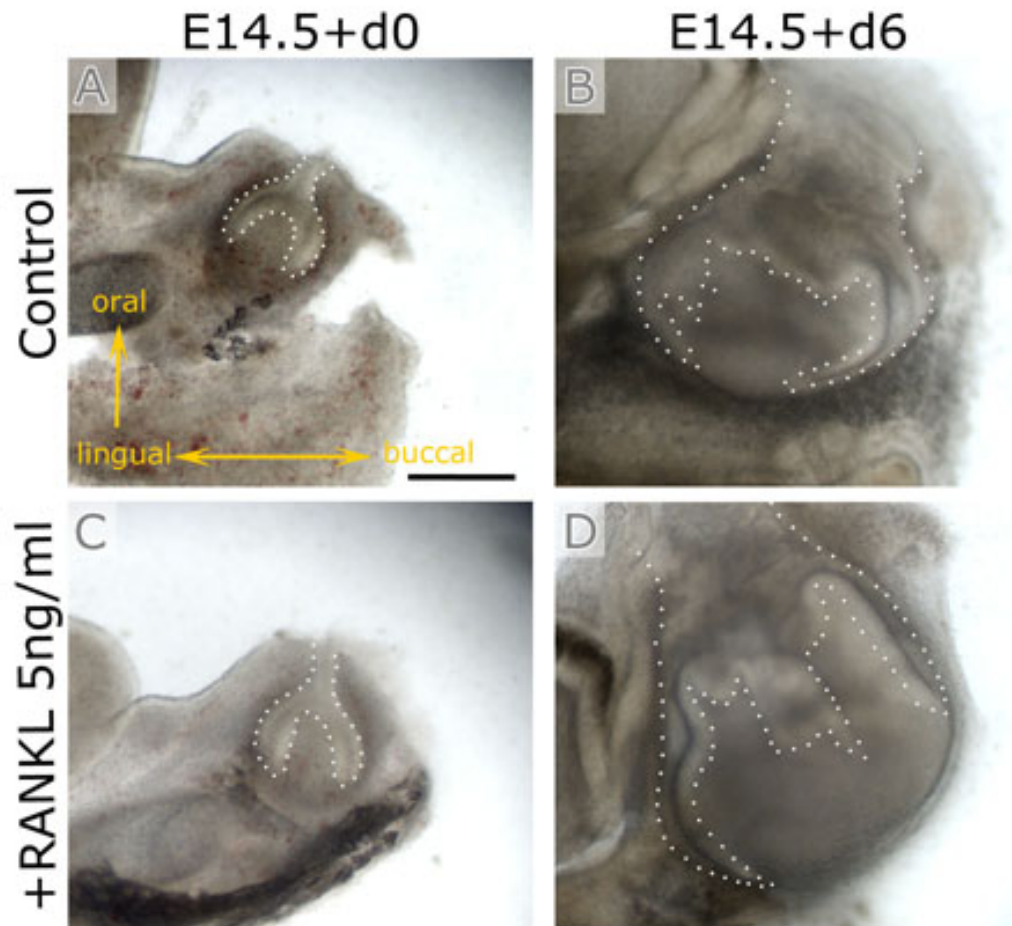
Figure 5.10 M1 development in explant culture at lower concentration of RANKL.

(**B** and **D**) Molar tooth after 6 days in culture. (**B**) Control medium. (**D**) RANKL, 5 ng/ml. RANKL- treated M1s developed to a greater extent than the untreated ones. Dental epithelium is outlined with white dots. Scale bar in **A** = 600 μm (same scale in **B**, **C**, and **D**).

In order to look at the effect of this lower RANKL concentration on the number of osteoclasts we stained the RANKL-treated M1s using the TRAP assay.
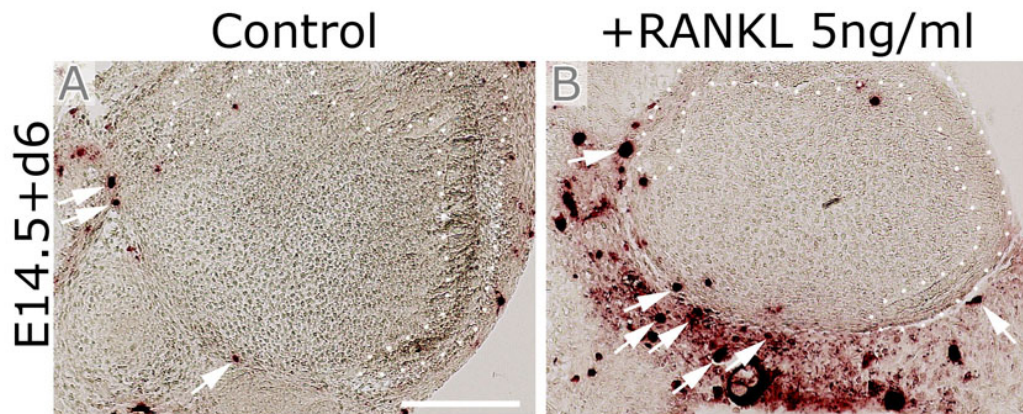
Figure 5.11 TRAP assay of the lower concentration RANKL-treated M1 explant.
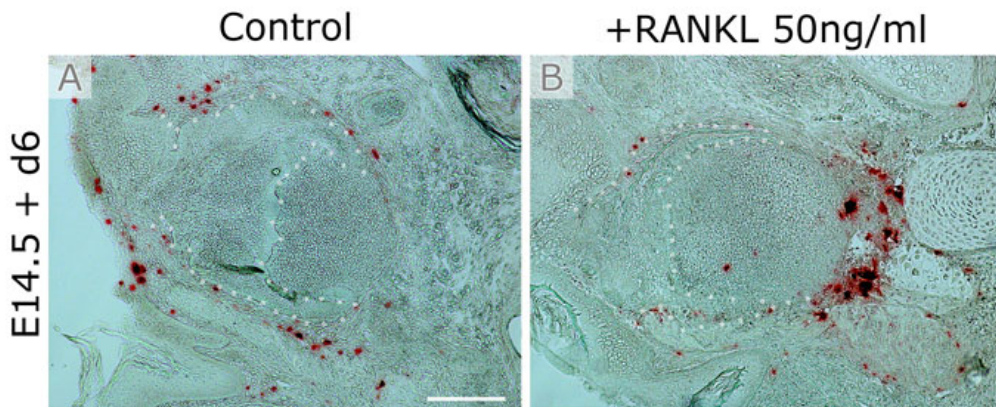
(**A**) Untreated M1 TRAP assay. (**B**) RANKL-treated M1 TRAP assay. TRAP assay showed an increased number of TRAP stained positive cells aligned on the alveolar bone at the border of the TBI in RANKL-treated explants compared to untreated explants. RANKL treatment was at a concentration of 5 ng/ml. Dental epithelium is outlined with white dots. Scale bar in **A** = 200 μm (same scale in **B**).

With the use of a lower concentration of RANKL, the TRAP assay of the RANKL-treated M1 revealed a huge increase in the number of cells that stained positively for TRAP, presumably osteoclasts, as displayed (Figure 5.11, B) compared to the untreated M1 as displayed (Figure 5.11, A).

5.3.3.4 *Quantitative analysis of TRAP cells*

As the graph (Figure 5.12) shows, the number of TRAP-stained positive cells in cultures treated with 5 ng/ml of RANKL was found to be significantly statistically higher than that of the untreated controls. The increased number of osteoclasts observed in the cultures was presumably derived from progenitor cells residing in the developing slice.
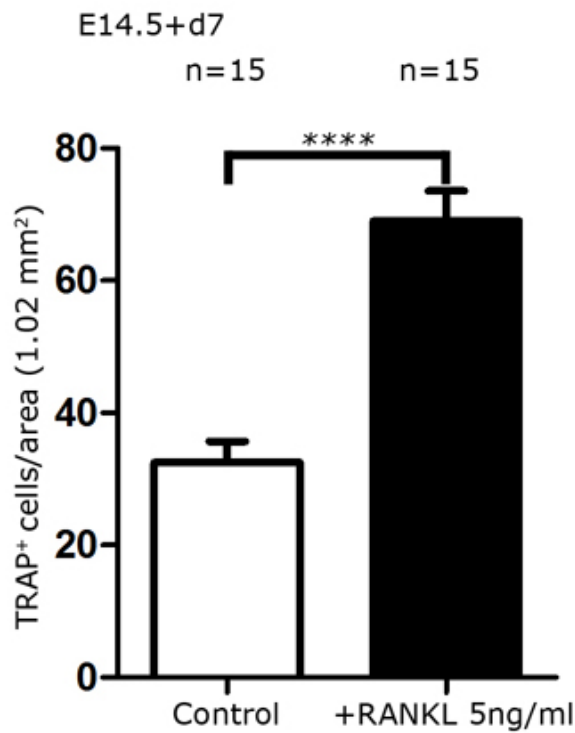
Figure 5.12 Graphical representation of the number of TRAP positive cells in the RANKL-treated at 5ng/ml and control cultures.

Graph showing the number of TRAP-positive cells in control and treated cultures. Four asterisks (****) correspond to $p \leq 0.0001$. Dose response to lower concentrations of RANKL as indicated by the average number of TRAP-positive cells counted within a cultured tooth germ. Lower levels of RANKL, 5 ng/ml, have positive effects on enhancement of osteoclastogenesis compared with controls. Unpaired student's t-test.

5.3.3.5   *Increase in TBI*

Having established the concentration of RANKL that led to an increase in osteoclastogenesis without toxicity, we moved to investigate the effect of manipulating the number of osteoclasts on regulation of the TBI. An increase in osteoclasts would be predicted to lead to an increase in bone removal, which might increase the relative size of the TBI. To investigate this we looked at the relative width of the TBI in cultures with greatly enhanced levels of TRAP positive cells in comparison to control cultures. In those cultures with large numbers of TRAP-positive cells around the developing tooth, the TBI between the tooth and bone was wider than in control cultures, indicating enhanced resorption of the bone (Figure 5.13, A, C, and E).
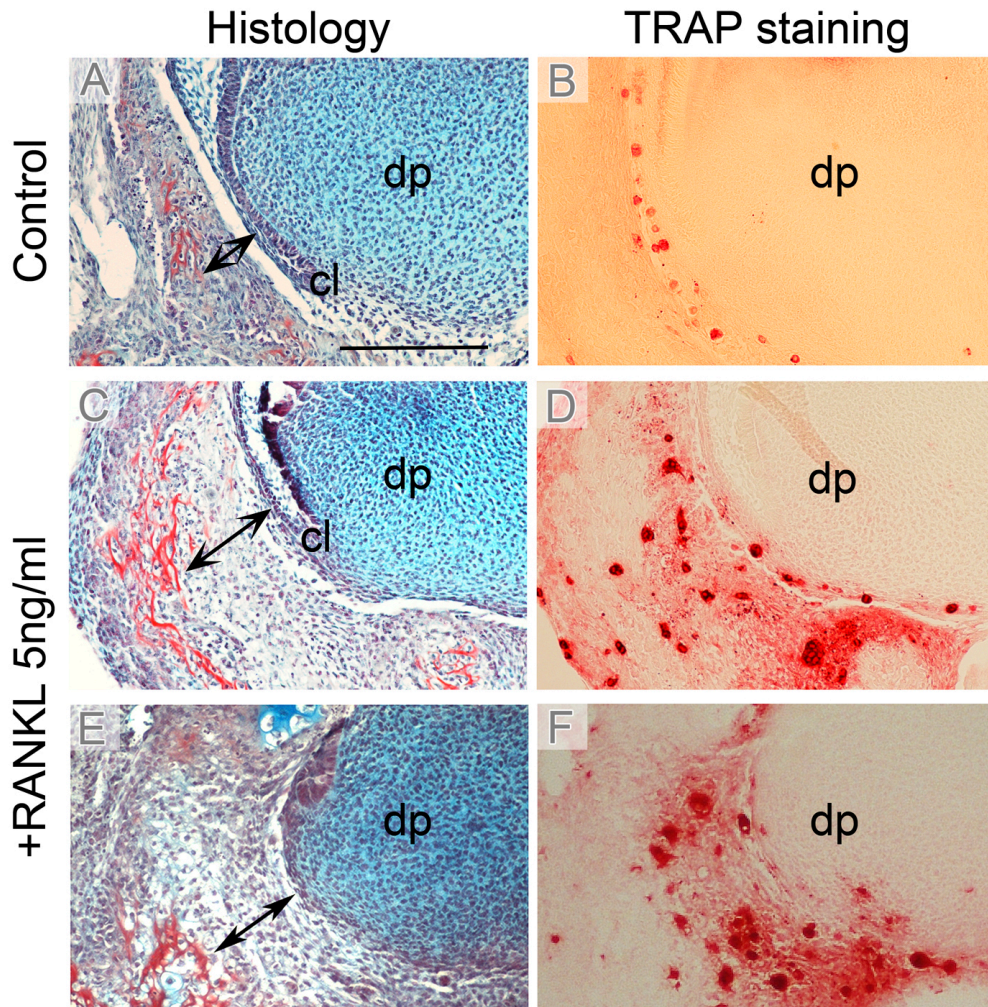
Figure 5.13 Enhancement of osteoclastogenesis widened the tooth-bone interface (TBI).

(**A-F**) E14.5 tooth germs cultured for 6 days. (**A** and **B**) Control culture. (**C**, **D**, **E**, and **F**) Cultures treated with 5 ng/ml RANKL. (**A**, **C**, and **E**) Trichrome stained tooth germs. (**B**, **D**, and **F**) Alternate sections stained for TRAP. (**A**) In control cultures, alveolar bone formed close to the outer enamel epithelium of the bell-stage tooth germ, with (**B**) TRAP stained positive cells lining the narrow TBI. (**C** and **E**) In RANKL-treated cultures, alveolar bone was found at a considerable distance from the tooth, and the TBI was expanded. (**D** and **F**) A large number of TRAP stained positive cells are observed filling the TBI. Arrows placed from the outer enamel epithelium near the cervical loop to the alveolar bone (stained red). cl = cervical loop, dp = dental papilla. Scale bar in **A** = 200 μm (same scale in **B**, **C**, **D**, **E**, and **F**).

5.3.3.5.1   Effect on tooth size

In the last chapter, we showed that removal of the tissues surrounding the tooth led to an expansion of the tooth germ, which was no longer constrained. We therefore wanted to test whether the removal of bone by an enhancement of osteoclasts production could also lead to an increase in the size of the developing tooth. To do this, we measured the increase in surface area of the tooth using the same surface area ratio used in the last chapter. Although there was a trend for the tooth germs to be larger after RANKL treatment, the result was not statistically significant (Figure 5.14). It was noteworthy that the standard error of the mean (SEM) was found to be larger in the RANKL-treated group indicating more variation in the surface area-ratios of that group compared to that of the untreated control.
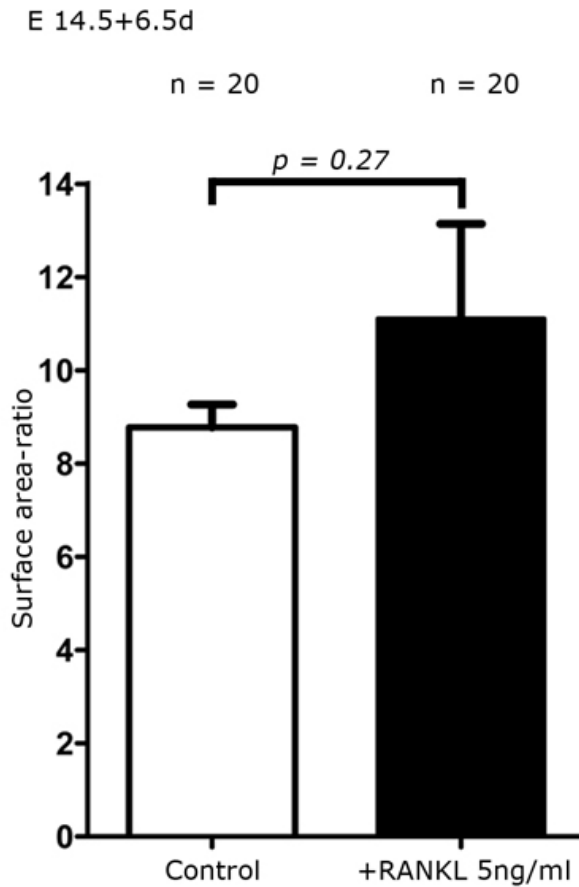
Figure 5.14 Morphometric analysis of the lower concentration RANKL-treated M1.

The graph shows a non-statistically significant difference in surface area between tooth germs cultured with or without RANKL, 5 ng/ml, after ≈ 6 days in culture. Unpaired student's t-test.

5.3.3.6   *Encroachment of bone (local response of osteoclasts)*

In some mandibular first molar (M1) explant cultures treated with RANKL, large areas of alveolar bone were present, associated with encroachment of the bone into the tooth (Figure 5.15). This result was seen in a subset of cultures at every RANKL concentration used 5, 25, and 50 ng/ml (Figure 5.15, E and I) and (Figure 5.6, B). This result was shown despite the presence of TRAP stained positive cells (Figure 5.15, F and J).
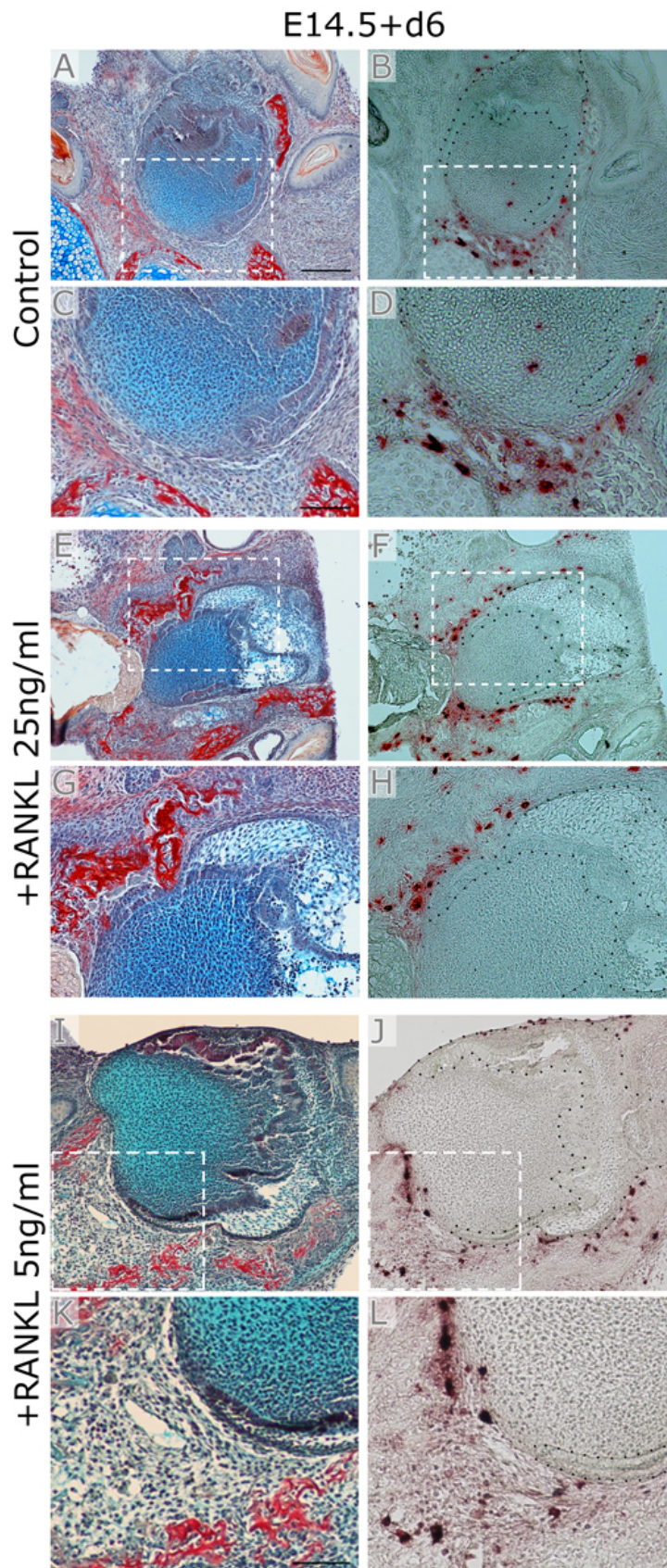
Figure 5.15 Histological sections of M1 RANKL-treated culture explant.

Figure 5.15 Histological sections of M1 RANKL-treated culture explant.

Invasion of the tooth germ by bone was seen after 6 days in culture. (**A**, **E** and **I**) The morphology after Trichrome staining. (**E**) RANKL treatment was at a concentration of 25 ng/ml. (**I**) RANKL treatment was at a concentration of 5 ng/ml. (**B**, **F** and **J**) TRAP staining of alternate histological sections shown in **A**, **E** and **I**. (**C**, **D**, **G**, **H**, **K** and **L**) Respectively, close-up views of **A**, **B**, **E**, **F**, **I** and **J**. Scale bar in **A** = 200 μm (same scale in **B**, **E**, **F**, **I** and **J**). Scale bar in **C** = 100 μm (same scale in **D**, **G** and **H**). Scale bar in **K** = 50 μm (same scale in **L**).

5.3.4 OPG experiments

5.3.4.1 *Treatment of M1 culture explant with OPG*

Having enhanced the RANK-RANKL signalling pathway, we moved to investigate the opposite effect by the addition of OPG to the mandibular first molar (M1) explant culture medium. The addition of OPG was predicted to have an inhibitory effect on osteoclastogenesis, and cause excess formation of bone as previously shown by Suzuki *et al.* (2004). In the experiments of Suzuki *et al.* (2004), the whole molar was cultured as a lump of tissue. The morphology of the tooth and surrounding tissue could therefore not be visualized during culture. In our system, however, as we are culturing slices of M1 rather than larger pieces of tissue, we could follow the tooth and bone throughout the culture period. OPG in the concentration range of 50 - 200 ng/ml was used and compared to control cultures. The concentration range chosen was in line with the experiments performed by Ohazama *et al.* (2004) and Suzuki *et al.* (2004).

Slice cultures of the OPG-treated mandibular first molar (M1) explants on day six were found to be less developed in relation to cuspal pattern and smaller in size in comparison to the untreated cultures (Figure 5.16, D' and C'). In approximately 30% of cultures, however, the tooth developed in a similar manner to the untreated examples (Figure 5.16, D and C). The effect of OPG at the concentration of 200 ng/ml on the development of M1 explants cultures was therefore regarded as inconsistent.
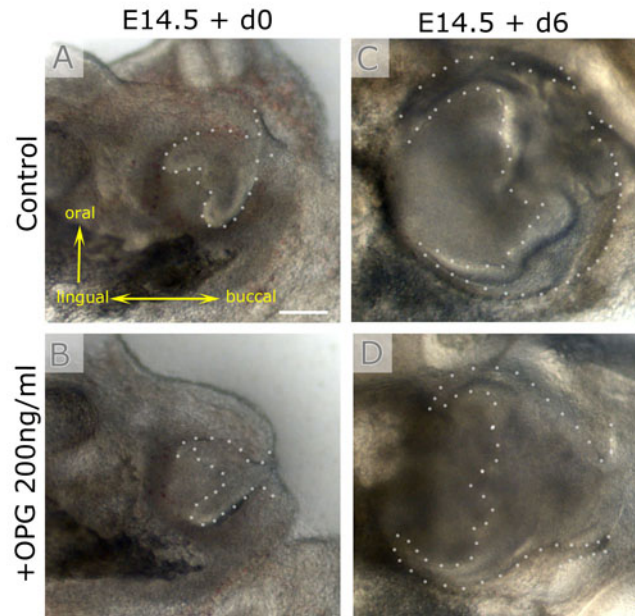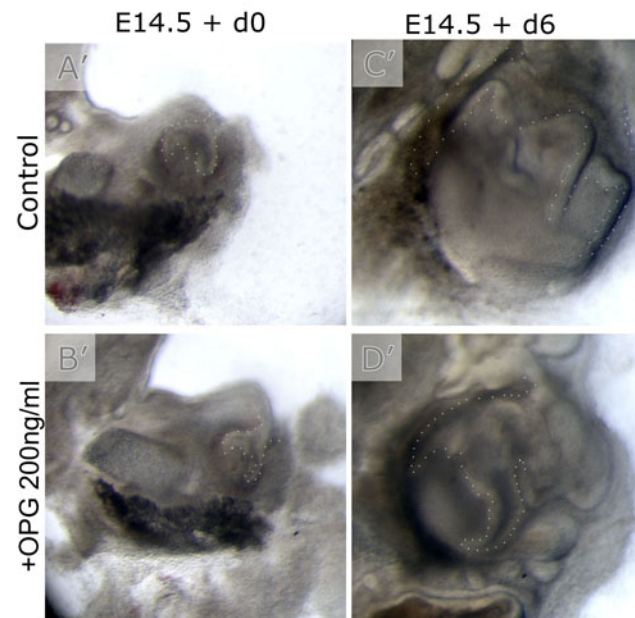
Figure 5.16 OPG-treated M1 development in explant culture.

(**C**, **D**, **C'**, and **D'**) Molar tooth after 6 days in culture. (**C** and **C'**) Control medium. (**D** and **D'**) OPG, 200 ng/ml. Dental epithelium is outlined with white dots. Scale bar in **A** = 300 μm (same scale in **B**, **C**, **D**, **A'**, **B'**, **C'**, and **D'**).

We then performed a TRAP assay to assess whether the addition of OPG had influenced the amount of osteoclasts produced. Less TRAP stained positive cells were observed in the OPG-treated M1 explant cultures (Figure 5.17, B) compared to the untreated ones (Figure 5.17, A), agreeing with the assumed negative effect of OPG on osteoclast production.
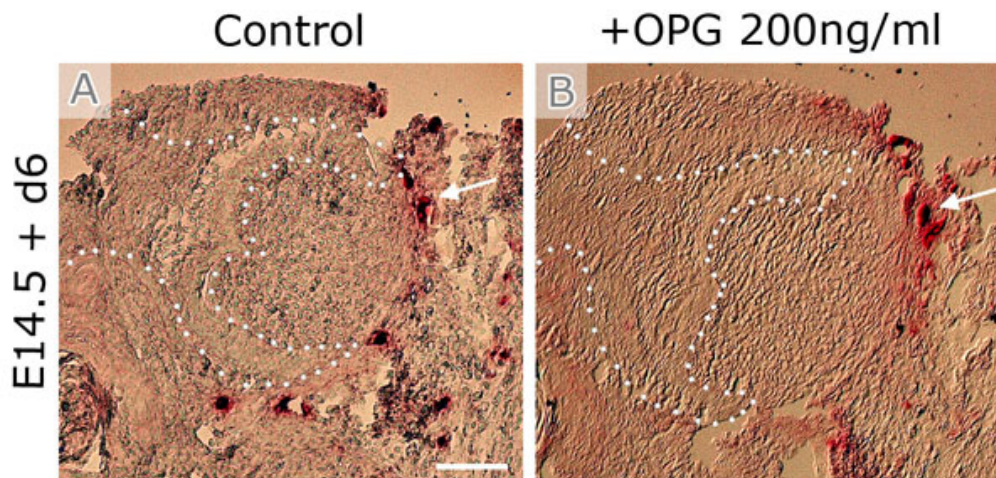
Figure 5.17 TRAP assay of OPG-treated M1 explant.

TRAP-assay showing a decreased number of TRAP positive cells aligning on the alveolar bone surface in OPG-treated explants (**B**) compared to (**A**) untreated explants. OPG treatment was at a concentration of 200 ng/ml. White arrows point to TRAP-positive osteoclasts. The dental epithelium is outlined with white dots. Scale bar in **A** = 200 μm (same scale in **B**).

5.3.4.2   *Quantitative analysis of TRAP cells after treatment*

In order to quantify the number of TRAP positive cells, these were counted. However, despite the findings in some cultures where the numbers of osetoclasts had reduced in the OPG treated cultures, when all the cultures were counted, there was no significant difference in number of cells (Figure 5.18). The variation among the samples in the OPG-treated M1s group was also found to be larger than that of the untreated group, the control, designated by the standard error of the mean (SEM).
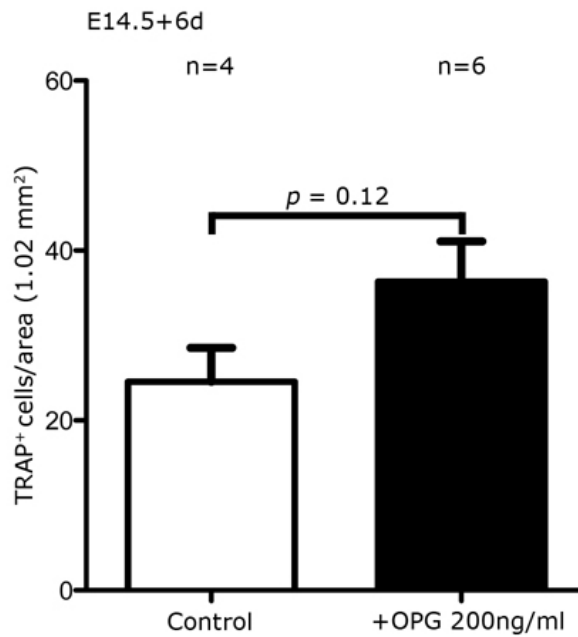
Figure 5.18 Graphical representation of the number of TRAP positive cells in the OPG-treated and control cultures.

Graph showing the number of TRAP-positive cells in the control and treated cultures. The *p* value was insignificant > 0.05. Unpaired student's t-test.

5.3.4.3   *Encroachment?*

When the OPG-treated mandibular first molar (M1) explant cultures, at the concentration of 200 ng/ml, were sectioned and the sections were Trichrome stained to assess the level of bone development, some thinning of the TBI was observed (Figure 5.19, B) although this appeared milder than that reported by Suzuki *et al.* (2004). An increase in the amount of bone together with a reduction in the space between the alveolar bone and tooth, and hence a narrower TBI, was observed in the OPG-treated M1 explant cultures (indicated by the two-sided white arrows in Figure 5.19, A and B), although in many cases the effect was not uniform around the tooth.
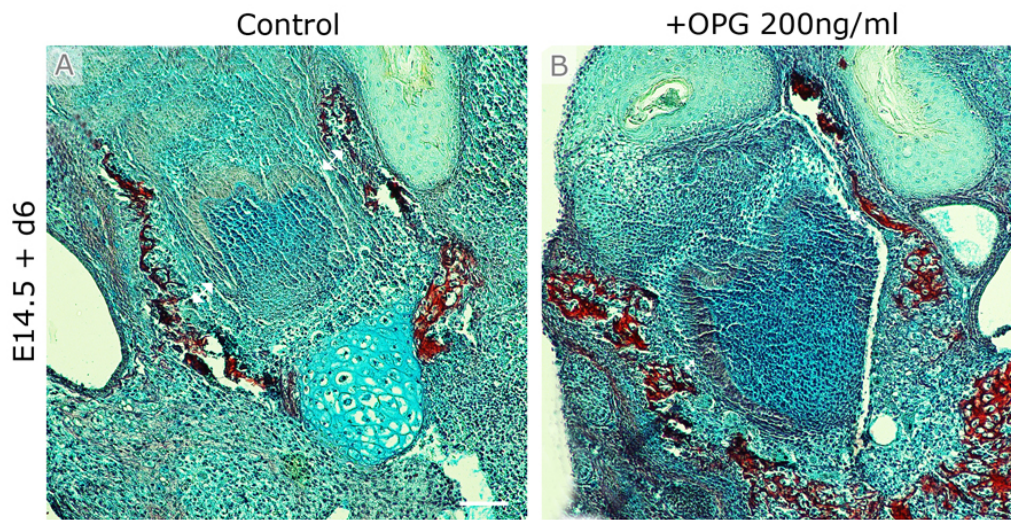
Figure 5.19 Histological sections of M1 OPG-treated culture explants.

(**A**) Untreated M1 morphology after Trichrome staining. (**B**) OPG-treated M1 morphology after Trichrome staining. OPG treatment was at a concentration of 200 ng/ml. More bone was seen in the OPG-treated M1s compared to the untreated ones, effectively narrowing the width of the TBI. White arrows indicate the width of the TBI in the OPG-treated and untreated M1s. Scale bar in **A** = 200 μm (same scale in **B**).

To correlate the difference in bone growth within a cultured tooth germ with the presence of osteoclasts, we analysed histological sections of M1 with alternate sections that were TRAP stained (Figure 5.20). A local loss of TRAP-positive stained cells, presumably osteoclasts, in the bone encroachment regions was seen and is indicated by the yellow arrows (Figure 5.20, A and B). However, where TRAP-positive stained cells were found, no bone encroachment was apparent as indicated by the white arrows (Figure 5.20, A and B). The effect of the addition of OPG therefore did not appear to be uniform within a developing culture.
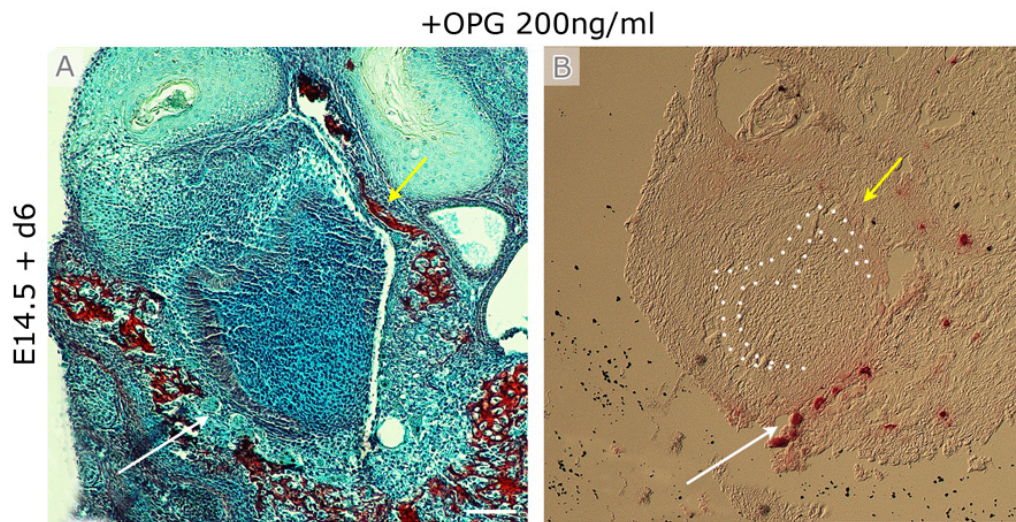
Figure 5.20 Histological sections of M1 OPG-treated culture explant.

(**A**) Morphology after Trichrome staining of OPG-treated culture (**B**) TRAP staining of an alternate histological section. OPG treatment was at a concentration of 200 ng/ml. The yellow arrow in **A** points to an area of bone encroachment. The yellow arrow in **B** reveals a local loss of TRAP stained positive cells in that area of bone encroachment. On the other hand, the white arrow in **B** points to an area that has TRAP stained positive cells. The white arrow in **A** highlights the area free from any invasion by bone. Scale bar in **A** = 200 μm (same scale in **B**).

5.4   Discussion

Although manipulation of the RANK/RANKL pathway has previously been carried out (Ohazama *et al.*, 2004; Suzuki *et al.*, 2004), our experiments have utilised the slice culture method to be able to follow development of the TBI during manipulation of the pathway. Unlike Ohazama *et al.* (2004), we have also concentrated on stages when osteoclasts are first found associated with the forming TBI. As a result I have been able to show the impact of increase and decrease of osteoclastogenesis specifically on the developing TBI. Addition of exogenous RANKL to tooth explants in culture resulted in a statistically significant increase in osteoclast numbers and a widening of the TBI. These experiments highlight the importance of RANK/RANKL signaling in controlling osteoclastogenesis and in control of the TBI.

In this chapter we concentrated on the role of the RANK/RANKL signalling pathway in regulating the TBI. *In situ* hybridization experiments depicted the localisation of OPG, RANK, and RANKL. Expression for all the three genes was found in the condensing mesenchyme that forms the alveolar bone. RANKL and OPG only were expressed in the tooth, in the differentiating tissues, such as ameloblasts. This is in contrast to the results published in previous studies that indicated that RANKL expression was not detected in tooth epithelium or mesenchyme but rather in the pre-osteogenic mesenchymal cells adjacent to the tooth germ (Ohazama *et al.*, 2004; Heinrich *et al.*, 2005). Differences in expression pattern may be due to the low levels of expression of these genes in some parts of the developing tooth and bone. The absence of RANK, the receptor of the RANK-RANKL signalling pathway, in the tooth epithelium at late stage of tooth development would imply that the tooth is not responding to the signal and the pathway cannot actually be active in the tooth. The finding of RANKL and OPG overlapping expression at sites far from RANK, indicates that these molecules may compete far from the receptor, with RANKL able to move large distances from the tooth to the bone and TBI to bind to RANK and trigger the

pathway. The RANK in the mesenchymal tissue surrounding the tooth could therefore receive RANKL signals from the tooth, in addition to the RANKL produced in the bone, implying a high activity of this pathway in the alveolar bone, particularly along the border with the tooth. This expression pattern, therefore, predicts osteoclast formation in this region, agreeing with the location of TRAP labeled cells.

The RANKL-treated M1 explant culture results were quite variable at the beginning, which may be due to problems of penetration of the ligand into the cultured tissue. This would have been confounded by the transient effects of the protein in the medium and raises the need for an appropriate culture scoring system to allow us to analyse our findings. The number of osteoclast progenitors found in each slice prior to culture might also differ, leading to variable findings.

The number of TRAP stained cells was counted in all M1 culture explants. An increase in the number of cells was found in control -RANKL versus experiment +RANKL 25 ng/ml, although it was not statistically significant this trend matches with the expected effect that occurs upon addition of RANKL to the RANK-RANKL signalling pathway which results in increased osteoclastogenesis. The statistically significant reduction of cells that was found in control -RANKL versus experiment +RANKL 50 ng/ml and experiment +RANKL 25ng/ml versus experiment +RANKL 50 ng/ml can be explained by the toxic effect the RANKL 50 ng/ml concentration might have on the osteoclastic cells. Many of the tooth germs were also small after the addition of high concentrations of RANKL. This may be due to the fact that at the cap stage RANK is expressed in the tooth as well as the developing bone (Ohazama *et al.*, 2004). Some of the effects we observed may therefore be due to influencing the role of this pathway in processes other than osteoclastogenesis.

The results after reducing the amount of the exogenous RANKL to 5 ng/ml, were more convincing. The 5 ng/ml RANKL treated M1s were well developed with a statistical increase in the number of TRAP positive cells. In keeping with this, a

cell death assay showed that the number of lysotracker stained cells in cultures treated with RANKL at the concentration of 5 ng/ml was not different from that of the untreated ones.

Enhancement of osteoclastogenesis led to a widening of the TBI, just as previous experiments have shown that a reduction in osteoclasts leads to tooth germ invasion by bone, and therefore loss of the TBI (Ida-Yonemochi *et al.*, 2002; Kitahara *et al.*, 2002). The number of osteoclasts is therefore very important for maintaining the size of the TBI during development.

We did not observe a statistically significant increase in the overall size of the tooth after TBI expansion as might have been predicted given our earlier isolation experiments. However, this may be because expansion of the TBI was not always uniform, with some patches of bone still forming close to the tooth at some points in some cultures. Larger teeth have not been reported in OPG knockout mice (Sheng *et al.*, 2010), and it would be interesting to assess whether these knockout tooth germs have a wider TBI during development. Given the high variation in our cultures, a larger number of samples might be necessary in order to dilute out some of these problems encountered.

Interestingly, bone encroachment occurred despite the presence of TRAP positive cells in some of the RANKL-treated M1 culture explants. Although TRAP staining indicates the presence of probable osteoclasts, it is possible that these cells were not functional, and therefore did not prevent bone encroachment. Alternatively, if functional osteoclasts were present at abnormal levels, this could disrupt the existing bone homeostatic equilibrium, which might also have triggered bone formation as a defensive mechanism. It is interesting that at the sites of bone encroachment, large numbers of TRAP-positive cells were observed, indicating that the tooth cells might 'sense' the invading bone and send out signals to recruit more osteoclasts to the area.

Our OPG cultures findings agreed with the findings of Ohazama *et al.* (2004) and Suzuki *et al.* (2004) to some degree but, similar to the RANKL results, showed large variation. At the high concentration of OPG used by Ohazama *et al.*, we also saw retardation of tooth development. This indicates that OPG has a direct effect on tooth morphogenesis and is in agreement with the analysis of the OPG knockout that showed tooth mineralization defects (Sheng *et al.*, 2010).

Suzuki *et al.* (2004) reported that many tooth germs were found compressed with the surrounding bone tissue in OPG-treated explants. A mild compression was observed in some of our cultures treated with OPG but the results were highly variable even within a tooth germ. It may be that the OPG has diffused unevenly in the tissue slices so that not all of the tissues had OPG at the same level, or it may be that different areas of tissues responded differently to the OPG. This variation in phenotype correlated with the variable presence of TRAP positive cells, with encroachment occurring in areas devoid of TRAP positive cells. In the future, trying different concentrations of OPG after ruling out its toxic effects on cells could yield better results.

Although our cultures were variable, we were still able to answer key questions about the role of the RANK-RANKL pathway in TBI development. We were able to show that stimulating the pathway (using RANKL) led to increased osteoclastogenesis and an expansion of the TBI, while reduction of the pathway (using OPG) led to reduced osteoclastogenesis in some areas and a smaller TBI. The RANK-RANKL signalling pathway is therefore critical in controlling the relative size of the TBI during tooth and bone development. Given the variable nature of our cultures we decided to move to a knockout mouse to understand the role of osteoclasts in development of the TBI in more detail (next chapter).

6 <u>Analysis of the tooth-bone interface in a mouse model of defective osteoclastogenesis and ankylosis: the *c-Fos* mutant</u>

6.1 Introduction

Having explored the tooth-bone interface during normal development in the third chapter of this thesis and following osteoclast manipulation in culture through modulation of the RANK-RANKL signaling pathway in the fifth chapter, in this chapter I have concentrated on the *c-Fos* mutant mouse. This knockout mouse is known to have a defect in osteoclastogenesis resulting in a lack of osteoclast production and the homozygous mice have a failure of tooth eruption (Johnson *et al.*, 1992; Wang *et al.*, 1992). We have therefore looked at this phenotype in more detail to investigate the tooth-bone-interface.

6.1.1 What is *c-Fos*?

The proto-oncogene *c-Fos* is the cellular homologue of v-fos which is the transforming gene identified in the FBJ, (Finkel, Biskis, Jinkins) and FBR (Finkel, Biskis, Reilly) murine sarcoma viruses (MSVs) (Finkel *et al.*, 1966).

c-Fos is a component of the activator protein-1 (Ap-1) complex which is a dimeric transcription factor composed mainly of Fos (c-Fos, FosB, Fra-1 and Fra-2) and Jun proteins (c-Jun, JunB and JunD) (Angel and Karin, 1991).

c-Fos was reported to have an important role in signal transduction, cell proliferation and differentiation (Muller and Wagner, 1984; Treisman, 1985; Morgan and Curran, 1991) as it contains transactivation domains required for

oncogenesis and cellular transformation (Wisdon and Verma, 1993; Jooss *et al.*, 1994; Funk *et al.*, 1997).

c-Fos is an essential gene for osteoclast differentiation, and osteoclast/macrophage lineage determination and therefore has a large impact on bone remodelling (Grigoriadis *et al.*, 1995). The mechanism by which *c-Fos* exerts its specific function in osteoclast differentiation is not understood, however, a retroviral-gene transfer study showed that all four Fos proteins, but not the Jun proteins, rescue the differentiation block *in vitro* (Grigoriadis *et al.*, 1993; Wisdon and Verma, 1993; Bergers *et al.*, 1995; Kustikova *et al.*, 1998). Moreover, *in vivo*, a transgene expressing *Fra-1* rescues the osteopetrosis of *c-Fos* mutant mice (Matsuo *et al.*, 2000). A link between RANK-RANKL signalling and the expression of Ap-1 proteins in osteoclast differentiation was established when the osteoclast differentiation factor RANKL was found to induce transcription of *Fosl1* in a *c-Fos* dependent manner (Matsuo *et al.*, 2000).

Figure 6.1 diagrammatically outlines the link between the RANK-RANKL signalling pathway and the action of Ap-1 proteins including *c-Fos*, in osteoclast differentiation.
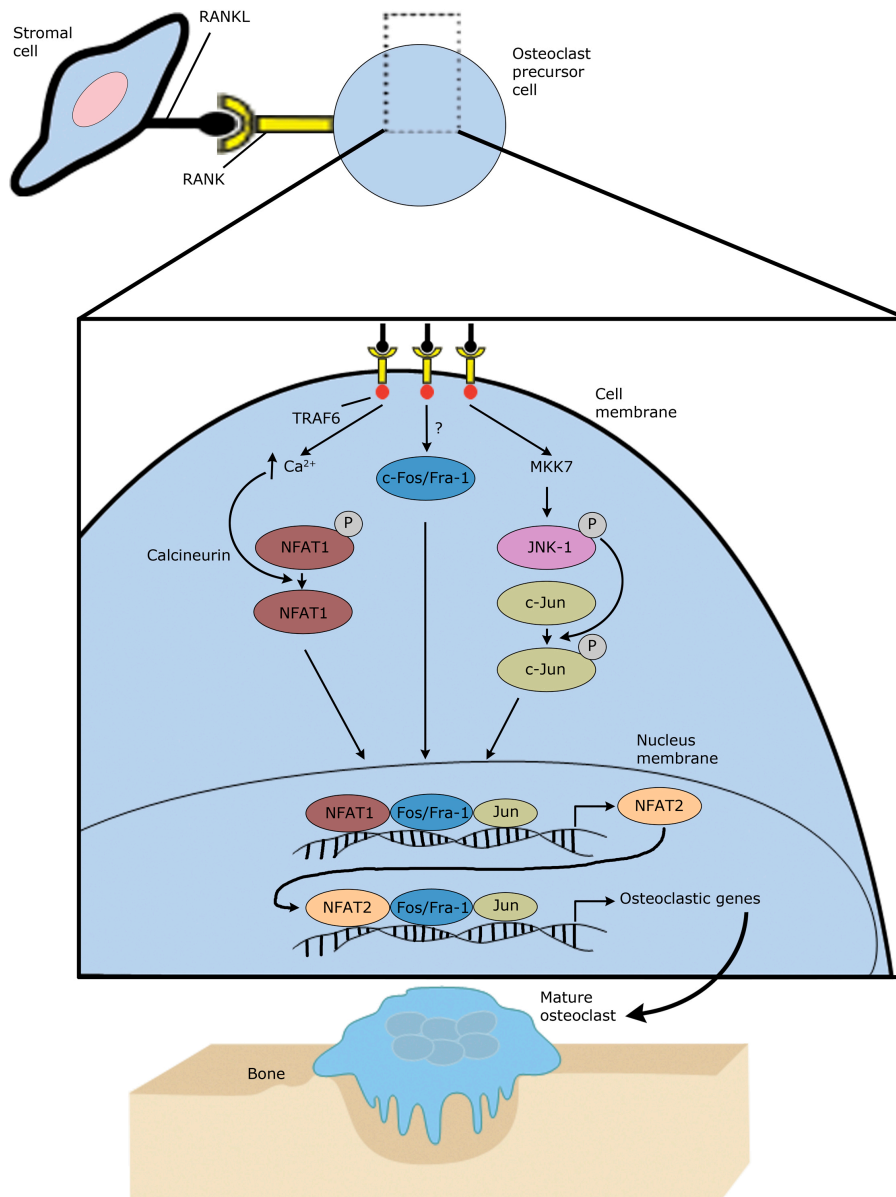
Figure 6.1 *c-Fos* and the RANK/RANKL pathway.

The AP-NFAT transcription complex mediates osteoclast precursor differentiation. Osteoclastogenesis is initiated by RANKL occupying RANK on the surface of osteoclast precursors. Subsequent recruitment of TRAF6 initiates the 3 depicted signalling cascades, in addition to other pathways not shown here. Phosphorylation (P) activates c-Jun in an MKK7/JNK-1-dependent manner, and NFAT1 is activated by dephosphorylation via calcium-mediated induction of calcineurin. RANKL/RANK also induces *c-Fos* expression by an incompletely understood mechanism. NFAT1 partners with the AP-1 proteins of the Fos/Jun families to transactivate the *NFAT2* gene, the product of which forms a similar ternary transcription complex on osteoclastic genes eventuating in the appearance of the mature osteoclast phenotype. *Adapted and modified from Teitelbaum (2004).*

In mice, expression of *c-Fos* has been shown in developing bones and teeth, haematopoietic cells, germ cells and in the central nervous system (Muller *et al.*, 1982; Dony and Gruss, 1987; Morgan *et al.*, 1987; Caubet and Bernaudin, 1988; De Togni *et al.*, 1988; Sandberg *et al.*, 1988; Pelto-Huikko *et al.*, 1991; Smeyne *et al.*, 1992; Cohen *et al.*, 1993).

6.1.2   Lack of *c-Fos*

Mice lacking *c-Fos*, generated using gene targeting in embryonic stem cells, provide an important paradigm for interpreting the function of *c-Fos in vivo*. Wang *et al.* (1992) reported growth-retardation, osteopetrosis with deficiencies in bone remodelling and tooth eruption, and altered haematopoiesis in all their homozygous c-*Fos* mutants although their heterozygous c-*Fos* mutants appeared normal; even so, females showed a distorted transmission frequency.

As the *c-Fos* mutant mice are born viable, Wang *et al.* (1992) and Johnson *et al.* (1992) implied that *Fos* is not essential for embryonic development. Nevertheless, osteopetrosis, a skeletal abnormality, is the principal phenotype, which develops in *c-Fos* knockout mice. Haematopoietic defects, in the form of a reduced number of B-lymphocytes and, T-lymphocytes, in some cases, were also exhibited in the *c-Fos* null mutant. However, the lymphopenia has been shown to be secondary to the bone defect as haematopoietic stem cells lacking *Fos* can still differentiate into all lymphoid and myeloid cells (Jain *et al.*, 1994; Okada *et al.*, 1994).

Johnson *et al.* (1992) demonstrated pleiotropic effects in homozygous null *c-Fos* mice. They reported loss of viability at birth, reduced fetal and placental weights, runting and osteopetrosis in postnatal development, abnormal germatogenesis, lymphonia and splenic extramedullary hematopoiesis, and hyperactivity and diminished response to external stimuli. In their work, distinction of the homozygous mutant mice from their heterozygous and wild-type littermates was

only attainable when they were 11 days old, when the homozygous mutants started falling behind their litter mates in weight. They continued to gain weight in a slow mode after the age of 2 weeks old, and they were shorter than half the size of normal of heterozygous littermates by the age of 5 weeks old. Lack of normal incisor eruption, slightly kinked tail tips, and a doomed skull, with a foreshortened snout were among the features displayed by these mutants. The foreshortening and increased density of the long bones and the lack of erupted teeth, which were characteristic of these mutants, were evident from radiographical analysis (Figure 6.2,1). The porous ends of the long bones could also be seen at the age of 3 weeks (Figure 6.2,2). Sections through the bone revealed abnormal bone formation, with disorganization at the epiphyseal growth plate and a small, ossified marrow cavity (Figure 6.2,3). The cortical bone of the diaphysis appeared normal, but the diaphysis medullary cavity contained thick bone trabecular with trapped chondrocytes and numerous associated osteoclasts. The Alcian blue positive stain of the trabecular matrix indicated the presence of acid mucopolysaccharides. At the age of 7 months old (the latest time point observed), their mutant mice remained about one-third to one-half the size of their littermates and their incisors and molars remained unerupted, and the characteristic domed skull shape was still maintained.
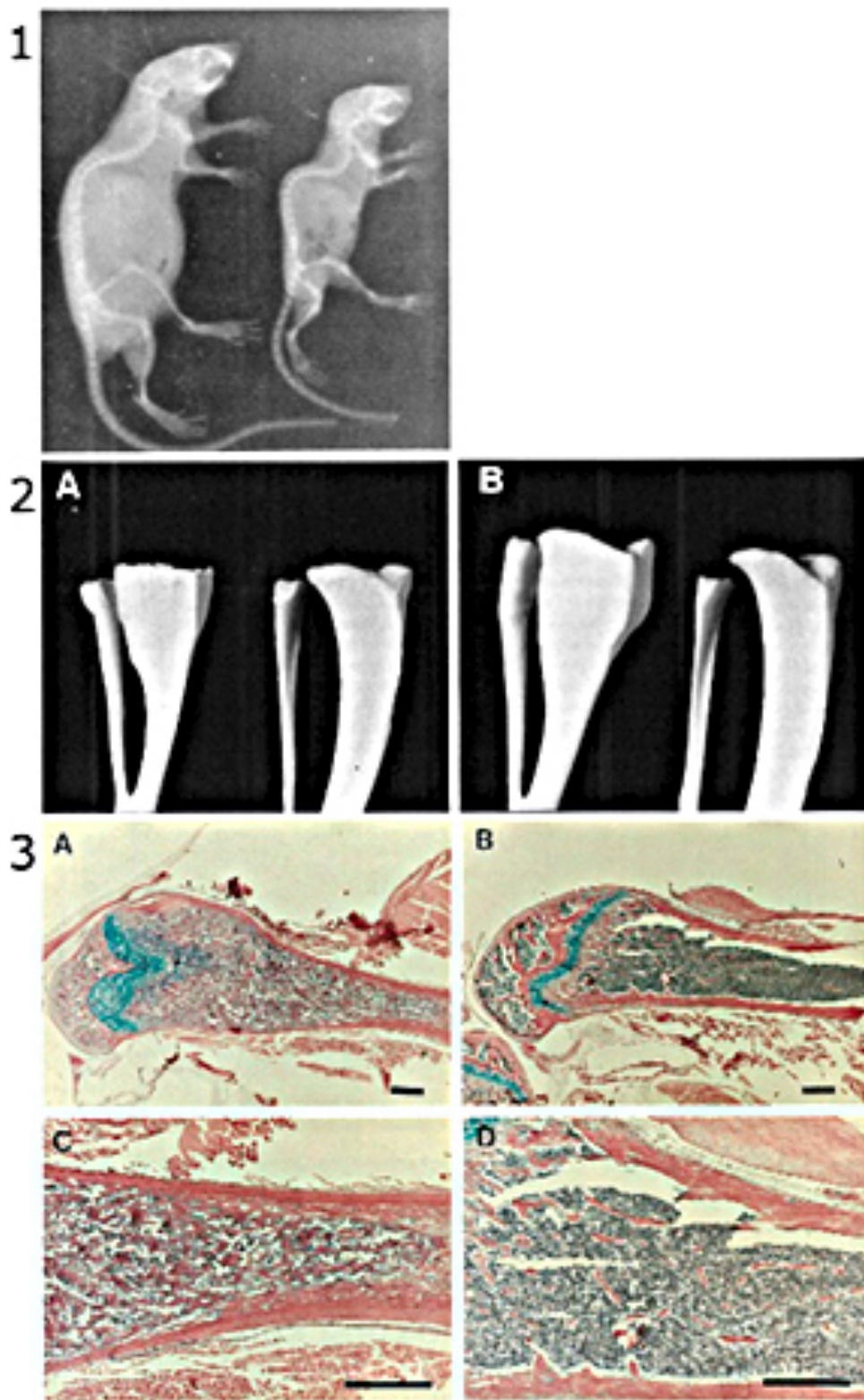
Figure 6.2 Radiograph of a 45 day old *c-Fos* null mutant and a normal littermate, long bones of normal and mutant mice, and histology of osteopetrotic long bones.

Figure 6.2 Radiograph of a 45 day old *c-Fos* null mutant and a normal littermate, long bones of normal and mutant mice, and histology of osteopetrotic long bones.

1 Radiograph of a 45 day old *c-Fos* null mutant and a normal littermate. Radiographs of a 45 day old *c-Fos* null mutant on the right and a littermate control on the left. The lack of incisors and erupted molars in the mutant is clearly evident, as are the dense long bones and minimal marrow cavities. **2** Long bones of normal and mutant mice. Dry bone preparations of the proximal end of the tibia and fibula of mutant (on the left) and littermate control animals (on the right). Three weeks old animals are shown in (**A**) and (**B**). **3** Histology of osteopetrotic long bones. Sections through the femur of an adult mutant (**A** and **C**) and a littermate control (**B** and **D**). Some disorganisations of the chondrocytes in the epiphysis is evident, and thick bone trabecular with trapped chondrocytes nearly fill the diaphysis medullary cavity. H&E, Alcian blue; bar = 0.5 mm. 1, 2, and 3. *Adapted and combined from Johnson et al. (1992).*

6.1.2.1   Osteopetrosis, Osteoclasts, and c-Fos

Osteopetroses are disorders of bone remodelling, characterized by impaired osteoclast function, resulting in a clear gain in skeletal mass (Marks, 1989). As previously mentioned, osteoclasts are bone-resorbing cells descended from hematopoietic precursors of the monocyte-macrophage lineage. The phenotypes described above in the *c-Fos* knockout mice have been shown to be caused by a defect in osteoclast differentiation at an early stage (Johnson *et al.*, 1992; Wang *et al.*, 1992; Grigoriadis *et al.*, 1994).

Osteoclastic defects in osteopetrosis can be haematopoietic, from abnormalities within the osteoclast lineage itself, or environmental, from defects in the supporting osteoblastic or stromal cell compartment, or both (Marks, 1989; Suda *et al.*, 1992). In the *c-Fos* null mouse the block in osteoclast differentiation was shown to be intrinsic to the osteoclast lineage, rather than due to an environmental defect (Grigoriadis *et al.*, 1994). A complete absence of functional, multinucleated osteoclasts and their immediate precursors was demonstrated in *c-Fos* mutant mice through a combination of *in vitro* and *in vivo* approaches (Grigoriadis *et al.*, 1994).

6.1.3   Overexpression of *c-Fos*

Ruther *et al.* (1987) studied transgenic mice expressing *c-Fos* genes generated under the control of the human metallothionein promoter. In a variety of tissues, they detected high levels of the *c-Fos* messenger RNA, though found that the deregulated *c-Fos* expression particularly interfered with normal bone development without inducing malignant tumours.

In hematopoietic tissues, Ruther *et al.* (1988) studied the function of the proto-oncogene *c-Fos* in generated transgenic mice that express *c-Fos* from the H2-Kb

promoter in several organs. Enlarged spleens and hyperplastic thymuses containing an increased number of thymic epithelial cells were found in these H2-*c-Fos* mice. T cell development in the thymus was specially affected by the exogenous *c-Fos* expression, increasing the fraction of mature thymocytes. Bone marrow radiation chimera results suggested that the altered distribution of T cell subsets was not a direct effect of *c-Fos* expression within the T cell lineage. In the spleen, no changes in the proportion of hematopoietic cell lineages were seen, and these mice did not develop lymphoid malignancies. However, H2-*c-Fos* mice are immune deficient animals as the B and T cell function was found to be impaired. Specifically, *c-Fos* appeared to stimulate the proliferation of thymic epithelial cells, and may thus indirectly affect T cell development.

Expression of the *c-Fos* gene in transgenic mice by Ruther *et al.* (1989) resulted in the development of bone lesions of which about half progressed to bone tumors, mainly chondrosarcomas. The tumors presented a strong preference for males and had a latency with a mean of 9.5 months. Mice without visible lesions, however, also developed bone tumors with the same sex favorite and latency. These reported outcomes of *c-Fos* expression were dependent on a replacement of 3' noncoding sequences of *c-Fos* by a long terminal repeat (LTR) of the FBJ-MSV virus but independent of the elected promoter.

Chimeric mice were generated with different embryonic stem cell clones and selected for high exogenous *c-Fos* expression (Wang *et al.*, 1991). In these mice a high frequency of cartilage tumors developed as early as 3-4 weeks of age independent of the degree of chimerism (Wang *et al.*, 1991). The tumors originated from cartilagenous tissues and contained many chondrocytes. The chimeric mice, however, were not affected during embryonic development. The expression of exogenous *c-Fos* RNA and Fos protein was highest in tumor tissues, mainly in differentiating chondrocytes. The same study established some primary and clonal tumor-derived cell lines in which high levels of *c-Fos*, *c-Jun*, and *cartilage-specific gene type II collagen* were expressed which gave rise to cartilage tumors *in vivo*, some of which additionally included bone.

Consequently, the chondrogenic cells and earlier progenitors were demonstrated to be especially transformed by Fos/Jun and, hence, represented a novel mesenchymal target cell for *c-Fos* overexpression.

As a tool to identify and isolate cell populations sensitive to altered levels of Fos protein, Grigoriadis *et al.* (1993) generated transgenic mice expressing the proto-oncogene *c-Fos* from an H-2Kb class I MHC promoter. They reported osteosarcomas with a short latency period in all homozygous H2-*c-Fos*LTR mice, which was found to be specific for *c-Fos*. Transgenic mice expressing the *Fos*- and *Jun*-related genes, *FosB* and *c-Jun*, from the same regulatory elements, did not develop any pathology despite high expression in bone tissues. The *c-Fos* transgene was expressed after birth in bone tissues before the onset of tumor formation, specifically in putative preosteoblasts, bone-forming osteoblasts, osteocytes, and osteoblastic cells present within the tumors, while no expression was reported during embryogenesis. High levels of exogenous *c-Fos* and the bone cell marker genes, type I collagen, alkaline phosphatase and osteopontin/2ar, were expressed in primary and clonal cell lines established from c-Fos-induced tumors, yet, the expression of osteocalcin/BGP was either low or absent. Some cell lines gave rise to osteosarcomas *in vivo*; all were tumorigenic, with osteoblastic cells expressing exogenous *c-Fos* mRNA, and Fos protein. They indicated bone-forming osteoblastic cells transformation by Fos after detailed analysis of one osteogenic cell line, P1, and several P1-derived clonal cell lines. In conclusion, they suggested that the normal growth control of osteoblastic cells is perturbed by high levels of Fos, and specific effects on the expression of the osteoblast phenotype were exerted by the same.

Enhancement of Fos-induced oncogenesis *in vivo* by coexpression of a *c-Jun* transgene was demonstrated, and a critical level of Fos was suggested to be necessary for osteosarcoma formation by Wang *et al.* (1995), as osteosarcomas developed at a higher frequency in *Fos-Jun* double-transgenic mice than single-*Fos* transgenic mice with the same time of the onset of tumor formation. Histological and histochemical analyses of the *Fos-Jun* tumors revealed greater

quantities of neoplastic bone, more remodelling, and a larger number of multinucleated osteoclast-like cells than tumors isolated from age-matched, single transgenic littermates. Overexpression of *Fos* in knockout mice that lack endogenous *Fos*, however, yielded a lower number of tumor-bearing mice; osteosarcomas were almost absent in *c-Fos*$^{-/-}$ mice, whereas tumor incidence was reduced to almost the half in *c-Fos*$^{+/-}$ mice. High levels of both transgenes were expressed in cell lines isolated from *Fos-Jun* transgenic tumors compared to significantly lower levels of the *Jun*-related gene *JunB* in cells expressing only a *c-Fos* transgene. Expression of interstitial collagenase (matrix metalloproteinase-1) was enhanced in cells derived from *Fos-Jun* tumors, and osteoblastic marker genes were expressed at varying levels in different cell lines.

Studies on the role of AP-1 family members in skeletal biology reported that overexpression of ΔFosB, using a tetracycline-regulated system, in transgenic mice resulted in increased bone formation throughout the skeleton and a continuous post-developmental increase in bone mass leading to profound osteosclerosis (Sabatakos *et al.*, 2000). ΔFosB is a naturally occurring truncated form of FosB, and is a Fos-related protein that arises from alternative splicing of the *FosB* transcript (Nakabeppu and Nathans, 1991). ΔFosB, however, was found to inhibit adipogenesis both *in vivo* and *in vitro* and to downregulate the expression of early markers of adipocyte differentiation. It was concluded that the transcriptional regulation of the process of osteoblastogenesis by ΔFosB could have possibly occurred at the expense of the process of adipogenesis (Sabatakos *et al.*, 2000) since osteoblasts and adipocytes are thought to originate from a common pluripotential precursor of a mesenchymal origin that is also capable of differentiation to other lineages such as chondrocytes and muscle (Bellows *et al.*, 1994).

The role of *c-Fos* in regulating the development and activities of bone and cartilage cells that form and maintain the skeleton is represented diagrammatically (Figure 6.3). As *c-Fos* can act both as a transforming oncogene and a cell-type-specific regulator of differentiation, a specific central function of

it has been proposed in the differentiation, activity and perhaps also the cellular interactions of the major skeletal cell types *in vivo*.
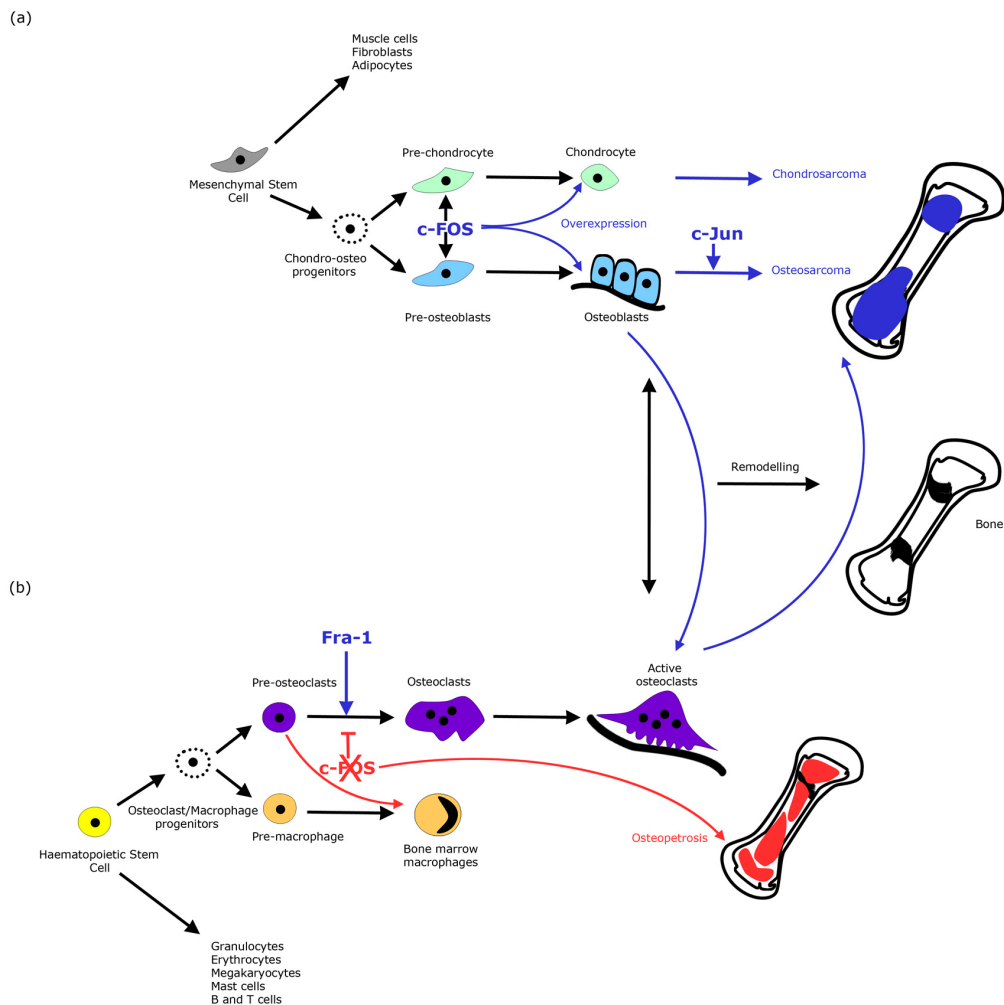
Figure 6.3 Model showing the effect of *c-Fos* overexpression and knockout on bone development.

Modulation of *c-Fos* expression disrupts the equilibrium between bone formation and resorption, which is crucial for normal bone remodelling and skeletogenesis. (**a**) *c-Fos* overexpression in transgenic and chimeric mice commands transformation of osteoblasts and chondrocytes, which ends in the formation of osteosarcomas and chondrosarcomas. *c-Jun* cooperates with *c-Fos* in osteoblast transformation and tumour formation. Overexpression of *c-Fos* also enhances osteoclast formation and activation, which in turn plays a vital role in tumour progression and tumour remodelling. (**b**) *c-Fos* knockout commands a block in osteoclast differentiation and an increase in macrophage numbers, which results in the evolution of osteopetrosis. Overexpression of *Fra-1* can recover the defect of osteoclastogenesis in the absence of *c-Fos*. In (**a**) and (**b**), the role of endogenous *c-Fos* is denoted by black arrows, the roles of the *c-Fos*, *c-Jun* and *Fra-1* transgenes are denoted by blue arrows and the outcomes of *c-Fos* deletion are represented by red arrows. *Adapted and modified from Zhao (2003) and Grigoriadis et al. (1995).*

6.1.4   *c-Fos* in the tooth

Lack of tooth eruption is a key feature of *c-Fos* null mice (Johnson *et al.*, 1992; Wang *et al.*, 1992). Ankylosis between the dentine of the tooth and the surrounding osteopetrotic bone around the mandibular first molar has been previously observed in adult *c-Fos* homozygous mutant mice (Foxworthy, 2003) (Figure 6.4).
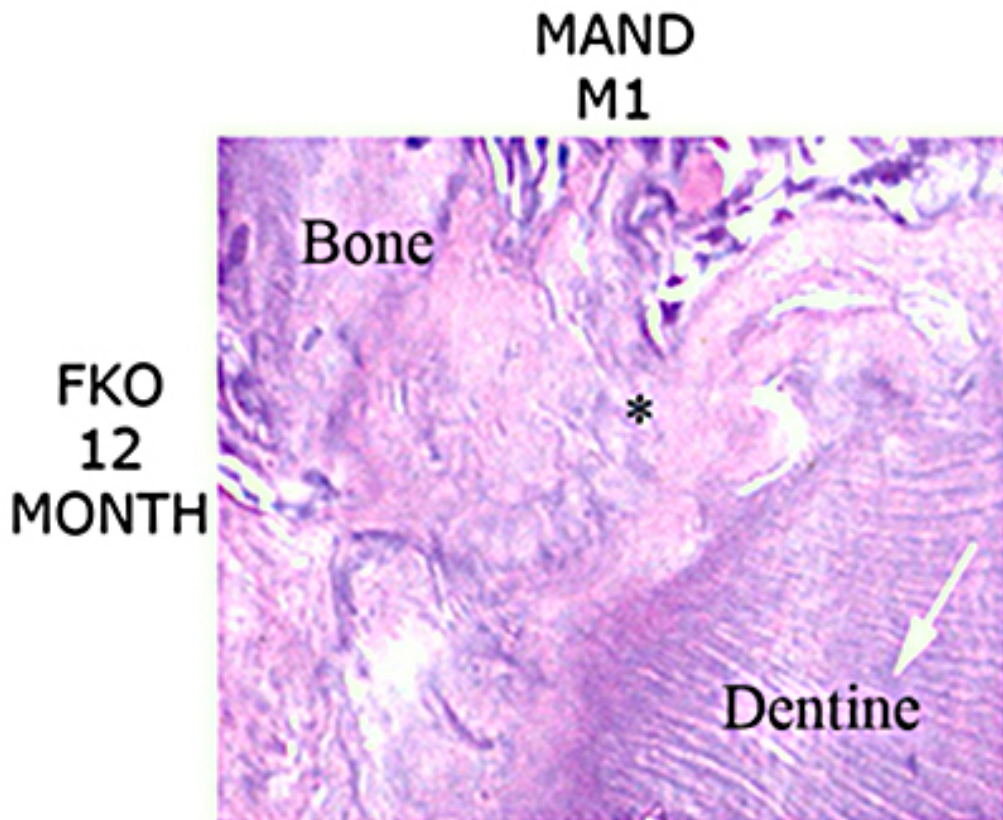
Figure 6.4 Ankylotic osteodentine in *c-Fos* mutants.

Adult FKO molars exhibit ankylosis between dentine and surrounding alveolar osteopetrotic bone, shown at 12 months around mandibular M1. In the areas of ankylosis, the tubular structure of the dentine (arrow) is lost as the bone (*) merges with the tooth structure to form the observed ankylotic osteodentine. *Adapted and modified from Foxworthy (2003)*.

The failure in eruption could represent a defect in the teeth or in the surrounding bone or both. During development the tooth is surrounded by bone, which needs to be removed to allow the tooth to erupt and for the roots to grow. In keeping with this, large numbers of osteoclasts are associated with the area under the forming roots and above the crown prior to eruption (Lungova *et al.*, 2011). Lack of osteoclasts in *c-Fos* mutants would therefore impact directly on this process.

In addition, however, *c-Fos* has been found to be expressed in the tissues of the tooth itself and may play a role in development of the tooth, independent of the bone. The earliest expression of the *c-Fos* during tooth development was by Caubet and Bernaudin (1988), who found a high level of expression of *c-Fos* in maturing odontoblasts at E18.

Analysis of the temporal and spatial patterns of expression of the Fos and the Fos-related antigens (Fra) in developing rat teeth by immunoreactivity at postnatal (P) 1-35 days revealed a transient gradient of Fos/Fra in all the molars in the coronal odontoblasts along sites of dentinogenesis, with numerous cells and intense staining near the pulp horn tip, and fewer cells and less staining in the mid-crown and cervical pulp. The gradient found was well established in first molars at P1, and was first seen in the second molars by P2, and in the third molars by P10. However, incisor teeth only had odontoblastic and ameloblastic immunoreactivity at P1 and molar root pulp lacked Fos/Fra-IR (Byers *et al.*, 1995).

In keeping with the expression in odontoblasts, *c-Fos* has been suggested to play a role in the transcriptional regulation of the dentin matrix protein 1 (DMP1), during the differentiation of the odontoblasts, which are the cells responsible for the synthesis of the calcified dentin matrix in the tooth (Narayanan *et al.*, 2002).

Prior to this, in 1999, Wise *et al.*, identified *c-Fos* as a resorption molecule and an eruption gene and demonstrated its maximal expression in the dental follicle

of the rat first mandibular molar at day 3 and day 5 postnatally in mice. They further commented that the expression timing in both studied models, in rats and mice, correlates with the time peak influx of mononuclear cells into the follicle, hence *c-Fos* may play a role in the cellular events of eruption.

In another study in postnatal rats, Wise *et al.* (1998) suggested that enhancement of the expression of *c-Fos* was one of the functions of colony stimulating factor-1 (CSF-1) in tooth eruption.

The results from the OPG experiments in chapter 5, results 3, were variable therefore I decided to use a different approach to investigate the effects of reduced osteoclastogenesis on the developing tooth-bone interface. This chapter aims to investigate the relationship between the tooth and bone *in vivo* using analysis of the *c-Fos* mutant. This mutant will be investigated using Micro-Computerized Tomography (Micro-CT) technology and histological study to assess the phenotype in the tooth and bone; TRAP staining, to identify the location of osteoclasts, and *in vivo* culture, to follow the relationship between the tooth and bone as they develop together.

Aims

- To analyse the developing tooth-bone interface in *c-Fos* mutants
- To describe the presence of osteoclasts, if any, in the *c-Fos* mutants.
- To monitor the progress of bone invasion into the tooth-bone interface in *c-Fos* mutants in explant culture.

6.2   Materials and Methods

6.2.1   Generation of *c-Fos* mutant

A male *c-Fos* heterozygous mutant mouse was obtained (to initiate our breeding programme, AE Grigoriadis, KCL).

The *c-Fos* heterozygous mouse was generated as described previously by Johnson *et al.* (1989) via targeting embryonic stem (ES) cells at the *c-Fos* locus by homologous recombination to generate chimeric mice that have transmitted the mutated allele through the germline.

6.2.2   *c-Fos* matings

We mated a *c-Fos* heterozygous mutant male (C57/BL6 background) with a wild-type female of the same background to obtain *c-Fos* heterozygous mutant males and females, which we further mated to generate *c-Fos* homozygous mutants.

6.2.3   Genomic DNA methods

6.2.3.1   *DNA Isolation from mouse tissue*

Tails were cut (approximately 4 mm) from *c-Fos* knockout litters and placed in 700 μl tail buffer (50 mM Tris-HCL, pH 8; 100 mM NaCl, 1% SDS) and digested overnight with 35 μl of 10 mg/ml proteinase K at 55°C. After adding concentrated (6M) NaCl (5 minutes with shaking) the samples were centrifuged for 5 minutes at 13,000 rpm and the supernatant was collected. The DNA was precipitated by the addition of 500 μl isopropanol and the DNA was pelleted by

centrifugation at 13,000 rpm for 2 minutes. The DNA pellet was washed with 70% ethanol, repelleted and incubated for 2 hours with TE at 37 °C and stored at room temperature.

6.2.3.2 *Polymerase chain reaction (PCR) genotyping*

Primers for sequences within the *c-Fos* wild type alleles and within the mutant neo zone were designed (shown in Table 6.1) for amplification of these wild type and knockout regions to distinguish between wild type and *c-Fos* knockout alleles for genotyping by polymerase chain reaction. 1 μl of genomic DNA was added to the PCR reaction, consisting of 15 μM Ton*Fos1*, 15 μM Ton*Fos2* and 15 μM Ton*Neo* primers, 1.5 mM MgCl2, 10 mM dNTPs, 1x PCR buffer and 2.5U Taq polymerase. Denaturation was performed at 94˚C for 1 minute, annealing at 56˚C for 1 minute and extension at 72˚C for 1 minute, for 30 cycles. The PCR products were run on a 2% ethidium bromide stained gel and viewed using ultraviolet transillumination.

Table 6.1 Primers used for *c-Fos* knockout PCR genotyping.

Primer	Sequence
Ton*Fos1*	5'-AGCTTTTATCTCCGATGAGG-3'
Ton*Fos2*	5'-CTGACACGGTCTTCACCATT-3'
Ton*Neo*	5'-TCTGTTGTGCCCAGTCATAG-3'

6.3   Results

6.3.1   Viability of mutants

Matings between *c-Fos* heterozygous mice were carried out but in general plug rates were low and we had unexpectedly low viability of homozygous mice after birth. In particular only one *c-Fos* homozygote survived to P21, the remainder being found dead at birth, or remnants found after the mother had eaten the dead pups. To assess whether the mice followed mendelian ratios prior to birth we complied the genotyping data from litters taken embryonically and compared these data from postnatal genotyping.

Table 6.2 Distribution of the *c-Fos* littermates genotyping.

Genotypes of Progeny of *c-Fos*$^{+/-}$/ *c-Fos*$^{+/-}$ Intercourses			
	c-Fos $^{+/+}$	*c-Fos* $^{+/-}$	*c-Fos* $^{-/-}$
Embryonic	8/43 (18.60%)	22/43 (51.16%)	13/43 (30.23%)
Post-natal	15/32 (46.96%)	13/32 (40.6%)	3/32 (9.4%) (dead at birth P0) 1/32 (3.1%) (alive at P21)

PCR was used to determine genotypes.

The genotyping showed clearly that prior to birth *c-Fos* homozygote and heterozygote mice were found at the expected ratios, indicating good survival to late embryonic stages. After birth, however, almost all the homozygotes died, although the cause of death was unclear. There were fewer than expected heterozygous mice at P21 indicating possible death of heterozygous mutants, in other words suggesting that viability in the heterozygous mutants was compromised.

6.3.2 Osteopetrosis, midline diastema, impaction, and lack of roots

6.3.2.1 Micro-CT WTs, Hets, and Homs

Lungova *et al.* (2011) studied the development of the mouse mandibular first molar and reported that its crown formation was completed during post-natal days 0-2, while root development was initiated at the age of post-natal day 4. Root development was completed on post-natal day 20, while tooth eruption of the first molar occurred at P15.

To discover gross variations among the *c-Fos* mutants, both homozygous and heterozygous, and wild-types, we used Micro-CT technology. Littermates were used at post-natal day 21, just before weaning.

Figure 6.5 Micro-CT analysis of mandibles in *c-Fos* wild-type and mutant mice.

Comparison of the mandibles of 3 week-old *c-Fos* wild-type, heterozygous and homozygous. In (**A**), the wild-type mandible exhibits completely erupted teeth; incisors and molars. The heterozygous mandible in (**B**) exhibits features similar to the wild-type. However, teeth are not shown to be erupting in the mandible of the homozygous mutant (**C**), and the morphology of the mandibles is somehow different from the wild-type and heterozygous mutant; as the reduced bone resorption is evident with bone buildup on the labial, buccal, and lingual surfaces of the mandible and mass of bone covering the incisal, occlusal, buccal, lingual, medial and posterior (lateral) surfaces of teeth is detectable.

188

In the *c-Fos* homozygous mutant, all teeth, molars and incisors could be seen to be impacted underneath a mass of bone (Figure 6.5, C), whereas the teeth were completely erupted in the wild-type when viewed coronally (Figure 6.5, A). The *c-Fos* homozygous mutant mandible itself (Figure 6.5, C) also accumulates bone on every surface visible from this aspect; labial, buccal, and lingual while it looks to have been remodelled properly in the wild-type (Figure 6.5, A). The *c-Fos* heterozygous mutant's mandible does not look to be any different from that of the wild-type (Figure 6.5, B).

Bony buildups could be seen on the labial, buccal, and palatal surfaces of the *c-Fos* homozygous mutant maxilla (Figure 6.6, C) and the zygomatic arch was bigger than that of the wild-type when viewed caudally (Figure 6.6, A). The molars' cusp tips and the incisors' edge tips were the only parts of the dental units visible in the *c-Fos* homozygous mutant (figure 6.6, C), while the crowns of the molars and incisors were fully erupted in the wild-type (Figure 6.6, A). The incisors as a mass are also seen diverging from each other in the homozygous mutant (Figure 6.6, C) while they were parallel to each other in the wild-type (Figure 6.6, A). The *c-Fos* heterozygous mutant (Figure 6.6, B) did not display any differences from the wild-type apart from the midline diastema.

Figure 6.6 Micro-CT analysis of maxillas in *c-Fos* wild-type and mutant mice.

Comparison of the maxillas of 3 week-old *c-Fos* wild-type, heterozygous and homozygous. In (**A**), the wild-type maxilla exhibits completely erupted teeth, incisors and molars. The heterozygous maxilla in (**B**) exhibits features similar to the wild-type. However, teeth are not shown to be erupting in the maxilla of the homozygous mutant (**C**), and the morphology of the maxilla is somehow changed from the wild-type and heterozygous mutant; as reduced bone resorption is evident with bone buildup on the labial, buccal, and palatal surfaces of the maxilla and the mass of bone covering the incisal, occlusal, buccal, palatal, medial and posterior (lateral) surfaces of teeth is detectable. The incisors are found to be divergent from each other and the zygomatic arch is also seen to be less remodelled than the wild-type and heterozygous mutant.

190

The mandibular first molar in each genotype was assessed from four directions, the buccal surface, lingual surface, and half and full bucco-lingual angles (Figure 6.7). The mandibular first molar lacked roots in the *c-Fos*-homozygous mutant (Figure 6.7, C, F, I, and M) while bone still covered its crown (Figure 6.7, C and F). The anatomy of the crown of the wild-type mandibular first molar could be seen, as the mid-buccal surface convexity and inter-cuspal depressions and cusp tips (Figure 6.7 A and D), and the bone extended from the cervical line of the tooth to cover the root portion (Figure 6.7, G and J). Two roots can be seen in the wild-type with an inter-radicular region (Figure 6.7 G and H). The mandibular first molar of the *c-Fos* heterozygous mutant (Figure 6.7, B, E, H, and L), crown and root, looked like the wild-type tooth morphology.
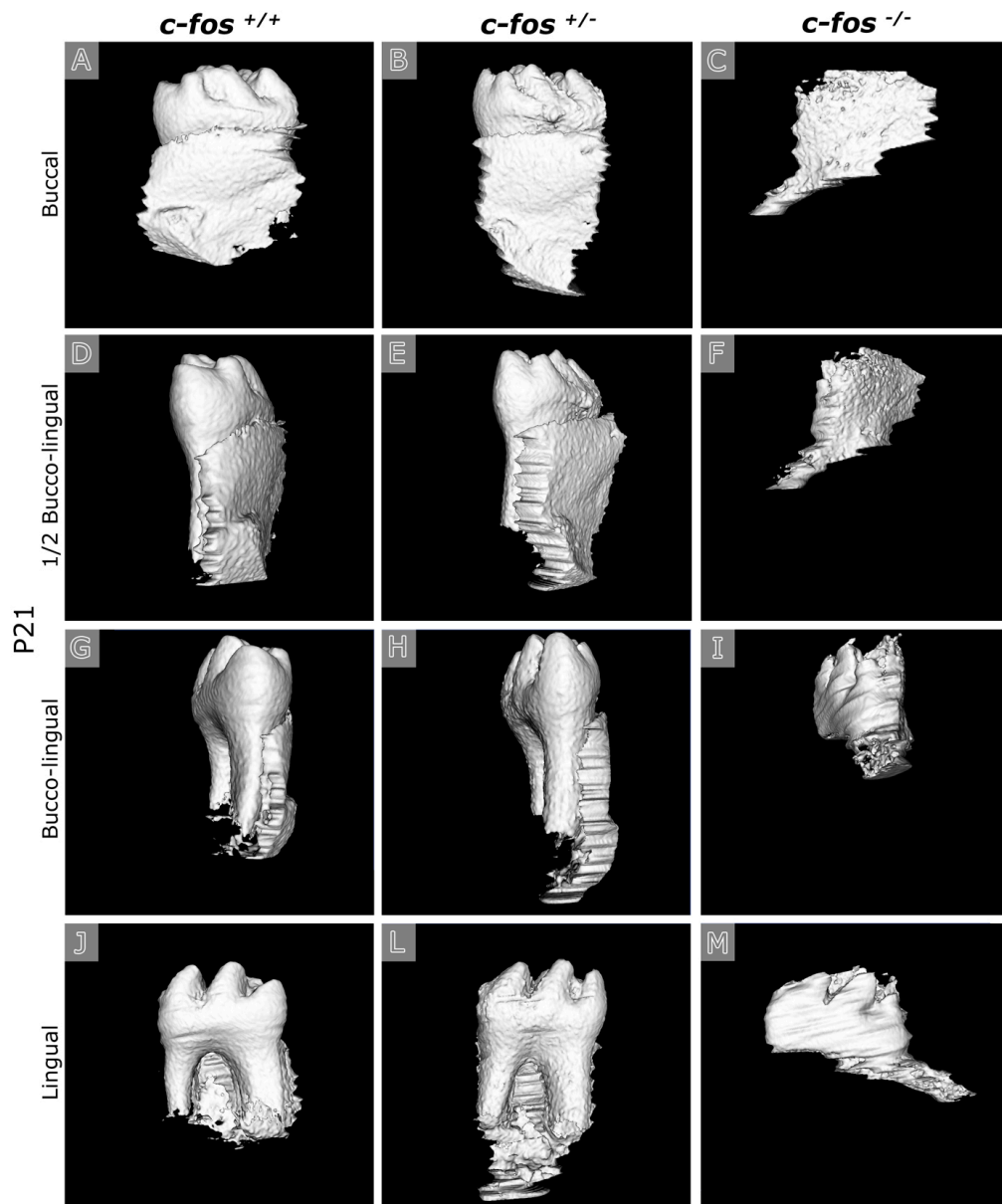
Figure 6.7 Micro-CT analysis of the mandibular first molars in *c-Fos* wild-type and mutant mice.

Figure 6.7 Micro-CT analysis of the mandibular first molars in *c-Fos* wild-type and mutant mice.

Comparison of the mandibular first molars of 3 week-old *c-Fos* wild-type, heterozygous and homozygous. In (**A**), the wild-type mandibular first molar as seen from the buccal side, the same view for the heterozygous mutant mandibular first molar (**B**) and the homozygous mutant's (**C**). The mandibular first molar in the *c-Fos* homozygous mutant (**C**) lacks root in comparison to the wild-type and heterozygous mutant, (**A and B**), respectively. The crown of the *c-Fos* homozygous mutant's mandibular first molar as seen in (**C**) is covered with bone, unlike the wild-type and heterozygous mutants where the anatomy of the crown can be seen clear in the form of mid-buccal surface convexity and inter-cuspal depressions and cusp tips. The mandibular first molar from half bucco-lingual angle can be seen in the wild-type, heterozygous and homozygous mutants, (**D**, **E**, and **F**), respectively. The level of bone ceases at the cervical line that connects the mandibular first molar's crown and root, in both the wild-type (**D**) and heterozygous mutant (**E**) whereas the crown of the mandibular first molar can only be imagined to lie behind the mass of bone seen in the homozygous mutant, in (**F**). The mandibular first molar as seen from a full bucco-lingual angle in the wild-type, heterozygous and homozygous mutants, (**G**, **H**, and **I**), respectively. The roots of the mandibular first molar start to be revealed from this Micro-CT point of imaging in the wild-type and heterozygous mutant, (**G and H**), respectively, but not in the homozygous mutant (**I**). The mandibular first molar of the wild-type, heterozygous mutant and homozygous mutant now are seen from the lingual side, (**J**, **L**, and **M**) respectively. The almost completely developed crown and root of the mandibular first molar can be seen in the wild-type and heterozygous mutant, (**J**) and (**L**) respectively. Two roots of the mandibular first molar are seen developing, and the inter-radicular region is seen in-between the roots. Roots are completely missing from the homozygous mutant's mandibular first molar in (**M**).

6.3.3   Bone invasion into the tooth-bone-interface encroaching on the first molars

6.3.3.1   Histology of developing TBI (E16.5 and NB/P0)

6.3.3.1.1   Histological study of *c-Fos* first molars

The teeth and bone were then assessed by histology staining to assess the interaction of the tooth and bone at the cellular level. For this, P0 pups were used, however, all the *c-Fos* homozygote pups were dead prior to tissue collection.

Interestingly, both the analysed *c-Fos* heterozygous and homozygous mutants showed signs of bone invasion into the tooth-bone interface encroaching on the first molars, the mandibular (Figure 6.8) and the maxillary (Figure 6.9), at birth. This invasion was particularly clear in the area of the forming roots.
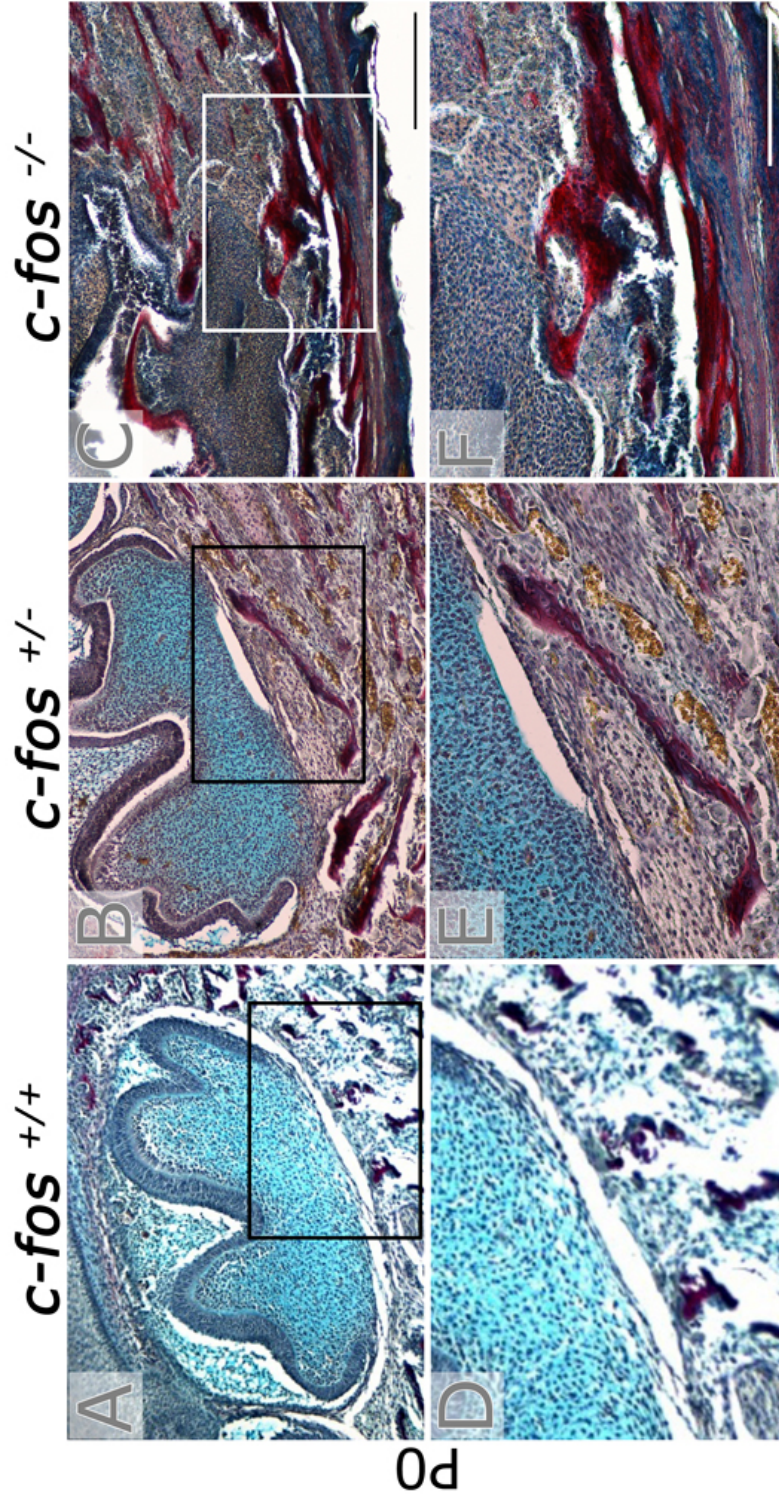
Figure 6.8 Histological sections of *c-Fos* mandibular first molars at birth.

Morphology after Trichrome staining at P0. At P0 both *c-Fos* heterozygous (**B**) and homozygous mutants (**C**) showed signs of bone invasion into the tooth-bone-interface encroaching on the tooth. (**D**, **E** and **F**) High power view of area boxed in (**A**, **B** and **C**) respectively. Scale bar in **C** = 300 μm (same scale in **A** and **B**). Scale bar in **F** = 200 μm (same scale in **D** and **E**).

195
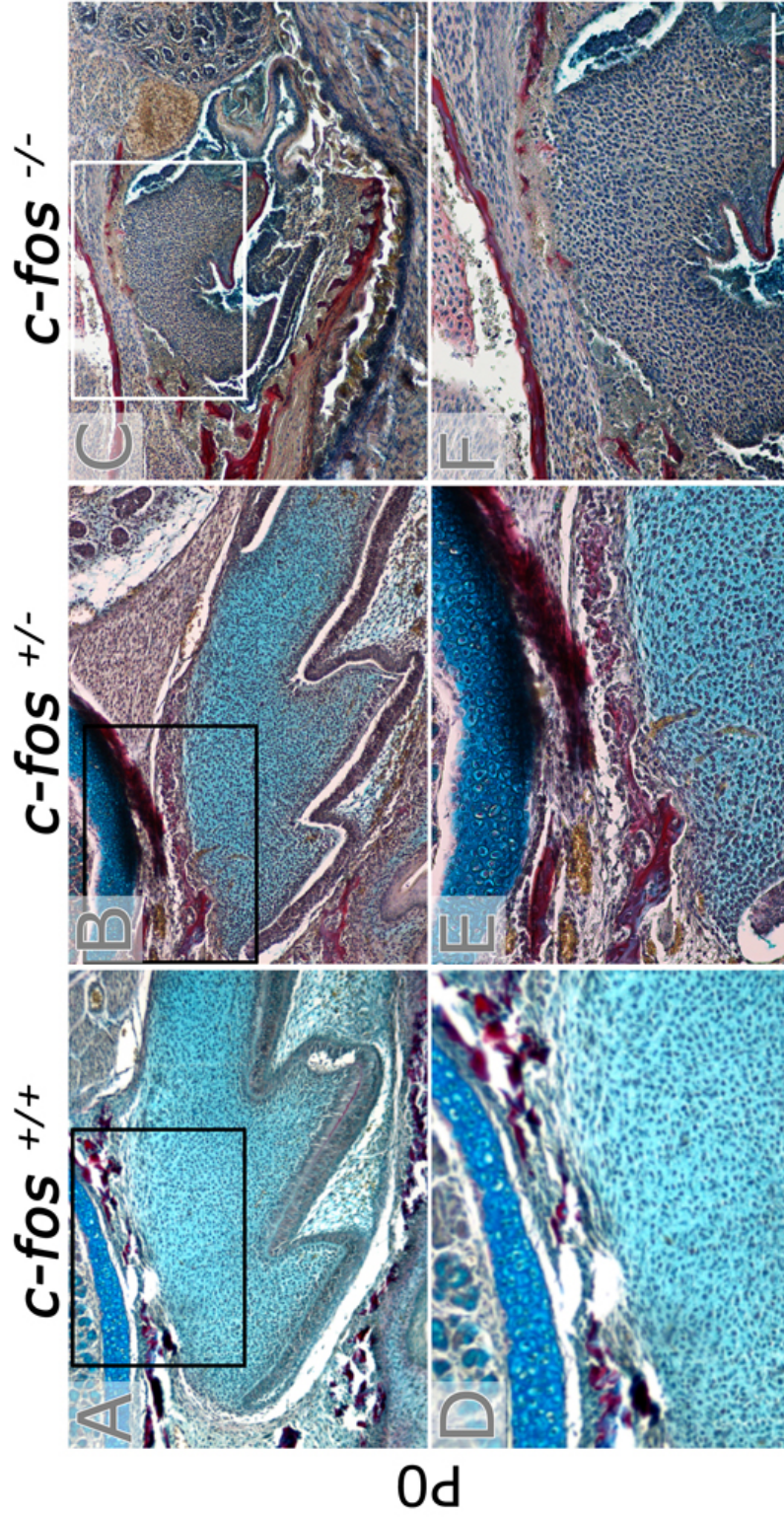
Figure 6.9 Histological sections of *c-Fos* maxillary first molars at birth.

Morphology after Trichrome staining at P0. At P0 both *c-Fos* heterozygous (**B**) and homozygous mutants (**C**) showed signs of bone invasion into the tooth-bone-interface encroaching on the tooth. (**D**, **E** and **F**) High power view of area boxed in (**A**, **B** and **C**) respectively. Scale bar in **C** = 300 μm (same scale in **A** and **B**). Scale bar in **F** = 200 μm (same scale in **D** and **E**).

196

In order to identify when this encroachment of bone happened, we looked at the tooth-bone interface of the mandibular first molar while the tooth was still developing at E16.5.

In Figure 6.10, an excellent tooth-bone-interface could be seen in the *c-Fos* wild-type, as a gap of reasonable size exists between the mandibular first molar tooth germ and the surrounding bone (Figure 6.10, D), whereas the gap was greatly narrowed in the *c-Fos* heterozygous mutant (Figure 6.10, C), as the bone was closer to the tooth germ epithelium with a resultant disrupted tooth-bone interface.
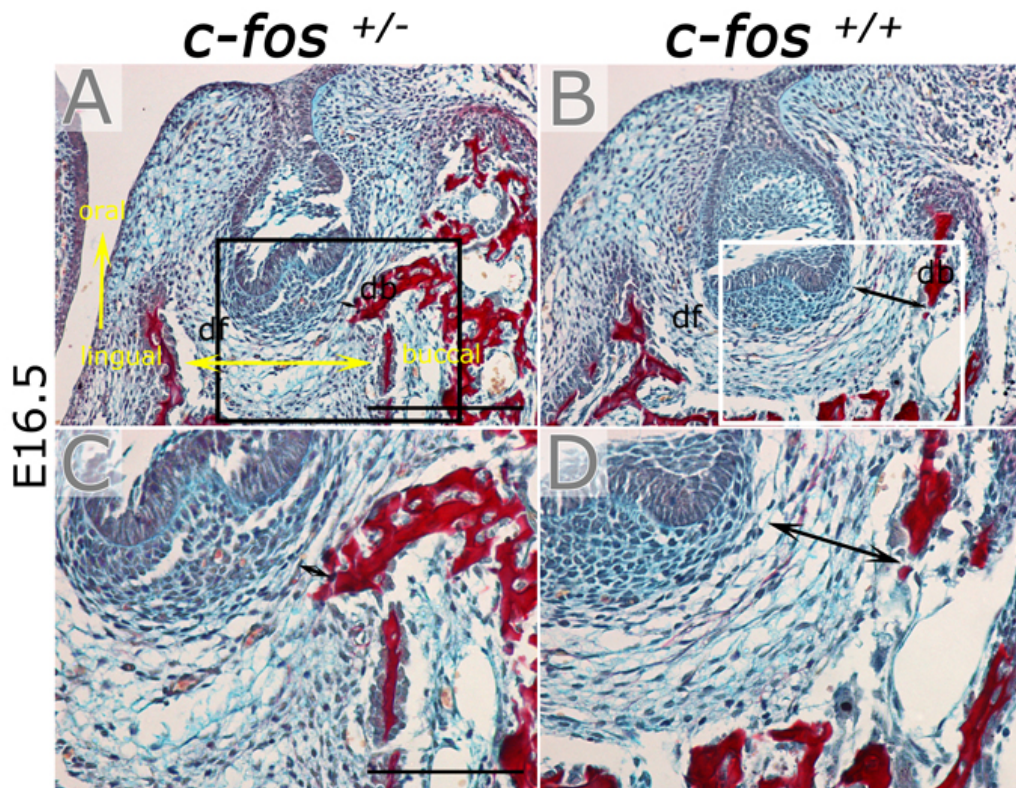
Figure 6.10 Histological sections of *c-Fos* mandibular first molars while developing.

Morphology after Trichrome staining at E16.5. (**A**) In the *c-Fos* heterozygous mutant, the alveolar bone forms very close to the outer enamel epithelium of the tooth germ in the cap stage. (**B**) In the *c-Fos* wild-type, the alveolar bone is found at a considerable distance from the tooth, and the tooth-bone interface is expanded. (**C**) and (**D**) High power view of area boxed in (**A**) and (**B**) respectively. Arrows placed from the outer enamel epithelium at the cervical loop to the alveolar bone (stained red). df = dental follicle, db = dentary bone. Scale bar in **A** = 200 μm (same scale in **B**). Scale bar in **C** = 100 μm (same scale in **D**).

6.3.4   Reduced osteoclastogenesis

6.3.4.1   TRAP staining

In order to see whether lower bone resorption, which is mainly the function of osteoclasts, has a role in the narrower tooth-bone interface observed in the *c-Fos* heterozygous mutant compared to the *c-Fos* wild-type, we stained histological

sections from both alternatively at E16.5 for Trichrome and TRAP. Afterwards, we counted the red stained positive TRAP cells and had the numbers compared.
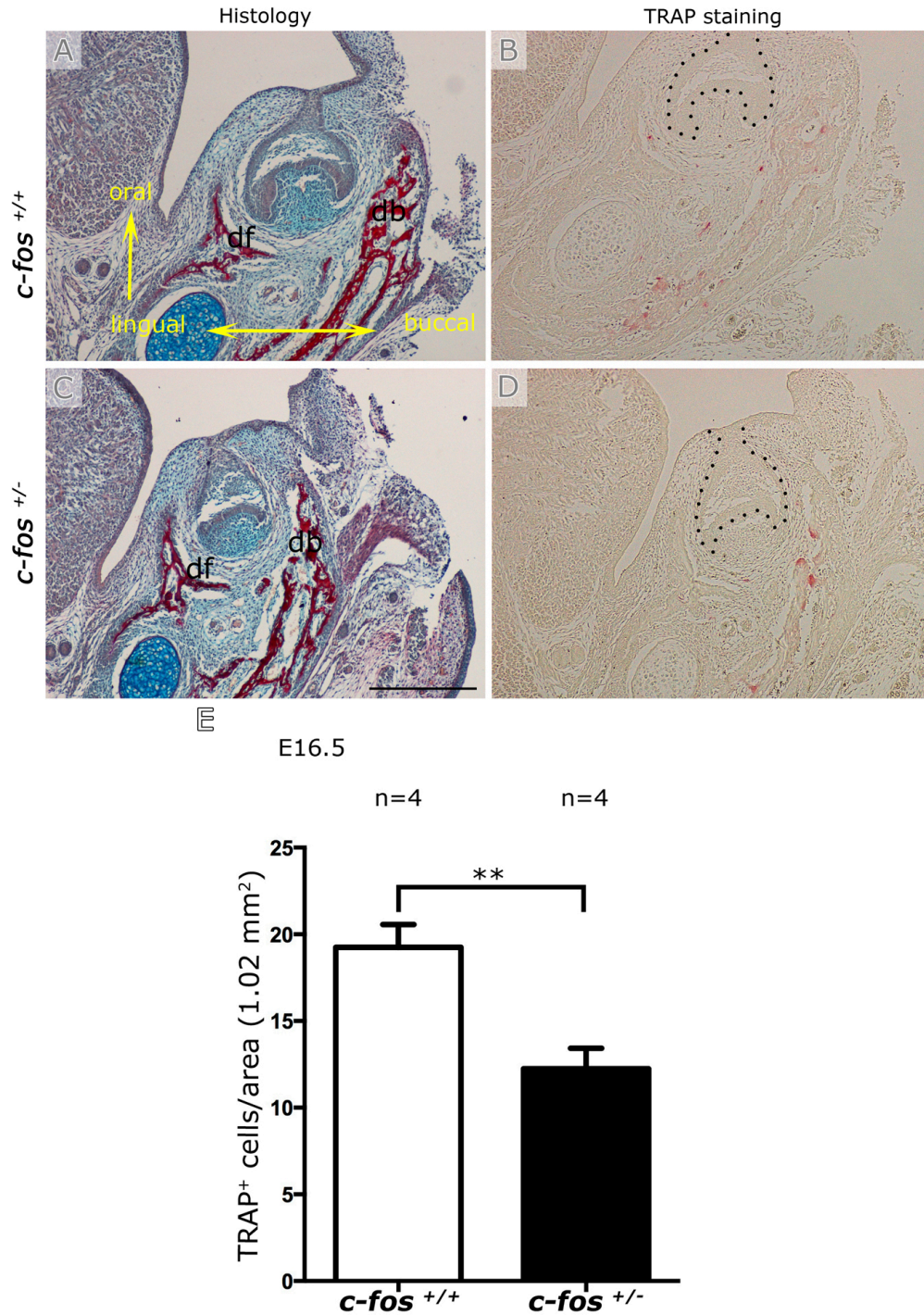
Figure 6.11 *c-Fos* **mandibular first molar TRAP positive cells count while developing.**

Figure 6.11 *c-Fos* **mandibular first molar TRAP positive cells count while developing.**

(**A** and **C**) Trichrome stain of an E16.5 mandibular first molar. *c-Fos* wild-type in (**A**) and *c-Fos* heterozygous mutant in (**C**). (**B** and **D**) Alternate sections stained for TRAP (red stain). (**E**) Graph showing the number of TRAP positive cells in *c-Fos* wild-types and *c-Fos* heterozygous mutants. Two (******) asterisks correspond to $p < 0.01$. Unpaired student's t-test. df = dental follicle, db = dentary bone. Epithelium of the tooth germ outlined with black dots in **B** and **D**. Scale bar in **C** = 300 μm (same scale bar in **A**, **B**, and **D**).

E16.5 first mandibular molars histological sections stained for Trichrome from wild-type and heterozygous *c-Fos* mutant (Figure 6.11, A and C), respectively. Alternate sections of the same stained for TRAP (Figure 6.11, B and D), respectively. The TRAP positive-stained cells were counted in both. After this, an unpaired t-test was applied on the numbers, and a statistically significant difference was found with the number of TRAP positive stained cells being larger around the *c-Fos* wild-type mandibular first molar than that of the *c-Fos* heterogeneous. The P value was found to be 0.0075, which is less than 0.05. The statistical findings were represented in the form of a graph (Figure 6.11, E).

We further investigated the difference in TRAP cells count between the *c-Fos* wild-type and *c-Fos* heterozygous mutant at the same age, E16.5, but focusing on the mandibular incisors in frontal section (Figure 6.12, A and B). The same results were obtained; the number of the TRAP positive stained cells was more statistically significant in the *c-Fos* wild-type incisor than the *c-Fos* heterozygous mutant one with a P value of 0.0015 being less than 0.05 after applying the unpaired t-test. The statistical finding was displayed graphically (Figure 6.12, C).

The heterozygous mice therefore do display a reduction in osteoclast numbers, which is likely to result in the subtle bone encroachment observed in the heterozygous mice during embryonic stages and at birth.
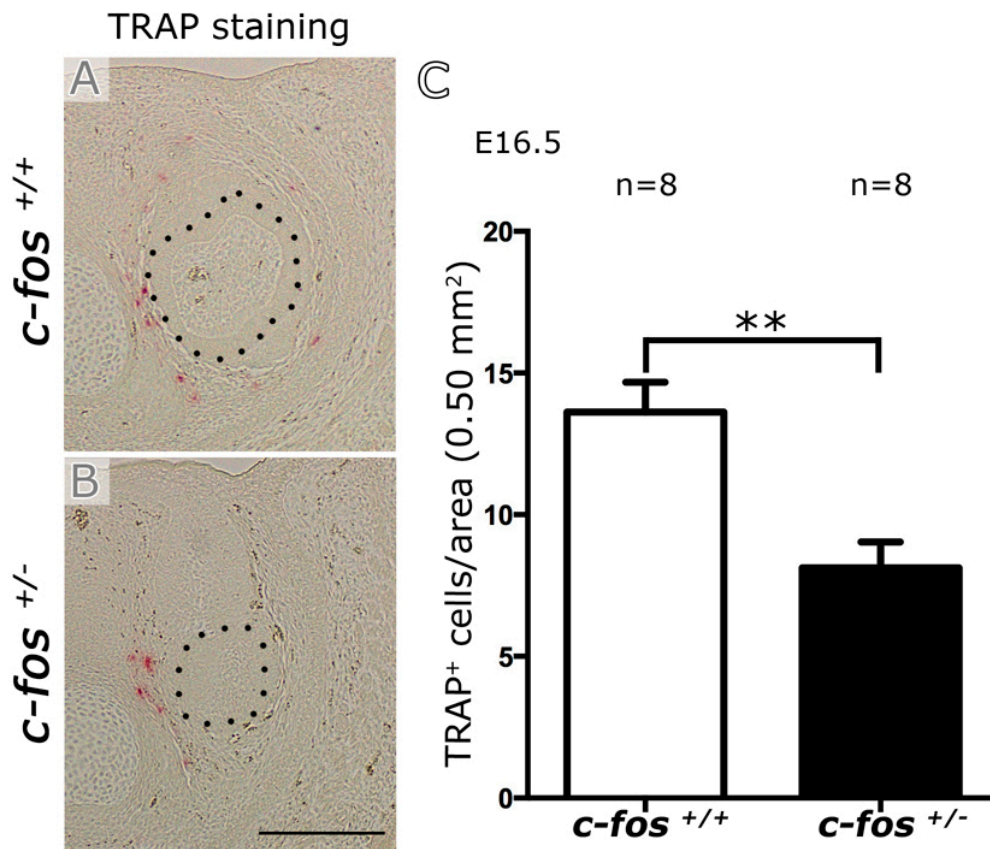
Figure 6.12 *c-Fos* **mandibular incisor TRAP positive cells count while developing.**

(**A** and **B**) TRAP stain of an E16.5 mandibular incisor. *c-Fos* wild-type in (**A**) and *c-Fos* heterozygous mutant in (**B**). (**C**) Graph showing the number of TRAP positive cells in *c-Fos* wild-type and *c-Fos* heterozygous mutant. Two (******) asterisks corresponds to $p<0.01$. Unpaired student's t-test. Epithelium of the tooth germ outlined with black dots in **A** and **B**. Scale bar in **B** = 200 μm (same scale bar in **A**).

6.3.5 Watching the process of bone encroachment

6.3.5.1 *Following the developing bone in mutant slice culture; Hets phenotype*

In order to follow this invasion of bone as the tooth developed, we moved to the slice culture technique to follow the relationship between the tooth and bone in the mutants as the teeth grew from the cap to the bell stages.
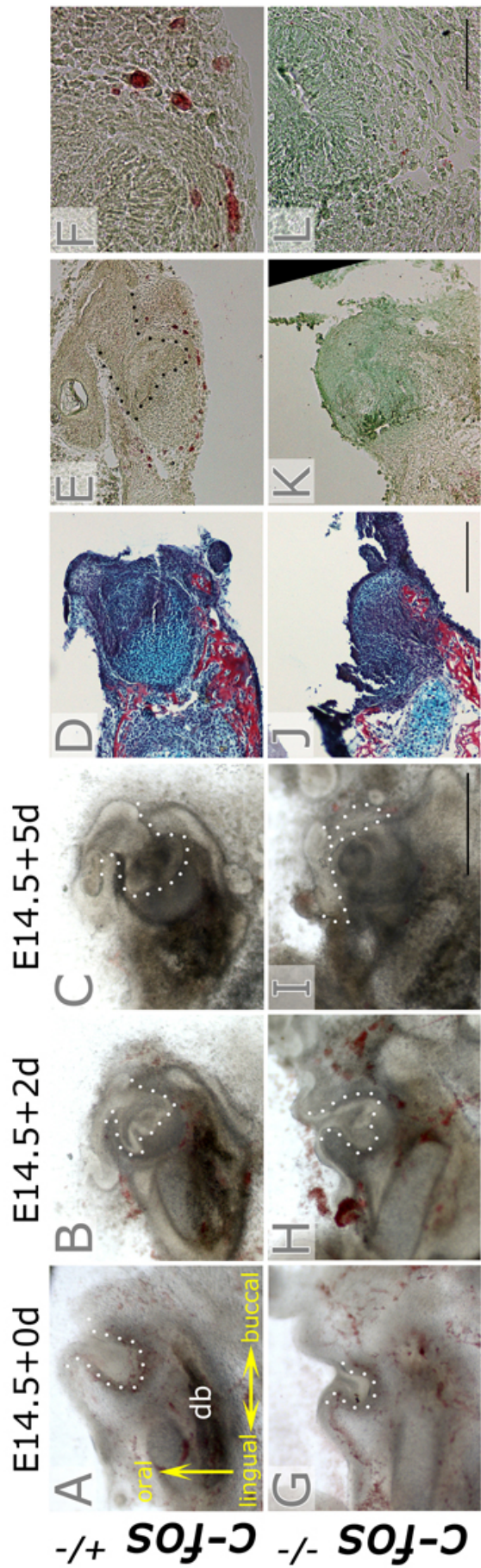
Figure 6.13 Cultures of *c-Fos* mutants, heterozygous and homozygous bud staged mandibular first molar tooth germs (E14.5) for 5 days.

(**A**) and (**G**) Day 0 *c-Fos* heterozygous and homozygous mutants respectively. (**B**) and (**H**) Day 2 of the same. (**C**) and (**I**) Day 5 of the same. (**D**) and (**J**) Trichrome stain of histological sections from (**C**) and (**I**) respectively. (**E**) and (**K**) Alternate sections of (**D**) and (**J**) stained for TRAP. (**F**) and (**L**) High power images from (**E**) and (**K**). db = dentary bone. Epithelium of the tooth germ outlined with white dots in **A**, **B**, **C**, **G**, **H**, and **I** while with black dots in **E**. Scale bar in **I** = 100 μm (same scale bar in **A**, **B**, **C**, **G**, and **H**). Scale bar in **J** = 200 μm (same scale bar in **D**, **E**, and **K**). Scale bar in **L** = 50 μm (same scale bar **F**).

203

The development of the mandibular first molar tooth germs from both *c-Fos* mutants, the heterozygous and the homozygous, was followed by using the slice culture method in explant cultures (Alfaqeeh and Tucker, 2013). E14.5 mandibular first molars from both mutants were followed over a period of 5 days (Figure 6.13, A to C and G to I). The mandibular first molar from both *c-Fos* mutants, the heterozygous and the homozygous, at E14.5 is found at the bud stage (Figure 6.13, A and G). Encroachment of the bone towards the dental papilla was also evident in the *c-Fos* heterozygous mutant in cultures (Figure 6.13, C), and close proximity of the alveolar bone to the external enamel epithelium of the mandibular first molar tooth germ was observed after Trichrome staining of histological section (Figure 6.13, D). Multinucleated red stained cells could be seen on the enlarged view of an alternate histological section stained for TRAP (Figure 6.13, F). The *c-Fos* homozygous mutant's mandibular first molar developed less than the heterozygous one while growing in slice culture (Figure 6.13, I). Histological section of the molar after Trichrome staining at the end of the culturing period revealed differentiating epithelium, interposing with the mesenchyme and loss of the classical tooth morphology (Figure 6.13, J).
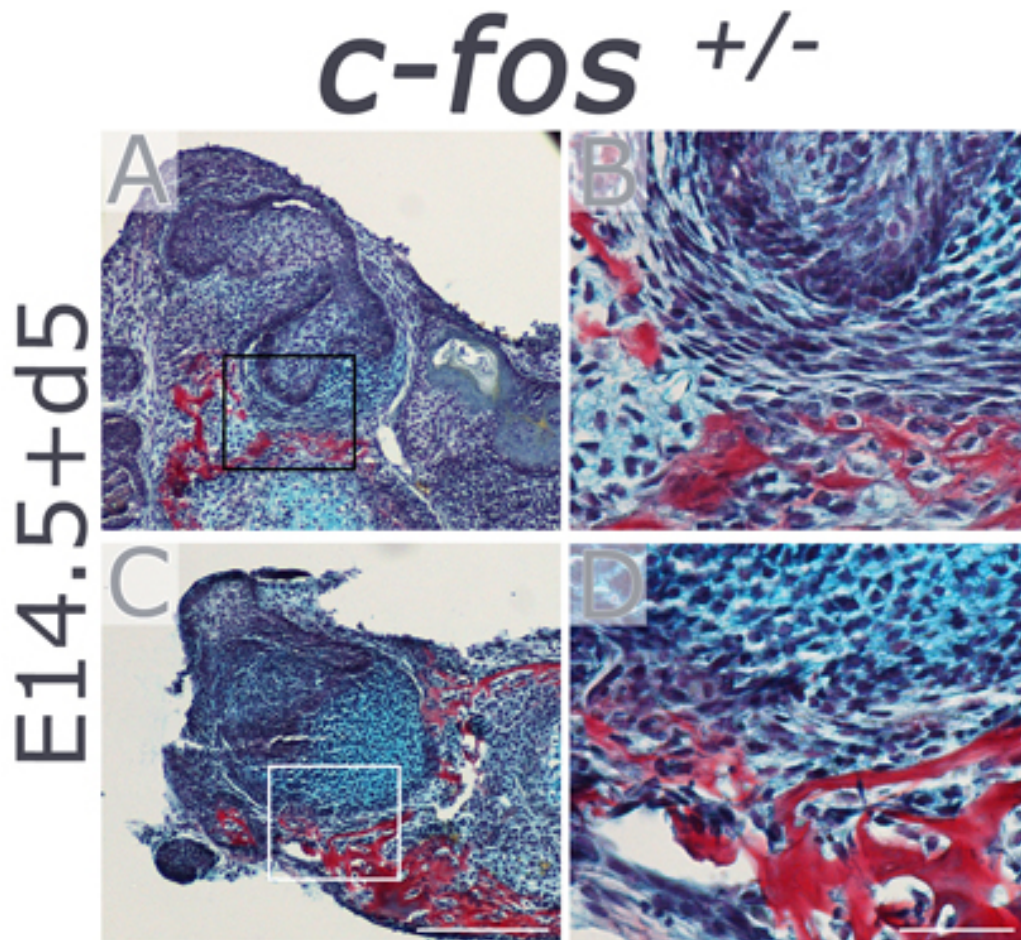
Figure 6.14 Histological sections showing signs of bone invasion into the tooth-bone interface of a *c-Fos* heterozygous mutant mandibular first molar after 5 days in culture.

(**A**) A bone-free tooth-bone-interface is shown in the first mandibular molar at the cap stage. (**C**) As the tooth expands it meets the bone, which starts to invade into the pulp. (**B**) and (**D**) High power view of area boxed in (**A**) and (**C**) respectively Scale bar in **C** = 200 μm (same scale bar in **A**). Scale bar in **D** = 50 μm (same scale bar in **B**).

Another example of an E14.5 mandibular first molar from a *c-Fos* heterozygous mutant that had been cultured for 5 days and then fixed for histology (Figure 6.14, A). The tooth germ can be noticed in the cap stage surrounded by a bone-free tooth bone interface (Figure 6.14, B); an enlarged view of the area boxed in Figure 6.14. In a second culture, however, the tooth has grown larger to the bell stage and has met the bone as it expands, obliterating the tooth-bone interface at this point and leading to bone contacting the epithelium of the tooth (Figure 6.14, C and D).
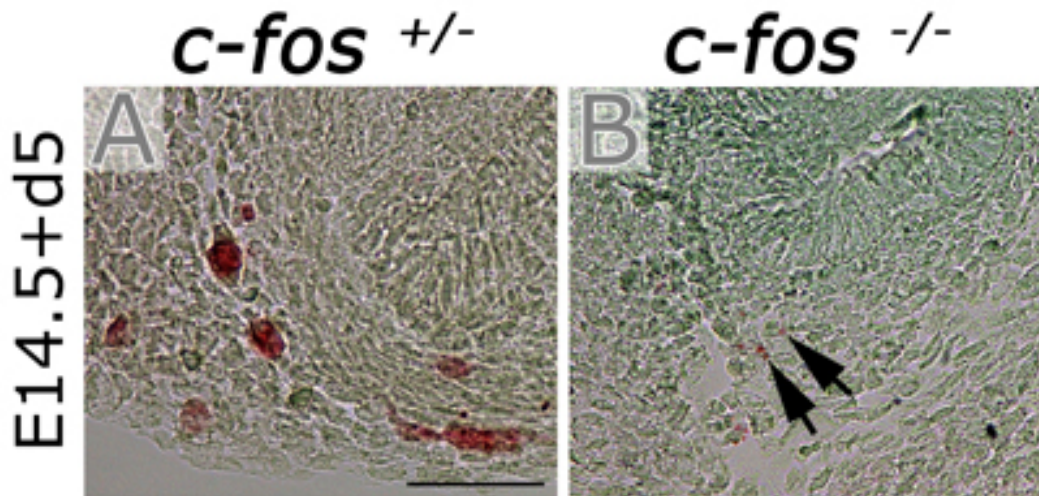
Figure 6.15 TRAP assay of a *c-Fos* heterozygous and homozygous mutants E14.5 mandibular first molar after 5 days in culture.

(**A**) Heterozygous *c-Fos*, (**B**) Homozygous *c-Fos* after culture of an E14.5 mandibular first molar for 5 days. (**A**) Multinucleated TRAP positive-stained cells observed around the TBI. (**B**) Weak TRAP staining in mono nucleated cells only, black arrows denote the some. Scale bar in **A** = 50 μm (same scale bar **B**).

Enlarged images of the TRAP stains of the E14.5 *c-Fos* heterozygous and homozygous mutants' mandibular first molar after 5 days in culture (Figure 6.15). Close up views reveal a few mononucleated red positive-stained cells in the *c-Fos* homozygous mutant (Figure 6.15, B), compared to the larger multinucleated red stained cells found in the *c-Fos* heterozygous mutant littermate (Figure 6.15, A). No multinucleated TRAP positive-stained cells were observed in the homozygotes, confirming the lack of active osteoclasts.

6.4   Discussion

The *c-Fos* mice have previously been investigated but the tooth phenotype has only been mentioned briefly in juvenile animals. Here I have characterized the defect, investigating the phenotype at a range of stages, both pre and post natal. I have characterized the mice using techniques not previously used on these mutants (Micro-CT, slice culture), and highlighted novel defects, for example the midline diastema, and shown that the heterozygous mice are not normal as previously indicated. Importantly, I was also able to show in my culture experiments that the bone was static and that the tooth invaded the bone, rather than the other way around. Tooth development in the homozygous mice was also seriously compromised in many cases and this would be interesting to study further.

The role of osteoclasts in preventing encroachment of bone was investigated in *c-Fos* knockout (KO) mice. Homozygous mutants have a cell-autonomous block in osteoclast differentiation and the teeth fail to erupt (Grigoriadis *et al.*, 1994). We evaluated the growth of *c-Fos* knockout and heterozygous$^{(+/-)}$ first molars (M1) and the distribution of osteoclasts *in vivo* and in tissue explant cultures.

The analysis of the *c-Fos* mutants demonstrated clear defects in bone remodeling and formation of the TBI in both homozygotes and heterozygotes. Unfortunately, the analysis of the *c-Fos* mice was hampered by poor reproductivity and neonatal death of the *c-Fos* homozygote mutants. Sterile matings have been reported in *c-Fos* mutants and smaller testes have been reported (Johnson *et al.*, 1992), perhaps explaining our reduced number of plugs. Sexual maturation of *c-Fos* null mutant mice of both genders was reported to occur around five weeks later than in wild-type (~10-15 weeks versus 4-5 weeks) (Wang *et al.*, 1992).

From those successful plugs, embryos displayed the expected Mendelian ratio, with heterozygous/heterozygous matings generating approximately 50%

heterozygotes and close to 25% wild type and homozygotes (Table 6.2). The situation at birth and at P21, however, was very different with only 3.13% of homomzygotes surviving to P21 (weaning). Death of homozygote neonates has been previously reported with 11% surviving to 15 days (Johnson *et al.*, 1992).

Often, traces of newborns were found in the cage in the form of a head or a limb indicating that the mother had eaten the dead or unhealthy pups. Interestingly, the number of heterozygous mice was lower than expected from Mendelian ratios. In heterozygous/heterozygous matings, double the numbers of heterozygotes would be expected compared to WT neonates, however similar numbers were recorded for the two groups (Table 6.2). This indicates that the heterozygotes also had reduced viability but more numbers would be necessary to confirm this finding. Wang *et al.* (1992) reported that the heterozygous *c-Fos* mutants in their study were normal with the females only having a problem with the transmission frequency.

The disorders of bone remodelling, in the *c-Fos* homozygous mutant skeleton were clearly evident using Micro-CT analysis, by the gain in skeletal mass of both the maxilla and the mandible, as well as the mass covering the crown of the teeth. Previous studies of defects in mice lacking *c-Fos* reported osteopetrosis and lack of incisors teeth in mice of 4 weeks old and above (Johnson *et al.*, 1992; Wang *et al.*, 1992). However, our examination of the incisors bearing areas confirmed at least the presence of the maxillary and mandibular incisors crowns in a 3 week old *c-Fos* homozygous mutant with a midline diastema in the maxilla. The midline diastema is a space between the maxillary central incisors; the presence of fibrosis or interdental bone mesiodens has been reported as a possible cause of diastemas (Huang and Creath, 1995), and the lower remodelling with the persistence of bone on both medial surfaces of the maxillary incisors could have accounted for the presence of the diastema. Although molar crown development appeared normal, no roots were evident in the homozygous mutant investigated. The investigated heterozygote mice, in

contrast to the homozygotes appeared relatively normal, with correct eruption of the teeth.

The failure of tooth eruption in the *c-Fos* knockout, as observed for all teeth, both molars and incisors, agrees with the findings of previous investigators (Johnson *et al.*, 1992; Wang *et al.*, 1992). Alveolar bone remodeling in association with root elongation has been reported as a basic parameter for tooth eruption (Marks and Schroeder, 1996), in view of this the lack of teeth eruption could be due to the absence of roots which are known to have a role in the eruption process (Riolo and Avery, 2002). Following completion of crown formation, the apical mesenchyme forms the developing periodontium while the inner and outer enamel epithelia fuse below the level of the crown cervical margin to produce the Hertwig's epithelial root sheath (HERS), a bilayered epithelial sheath, during tooth development (Zeichner-David *et al.*, 2003). Proliferation of the HERS is essential for root development (Lungova *et al.*, 2011), and for correct root development, the bone surrounding the base of the tooth needs to be cleared. In the *c-Fos* homozgote, it appears likely that the failure in bone resorption meant that a path for root development was not cleared, hindering the process of HERS proliferation and hence the process of root development. From the histology sections at P0, the fusion of the inner and outer enamel epithelia appeared normal, indicating the defect was not due to an innate problem in HERS formation, however, later stage mutants (from P4) would be needed to assess HERS development precisely. At this stage, a reduction in the TBI was evident in both homozygotes and heterozgotes, particularly associated with the area where the roots would form. In keeping with this phenotype at P0, heterozygotes also showed a defect in the TBI at E16.5. The presence of a TBI defect in heterozygous mice at two developmental stages but not at weaning (as indicated by Micro-CT) indicates that the heterozygous defect might be fairly variable, or alternatively might suggest that strongly affected individuals did not survive to weaning. More numbers would be necessary to assess this further.

The histological study of the *c-Fos* heterogeneous E14.5 first mandibular molars following five days in culture revealed two different tooth-bone-interface phenotypes; a bone-free one in one tooth germ and a bone-invaded one in another. The static nature of the dentary bone during development in the *c-Fos* mice model, and the extent to which the tooth germ grows, could be a possible interpretation of such findings. At earlier stages of tooth germ development, a clear tooth-bone interface at a reasonable distance from the tooth germ epithelium was observed but as the tooth germ grew, it started to impact on the static dentary bone, resulting in the bone encroachment seen in some samples. Loss of bone retraction as the tooth advances would be a result of the defect in the process of bone resorption. Heterozygous cultures showed different degrees of bone encroachment, indicating a range in the extent of the phenotype.

Osteoclasts create the space in which the tooth grows intact from any bone invasion and reserves the gap between the tooth and the bone required for the soft tissues of the periodontium development (Fleischmannova *et al.*, 2010; Alfaqeeh *et al.*, 2013). The reduced number of TRAP positive stained cells detected in the *c-Fos* heterogeneous first mandibular molar at E16.5 appears to impact on bone clearance so that the tooth germs encountered bone as it grew. The reduced number of TRAP positive stained cells in the *c-Fos* heterozygous surrounding the molars was further confirmed by analysis of the lower incisor tooth germ, which showed a similar reduction in TRAP positive cells in the heterozygote.

The homozygous mutants showed poor development in culture, with a delay in reaching the cap stage compared to WT littermates.

A previous study reported reduced fetal and placental weights at E15.5 of *c-Fos* homozygous and heterozygous mutant suggesting *c-Fos* expression being involved in some aspect of placental development and function (Johnson *et al.*, 1992). *c-Fos* null mutants' significant loss of viability at birth was reported in the

same study due to placental insufficiency in the embryo. After 5 days in culture, cyst-like tissue was evident, surrounded by large amounts of bone, showing normal tooth development had been disrupted.

In cultured homozygote molars, some TRAP stain was evident, indicating the presence of mononucleated TRAP positive stained cells in the tooth-bone interface of the *c-Fos* mutant first mandibular molar. The hypothesis that osteoclasts and macrophage progenitors are developmentally related was supported earlier and a lineage shift between osteoclasts and macrophages with a resultant increase of bone marrow macrophages has previously been reported due to the lack of *Fos* (Grigoriadis *et al.*, 1994). In view of this report, the TRAP stained mononucleated cells could be macrophages instead of osteoclasts.

When the process of bone remodelling is disrupted; the amount of bone produced is affected i.e. Overall amount. The bone invasion seen in the tooth-bone interface is not due to enhancement in bone formation in the mutants as osteoblasts differentiation appears normal (Foxworthy, 2003). The defect is therefore due to disruption in the process of bone resorption.

In conclusion these results show that osteoclasts in the alveolar bone play an essential role in promoting the maintenance of the TBI, removing bone as the tooth advances and providing the space required to accommodate the developing tooth. Defects in this process lead to ankylosis and may restrict the growth of the tooth.

7   <u>General Discussion</u>

In the first results chapter, the close relationship between the tooth and bone during development was described, illustrating the localisation of osteoclasts. Osteoclasts were found to be closely associated with the border of the developing bone, lining the TBI, but not within the TBI itself. Next, the slice culture was used to follow tooth development in explant culture, providing an excellent opportunity for manipulation and lineage tracing. Finally, DiI labelling experiments showed the contribution of two sources of cells in the formation of alveolar bone namely, dental follicle cells from around the tooth and, bone cells from the margins of the dentary.

In the second results chapter, the impact of the tooth on the bone and bone on the tooth was addressed. Isolation of the mandibular first molar (M1) tooth germ from the surrounding mesenchyme and alveolar bone led to an expansion of the tooth germ, therefore, the presence of the surrounding tissue appeared to restrict the growth of developing tooth germs. Next, the impact of the tooth epithelium on the pattern of osteoclasts was examined. Removing the tooth epithelium in culture experiments still led to the normal layout of osteoclasts at E14.5 indicating either that their pattern was controlled by a signal released from the dental epithelium prior to its removal or that the pattern was controlled by a signal from the dental mesenchyme. Lastly, the effect of manipulating the BMP signalling pathway on the differentiation of cells in the TBI during tooth development was studied. Following local application of BMP-4 and Noggin on agarose coated beads in culture, a change in fate of the TBI was observed. We observed a local reduction in the TBI near to the BMP-4 bead with enhanced bone formation. In contrast, we observed a local widening in the TBI when Noggin beads were implanted with a loss of bone.

In the third results chapter, disrupting the process of osteoclastogenesis through manipulation of the RANK-RANKL signalling pathway was investigated. The expression of OPG, RANK, and RANKL genes involved in the pathway was

first examined. *In situ* hybridisation revealed the presence of all three genes in the alveolar bone and the OPG and RANKL only in the dental epithelium. Addition of exogenous RANKL to tooth explants in culture resulted in a statistically significant increase in osteoclast numbers and a widening of the TBI. On the other hand, the results obtained after exogenous OPG addition were regarded as inconsistent due to high variability. However, correlation of the difference in bone growth within a cultured tooth germ with the presence of osteoclasts showed absence of osteoclasts in areas of bone encroachment and the opposite, presence of osteoclasts in areas devoid of bone. These experiments highlighted the importance of RANK signaling in controlling osteoclastogenesis and in control of the TBI.

In the fourth and final results chapter, the TBI in *c-Fos* mutants, a knockout mouse known to have a defect in osteoclastogenesis, resulting in lack of osteoclast production, was analysed. From genotyping, *c-Fos* mutant embryos displayed the expected Mendelian ratio, however, after birth, almost all the homozygotes died and the heterozygotes viability was compromised. In a 3 week old *c-Fos* homozygote, Micro-CT analysis made evident the osteopetrotic phenotype, as there was a net gain in the skeletal mass of both the maxilla and mandible, as well as a mass covering the crown of the teeth. We also observed defects in the midline diastema, tooth impaction, and lack of roots. In the *c-Fos* heterozygous and homozygous mutants, the TBI showed signs of bone invasion, encroaching on the M1. TRAP assay could not detect osteoclasts in the homozygotes; instead a few positive-stained mononucleated cells were observed which were probably macrophages. In the heterozygous mice, a reduction of osteoclasts was observed during embryonic development, showing that osteoclastogenesis was also compromised in the heterozygotes. In general, the M1s of the homozygotes had retarded development when compared to the heterozygotes M1s in culture, and at the end of the culturing period, loss of the classical tooth morphology was observed in the homozygotes with the dental epithelium interposing with the mesenchyme.

These results are summed up in Figure 7.1. Control of the TBI appears to be a two-pronged process with:

1. Control of osteoclasts used to remove the bone (osteoclastogenesis).

2. Inhibition of bone induction (osteogenesis).

Together these two processes create a bone-free zone around the tooth. By changing either of these processes; the TBI is disrupted and tooth development is altered.
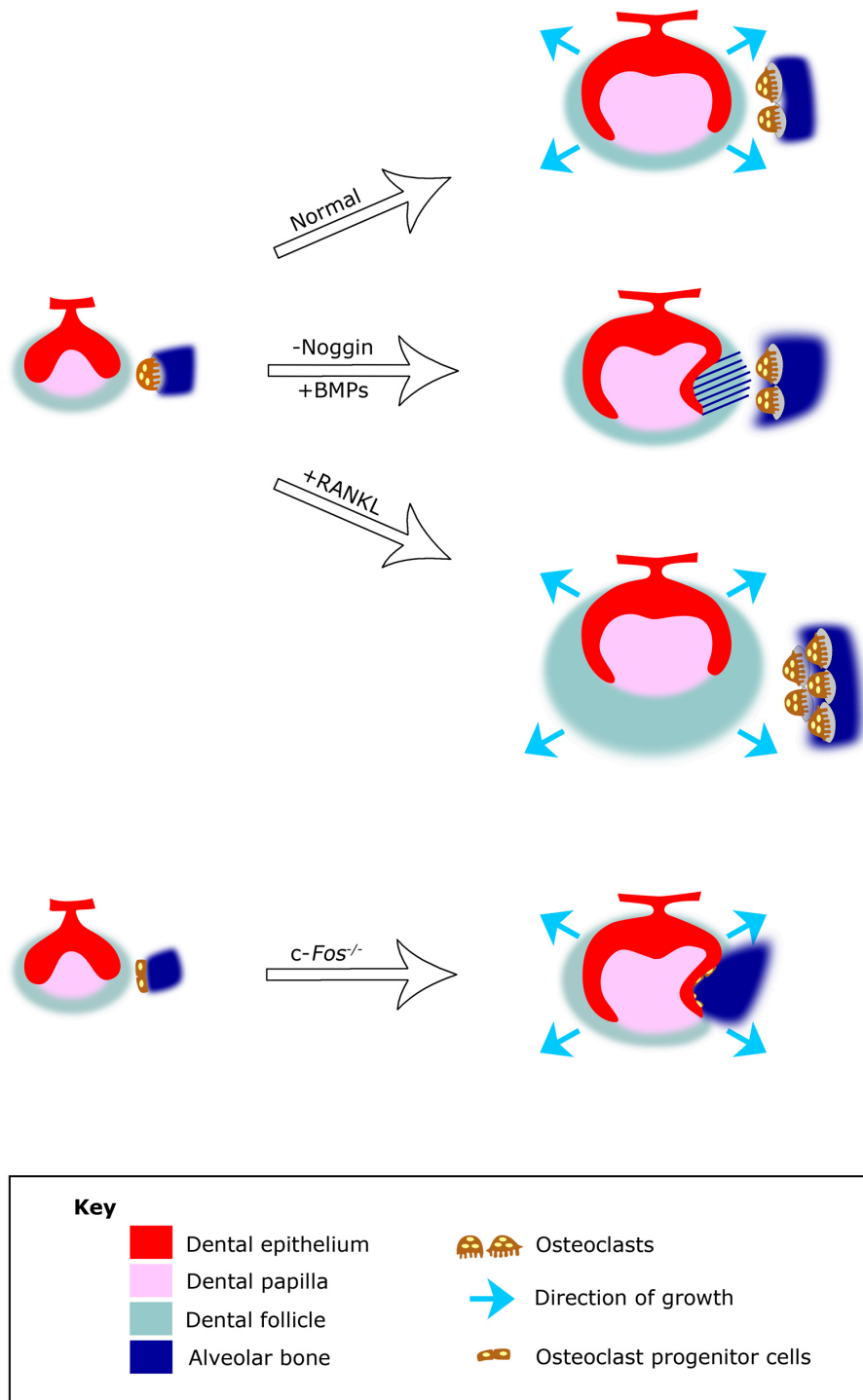
Figure 7.1 Diagrammatic representation of the TBI and alveolar bone formation during development in the different models studied in this thesis.

From data collected in this thesis on gene expression and osteoclast position, combined with published data on gene and protein expression levels, we can start to put together a picture of signaling in the TBI, tooth and bone. This can be used to predict where various pathways are active. For example, the lack of RANK expression in the tooth compared to the bone, in contrast to expression of the soluble factors RANKL and OPG in the tooth and bone, indicates that the highest area of activation of this pathway would be on the border of the bone adjacent to the tooth. Such localized activation would explain the high numbers of osteoclasts positioned along this border region. (Figure 7.2, A).

A similar activation area can be predicted from the known expression of Noggin and BMP in the tooth, bone and TBI. Here, Noggin in the TBI would exclude activity of BMP in this region, preventing osteoblast induction, while in the surrounding mesenchyme the lack of Noggin would allow the high levels of BMP to start generating bone (Figure 7.2, B).
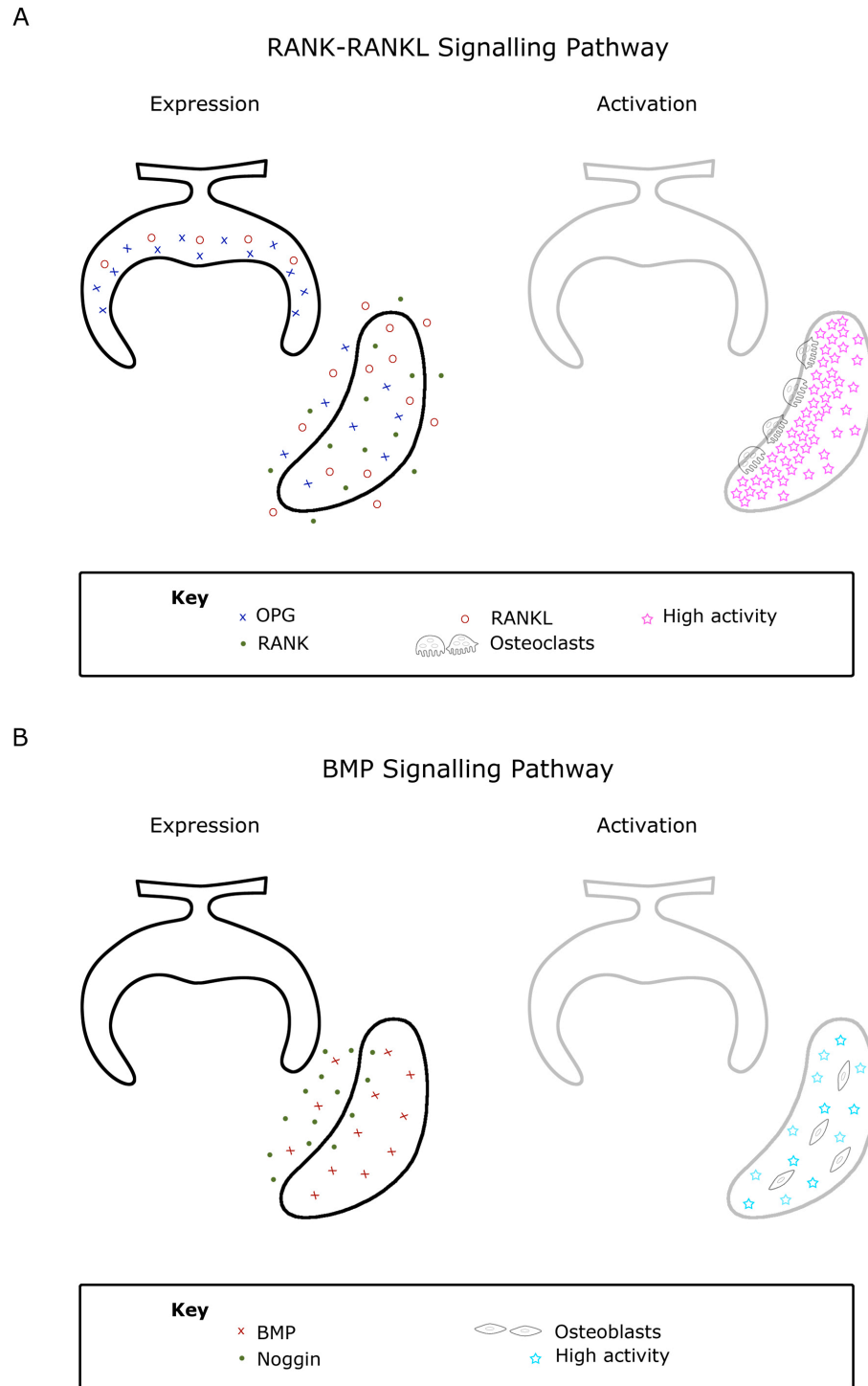
Figure 7.2 Diagrammatic representation of the expression of the signalling pathways studied in the TBI and alveolar bone and visualization of the activation of the pathway.

In the experiments where the surrounding mesenchyme and bone were physically removed, the tooth expanded (Figure 7.3). One can therefore imagine two sets of pressures: one exerted by the tooth as it proliferates, signaling to the osteoclasts to clear a path for expansion, and a second opposing force from the surrounding bone constraining growth and controlling the final tooth size or rate of growth. Interestingly, although some tooth germs appeared larger after RANKL treatment, and the TBI expanded, the effect on size was not statistically significant. It is possible that manipulating the osteoclast levels (as in results chapter 3) is not able to have the same effect as physically removing the bone (as in results chapter 2). It would be interesting to investigate this further.
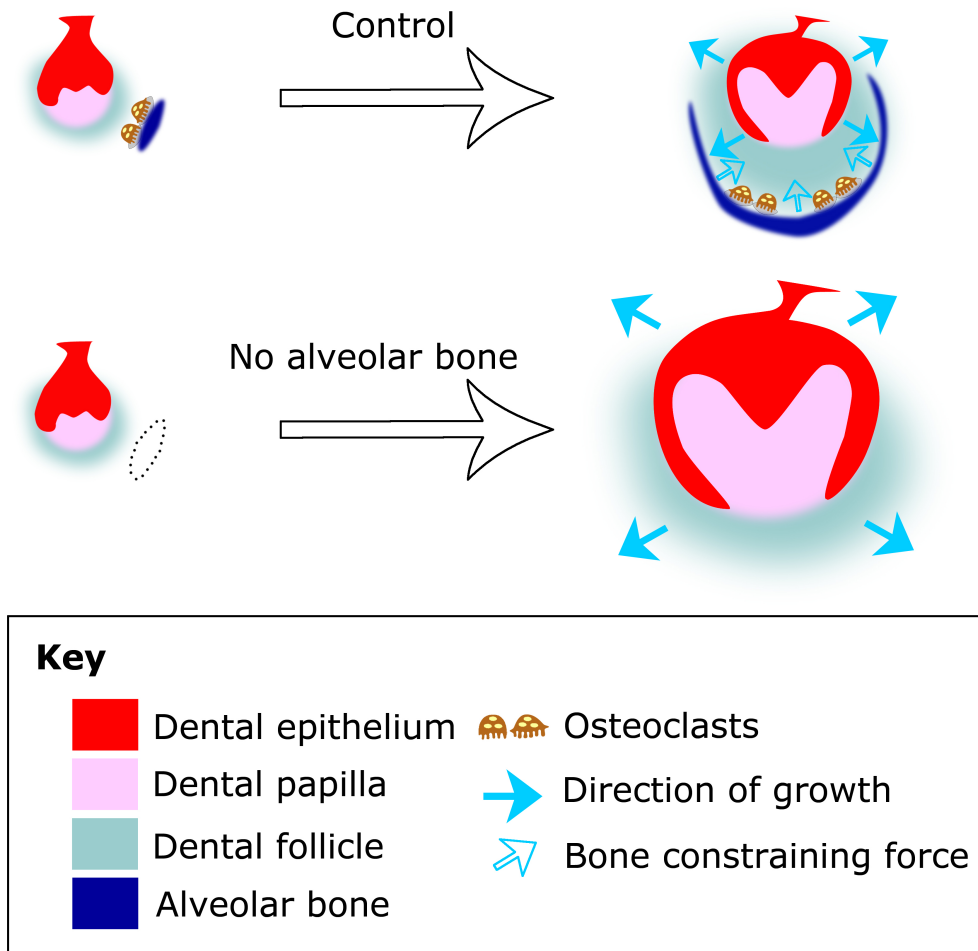
Figure 7.3 Diagrammatic representation of the findings of the TBI formation during development with and without the surrounding tissues, including the alveolar bone.

Although this is a basic science project, the scope of this thesis provides hints that could help shed light on clinical problems. For example, this work can provide an understanding of the mechanisms that underlie ankylosis, in which it is impossible to move teeth when a force is applied. For example, in cases of retained primary molars, this could be caused by genetic defects (for example defects in osteoclastogenesis) or environmental effects (for example changes to the mechanical forces). How the TBI forms can also enhance our understanding of cases of ankylosis that occurs later in life, informing how the TBI (containing the periodontal ligament) is maintained around the root in adults.

Having approached ankylosis using the binocular of molecular and developmental biology, we could elaborate on the causes of ankylosis and create new opportunities for having the condition reverted or diminished.

The key of ankylosis treatment would be to restore the natural biology of the tooth-bone interface, and the normal rate of bone remodeling.

This study highlights that ankylosis can form by incorrect bone deposition or incorrect removal of bone, for example, an incorrect balance of osteoblasts, due to a disruption of BMPs or Noggin pathways, or the invasion of bone due to a problem in the osteoclastogenesis driven by defects in RANKL signalling or c-Fos. Such diverse causes should be taken into account before treatments are considered. For example, is it necessary to stimulate osteoclasts or inhibit osteoblasts to shift the balance back to normal? Therefore, the detection of the balance of osteoblasts and osteoclasts, and the rate of bone remodeling, needs to be able to be identified prior to the local application of drugs. Whether such treatments are possible through the local application of available drugs that treat these conditions, for example via injection or new methods such as nano-drops, is something that warrants investigation. For example, there are drugs that can enhance or block activity of osteoblast receptors and therefore modulate bone remodelling and tooth movement (Davidovitch and Murphy, 2009). Meanwhile, transfer of the RANKL gene to the periodontal tissue has been shown to activate osteoclastogenesis and accelerate the amount of experimental tooth movement

(Kanzaki *et al.*, 2006). Gene transfer of OPG to the periodontal tissue in contrast inhibited experimental tooth movement (Kanzaki *et al.*, 2004). Local RANKL gene transfer might therefore be a useful tool not only for shortening orthodontic treatment, but also for moving ankylosed teeth, where the teeth are fused to the surrounding bone (Kanzaki *et al.*, 2006).

An understanding of the TBI biology could also be important to be able to artificially recreate and sustain a TBI with a periodontal ligament, for example in cases such as a prosthetic dental implant or an avulsed tooth that has been put back. Upon replacing missing teeth with an implant, prior to placement of the implant, the socket could be treated with drugs that would facilitate PDL recreation in the form of a special coating of the implant that would stimulate PDL attachment. Alternatively, periodontal precursor cells could be used to try and recreate the TBI. Special treatment of avulsed teeth prior to re-implantation could also reduce risk of them ending up ankylosed.

There are many experiments that I would like to now try to move my studies in a more translational direction. In particular, having established the *c-Fos* mice as a great model for ankylosis I would like to try and rescue the phenotype. This could be achieved by trying to stimulate the osteoclast pathway downstream of *c-Fos*. Having characterised the TBI in the developing tooth in the embryo and neonate, it would be a natural progression to study the TBI in the adult, when the TBI houses the periodontal ligament. Whether similar forces and signalling occur in the adult as the embryo would be really interesting. Lastly I would like to compare development of the TBI in the first and last molar (M1 and M3) as these teeth develop at different time-points and in very different surroundings. The M1 develops with the forming bone, while the M3 develops within an already mature bony mandible. The TBI is therefore set up in a different way in these two similar tooth types.

Such future work and new innovative treatments would make moving any tooth that is present in the oral cavity possible and would assure that the biological processes associated with aging happen naturally so everyone could posses a bright smile.

Bibliography

Abe, M., Tamamura, Y., Yamagishi, H., Maeda, T., Kato, J., Tabata, M. J., Srivastava, D., Wakisaka, S. and Kurisu, K. (2002) 'Tooth-type specific expression of dHAND/Hand2: possible involvement in murine lower incisor morphogenesis', *Cell and Tissue Research* 310(2): 201-12.

Aberg, T., Wozney, J. and Thesleff, I. (1997) 'Expression patterns of bone morphogenetic proteins (Bmps) in the developing mouse tooth suggest roles in morphogenesis and cell differentiation', *Developmental Dynamics* 210(4): 383-96.

Abu-Amer, Y., Erdmann, J., Alexopoulou, L., Kollias, G., Ross, F. P. and Teitelbaum, S. L. (2000) 'Tumor necrosis factor receptors types 1 and 2 differentially regulate osteoclastogenesis', *Journal of Biological Chemistry* 275(35): 27307-10.

Acharya, A., Shetty, S. and Deshmukh, V. (2010) 'Periodontal Ligament Stem Cells: An Overview', *Journal of Oral Biosciences* 52(3): 275–282.

Aeschlimann, D. and Evans, B. A. (2004) 'The vital osteoclast: how is it regulated?', *Cell Death and Differentiation* 11 Suppl 1: S5-7.

Akiyama, T., Dass, C. R., Shinoda, Y., Kawano, H., Tanaka, S. and Choong, P. F. (2010) 'PEDF regulates osteoclasts via osteoprotegerin and RANKL', *Biochemical and Biophysical Research Communications* 391(1): 789-94.

Albers, D. D. (1986) 'Ankylosis of teeth in the developing dentition', *Quintessence International* 17(5): 303-8.

Alfaqeeh, S. A., Gaete, M. and Tucker, A. S. (2013) 'Interactions of the Tooth and Bone during Development', *Journal of Dental Research* 92(12): 1129-35.

Alfaqeeh, S. A. and Tucker, A. S. (2013) 'The Slice Culture Method for Following Development of Tooth Germs In Explant Culture', *Journal of Visualized Experiments* 81(e50824).

Alvarez-Perez, M. A., Narayanan, S., Zeichner-David, M., Rodriguez Carmona, B. and Arzate, H. (2006) 'Molecular cloning, expression and

immunolocalization of a novel human cementum-derived protein (CP-23)', *Bone* 38(3): 409-19.

Anderson, G. J. and Darshan, D. (2008) 'Small-molecule dissection of BMP signaling', *Nature Chemical Biology* 4(1): 15-6.

Angel, P. and Karin, M. (1991) 'The role of Jun, Fos and the AP-1 complex in cell-proliferation and transformation', *Biochimica et Biophysica Acta* 1072(2-3): 129-57.

Aspenberg, P., Jeppsson, C. and Economides, A. N. (2001) 'The bone morphogenetic proteins antagonist Noggin inhibits membranous ossification', *Journal of Bone and Mineral Research* 16(3): 497-500.

Azria, M., Copp, D. H. and Zanelli, J. M. (1995) '25 years of salmon calcitonin: from synthesis to therapeutic use', *Calcified Tissue International* 57(6): 405-8.

Baran, D. T. and Braverman, L. E. (1991) 'Thyroid hormones and bone mass', *Journal of Clinical Endocrinology and Metabolism* 72(6): 1182-3.

Beertsen, W., McCulloch, C. A. and Sodek, J. (1997) 'The periodontal ligament: a unique, multifunctional connective tissue', *Periodontology* 2000 13: 20-40.

Bellows, C. G., Wang, Y. H., Heersche, J. N. and Aubin, J. E. (1994) '1,25-dihydroxyvitamin D3 stimulates adipocyte differentiation in cultures of fetal rat calvaria cells: comparison with the effects of dexamethasone', *Endocrinology* 134(5): 2221-9.

Bergers, G., Graninger, P., Braselmann, S., Wrighton, C. and Busslinger, M. (1995) 'Transcriptional activation of the fra-1 gene by AP-1 is mediated by regulatory sequences in the first intron', *Molecular and Cellular Biology* 15(7): 3748-58.

Birkedal-Hansen, H. (1993) 'Role of matrix metalloproteinases in human periodontal diseases', *Journal of Periodontology* 64(5 Suppl): 474-84.

Bonucci, E. (1990) The ultrastructure of the osteocyte *Ultrastructure of skeletal tissues: bone and cartilage in health and disease*. Boston: Kluwer Academic Publishers.

Bord, S., Ireland, D. C., Beavan, S. R. and Compston, J. E. (2003) 'The effects of estrogen on osteoprotegerin, RANKL, and estrogen receptor expression in human osteoblasts', *Bone* 32(2): 136-41.

Bosshardt, D. D. (2005) 'Are cementoblasts a subpopulation of osteoblasts or a unique phenotype?', *Journal of Dental Research* 84(5): 390-406.

Bosshardt, D. D. and Schroeder, H. E. (1996) 'Cementogenesis reviewed: a comparison between human premolars and rodent molars', *Anatomical Record* 245(2): 267-92.

Bostanci, N., Ilgenli, T., Emingil, G., Afacan, B., Han, B., Toz, H., Atilla, G., Hughes, F. J. and Belibasakis, G. N. (2007a) 'Gingival crevicular fluid levels of RANKL and OPG in periodontal diseases: implications of their relative ratio', *Journal of Clinical Periodontology* 34(5): 370-6.

Bostanci, N., Ilgenli, T., Emingil, G., Afacan, B., Han, B., Toz, H., Berdeli, A., Atilla, G., McKay, I. J., Hughes, F. J. *et al.* (2007b) 'Differential expression of receptor activator of nuclear factor-kappaB ligand and osteoprotegerin mRNA in periodontal diseases', *Journal of Periodontal Research* 42(4): 287-93.

Boughner, J. C. (2011) 'Making Space for Permanent Molars in Growing Baboon (Papio anubis) and Great Ape (Pan paniscus and P. troglodytes) Mandibles: Possible Ontogenetic Strategies and Solutions', *Anatomy Research International* 2011: 484607.

Brunet, L. J., McMahon, J. A., McMahon, A. P. and Harland, R. M. (1998) 'Noggin, cartilage morphogenesis, and joint formation in the mammalian skeleton', *Science* 280(5368): 1455-7.

Bucay, N., Sarosi, I., Dunstan, C. R., Morony, S., Tarpley, J., Capparelli, C., Scully, S., Tan, H. L., Xu, W., Lacey, D. L. et al. (1998) 'osteoprotegerin-deficient mice develop early onset osteoporosis and arterial calcification', *Genes and Development* 12(9): 1260-8.

Byers, M. R., Mecifi, K. B. and Iadarola, M. J. (1995) 'Focal c-fos expression in developing rat molars: correlations with subsequent intradental and epithelial sensory innervation', *International Journal of Developmental Biology* 39(1): 181-9.

Cao, X. (2011) 'Targeting osteoclast-osteoblast communication', *Nature Medicine* 17(11): 1344-6.

Capdevila, J. and Johnson, R. L. (1998) 'Endogenous and ectopic expression of noggin suggests a conserved mechanism for regulation of BMP function

during limb and somite patterning', *Developmental Biology* 197(2): 205-17.

Capulli, M., Paone, R. and Rucci, N. (2014) 'Osteoblast and osteocyte: games without frontiers', *Archives of Biochemistry and Biophysics* 561: 3-12.

Caton, J. and Tucker, A. S. (2009) 'Current knowledge of tooth development: patterning and mineralization of the murine dentition', *Journal of Anatomy* 214(4): 502-15.

Caubet, J. F. and Bernaudin, J. F. (1988) 'Expression of the c-fos proto-oncogene in bone, cartilage and tooth forming tissues during mouse development', *Biology of the Cell* 64(1): 101-4.

Chai, Y., Jiang, X., Ito, Y., Bringas, P., Jr., Han, J., Rowitch, D. H., Soriano, P., McMahon, A. P. and Sucov, H. M. (2000) 'Fate of the mammalian cranial neural crest during tooth and mandibular morphogenesis', *Development* 127(8): 1671-9.

Chen, Q., Kaji, H., Kanatani, M., Sugimoto, T. and Chihara, K. (2004) 'Testosterone increases osteoprotegerin mRNA expression in mouse osteoblast cells', *Hormone and Metabolic Research* 36(10): 674-8.

Cho, M. I. and Garant, P. R. (2000) 'Development and general structure of the periodontium', *Periodontology* 2000 24: 9-27.

Chu, K., Kim, M., Chae, S. H., Jeong, S. W., Kang, K. S., Jung, K. H., Kim, J., Kim, Y. J., Kang, L., Kim, S. U. et al. (2004) 'Distribution and in situ proliferation patterns of intravenously injected immortalized human neural stem-like cells in rats with focal cerebral ischemia', *Neuroscience Research* 50(4): 459-65.

Cohen, D. R., Vandermark, S. E., McGovern, J. D. and Bradley, M. P. (1993) 'Transcriptional regulation in the testis: a role for transcription factor AP-1 complexes at various stages of spermatogenesis', *Oncogene* 8(2): 443-55.

D'Souza, D. and Patel, K. (1999) 'Involvement of long- and short-range signalling during early tendon development', *Anatomy and Embryology* 200(4): 367-75.

D'Souza, R. N., Aberg, T., Gaikwad, J., Cavender, A., Owen, M., Karsenty, G. and Thesleff, I. (1999) 'Cbfa1 is required for epithelial-mesenchymal

interactions regulating tooth development in mice', *Development* 126(13): 2911-20.

Davidovitch, Z. and Murphy, N. C. (2009) The Adaptation and Development of Biological Concepts in Orthodontics. In: *Biological Mechanisms of Tooth Movement*: Wiley-Blackwell Publishing Ltd.

De Togni, P., Niman, H., Raymond, V., Sawchenko, P. and Verma, I. M. (1988) 'Detection of fos protein during osteogenesis by monoclonal antibodies', *Molecular and Cellular Biology* 8(5): 2251-6.

Delany, A. M., Pash, J. M. and Canalis, E. (1994) 'Cellular and clinical perspectives on skeletal insulin-like growth factor I', *Journal of Cellular Biochemistry* 55(3): 328-33.

Delmas, P. and Malaval, L. (1993) *Handbook of experimental pharmacology. Vol. 107. Physiology and pharmacology of bone, Berlin: Springer-Verlag.*

DeLuca, H. F. (1980) 'Vitamin D: revisited 1980', *Clinics in Endocrinology and Metabolism* 9(1): 1-26.

Diekwisch, T. G. (2001) 'The developmental biology of cementum', *International Journal of Developmental Biology* 45(5-6): 695-706.

Diekwisch, T. G. (2002) 'Pathways and fate of migratory cells during late tooth organogenesis', *Connective Tissue Research* 43(2-3): 245-56.

Diep, L., Matalova, E., Mitsiadis, T. A. and Tucker, A. S. (2009) 'Contribution of the tooth bud mesenchyme to alveolar bone', *Journal of Experimental Zoology Part B Molecular and Developmental Evolution* 312B(5): 510-7.

Dony, C. and Gruss, P. (1987) 'Proto-oncogene c-fos expression in growth regions of fetal bone and mesodermal web tissue', *Nature* 328(6132): 711-4.

Ducy, P., Schinke, T. and Karsenty, G. (2000) 'The osteoblast: a sophisticated fibroblast under central surveillance', *Science* 289(5484): 1501-4.

Ducy, P., Zhang, R., Geoffroy, V., Ridall, A. L. and Karsenty, G. (1997) 'Osf2/Cbfa1: a transcriptional activator of osteoblast differentiation', *Cell* 89(5): 747-54.

Edgar, C. M., Chakravarthy, V., Barnes, G., Kakar, S., Gerstenfeld, L. C. and Einhorn, T. A. (2007) 'Autogenous regulation of a network of bone

morphogenetic proteins (BMPs) mediates the osteogenic differentiation in murine marrow stromal cells', *Bone* 40(5): 1389-98.

Eghbali-Fatourechi, G., Khosla, S., Sanyal, A., Boyle, W. J., Lacey, D. L. and Riggs, B. L. (2003) 'Role of RANK ligand in mediating increased bone resorption in early postmenopausal women', *Journal of Clinical Investigation* 111(8): 1221-30.

Erlebacher, A., Filvaroff, E. H., Gitelman, S. E. and Derynck, R. (1995) 'Toward a molecular understanding of skeletal development', *Cell* 80(3): 371-8.

Finkel, M. P., Biskis, B. O. and Jinkins, P. B. (1966) 'Virus induction of osteosarcomas in mice', *Science* 151(3711): 698-701.

Fischer, A. H., Jacobson, K. A., Rose, J. and Zeller, R. (2008) 'Hematoxylin and eosin staining of tissue and cell sections', *Cold Spring Harbor Protocols* 2008: pdb prot4986.

Fleischmannova, J., Matalova, E., Sharpe, P. T., Misek, I. and Radlanski, R. J. (2010) 'Formation of the tooth-bone interface', *Journal of Dental Research* 89(2): 108-15.

Foxworthy, M. (2003) 'The role of c-fos in the development and eruption of the murine dentition', PhD thesis, *King's College London Library*.

Franzoso, G., Carlson, L., Xing, L., Poljak, L., Shores, E. W., Brown, K. D., Leonardi, A., Tran, T., Boyce, B. F. and Siebenlist, U. (1997) 'Requirement for NF-kappaB in osteoclast and B-cell development', *Genes and Development* 11(24): 3482-96.

Frazier-Bowers, S. A., Puranik, C. P. and Mahaney, M. C. (2010) 'The etiology of eruption disorders - further evidence of a 'genetic paradigm'', *Seminars in Orthodontics* 16(3): 180-185.

Frost, H. M. (1969) 'Tetracycline-based histological analysis of bone remodeling', *Calcified Tissue Research* 3(3): 211-37.

Funk, M., Poensgen, B., Graulich, W., Jerome, V. and Muller, R. (1997) 'A novel, transformation-relevant activation domain in Fos proteins', *Molecular and Cellular Biology* 17(2): 537-44.

Gage, F. H. (2000) 'Mammalian neural stem cells', *Science* 287(5457): 1433-8.

Genco, R. J. (1992) 'Host responses in periodontal diseases: current concepts', *Journal of Periodontology* 63(4 Suppl): 338-55.

Giannobile, W. V., Ryan, S., Shih, M. S., Su, D. L., Kaplan, P. L. and Chan, T. C. (1998) 'Recombinant human osteogenic protein-1 (OP-1) stimulates periodontal wound healing in class III furcation defects', *Journal of Periodontology* 69(2): 129-37.

Grigoriadis, A. E., Schellander, K., Wang, Z. Q. and Wagner, E. F. (1993) 'Osteoblasts are target cells for transformation in c-fos transgenic mice', *Journal of Cell Biology* 122(3): 685-701.

Grigoriadis, A. E., Wang, Z. Q., Cecchini, M. G., Hofstetter, W., Felix, R., Fleisch, H. A. and Wagner, E. F. (1994) 'c-Fos: a key regulator of osteoclast-macrophage lineage determination and bone remodeling', *Science* 266(5184): 443-8.

Grigoriadis, A. E., Wang, Z. Q. and Wagner, E. F. (1995) 'Fos and bone cell development: lessons from a nuclear oncogene', *Trends in Genetics* 11(11): 436-41.

Guerrini, M. M., Sobacchi, C., Cassani, B., Abinun, M., Kilic, S. S., Pangrazio, A., Moratto, D., Mazzolari, E., Clayton-Smith, J., Orchard, P. et al. (2008) 'Human osteoclast-poor osteopetrosis with hypogammaglobulinemia due to TNFRSF11A (RANK) mutations', *American Journal of Human Genetics* 83(1): 64-76.

Hadjidakis, D. J. and Androulakis, II (2006) 'Bone remodeling', *Annals of the New York Academy of Sciences* 1092: 385-96.

Hahn, C. G., Han, L. Y., Rawson, N. E., Mirza, N., Borgmann-Winter, K., Lenox, R. H. and Arnold, S. E. (2005) 'In vivo and in vitro neurogenesis in human olfactory epithelium', *Journal of Comparative Neurology* 483(2): 154-63.

Hakki, S. S., Bozkurt, B., Hakki, E. E., Kayis, S. A., Turac, G., Yilmaz, I. and Karaoz, E. (2014) 'Bone morphogenetic protein-2, -6, and -7 differently regulate osteogenic differentiation of human periodontal ligament stem cells', *Journal of Biomedical Materials Research Part B: Applied Biomaterials* 102(1): 119-30.

Hall, B. K. and Miyake, T. (1992) 'The membranous skeleton: the role of cell condensations in vertebrate skeletogenesis', *Anatomy and Embryology* 186(2): 107-24.

Hayamizu, T. F., Sessions, S. K., Wanek, N. and Bryant, S. V. (1991) 'Effects of localized application of transforming growth factor beta 1 on developing chick limbs', *Developmental Biology* 145(1): 164-73.

Hayek, A., Culler, F. L., Beattie, G. M., Lopez, A. D., Cuevas, P. and Baird, A. (1987) 'An in vivo model for study of the angiogenic effects of basic fibroblast growth factor', *Biochemical and Biophysical Research Communications* 147(2): 876-80.

Hayman, A. R., Bune, A. J. and Cox, T. M. (2000) 'Widespread expression of tartrate-resistant acid phosphatase (Acp 5) in the mouse embryo', *Journal of Anatomy* 196 (Pt 3): 433-41.

Heinegard, D., Hultenby, K., Oldberg, A., Reinholt, F. and Wendel, M. (1989) 'Macromolecules in bone matrix', *Connective Tissue Research* 21(1-4): 3-11.

Heinrich, J., Bsoul, S., Barnes, J., Woodruff, K. and Abboud, S. (2005) 'CSF-1, RANKL and OPG regulate osteoclastogenesis during murine tooth eruption', *Archives of Oral Biology* 50(10): 897-908.

Helfrich, M. H. (2005) 'Osteoclast diseases and dental abnormalities', *Archives of Oral Biology* 50(2): 115-22.

Helpin, M. L. and Duncan, W. K. (1986) 'Ankylosis in monozygotic twins', *American Society Journal of Dentistry for Children* 53(2): 135-9.

Hofbauer, L. C., Gori, F., Riggs, B. L., Lacey, D. L., Dunstan, C. R., Spelsberg, T. C. and Khosla, S. (1999a) 'Stimulation of osteoprotegerin ligand and inhibition of osteoprotegerin production by glucocorticoids in human osteoblastic lineage cells: potential paracrine mechanisms of glucocorticoid-induced osteoporosis', *Endocrinology* 140(10): 4382-9.

Hofbauer, L. C., Hicok, K. C., Chen, D. and Khosla, S. (2002) 'Regulation of osteoprotegerin production by androgens and anti-androgens in human osteoblastic lineage cells', *European Journal of Endocrinology* 147(2): 269-73.

Hofbauer, L. C., Lacey, D. L., Dunstan, C. R., Spelsberg, T. C., Riggs, B. L. and Khosla, S. (1999b) 'Interleukin-1beta and tumor necrosis factor-alpha, but not interleukin-6, stimulate osteoprotegerin ligand gene expression in human osteoblastic cells', *Bone* 25(3): 255-9.

Holleville, N., Quilhac, A., Bontoux, M. and Monsoro-Burq, A. H. (2003) 'BMP signals regulate Dlx5 during early avian skull development', *Developmental Biology* 257(1): 177-89.

Horton, W. A. (1993) Morphology of connective tissue: Cartilage. In: *Connective tissue and its heritable disorders*. New York, NY: Wiley-Liss.

Huang, L. F., Fukai, N., Selby, P. B., Olsen, B. R. and Mundlos, S. (1997) 'Mouse clavicular development: analysis of wild-type and cleidocranial dysplasia mutant mice', *Developmental Dynamics* 210(1): 33-40.

Huang, W. J. and Creath, C. J. (1995) 'The midline diastema: a review of its etiology and treatment', *Pediatric Dentistry* 17(3): 171-9.

Huang, X., Bringas, P., Jr., Slavkin, H. C. and Chai, Y. (2009) 'Fate of HERS during tooth root development', *Developmental Biology* 334(1): 22-30.

Hughes, A. E., Shearman, A. M., Weber, J. L., Barr, R. J., Wallace, R. G., Osterberg, P. H., Nevin, N. C. and Mollan, R. A. (1994) 'Genetic linkage of familial expansile osteolysis to chromosome 18q', *Human Molecular Genetics* 3(2): 359-61.

Hughes, F. J., Collyer, J., Stanfield, M. and Goodman, S. A. (1995) 'The effects of bone morphogenetic protein-2, -4, and -6 on differentiation of rat osteoblast cells in vitro', *Endocrinology* 136(6): 2671-7.

Ida-Yonemochi, H., Noda, T., Shimokawa, H. and Saku, T. (2002) 'Disturbed tooth eruption in osteopetrotic (op/op) mice: histopathogenesis of tooth malformation and odontomas', *Journal of Oral Pathology and Medicine* 31(6): 361-73.

Ikezawa, K., Ohtsubo, M., Norwood, T. H. and Narayanan, A. S. (1998) 'Role of cyclin E and cyclin E-dependent kinase in mitogenic stimulation by cementum-derived growth factor in human fibroblasts', *Federation of American Societies for Experimental Biology Journal* 12(12): 1233-9.

Jain, J., Nalefski, E. A., McCaffrey, P. G., Johnson, R. S., Spiegelman, B. M., Papaioannou, V. and Rao, A. (1994) 'Normal peripheral T-cell function in c-Fos-deficient mice', *Molecular and Cellular Biology* 14(3): 1566-74.

Jernvall, J., Aberg, T., Kettunen, P., Keranen, S. and Thesleff, I. (1998) 'The life history of an embryonic signaling center: BMP-4 induces p21 and is

associated with apoptosis in the mouse tooth enamel knot', *Development* 125(2): 161-9.

Jilka, R. L., Hangoc, G., Girasole, G., Passeri, G., Williams, D. C., Abrams, J. S., Boyce, B., Broxmeyer, H. and Manolagas, S. C. (1992) 'Increased osteoclast development after estrogen loss: mediation by interleukin-6', *Science* 257(5066): 88-91.

Jin, Q. M., Anusaksathien, O., Webb, S. A., Rutherford, R. B. and Giannobile, W. V. (2003) 'Gene therapy of bone morphogenetic protein for periodontal tissue engineering', *Journal of Periodontology* 74(2): 202-13.

Jin, Q. M., Zhao, M., Economides, A. N., Somerman, M. J. and Giannobile, W. V. (2004) 'Noggin gene delivery inhibits cementoblast-induced mineralization', *Connective Tissue Research* 45(1): 50-9.

Johnson, R. B., Gilbert, J. A., Cooper, R. C., Dai, X., Newton, B. I., Tracy, R. R., West, W. F., DeMoss, T. L., Myers, P. J. and Streckfus, C. F. (1997) 'Alveolar bone loss one year following ovariectomy in sheep', *Journal of Periodontology* 68(9): 864-71.

Johnson, R. S., Sheng, M., Greenberg, M. E., Kolodner, R. D., Papaioannou, V. E. and Spiegelman, B. M. (1989) 'Targeting of nonexpressed genes in embryonic stem cells via homologous recombination', *Science* 245(4923): 1234-6.

Johnson, R. S., Spiegelman, B. M. and Papaioannou, V. (1992) 'Pleiotropic effects of a null mutation in the c-fos proto-oncogene', *Cell* 71(4): 577-86.

Jooss, K. U., Funk, M. and Muller, R. (1994) 'An autonomous N-terminal transactivation domain in Fos protein plays a crucial role in transformation', *European Molecular Biology Organization Journal* 13(6): 1467-75.

Kaku, M., Komatsu, Y., Mochida, Y., Yamauchi, M., Mishina, Y. and Ko, C. C. (2012) 'Identification and characterization of neural crest-derived cells in adult periodontal ligament of mice', *Archives of Oral Biology* 57(12): 1668-75.

Kanzaki, H., Chiba, M., Arai, K., Takahashi, I., Haruyama, N., Nishimura, M. and Mitani, H. (2006) 'Local RANKL gene transfer to the periodontal

tissue accelerates orthodontic tooth movement', *Gene Therapy* 13(8): 678-85.

Kanzaki, H., Chiba, M., Shimizu, Y. and Mitani, H. (2001) 'Dual regulation of osteoclast differentiation by periodontal ligament cells through RANKL stimulation and OPG inhibition', *Journal of Dental Research* 80(3): 887-91.

Kanzaki, H., Chiba, M., Takahashi, I., Haruyama, N., Nishimura, M. and Mitani, H. (2004) 'Local OPG gene transfer to periodontal tissue inhibits orthodontic tooth movement', *Journal of Dental Research* 83(12): 920-5.

Karsenty, G. (1999) 'The genetic transformation of bone biology', *Genes and Development* 13(23): 3037-51.

Katagiri, T., Yamaguchi, A., Ikeda, T., Yoshiki, S., Wozney, J. M., Rosen, V., Wang, E. A., Tanaka, H., Omura, S. and Suda, T. (1990) 'The non-osteogenic mouse pluripotent cell line, C3H10T1/2, is induced to differentiate into osteoblastic cells by recombinant human bone morphogenetic protein-2', *Biochemical and Biophysical Research Communications* 172(1): 295-9.

Katagiri, T., Yamaguchi, A., Komaki, M., Abe, E., Takahashi, N., Ikeda, T., Rosen, V., Wozney, J. M., Fujisawa-Sehara, A. and Suda, T. (1994) 'Bone morphogenetic protein-2 converts the differentiation pathway of C2C12 myoblasts into the osteoblast lineage', *Journal of Cell Biology* 127(6 Pt 1): 1755-66.

Kearns, A. E., Khosla, S. and Kostenuik, P. J. (2008) 'Receptor activator of nuclear factor kappaB ligand and osteoprotegerin regulation of bone remodeling in health and disease', *Endocrine Reviews* 29(2): 155-92.

Khanna-Jain, R., Agata, H., Vuorinen, A., Sandor, G. K., Suuronen, R. and Miettinen, S. (2010) 'Addition of BMP-2 or BMP-6 to dexamethasone, ascorbic acid, and beta-glycerophosphate may not enhance osteogenic differentiation of human periodontal ligament cells', *Growth Factors* 28(6): 437-46.

Khosla, S. (2001) 'Minireview: the OPG/RANKL/RANK system', *Endocrinology* 142(12): 5050-5.

Khosla, S., Atkinson, E. J., Dunstan, C. R. and O'Fallon, W. M. (2002) 'Effect of estrogen versus testosterone on circulating osteoprotegerin and other

cytokine levels in normal elderly men', *Journal of Clinical Endocrinology and Metabolism* 87(4): 1550-4.

Kim, J. Y., Cho, S. W., Hwang, H. J., Lee, M. J., Lee, J. M., Cai, J., Choi, S. H., Kim, C. K. and Jung, H. S. (2007) 'Evidence for expansion-based temporal BMP4/NOGGIN interactions in specifying periodontium morphogenesis', *Cell and Tissue Research* 330(1): 123-32.

Kimble, R. B., Srivastava, S., Ross, F. P., Matayoshi, A. and Pacifici, R. (1996) 'Estrogen deficiency increases the ability of stromal cells to support murine osteoclastogenesis via an interleukin-1and tumor necrosis factor-mediated stimulation of macrophage colony-stimulating factor production', *Journal of Biological Chemistry* 271(46): 28890-7.

King, G. N. and Hughes, F. J. (1999) 'Effects of occlusal loading on ankylosis, bone, and cementum formation during bone morphogenetic protein-2-stimulated periodontal regeneration in vivo', *Journal of Periodontology* 70(10): 1125-35.

King, G. N., King, N. and Hughes, F. J. (1998) 'Effect of two delivery systems for recombinant human bone morphogenetic protein-2 on periodontal regeneration in vivo', *Journal of Periodontal Research* 33(4): 226-36.

Kitahara, Y., Suda, N., Kuroda, T., Beck, F., Hammond, V. E. and Takano, Y. (2002) 'Disturbed tooth development in parathyroid hormone-related protein (PTHrP)-gene knockout mice', *Bone* 30(1): 48-56.

Kitazawa, R., Kitazawa, S. and Maeda, S. (1999) 'Promoter structure of mouse RANKL/TRANCE/OPGL/ODF gene', *Biochimica et Biophysica Acta* 1445(1): 134-41.

Knothe Tate, M. L., Falls, T. D., McBride, S. H., Atit, R. and Knothe, U. R. (2008) 'Mechanical modulation of osteochondroprogenitor cell fate', *International Journal of Biochemistry and Cell Biology* 40(12): 2720-38.

Komaki, M., Karakida, T., Abe, M., Oida, S., Mimori, K., Iwasaki, K., Noguchi, K., Oda, S. and Ishikawa, I. (2007) 'Twist negatively regulates osteoblastic differentiation in human periodontal ligament cells', *Journal of Cellular Biochemistry* 100(2): 303-14.

Komaki, M., Katagiri, T. and Suda, T. (1996) 'Bone morphogenetic protein-2 does not alter the differentiation pathway of committed progenitors of osteoblasts and chondroblasts', *Cell and Tissue Research* 284(1): 9-17.

Komuro, H., Olee, T., Kuhn, K., Quach, J., Brinson, D. C., Shikhman, A., Valbracht, J., Creighton-Achermann, L. and Lotz, M. (2001) 'The osteoprotegerin/receptor activator of nuclear factor kappaB/receptor activator of nuclear factor kappaB ligand system in cartilage', *Arthritis and Rheumatism* 44(12): 2768-76.

Kong, Y. Y., Feige, U., Sarosi, I., Bolon, B., Tafuri, A., Morony, S., Capparelli, C., Li, J., Elliott, R., McCabe, S. et al. (1999) 'Activated T cells regulate bone loss and joint destruction in adjuvant arthritis through osteoprotegerin ligand', *Nature* 402(6759): 304-9.

Kratochwil, K., Dull, M., Farinas, I., Galceran, J. and Grosschedl, R. (1996) 'Lef1 expression is activated by BMP-4 and regulates inductive tissue interactions in tooth and hair development', *Genes and Development* 10(11): 1382-94.

Kurihara, S. and Enlow, D. H. (1980) 'An electron microscopic study of attachments between periodontal fibers and bone during alveolar remodeling', *American Journal of Orthodontics* 77(5): 516-31.

Kustikova, O., Kramerov, D., Grigorian, M., Berezin, V., Bock, E., Lukanidin, E. and Tulchinsky, E. (1998) 'Fra-1 induces morphological transformation and increases in vitro invasiveness and motility of epithelioid adenocarcinoma cells', *Molecular and Cellular Biology* 18(12): 7095-105.

Lacey, D. L., Timms, E., Tan, H. L., Kelley, M. J., Dunstan, C. R., Burgess, T., Elliott, R., Colombero, A., Elliott, G., Scully, S. et al. (1998) 'Osteoprotegerin ligand is a cytokine that regulates osteoclast differentiation and activation', *Cell* 93(2): 165-76.

Lee, S. K. and Lorenzo, J. A. (1999) 'Parathyroid hormone stimulates TRANCE and inhibits osteoprotegerin messenger ribonucleic acid expression in murine bone marrow cultures: correlation with osteoclast-like cell formation', *Endocrinology* 140(8): 3552-61.

Lekic, P. and McCulloch, C. A. (1996) 'Periodontal ligament cell population: the central role of fibroblasts in creating a unique tissue', *Anatomical Record* 245(2): 327-41.

Li, J., Sarosi, I., Yan, X. Q., Morony, S., Capparelli, C., Tan, H. L., McCabe, S., Elliott, R., Scully, S., Van, G. et al. (2000) 'RANK is the intrinsic

hematopoietic cell surface receptor that controls osteoclastogenesis and regulation of bone mass and calcium metabolism', *Proceedings of the National Academy of Sciences of the United States of America* 97(4): 1566-71.

Liu, C., Walter, T. S., Huang, P., Zhang, S., Zhu, X., Wu, Y., Wedderburn, L. R., Tang, P., Owens, R. J., Stuart, D. I. et al. (2010) 'Structural and functional insights of RANKL-RANK interaction and signaling', *Journal of Immunology* 184(12): 6910-9.

Liu, J. G., Tabata, M. J., Fujii, T., Ohmori, T., Abe, M., Ohsaki, Y., Kato, J., Wakisaka, S., Iwamoto, M. and Kurisu, K. (2000) 'Parathyroid hormone-related peptide is involved in protection against invasion of tooth germs by bone via promoting the differentiation of osteoclasts during tooth development', *Mechanisms of Development* 95(1-2): 189-200.

Liu, J. G., Tabata, M. J., Yamashita, K., Matsumura, T., Iwamoto, M. and Kurisu, K. (1998) 'Developmental role of PTHrP in murine molars', *European Journal of Oral Sciences* 106 Suppl 1: 143-6.

Lojda, Z., Gossran, R., Schiebler, T. H. and eds. (1979) *Enzyme Histochemistry - A Laboratory Manual*, Berlin: Springer-Verlag.

Lungova, V., Radlanski, R. J., Tucker, A. S., Renz, H., Misek, I. and Matalova, E. (2011) 'Tooth-bone morphogenesis during postnatal stages of mouse first molar development', *Journal of Anatomy* 218(6): 699-716.

Marks, S. C., Jr. (1989) 'Osteoclast biology: lessons from mammalian mutations', *American Journal of Medical Genetics* 34(1): 43-54.

Marks, S. C., Jr. and Schroeder, H. E. (1996) 'Tooth eruption: theories and facts', *Anatomical Record* 245(2): 374-93.

Marotti, G. (1977) Decrement in volume of osteoblasts during osteon formation and its effect on the size of the corresponding osteocytes *Bone Histomorphometry*. Paris: Armour Montagu.

Martin, T. J., Romas, E. and Gillespie, M. T. (1998) 'Interleukins in the control of osteoclast differentiation', *Critical Reviews in Eukaryotic Gene Expression* 8(2): 107-23.

Matalova, E., Svandova, E. and Tucker, A. S. (2012) 'Apoptotic signaling in mouse odontogenesis', *OMICS: A Journal of Integrative Biology* 16(1-2): 60-70.

Matsuo, K., Owens, J. M., Tonko, M., Elliott, C., Chambers, T. J. and Wagner, E. F. (2000) 'Fosl1 is a transcriptional target of c-Fos during osteoclast differentiation', *Nature Genetics* 24(2): 184-7.

McKee, M. and A., N. (1993) Ultrastructural, cytochemical and immunocytochemical studies on bone and its interfaces. *Cells Mater*.

McMahon, J. A., Takada, S., Zimmerman, L. B., Fan, C. M., Harland, R. M. and McMahon, A. P. (1998) 'Noggin-mediated antagonism of BMP signaling is required for growth and patterning of the neural tube and somite', *Genes and Development* 12(10): 1438-52.

McSheehy, P. M. and Chambers, T. J. (1986) 'Osteoblastic cells mediate osteoclastic responsiveness to parathyroid hormone', *Endocrinology* 118(2): 824-8.

Mekaapiruk, K., Suda, N., Hammond, V. E., Beck, F., Kuroda, T., Takano, Y. and Terashima, T. (2002) 'The influence of parathyroid hormone-related protein (PTHrP) on tooth-germ development and osteoclastogenesis in alveolar bone of PTHrP-knock out and wild-type mice in vitro', *Archives of Oral Biology* 47(9): 665-72.

Mitchell, C. A., Kennedy, J. G. and Wallace, R. G. (1990) 'Dental abnormalities associated with familial expansile osteolysis: a clinical and radiographic study', *Oral Surgery, Oral Medicine, and Oral Pathology* 70(3): 301-7.

Mizuno, A., Amizuka, N., Irie, K., Murakami, A., Fujise, N., Kanno, T., Sato, Y., Nakagawa, N., Yasuda, H., Mochizuki, S. et al. (1998) 'Severe osteoporosis in mice lacking osteoclastogenesis inhibitory factor/osteoprotegerin', *Biochemical and Biophysical Research Communications* 247(3): 610-5.

Mizuno, N., Shiba, H., Mouri, Y., Xu, W., Kudoh, S., Kawaguchi, H. and Kurihara, H. (2005) 'Characterization of epithelial cells derived from periodontal ligament by gene expression patterns of bone-related and enamel proteins', *Cell Biology International* 29(2): 111-7.

Morgan, J. I., Cohen, D. R., Hempstead, J. L. and Curran, T. (1987) 'Mapping patterns of c-fos expression in the central nervous system after seizure', *Science* 237(4811): 192-7.

Morgan, J. I. and Curran, T. (1991) 'Stimulus-transcription coupling in the nervous system: involvement of the inducible proto-oncogenes fos and jun', *Annual Review of Neuroscience* 14: 421-51.

Mowry, R. W. (1956) 'Alcian blue technics for the histochemical study of acidic carbohydrates', *Journal of Histochemistry and Cytochemistry* 4: 407.

Muller, R., Slamon, D. J., Tremblay, J. M., Cline, M. J. and Verma, I. M. (1982) 'Differential expression of cellular oncogenes during pre- and postnatal development of the mouse', *Nature* 299(5884): 640-4.

Muller, R. and Wagner, E. F. (1984) 'Differentiation of F9 teratocarcinoma stem cells after transfer of c-fos proto-oncogenes', *Nature* 311(5985): 438-42.

Munne, P. M., Tummers, M., Jarvinen, E., Thesleff, I. and Jernvall, J. (2009) 'Tinkering with the inductive mesenchyme: Sostdc1 uncovers the role of dental mesenchyme in limiting tooth induction', *Development* 136(3): 393-402.

Muthukuru, M. (2013) 'Bone morphogenic protein-2 induces apoptosis and cytotoxicity in periodontal ligament cells', *Journal of Periodontology* 84(6): 829-38.

Nakabeppu, Y. and Nathans, D. (1991) 'A naturally occurring truncated form of FosB that inhibits Fos/Jun transcriptional activity', *Cell* 64(4): 751-9.

Nakamura, M., Bringas, P., Jr., Nanci, A., Zeichner-David, M., Ashdown, B. and Slavkin, H. C. (1994) 'Translocation of enamel proteins from inner enamel epithelia to odontoblasts during mouse tooth development', *Anatomical Record* 238(3): 383-96.

Nakamura, Y., Nakaya, H., Saito, N. and Wakitani, S. (2006) 'Coordinate expression of BMP-2, BMP receptors and Noggin in normal mouse spine', *Journal of Clinical Neuroscience* 13(2): 250-6.

Nakatsuka, K., Nishizawa, Y. and Ralston, S. H. (2003) 'Phenotypic characterization of early onset Paget's disease of bone caused by a 27-bp duplication in the TNFRSF11A gene', *Journal of Bone and Mineral Research* 18(8): 1381-5.

Narayanan, K., Ramachandran, A., Hao, J. and George, A. (2002) 'Transcriptional regulation of dentin matrix protein 1 (DMP1) by AP-1 (c-fos/c-jun) factors', *Connective Tissue Research* 43(2-3): 365-71.

Negishi-Koga, T., Shinohara, M., Komatsu, N., Bito, H., Kodama, T., Friedel, R. H. and Takayanagi, H. (2011) 'Suppression of bone formation by osteoclastic expression of semaphorin 4D', *Nature Medicine* 17(11): 1473-80.

Nguyen, D. H. and Martin, J. T. (2008) 'Common dental infections in the primary care setting', *American Family Physician* 77(6): 797-802.

Nieoullon, V., Belvindrah, R., Rougon, G. and Chazal, G. (2005) 'mCD24 regulates proliferation of neuronal committed precursors in the subventricular zone', *Molecular and Cellular Neurosciences* 28(3): 462-74.

Nohe, A., Keating, E., Knaus, P. and Petersen, N. O. (2004) 'Signal transduction of bone morphogenetic protein receptors', *Cellular Signalling* 16(3): 291-9.

Ohazama, A., Courtney, J. M. and Sharpe, P. T. (2004) 'Opg, Rank, and Rankl in tooth development: co-ordination of odontogenesis and osteogenesis', *Journal of Dental Research* 83(3): 241-4.

Okada, S., Wang, Z. Q., Grigoriadis, A. E., Wagner, E. F. and von Ruden, T. (1994) 'Mice lacking c-fos have normal hematopoietic stem cells but exhibit altered B-cell differentiation due to an impaired bone marrow environment', *Molecular and Cellular Biology* 14(1): 382-90.

Overall, C. M. and Sodek, J. (1990) 'Concanavalin A produces a matrix-degradative phenotype in human fibroblasts. Induction and endogenous activation of collagenase, 72-kDa gelatinase, and Pump-1 is accompanied by the suppression of the tissue inhibitor of matrix metalloproteinases', *Journal of Biological Chemistry* 265(34): 21141-51.

Palmer, R. M. and Lumsden, A. G. (1987) 'Development of periodontal ligament and alveolar bone in homografted recombinations of enamel organs and papillary, pulpal and follicular mesenchyme in the mouse', *Archives of Oral Biology* 32(4): 281-9.

Palumbo, C. (1986) 'A three-dimensional ultrastructural study of osteoid-osteocytes in the tibia of chick embryos', *Cell and Tissue Research* 246(1): 125-31.

Palumbo, C., Palazzini, S. and Marotti, G. (1990) 'Morphological study of intercellular junctions during osteocyte differentiation', *Bone* 11(6): 401-6.

Pelto-Huikko, M., Schultz, R., Koistinaho, J. and Hokfelt, T. (1991) 'Immunocytochemical demonstration of c-fos protein in sertoli cells and germ cells in rat testis', *Acta Physiologica Scandinavica* 141(2): 283-4.

Ponchel, F., Cuthbert, R. J. and Goeb, V. (2011) 'IL-7 and lymphopenia', *International Journal of Clinical Chemistry* 412(1-2): 7-16.

Radlanski, R. J., Mocker, E. and Rahlfs, D. (1998) 'Computer-aided graphical reconstructions of the development of murine dental primordia and surrounding structures from day 12 until birth', *European Journal of Oral Sciences* 106 Suppl 1: 71-9.

Rajshankar, D., McCulloch, C. A., Tenenbaum, H. C. and Lekic, P. C. (1998) 'Osteogenic inhibition by rat periodontal ligament cells: modulation of bone morphogenic protein-7 activity in vivo', *Cell and Tissue Research* 294(3): 475-83.

Ramaesh, T. and Bard, J. B. (2003) 'The growth and morphogenesis of the early mouse mandible: a quantitative analysis', *Journal of Anatomy* 203(2): 213-22.

Reddi, A. H. (1997) 'BMPs: actions in flesh and bone', *Nature Medicine* 3(8): 837-9.

Reddi, A. H. (2001) 'Bone morphogenetic proteins: from basic science to clinical applications', *Journal of Bone and Joint Surgery*. American volume 83-A Suppl 1(Pt 1): S1-6.

Riolo, M. L. and Avery, J. K. (2002) *Essentials for Orthodontic* Practice 1 ed.: EFOP Press.

Ripamonti, U., Heliotis, M., Rueger, D. C. and Sampath, T. K. (1996) 'Induction of cementogenesis by recombinant human osteogenic protein-1 (hop-1/bmp-7) in the baboon (Papio ursinus)', *Archives of Oral Biology* 41(1): 121-26.

Ripamonti, U., Heliotis, M., van den Heever, B. and Reddi, A. H. (1994) 'Bone morphogenetic proteins induce periodontal regeneration in the baboon (Papio ursinus)', *Journal of Periodontal Research* 29(6): 439-45.

Roberts-Harry, D. and Sandy, J. (2004) 'Orthodontics. Part 11: orthodontic tooth movement', *British Dental Journal* 196(7): 391-4; quiz 426.

Roodman, G. D., Ibbotson, K. J., MacDonald, B. R., Kuehl, T. J. and Mundy, G. R. (1985) '1,25-Dihydroxyvitamin D3 causes formation of multinucleated cells with several osteoclast characteristics in cultures of primate marrow', *Proceedings of the National Academy of Sciences of the United States of America* 82(23): 8213-7.

Roshandel, D., Holliday, K. L., Pye, S. R., Boonen, S., Borghs, H., Vanderschueren, D., Huhtaniemi, I. T., Adams, J. E., Ward, K. A., Bartfai, G. et al. (2010) 'Genetic variation in the RANKL/RANK/OPG signaling pathway is associated with bone turnover and bone mineral density in men', *Journal of Bone and Mineral Research* 25(8): 1830-8.

Rothova, M., Thompson, H., Lickert, H. and Tucker, A. S. (2012) 'Lineage tracing of the endoderm during oral development', *Developmental Dynamics* 241(7): 1183-91.

Ruther, U., Garber, C., Komitowski, D., Muller, R. and Wagner, E. F. (1987) 'Deregulated c-fos expression interferes with normal bone development in transgenic mice', *Nature* 325(6103): 412-6.

Ruther, U., Komitowski, D., Schubert, F. R. and Wagner, E. F. (1989) 'c-fos expression induces bone tumors in transgenic mice', *Oncogene* 4(7): 861-5.

Ruther, U., Muller, W., Sumida, T., Tokuhisa, T., Rajewsky, K. and Wagner, E. F. (1988) 'c-fos expression interferes with thymus development in transgenic mice', *Cell* 53(6): 847-56.

Rutherford, R. B., Sampath, T. K., Rueger, D. C. and Taylor, T. D. (1992) 'Use of bovine osteogenic protein to promote rapid osseointegration of endosseous dental implants', *International Journal of Oral and Maxillofacial Implants* 7(3): 297-301.

Sabatakos, G., Sims, N. A., Chen, J., Aoki, K., Kelz, M. B., Amling, M., Bouali, Y., Mukhopadhyay, K., Ford, K., Nestler, E. J. et al. (2000) 'Overexpression of DeltaFosB transcription factor(s) increases bone formation and inhibits adipogenesis', *Nature Medicine* 6(9): 985-90.

Saffar, J. L., Lasfargues, J. J. and Cherruau, M. (1997) 'Alveolar bone and the alveolar process: the socket that is never stable', *Periodontology 2000* 13: 76-90.

Sandberg, M., Vuorio, T., Hirvonen, H., Alitalo, K. and Vuorio, E. (1988) 'Enhanced expression of TGF-beta and c-fos mRNAs in the growth plates of developing human long bones', *Development* 102(3): 461-70.

Saygin, N. E., Giannobile, W. V. and Somerman, M. J. (2000) 'Molecular and cell biology of cementum', *Periodontology 2000* 24: 73-98.

Scherft, J. and Groot, C. (1990) The electron microscopic structure of the osteoblast *Ultrastructure of skeletal tissues: bone and cartilage in health and disease*. Boston: Kluwer Academic Publishers.

Schreiber, A. B., Winkler, M. E. and Derynck, R. (1986) 'Transforming growth factor-alpha: a more potent angiogenic mediator than epidermal growth factor', *Science* 232(4755): 1250-3.

Schroeder, H. E. (1992) 'Biological problems of regenerative cementogenesis: synthesis and attachment of collagenous matrices on growing and established root surfaces', *International Review of Cytology* 142: 1-59.

Schweitzer, R., Chyung, J. H., Murtaugh, L. C., Brent, A. E., Rosen, V., Olson, E. N., Lassar, A. and Tabin, C. J. (2001) 'Analysis of the tendon cell fate using Scleraxis, a specific marker for tendons and ligaments', *Development* 128(19): 3855-66.

Sheng, Z. F., Ye, W., Wang, J., Li, C. H., Liu, J. H., Liang, Q. C., Li, S., Xu, K. and Liao, E. Y. (2010) 'OPG knockout mouse teeth display reduced alveolar bone mass and hypermineralization in enamel and dentin', *Archives of Oral Biology* 55(4): 288-93.

Sigurdsson, T. J., Nygaard, L., Tatakis, D. N., Fu, E., Turek, T. J., Jin, L., Wozney, J. M. and Wikesjo, U. M. (1996) 'Periodontal repair in dogs: evaluation of rhBMP-2 carriers', *International Journal of Periodontics and Restorative Dentistry* 16(6): 524-37.

Simonet, W. S., Lacey, D. L., Dunstan, C. R., Kelley, M., Chang, M. S., Luthy, R., Nguyen, H. Q., Wooden, S., Bennett, L., Boone, T. et al. (1997) 'Osteoprotegerin: a novel secreted protein involved in the regulation of bone density', *Cell* 89(2): 309-19.

Smeyne, R. J., Schilling, K., Robertson, L., Luk, D., Oberdick, J., Curran, T. and Morgan, J. I. (1992) 'fos-lacZ transgenic mice: mapping sites of gene induction in the central nervous system', *Neuron* 8(1): 13-23.

Smith, E. L., Locke, M., Waddington, R. J. and Sloan, A. J. (2010) 'An ex vivo rodent mandible culture model for bone repair', *Tissue Engineering Part C: Methods* 16(6): 1287-96.

Sobacchi, C., Frattini, A., Guerrini, M. M., Abinun, M., Pangrazio, A., Susani, L., Bredius, R., Mancini, G., Cant, A., Bishop, N. et al. (2007) 'Osteoclast-poor human osteopetrosis due to mutations in the gene encoding RANKL', *Nature Genetics* 39(8): 960-2.

Sodek, J. (1977) 'A comparison of the rates of synthesis and turnover of collagen and non-collagen proteins in adult rat periodontal tissues and skin using a microassay', *Archives of Oral Biology* 22(12): 655-65.

Sodek, J. and McKee, M. D. (2000) 'Molecular and cellular biology of alveolar bone', *Periodontology 2000* 24: 99-126.

Somerman, M. J., Ouyang, H. J., Berry, J. E., Saygin, N. E., Strayhorn, C. L., D'Errico, J. A., Hullinger, T. and Giannobile, W. V. (1999) 'Evolution of periodontal regeneration: from the roots' point of view', *Journal of Periodontal Research* 34(7): 420-4.

Spooner, B. S., Bassett, K. E. and Spooner, B. S., Jr. (1989) 'Embryonic salivary gland epithelial branching activity is experimentally independent of epithelial expansion activity', *Developmental Biology* 133(2): 569-75.

Suda, T., Takahashi, N. and Martin, T. J. (1992) 'Modulation of osteoclast differentiation', *Endocrine Reviews* 13(1): 66-80.

Sun, L., Peng, Y., Sharrow, A. C., Iqbal, J., Zhang, Z., Papachristou, D. J., Zaidi, S., Zhu, L. L., Yaroslavskiy, B. B., Zhou, H. et al. (2006) 'FSH directly regulates bone mass', *Cell* 125(2): 247-60.

Suzuki, T., Suda, N. and Ohyama, K. (2004) 'Osteoclastogenesis during mouse tooth germ development is mediated by receptor activator of NFKappa-B ligand (RANKL)', *Journal of Bone and Mineral Metabolism* 22(3): 185-91.

Tabata, M. J., Fujii, T., Liu, J. G., Ohmori, T., Abe, M., Wakisaka, S., Iwamoto, M. and Kurisu, K. (2002) 'Bone morphogenetic protein 4 is involved in

cusp formation in molar tooth germ of mice', *European Journal of Oral Sciences* 110(2): 114-20.

Tabata, M. J., Kim, K., Liu, J. G., Yamashita, K., Matsumura, T., Kato, J., Iwamoto, M., Wakisaka, S., Matsumoto, K., Nakamura, T. et al. (1996) 'Hepatocyte growth factor is involved in the morphogenesis of tooth germ in murine molars', *Development* 122(4): 1243-51.

Takano-Yamamoto, T., Takemura, T., Kitamura, Y. and Nomura, S. (1994) 'Site-specific expression of mRNAs for osteonectin, osteocalcin, and osteopontin revealed by in situ hybridization in rat periodontal ligament during physiological tooth movement', *Journal of Histochemistry and Cytochemistry* 42(7): 885-96.

Takayama, K., Suzuki, A., Manaka, T., Taguchi, S., Hashimoto, Y., Imai, Y., Wakitani, S. and Takaoka, K. (2009) 'RNA interference for noggin enhances the biological activity of bone morphogenetic proteins in vivo and in vitro', *Journal of Bone and Mineral Metabolism* 27(4): 402-11.

Talwar, R., Di Silvio, L., Hughes, F. J. and King, G. N. (2001) 'Effects of carrier release kinetics on bone morphogenetic protein-2-induced periodontal regeneration in vivo', *Journal of Clinical Periodontology* 28(4): 340-7.

Teitelbaum, S. L. (2000) 'Bone resorption by osteoclasts', *Science* 289(5484): 1504-8.

Teitelbaum, S. L. (2004) 'RANKing c-Jun in osteoclast development', *Journal of Clinical Investigation* 114(4): 463-5.

Ten Cate, A. R. (1994) In: *Oral Histology*, St. Louis, MO: Mosby.

Ten Cate, A. R. and Mills, C. (1972) 'The development of the periodontium: the origin of alveolar bone', *Anatomical Record* 173(1): 69-77.

Ten Cate, A. R., Mills, C. and Solomon, G. (1971) 'The development of the periodontium. A transplantation and autoradiographic study', *Anatomical Record* 170(3): 365-79.

Thesleff, I. (2006) 'The genetic basis of tooth development and dental defects', *American Journal of Medical Genetics Part A* 140(23): 2530-5.

Thesleff, I. and Pirinen, S. (2003) Genetics of dental defects *Encyclopedia of Human Genome. Genes & Disease*, vol. Genes & Disease: John Wiley & Sons, Ltd.

Thesleff, I. and Tummers, M. (2008) Tooth organogenesis and regeneration *StemBook*. Cambridge (MA).

Thomadakis, G., Ramoshebi, L. N., Crooks, J., Rueger, D. C. and Ripamonti, U. (1999) 'Immunolocalization of Bone Morphogenetic Protein-2 and -3 and Osteogenic Protein-1 during murine tooth root morphogenesis and in other craniofacial structures', *European Journal of Oral Sciences* 107(5): 368-77.

Treisman, R. (1985) 'Transient accumulation of c-fos RNA following serum stimulation requires a conserved 5' element and c-fos 3' sequences', *Cell* 42(3): 889-902.

Trouvin, A. P. and Goeb, V. (2010) 'Receptor activator of nuclear factor-kappaB ligand and osteoprotegerin: maintaining the balance to prevent bone loss', *Clinical Interventions in Aging* 5: 345-54.

Tsoukas, C. D., Provvedini, D. M. and Manolagas, S. C. (1984) '1,25-dihydroxyvitamin D3: a novel immunoregulatory hormone', *Science* 224(4656): 1438-40.

Tucker, A. S., Al Khamis, A. and Sharpe, P. T. (1998) 'Interactions between Bmp-4 and Msx-1 act to restrict gene expression to odontogenic mesenchyme', *Developmental Dynamics* 212(4): 533-9.

Vaananen, H. K., Zhao, H., Mulari, M. and Halleen, J. M. (2000) 'The cell biology of osteoclast function', *Journal of Cell Science* 113 (Pt 3): 377-81.

Vainio, S., Jalkanen, M. and Thesleff, I. (1989) 'Syndecan and tenascin expression is induced by epithelial-mesenchymal interactions in embryonic tooth mesenchyme', *Journal of Cell Biology* 108(5): 1945-53.

Van Den Bergh, J. P., ten Bruggenkate, C. M., Groeneveld, H. H., Burger, E. H. and Tuinzing, D. B. (2000) 'Recombinant human bone morphogenetic protein-7 in maxillary sinus floor elevation surgery in 3 patients compared to autogenous bone grafts. A clinical pilot study', *Journal of Clinical Periodontology* 27(9): 627-36.

Waite, K. A. and Eng, C. (2003) 'From developmental disorder to heritable cancer: it's all in the BMP/TGF-beta family', *Nature Reviews*. Genetics 4(10): 763-73.

Wan Hassan, W. N., Stephenson, P. A., Waddington, R. J. and Sloan, A. J. (2012) 'An ex vivo culture model for orthodontically induced root resorption', *Journal of Dentistry* 40(5): 406-15.

Wang, Z. Q., Grigoriadis, A. E., Mohle-Steinlein, U. and Wagner, E. F. (1991) 'A novel target cell for c-fos-induced oncogenesis: development of chondrogenic tumours in embryonic stem cell chimeras', *European Molecular Biology Organization Journal* 10(9): 2437-50.

Wang, Z. Q., Liang, J., Schellander, K., Wagner, E. F. and Grigoriadis, A. E. (1995) 'c-fos-induced osteosarcoma formation in transgenic mice: cooperativity with c-jun and the role of endogenous c-fos', *Cancer Research* 55(24): 6244-51.

Wang, Z. Q., Ovitt, C., Grigoriadis, A. E., Mohle-Steinlein, U., Ruther, U. and Wagner, E. F. (1992) 'Bone and haematopoietic defects in mice lacking c-fos', *Nature* 360(6406): 741-5.

Weinstein, R. S., Chen, J. R., Powers, C. C., Stewart, S. A., Landes, R. D., Bellido, T., Jilka, R. L., Parfitt, A. M. and Manolagas, S. C. (2002) 'Promotion of osteoclast survival and antagonism of bisphosphonate-induced osteoclast apoptosis by glucocorticoids', *Journal of Clinical Investigation* 109(8): 1041-8.

Whyte, M. P., Obrecht, S. E., Finnegan, P. M., Jones, J. L., Podgornik, M. N., McAlister, W. H. and Mumm, S. (2002) 'Osteoprotegerin deficiency and juvenile Paget's disease', *New England Journal of Medicine* 347(3): 175-84.

Wilkinson, D. G. (1992) *In situ hybridisation: a practical approach*, Oxford: Oxford University Press.

Winkler, S. (2002) 'Implant site development and alveolar bone resorption patterns', *Journal of Oral Implantology* 28(5): 226-9.

Wisdon, R. and Verma, I. M. (1993) 'Transformation by Fos proteins requires a C-terminal transactivation domain', *Molecular and Cellular Biology* 13(12): 7429-38.

Wise, G. E., Huang, H. and Que, B. G. (1999) 'Gene expression of potential tooth eruption molecules in the dental follicle of the mouse', *European Journal of Oral Sciences* 107(6): 482-6.

Wise, G. E. and King, G. J. (2008) 'Mechanisms of tooth eruption and orthodontic tooth movement', *Journal of Dental Research* 87(5): 414-34.

Wise, G. E., Marks, S. C., Jr. and Zhao, L. (1998) 'Effect of CSF-1 on in vivo expression of c-fos in the dental follicle during tooth eruption', *European Journal of Oral Sciences* 106 Suppl 1: 397-400.

Wozney, J. M. (1992) 'The bone morphogenetic protein family and osteogenesis', *Molecular Reproduction and Development* 32(2): 160-7.

Yamada, S., Tomoeda, M., Ozawa, Y., Yoneda, S., Terashima, Y., Ikezawa, K., Ikegawa, S., Saito, M., Toyosawa, S. and Murakami, S. (2007) 'PLAP-1/asporin, a novel negative regulator of periodontal ligament mineralization', *Journal of Biological Chemistry* 282(32): 23070-80.

Yamashiro, T., Tummers, M. and Thesleff, I. (2003) 'Expression of bone morphogenetic proteins and Msx genes during root formation', *Journal of Dental Research* 82(3): 172-6.

Yamazaki, H., Tsuneto, M., Yoshino, M., Yamamura, K. and Hayashi, S. (2007) 'Potential of dental mesenchymal cells in developing teeth', *Stem Cells* 25(1): 78-87.

Yanagita, M. (2005) 'BMP antagonists: their roles in development and involvement in pathophysiology', *Cytokine and Growth Factor Reviews* 16(3): 309-17.

Yao, S., Ring, S., Henk, W. G. and Wise, G. E. (2004) 'In vivo expression of RANKL in the rat dental follicle as determined by laser capture microdissection', *Archives of Oral Biology* 49(6): 451-6.

Yoshida, T., Vivatbutsiri, P., Morriss-Kay, G., Saga, Y. and Iseki, S. (2008) 'Cell lineage in mammalian craniofacial mesenchyme', *Mechanisms of Development* 125(9-10): 797-808.

Yoshikawa, D. K. and Kollar, E. J. (1981) 'Recombination experiments on the odontogenic roles of mouse dental papilla and dental sac tissues in ocular grafts', *Archives of Oral Biology* 26(4): 303-7.

Yoshizawa, T., Takizawa, F., Iizawa, F., Ishibashi, O., Kawashima, H., Matsuda, A. and Endo, N. (2004) 'Homeobox protein MSX2 acts as a molecular defense mechanism for preventing ossification in ligament fibroblasts', *Molecular and Cellular Biology* 24(8): 3460-72.

Zeichner-David, M., Oishi, K., Su, Z., Zakartchenko, V., Chen, L. S., Arzate, H. and Bringas, P., Jr. (2003) 'Role of Hertwig's epithelial root sheath cells in tooth root development', *Developmental Dynamics* 228(4): 651-63.

Zhang, Z., Song, Y., Zhang, X., Tang, J., Chen, J. and Chen, Y. (2003) 'Msx1/Bmp4 genetic pathway regulates mammalian alveolar bone formation via induction of Dlx5 and Cbfa1', *Mechanisms of Development* 120(12): 1469-79.

Zhao, H. Y., Liu, J. M., Ning, G., Zhao, Y. J., Chen, Y., Sun, L. H., Zhang, L. Z., Xu, M. Y. and Chen, J. L. (2008) 'Relationships between insulin-like growth factor-I (IGF-I) and OPG, RANKL, bone mineral density in healthy Chinese women', *Osteoporosis International* 19(2): 221-6.

Zhao, M., Berry, J. E. and Somerman, M. J. (2003) 'Bone morphogenetic protein-2 inhibits differentiation and mineralization of cementoblasts in vitro', *Journal of Dental Research* 82(1): 23-7.

Zhao, Y. (2003) 'Phenotypic analysis of the osteoclast lineage in c-fos mutant mice', PhD thesis, *King's College London Library*.

Appendices

Appendix *i*

Published papers from PhD

See attached disc for video.

Video Article

The Slice Culture Method for Following Development of Tooth Germs In Explant Culture

Sarah A. Alfaqeeh[1,2], Abigail S. Tucker[1,2]

[1]Department of Craniofacial Development and Stem Cell Biology, and Department of Orthodontics, Dental Institute, King's College

[2]Department of Pediatric Dentistry and Orthodontics, College of Dentistry, king saud university

Abstract

Explant culture allows manipulation of developing organs at specific time points, and is therefore an important method for the developmental biologist. For many organs it is difficult to access developing tissue to allow monitoring during *ex vivo* culture. The slice culture method allows access to tissue so that morphogenetic movements can be followed and specific cell populations can be targeted for manipulation or lineage tracing.

In this paper we describe a method of slice culture that has been very successful for culture of tooth germs in a range of species. The method provides excellent access to the tooth germs, which develop at a similar rate to that observed *in vivo*, surrounded by the other jaw tissues. This allows tissue interactions between the tooth and surrounding tissue to be monitored. Although this paper concentrates on tooth germs, the same protocol can be applied to follow development of a number of other organs, such as salivary glands, Meckel's cartilage, nasal glands, tongue, and ear.

Introduction

For a number of experiments it is important to be able to culture tissue *ex vivo* to follow development. Culture of developing tissue provides access at defined periods of development and allows manipulation of genes by the addition of factors to the culture medium, or on loaded beads, and by the use of transfection and electroporation [1]. For many experiments it is important to be able to visualize the tissue as it grows, for example, to follow the fate of lineage labeled cells as the tissue undergoes morphogenesis. This can be particularly problematic for tissues that develop deep within the embryo, which are not obvious when a block of tissue from the embryo is cultured. Teeth are good examples of this, as they develop within the mandible, maxilla and frontal nasal process. When the whole mandible is cultured the superficial structures of the tooth can be viewed but changes in morphology can only be analyzed after sectioning of fixed tissue [2]. We have adapted a live slice culture technique allowing us to follow tooth germ development and providing access to the different parts of the tooth during development. The technique cultures the tooth germ slices at the gas-liquid interface, using a modified Trowell method [3]. These slice cultures have been very useful in directly following morphogenesis of the tooth, and allowing lineage tracing of distinct component, such as the enamel knot and the dental papilla and follicle [1,4-7]. The technique is not limited to mouse embryos and has successfully been used to culture live slices of pig and snake dental tissue [8,9]. In addition to the benefit of being able to visualize tooth development, the slice methods also has the advantage that the thin slices of tissue have increased access to nutrients from the medium and air from the incubator. This results in improved growth of the tooth germs, which match development *in vivo*, and show invasion of endothelial cells into the papilla [7]. In contrast tooth germs in whole mandible cultures develop slower than those *in vivo* and the centre of the culture is often necrotic in long-term cultures. In slice culture, the tooth develops within a slice of the jaw, and its interaction with the surrounding developing bone and other tissues can be monitored. In our method the tissue is chopped straight after dissection with no need to embed in a support medium [10,11], and no need for any system to attach the tissue to the chopping block. The method is therefore non-invasive and rapid, allowing many mandibles to be sectioned in one session.

Protocol

1. Set Up

1. Sharpen the dissection instruments (using a sharpening stone lubricated with mineral oil) and sterilize prior to use for organ culture using a 70% ethanol spray and dry-heat sterilization. Sharpen the dissection needles using electrolysis in 2M sodium hydroxide using a 12V supply.
2. Prepare the culture medium used for the dissection and culture of embryonic organs, consisting of Advanced Dulbecco's Modified Eagle Medium F12 (DMEM F12) supplemented with 1% Glutamax and 1% penicillin-streptomycin.

248

2. Embryo Dissection

1. Cull a timed mated pregnant female using a schedule one method as approved by the Home Office or other governing body. Dissect away the skin around the lower abdomen, and cut open the abdomen using scissors. Locate the two uterine horns, which connect together at the lower midline.
2. Dissect out the uterus and place in a tube filled with medium on ice. When on ice, the tissue can be left for several hours.
3. Remove the uterus and place in a petri dish in medium under the microscope. Where possible embryo dissections should be performed in a laminar-flow hood to minimize contamination.
4. Dissect out the embryos from the uterus and free them from their extra-embryonic tissues.
5. Decapitate the embryos using a tungsten needle and transfer the heads into a fresh dish of medium.
6. Isolate the mandibles from the heads by placing a needle into the oral cavity and cut through towards the back of the head (**Figure 1A, B**). Isolated mandibles can be temporarily stored in medium on ice while waiting for chopping.
7. For whole mandible slices stages E11.5 to E15.5 are ideal for tooth germ culture. After E15.5 the developing bone in the mandible is too hard for chopping. Tooth slices can still be made but the bone (dentary and forming alveolar bone) must first be removed by dissection before chopping [9]. Remove bone carefully using tungsten needles and forceps.

3. Embryo Slicing

1. Prepare the mandible tissue slices using a standard table tissue chopper (**Figure 1C**). Use a fresh blade after approximately 200 mandibles, and make sure it lies flush with the mounting disc when it falls.
2. Clean the mounting disc and blade with 70% Ethanol before use. Care must be taken when using the machine, as the blade is very sharp.
3. Set the chopper at a cutting distance of between 200 and 400 µm according to the age of the specimen, and depending on whether the whole tooth germ is required. Set the blade force on maximum.
4. Transfer a mandible to the plastic mounting disc using a pipette or forceps. Arrange the mandible on the disc making sure the orientation is still clear. The developing tongue can be used as a useful landmark for determining orientation. For molars use a frontal/transverse orientation (see plane of chopping in **Figure 1B**), while for incisors use a sagittal slice through the mandible to reflect the different orientation of these teeth as they grow (see plane of chopping in **Figure 2A**).
5. Remove the excess medium from around the tissue using filter paper in order to slightly dry the mandible on the mounting disc.
6. Immediately after drying, place the disc on the circular stainless steel table of the chopper. Turn the machine on and press start. The table traverses automatically from left to right while at the same time the chopping arm carrying the blade is raised and dropped at up to 200 strokes per minute.
7. Turn off the machine once the tissue has been completely sliced. Make sure the blade arm is in the raised position and remove the disc. Do not place fingers under the blade arm or leave the machine unattended when chopping.
8. Take the mounting disc and immediately add medium to the slices on the disc in order to prevent excessive drying. Carefully dislodge the sliced tissue from the bottom of the disc using a tungsten needle and then pipette into a small petri dish of medium (**Figure 2A**).
9. Separate the slices using a needle and then select the tissue slices containing the tissue of interest under a stereomicroscope (**Figure 1D,E & Figure 2B**). Place selected slices in fresh culture dishes with medium.

4. Slice Culture

1. Prepare central-well organ culture dishes ready for culture by adding approximately 2 mls of autoclaved water to the outer well to prevent dehydration, and by positioning a metal grid across the centre of the dish (**Figure 3A,B**).
2. Prepare metal grids by cutting strips approximately 4 cm by 1.5 cms from sheets of stainless steel mesh. Use a hole punch to make a hole in the centre and bend the sides to create a staggered end. The grid should fit flat across the central well, lying parallel to the bottom of the dish (**Figure 3A,B**). Autoclave the grids to sterilize before use.
3. Cut a piece of transparent polyethylene terephthalate (PET) membrane (pore size 0.4 µm) large enough to cover the hole in the grid. Place the cut membrane into the dish with the selected slice.
4. Place the slice on top of the membrane and then carefully lift the membrane out of the medium, with slice flattened in the centre.
5. Place the filter on the grid over the circular hole in the centre, and add approximately 1 ml of culture medium to the well, up to the level of the membrane.
6. For manipulations add proteins or small molecule inhibitors to the medium (for example[8]).
7. Photograph the slice for a record of morphology at day 0 of culture.
8. Place the dishes in a humidified atmosphere of 5% CO_2 at 37 °C in an incubator.
9. Photograph the cultures at regular intervals for on average 7 days. Change the culture medium every 48-72 hr. For photography view the slices with a light source from underneath (**Figure 2C-E**).

5. Lineage Tracing

If lineage tracing is required, lipophilic dyes such as DiI or DiO can be injected into the tooth germ before step 4, slice culture.

1. Pull glass capillary needles using a needle puller.
2. Break the tip of the needle using forceps and place tip down into the dye solution. Leave for a few minutes while the dye fills the tip by capillary action.
3. Place the filled needle into a holder and attach via tubing to an injector or mouth pipette.
4. Position the tip of the needle in the culture medium touching the area of the slice due to be labeled. Apply air pressure to displace a small amount of dye out of the needle and onto the tissue.
5. Remove needle and check for labeling under fluorescence.

6. Successfully labeled slices can be transferred to filters and cultured as described in step 4.

Representative Results

In order to follow the movement of the first molar dental follicle, 250 μm frontal slices were taken through a mandible using the method described above. The dental follicle is the layer of mesenchyme that surrounds the outer enamel epithelium (OEE) of the developing tooth, and has previously been shown to take part in the formation of tissue of the periodontium [6]. Mandibles were dissected at E14.5, the cap stage of tooth development. In the slice the outline of the dental epithelium was clear, and the condensing dental mesenchyme could be identified as a darker ring around the tooth epithelium (**Figure 4A**). DiI was injected in the mesenchyme next to the outer enamel epithelium of the tooth slice on the lingual side (**Figure 4A**). After labeling the slices were cultured for 4 days and photographed at intervals (**Figure 4B,C**). *In vivo* the tooth germs would have reached the bell stage by E18.5, and a distinct bell stage shape was observed in the slices, indicating a similar progression over this time period. The spot of DiI was seen to extend into a band of cells extending around the outer dental epithelium as the tooth grew (**Figure 4B,C**).
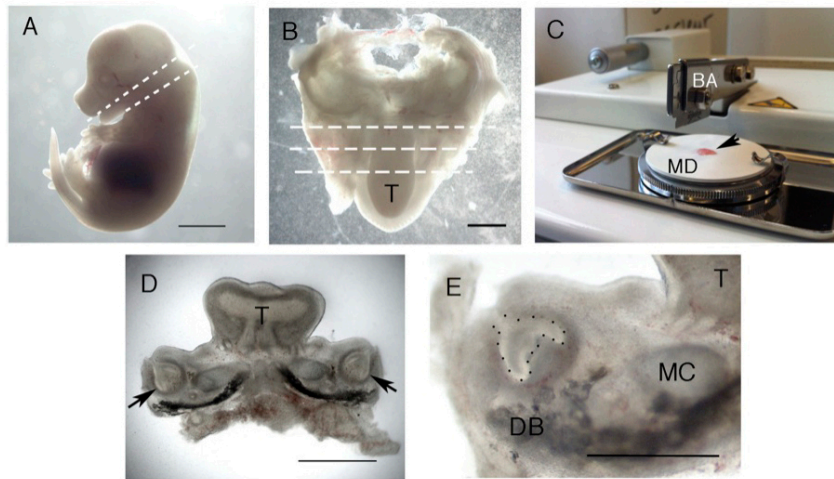
Figure 1. Formation of live slices. (A) E14.5 embryo. Dashed lines indicate the planes cut with a dissecting needle, starting with the lower cut for decapitation. (B) Dissected lower jaw. The tongue is facing downwards. The plane of section for the tissue chopper is shown using dashed lines. (C) Tissue chopper showing blade arm (BA) and white mounting disc (MD) with prepared specimen (arrow). (D) Representative slice through the molar region. Arrows point to molar tooth germs. (E) High power view of a molar slice. The tooth germ epithelium is outlined with black spots. Images sharpened using photoshop. T = Tongue, DB = Dentary bone, MC = Meckel's cartilage. Scale bar in A = 3 mm. Scale bar in B & D = 1 mm. Scale bar in E = 500 μm. Click here to view larger figure.
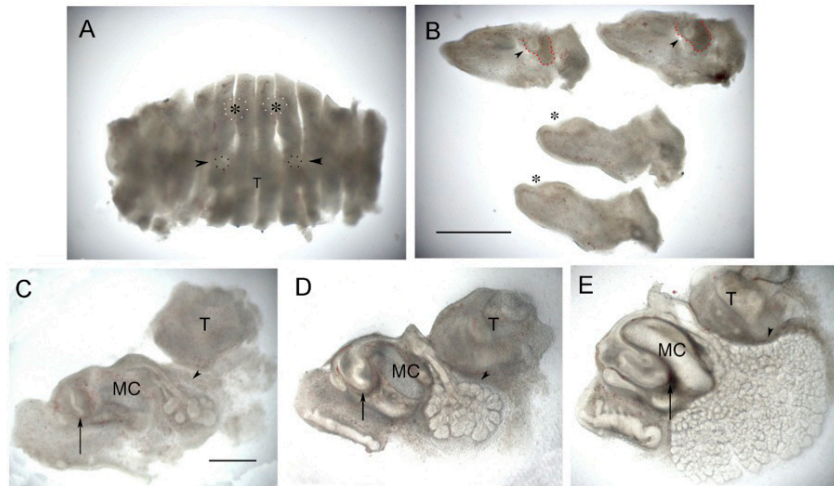
Figure 2. Incisor and gland culture. (A) E12.5 Mandible that has been chopped sagittally. Developing incisors (outlined white spots with asterix) and submandibular glands (outlined with black spots and arrowed) can be just made out. (B) Same mandible showing central 4 slices separated out. The developing submandibular gland can be seen as a bud surrounded by condensed mesenchyme (arrowheads) in the two more lateral sections (top of image). The condensing mesenchyme around the gland is outlined in red. The incisors are at the epithelial thickening stage (asterix) in the two central slices (bottom of image). (C) Sagittal slice through an incisor at E14.0 at Day 0. (D) Same slice 1 day later. (E) Same slice after 3 days in culture. (C-E) Arrow points to incisor and forming labial cervical loop. Arrowhead points to developing submandibular gland. In culture the tooth germ extends backwards as the cervical loops grow, while the salivary gland continues to undergo branching morphogenesis and lumen formation. Images sharpened using photoshop. T = Tongue, MC = Meckel's cartilage. Scale bar in B = 1 mm, same scale in A, Scale bar in C = 500 μm. Same scale in D,E. Click here to view larger figure.
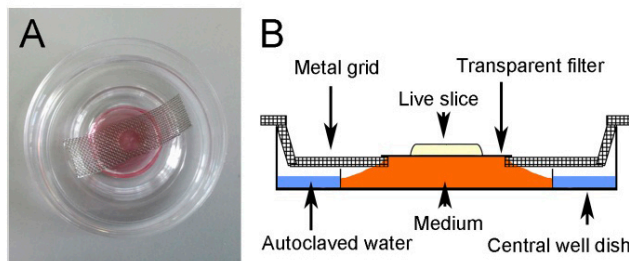
Figure 3. Culture method. (A) Cultured slice. The culture sits on a transparent filter suspended over medium via a metal grid. A hole in the grid allows the slice to be visualized with light from below. (B) Schematic of culture method.
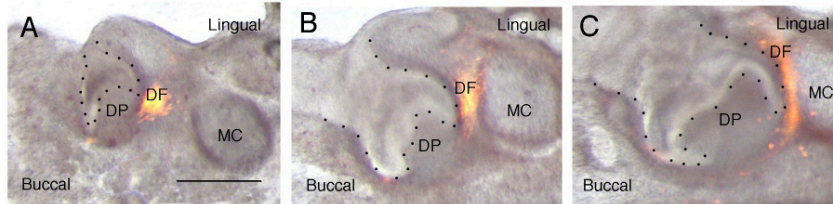
Figure 4. DiI labeling of the dental follicle. (A-C) Merged light and dark field images showing developing molar tooth germ and location of DiI lineage label. (A) Day 0. The tooth germ (arrowhead) is at the cap stage. DiI labels cells of the dental follicle on the lingual side of the tooth. (B) Day 1. (C) Day 4. The tooth germ has reached the bell stage and the DiI labeled cells are seen to spread out in an arc around the developing outer enamel epithelium. Images have been sharpened in photoshop after merging layers using the screen mode. Epithelium of tooth outlined with black spots. DP = dental papilla lying within the inner enamel epithelium. DF = dental follicle, which runs around the outer enamel epithelium. MC = Meckel's cartilage. Scale bar in A: 500 µm (same scale in B,C). Click here to view larger figure.

Discussion

This method of tooth culture has the advantage that access to the tooth germ is excellent, allowing accurate lineage tracing and placement of beads within the epithelium or the mesenchyme. Defined regions of the developing tooth germ can therefore be specifically targeted. During culture the changing morphology of the tooth germ can be followed, and the effect of manipulations quickly assessed.

The method, however, is only suitable for young tooth germs before substantial formation of hard tissues, such as dentine and enamel, as these cannot be chopped accurately. For mandibles after E15.5 it is necessary to remove the bone before chopping. This has the disadvantage of potentially damaging the tooth germ, which is closely associated with the bone from E16.5. We have successfully sliced dissected tooth germs up to postnatal day 4, after which the tooth becomes too hard for the chopper to cut due to the deposition of enamel. The slice method works well on tooth germs from E13.5, *i.e.* the bud stage[1,6]. Before this time-point, when the tooth is at the epithelial thickening stage, the tooth germs do develop but the success rate is reduced and the morphology can be affected over the long term.

One major disadvantage with the method is that the chopping occurs at random through the tooth. In some slices a whole tooth germ will be found within a slice, while in others the chopper may cut the tooth germ through the middle. This means that it may be difficult to obtain large numbers of identical slices. To combat this problem, it is possible to divide a slice down the middle and use the right and left sides as experimental and control. For this, however, the mandible must be carefully placed on the chopping disc to ensure the slice is cut symmetrically. For some experiments it is an advantage to have slices that dissect the tooth so that internal structures, such as the enamel knot, can be accessed for lineage labeling [4]. The tooth germ appears very robust and such half tooth germs are able to develop well in culture with compensation from the surrounding tissue, as previously shown in halved molar tooth germs [12,13].

As an alternative to slice culture, tooth germs can be dissected out of the mandible and cultured in isolation [14]. This removes the problem of poor nutrition and oxygenation associated with culturing large blocks of tissue and leads to good tooth development but as a consequence the tooth develops without interaction with the surrounding tissue. When large amounts of the surrounding mesenchyme are removed the number of tooth germs that form can be altered, highlighting the importance of the surrounding mesenchyme for normal tooth development [15]. Slice culture is therefore a good method for studying the interactions of tissues, for example how the bone and tooth interact in the formation of the alveolar bone, or how the salivary glands interact with the tongue and oral epithelium, something that is lost when these tissues are cultured in isolation.

This paper highlights the use of this method for culturing the tooth germs but the same method is also excellent for culturing developing submandibular and sublingual glands and following the development of structure such as Meckel's cartilage (**Figure 2**).

Disclosures

The authors declare that they have no competing financial interests

Acknowledgements

References

1. Rothova, M., Peterkova, R. & Tucker, A.S. Fate map of the dental mesenchyme: dynamic development of the dental papilla and follicle. *Developmental biology.* **366**, 244-254, doi:10.1016/j.ydbio.2012.03.018 (2012).
2. Ferguson, C.A., *et al.* Activin is an essential early mesenchymal signal in tooth development that is required for patterning of the murine dentition. *Genes & development.* **12**, 2636-2649 (1998).
3. Trowell, O.A. The culture of mature organs in a synthetic medium. *Experimental cell research.* **16**, 118-147 (1959).

4. Matalova, E., Antonarakis, G.S., Sharpe, P.T., & Tucker, A.S. Cell lineage of primary and secondary enamel knots. *Developmental dynamics : an official publication of the American Association of Anatomists.* **233**, 754-759, doi:10.1002/dvdy.20396 (2005).

5. Mitsiadis, T.A., Tucker, A.S., De Bari, C., Cobourne, M.T., & Rice, D.P. A regulatory relationship between Tbx1 and FGF signaling during tooth morphogenesis and ameloblast lineage determination. *Developmental biology.* **320**, 39-48, doi:10.1016/j.ydbio.2008.04.006 (2008).

6. Diep, L., Matalova, E., Mitsiadis, T.A., & Tucker, A.S. Contribution of the tooth bud mesenchyme to alveolar bone. *Journal of experimental zoology. Part B, Molecular and developmental evolution.* **312B**, 510-517, doi:10.1002/jez.b.21269 (2009).

7. Rothova, M., Feng, J., Sharpe, P.T., Peterkova, R., & Tucker, A.S. Contribution of mesoderm to the developing dental papilla. *The International journal of developmental biology.* **55**, 59-64, doi:10.1387/ijdb.103083mr (2011).

8. Buchtova, M., *et al.* Initiation and patterning of the snake dentition are dependent on Sonic hedgehog signaling. *Developmental biology.* **319**, 132-145, doi:10.1016/j.ydbio.2008.03.004 (2008).

9. Buchtova, M., Stembirek, J., Glocova, K., Matalova, E., & Tucker, A.S. Early regression of the dental lamina underlies the development of diphyodont dentitions. *Journal of dental research.* **91**, 491-498, doi:10.1177/0022034512442896 (2012).

10. Cho, S.W., *et al.* The primary enamel knot determines the position of the first buccal cusp in developing mice molars. *Differentiation; research in biological diversity.* **75**, 441-451, doi:10.1111/j.1432-0436.2006.00153.x (2007).

11. Sakano, M., *et al.* Cell dynamics in cervical loop epithelium during transition from crown to root: implications for Hertwig's epithelial root sheath formation. *Journal of periodontal research.* doi:10.1111/jre.12003 (2012).

12. Fisher, A.R. Morphological development in vitro of the whole and halved lower molar tooth germ of the mouse. *Archives of oral biology.* **16**, 1481-1496 (1971).

13. Coin, R., Schmitt, R., Lesot, H., Vonesch, J.L., & Ruch, J.V. Regeneration of halved embryonic lower first mouse molars: correlation with the distribution pattern of non dividing IDE cells, the putative organizers of morphogenetic units, the cusps. *The International journal of developmental biology.* **44**, 289-295 (2000).

14. Kavanagh, K.D., Evans, A.R., & Jernvall, J. Predicting evolutionary patterns of mammalian teeth from development. *Nature.* **449**, 427-432, doi:10.1038/nature06153 (2007).

15. Munne, P.M., Tummers, M., Jarvinen, E., Thesleff, I., & Jernvall, J. Tinkering with the inductive mesenchyme: Sostdc1 uncovers the role of dental mesenchyme in limiting tooth induction. *Development.* **136**, 393-402, doi:10.1242/dev.025064 (2009).

253

jove Journal of Visualized Experiments

www.jove.com

Materials List for:

The Slice Culture Method for Following Development of Tooth Germs In Explant Culture

Sarah A. Alfaqeeh[1,2], Abigail S. Tucker[1]

[1]Department of Craniofacial Development and Stem Cell Biology, and Department of Orthodontics, Dental Institute, Guy's Hospital, UK, King's College London

[2]Department of Pediatric Dentistry and Orthodontics, College of Dentistry, King Saud University, Kingdom of Saudi Arabia

Correspondence to: Abigail S. Tucker at Abigail.tucker@kcl.ac.uk

Materials

Name	Company	Catalog Number	Comments
Ethanol	VWR	101077Y	100% ethanol was diluted in distilled H_2O to 70%.
DMEM F12	Gibco	12634-010	Advanced Dulbecco's Modified Eagle Medium F12
GlutaMAX	Gibco	35050-061	
Penicillin-streptomycin	Sigma	P0781	
DiI (Molecular probes)	Vybrant	V-22885	Cell-labeling solution
	Invitrogen		Cell tracker CM-DiI, C-7000
DiO (Molecular probes)	Vybrant	V22886	
Geminator 500	Thomas	Thomas No. 3885A20	Dry-heat sterilization
McIlwain tissue chopper	Ted Pella, Inc.	10180	Standard table
Organ culture dish (Center-Well Organ Culture Dish)	Falcon	353037	
Membranes (Cell Culture Inserts, 0.4 μm pore size)	BD Falcon	353090	PET track-etched membrane, 6-well format
Metal grids (Stainless Steel - AISI 304 - Mesh)	Goodfellow	FE228710	(Fe/Cr18/Ni10)
AutoFlow Direct Heat CO_2 Incubator	Nuaire	NU-5500	
Picospritzer III	Intracel Ltd	051-0500-900 0-100 psi	Single channel picospritzer III
Glass capillary with filament 1 mm	WPI	TW100F-4	
Tungsten wire 0.1 mm	Goodfellow	W005138	
Tungsten wire 0.38 mm	Goodfellow	W005155	
Aspirator tubes	Sigma	A5177	Used for mouth aspiration lineage tracers

Journal of Dental Research

Interactions of the Tooth and Bone during Development
S.A. Alfaqeeh, M. Gaete and A.S. Tucker
J DENT RES 2013 92: 1129 originally published online 23 October 2013
DOI: 10.1177/0022034513510321

The online version of this article can be found at:
http://jdr.sagepub.com/content/92/12/1129
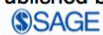
RESEARCH REPORTS
Biological

S.A. Alfaqeeh[1,2], M. Gaete[1,3],
and A.S. Tucker[1]*

[1]Department of Craniofacial Development and Stem Cell Biology, Department of Orthodontics, King's College London, London, UK, SE1 9RT; [2]Department of Pediatric Dentistry and Orthodontics, College of Dentistry, King Saud University, Riyadh, Kingdom of Saudi Arabia; and [3]Department of Anatomy, Faculty of Medicine, Pontificia Universidad Católica de Chile, Santiago, Chile; *corresponding author, abigail.tucker@kcl.ac.uk

Interactions of the Tooth and Bone during Development

ABSTRACT

The tooth works as a functional unit with its surrounding bony socket, the alveolar bone. The growth of the tooth and alveolar bone is coordinated so that a studied distance always separates the 2, known as the tooth-bone interface (TBI). Lack of mineralization, a crucial feature of the TBI, creates the space for the developing tooth to grow and the soft tissues of the periodontium to develop. We have investigated the interactions between the tooth and its surrounding bone during development, focusing on the impact of the developing alveolar bone on the development of the mouse first molar (M1). During development, TRAP-positive osteoclasts are found to line the TBI as bone starts to be deposited around the tooth, removing the bone as the tooth expands. An enhancement of osteoclastogenesis through RANK-RANKL signaling results in an expansion of the TBI, showing that osteoclasts are essential for defining the size of this region. Isolation of the M1 from the surrounding mesenchyme and alveolar bone leads to an expansion of the tooth germ, driven by increased proliferation, indicating that, during normal development, the growth of the tooth germ is constrained by the surrounding tissues.

KEY WORDS: dental follicle, ankylosis, odontogenesis, osteoclasts, RANK/RANKL, periodontium-gingiva.

INTRODUCTION

Mammalian tooth formation is a complex process involving epithelial-mesenchymal interactions between the ectoderm and neural-crest-derived mesenchyme (Chai *et al.*, 2000; Rothova *et al.*, 2012). These cells gradually undergo morphogenesis and differentiation, forming both the tooth and the surrounding periodontal tissue [alveolar bone, periodontal ligament (PDL), and cementum], creating a functional unit for mastication (Cho and Garant, 2000; Diep *et al.*, 2009). The region between the alveolar bone and the dental cementum of the tooth can be defined as the tooth-bone interface (TBI) (Fleischmannova *et al.*, 2010). In functional teeth, the TBI houses the soft tissues of the PDL, a mainly neural-crest-derived structure that anchors the tooth and jawbone together (Kaku *et al.*, 2012). The TBI accommodates the shock-absorbing function of the PDL and distributes the mechanical stress generated during mastication, tooth movement, and bone remodeling (Lekic and McCulloch, 1996; Sodek and McKee, 2000). During tooth crown development, a TBI is found between the tooth germ and the surrounding alveolar bone and creates a space for the developing tooth to grow, while during root development it forms a soft-tissue space in which the periodontal ligament can develop.

When the TBI is compromised, the bone can fuse with the tooth, resulting in ankylosis (Albers, 1986). For ankylosis to be avoided, it is essential that the TBI remain free from mineralization. Tissue-culture experiments have shown that the developing TBI possesses osteogenic potential, since isolated dental follicle containing TBI at the cap stage (E14.5) can form bone when cultured under a kidney capsule (Kim *et al.*, 2007). In addition to inhibition of osteogenesis of the TBI cells, encroachment of bone from the jaw into the TBI also needs to be prevented. This appears to involve the action of osteoclasts, which regulate bone resorption. In mice with impaired osteoclast function, the alveolar bone starts to encroach into the TBI, disrupting development of the growing tooth germ (Liu *et al.*, 2000; Kitahara *et al.*, 2002; Ida-Yonemochi *et al.*, 2002; Mekaapiruk *et al.*, 2002; Suzuki *et al.*, 2004; Helfrich, 2005). Regulation of osteoclastogenesis also has a critical role in facilitating dental eruption, clearing the bone away from the path of eruption (Wise and King, 2008). In keeping with this, failure in osteoclast formation leads to primary failure of eruption in humans and rats (Helfrich, 2005; Frazier-Bowers *et al.*, 2010).

In this article, we report the results of a study in which we examined the interaction between the bone and tooth during embryonic development of the first lower molar (M1). We used explant culture, lineage labeling, and histochemistry to follow the relationship between the bone and tooth, and show
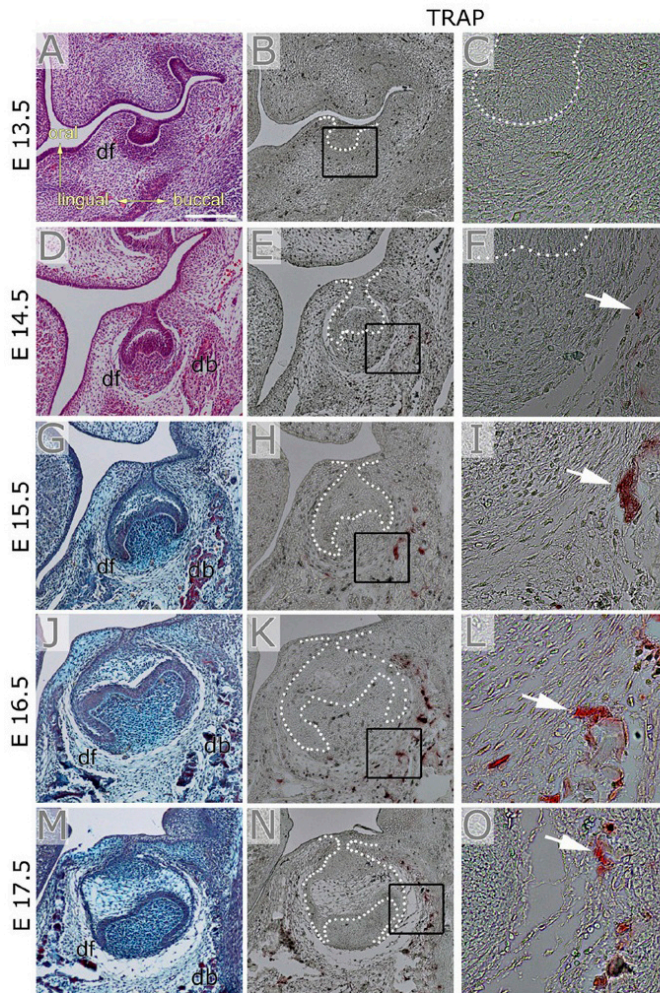
Alfaqeeh *et al.*

Figure 1. Initiation of the alveolar bone and osteoclastogenesis. **(A, D)** H&E-stained developing tooth germs, frontal section. **(G,J,M)** Trichrome stain of developing tooth germs, frontal section. **(B,C,E,F,H,I,K,L,N,O)** Alternate sections stained for TRAP (red stain). **(C,F,I,L,O)** High-power view of area boxed in (B,E,H,K,N). (A-C) E13.5. At the tooth bud stage of development, no TRAP-positive cells were evident. (D-F) By the cap stage, E14.5, small patches of alveolar bone were evident on the buccal side of the tooth, with a few TRAP-positive cells lining the tooth-bone interface (TBI) (arrow). (G-I) At E15.5, alveolar bone was obvious on the buccal side, again associated with TRAP-positive cells lining the TBI (arrow). (J-L) By the bell stage (E16.5), alveolar bone was clearly seen also on the lingual side of the tooth, with TRAP cells lining the TBI (arrow). (M-O) By the late bell stage (E17.5), the alveolar bone had extended up toward the oral epithelium on both sides of the tooth, with TRAP cells lining the TBI (arrow). df = dental follicle, db = dentary bone. Scale bar in A = 300 μm (same scale in B,D,E,G,H,J,K,M, and N).

MATERIALS & METHODS

Embryo Collection and Culture

Wild-type CD1 embryos were collected according to Home Office regulations. Heads for histology and histochemistry were fixed in 4% paraformaldehyde from E13.5 to newborn (P0).

Tissue slices containing molar tooth germs were prepared from the mandibles of E14.5 mice by means of a standard table McIlwain™ Tissue Chopper (Mickle, Guildford, UK) (Diep *et al.*, 2009). Further information on culture, confocal imaging, and analysis of proliferation, surface area, volume, and density can be found in the online Appendix.

DiI Labeling

DiI is a lipophilic dye that intercalates in the cell membrane, marking groups of cells. DiI (Cell tracker CM-DiI, C-7000, Molecular Probes, Eugene, OR, USA) was dissolved in 100% EtOH. Before culture, small amounts of DiI were injected into the slices by means of a mouth aspirator. The position of the DiI was recorded with a fluorescence Leica dissecting microscope every 24 hrs (N = 20).

RANKL Experiments

RANKL protein (R&D Systems, Minneapolis, MN, USA) (diluted in sterile PBS containing 1% BSA and stored in a stock concentration, 10 μg/mL) was added to the culture medium at a concentration of 5 ng/mL (N = 24).

RESULTS

Formation of the TBI during Development

To understand development of the murine TBI, we first followed its development from initiation of the alveolar bone to complete enclosure of the developing tooth, just before birth. At the same time, the presence and location of osteoclasts were followed by the TRAP assay for visualization of the timing of osteoclast and bone formation. TRAP staining labels cells from the macrophage/osteoclast lineage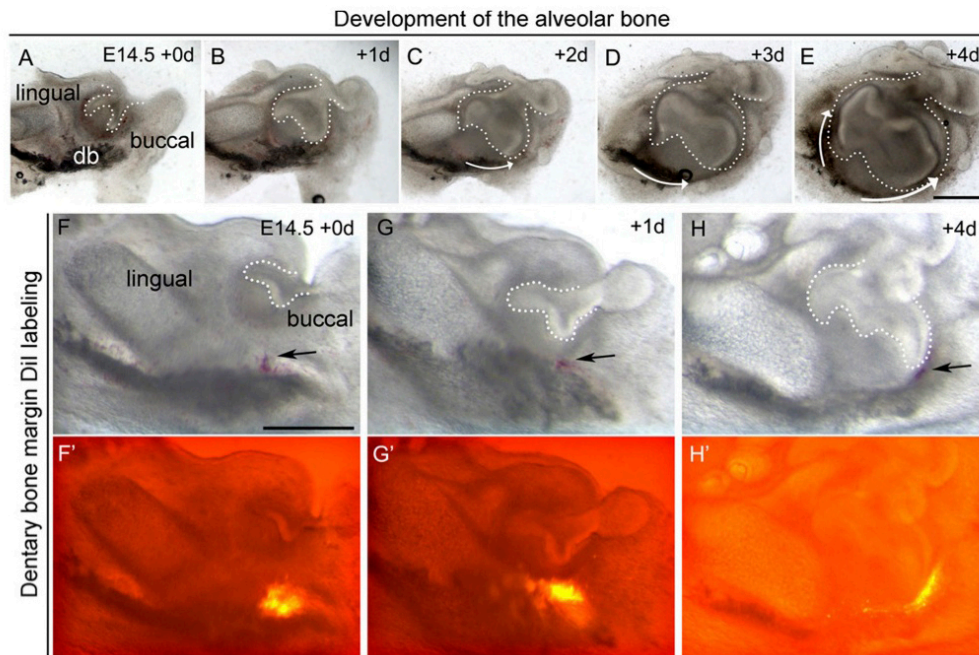 in addition to dendritic cells (Hayman *et al.*, 2000). At E13.5, when the tooth had reached the bud stage, no evidence of alveolar bone was observed from histology, and no TRAP-positive cells were evident (Figs. 1A-1C). By the cap stage, however, at

that the surrounding tissues act to constrain the growth rate of the tooth germ in culture and that osteoclasts play an important role in defining the size of the tooth-bone interface.

Figure 2. Development of the alveolar socket. **(A-E)** Culture of a cap-stage tooth germ (E14.5) for 4 days. (A) Day 0. (B) Day 1. (C) Day 2. (D) Day 3. (E) Day 4. The bone appeared dark under transmission light. Initially, the bone was at a distance from the tooth (A) and then started to appear on the buccal side of the tooth (arrow in C), followed by the lingual side (arrow in E). db = dentary bone. **(F-H)** Bright field of developing tooth germ in culture. **(F´-H´)** images in merged bright and dark field. (F, F´) Day 0. A Dil dot is placed at the margin of the dentary bone (arrow). (G, G´) Day 1. No movement of the Dil-labeled cells was observed, but the tooth germ had grown toward the injection site. (H, H´) Day 4. The tooth had grown toward the dentary bone, and labeled cells were observed around the buccal side of the tooth germ in the developing alveolar bone. Epithelium of the tooth germ outlined with white dots. Scale bar in E = 300 µm (same scale in A-D). Scale bar in F= 500 µm (same scale in F´, G, G´, H, H´).

E14.5, the alveolar bone, connected to the dentary bone (also known as the mandibular bone), was observed forming adjacent to the buccal side of the tooth, and a few TRAP-positive cells were located lining the bone facing the tooth-bone interface (TBI) (Figs. 1D-1F). As the tooth developed from the late cap to the bell stage, the alveolar bone reached around the buccal side of the tooth and started to form on the lingual side (Figs. 1G-1L). By the late-bell stage, the bone was observed on both sides of the tooth, reaching up toward the oral epithelium (Figs. 1M-O). At all these stages, a distinct non-mineralized TBI was evident, with TRAP-positive cells lining the bone side.

To follow the development of the alveolar bone during tooth development, we used a slice-culture approach to watch the relationship between the developing bone and tooth from E14.5. In slice cultures, the bone was evident as a darkly stained region that appeared to extend out from the dentary bone of the jaw, wrapping itself around the bone during the culture period (Figs. 2A-2E). As observed from histology, the bone first progressed around the buccal side of the tooth (Figs. 2B, 2C) and then was seen around the lingual side, reaching up toward the oral epithelium (Figs. 2D, 2E). This pattern of development has been suggested to be generated by

the osteogenic cells migrating around the tooth extending out from the dentary bone (Ramaesh and Bard, 2003). Alternatively, it could represent a wave of differentiation of the mesenchyme around the tooth forming bone. To distinguish between these 2 possibilities, we labeled the cells next to the dentary bone with the fluorescent label Dil. Initially, the Dil-labeled cells remained in position next to the border of the dentary bone as the tooth grew (Figs. 2F, 2F´, 2G, 2G´). After 4 days in culture, the tooth germ had grown considerably, meeting the original site of injection, and labeled cells were observed in an arc along the outer enamel epithelium on the buccal side (Figs. 2H, 2H´). The labeled cells therefore were recruited into the alveolar bone.

Increasing Osteoclast Numbers Lead to a Wider TBI

To investigate the role of osteoclasts in regulation of the TBI, we manipulated the level of osteoclasts in our cultures using the addition of RANKL (receptor activator of nuclear factor kappa-B ligand). RANK-RANKL signaling mediates osteoclastogenesis, with RANK, the receptor for RANKL, expressed on the surfaces of osteoclasts (Li *et al.*, 2000). Loss of osteoclasts has
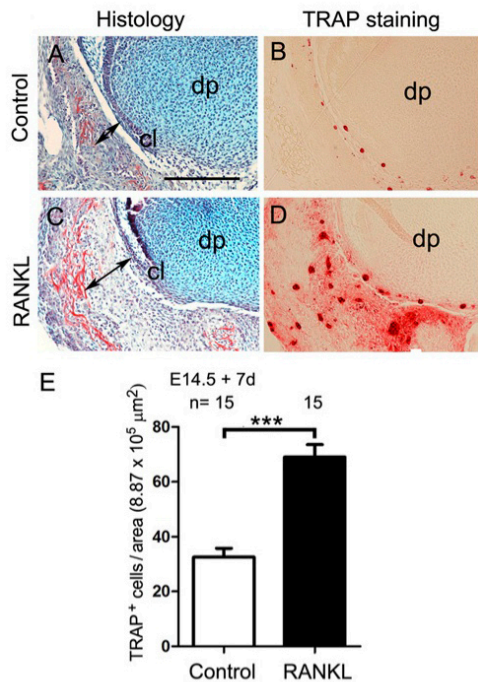
Figure 3. Enhancement of osteoclastogenesis widened the tooth-bone interface (TBI). **(A-D)** E14.5 tooth germs cultured for 6 days. (A,B) Control culture. (C,D) Cultures treated with 5 ng/mL RANKL. (A,C) Trichrome-stained tooth germs. (B,D) Alternate sections stained for TRAP. (A) In control cultures, alveolar bone formed close to the outer enamel epithelium of the bell-stage tooth germ, with (B) TRAP-positive cells lining the narrow TBI. (C) In RANKL-treated cultures, alveolar bone was found at a considerable distance from the tooth, and the TBI was expanded. (D) A large number of trap-positive cells is observed filling the TBI. **(E)** Graph showing the number of TRAP-positive cells in control and treated cultures. Three asterisks (***) correspond to $p < .001$. Arrows placed from the outer enamel epithelium near the cervical loop to the alveolar bone (stained red). cl = cervical loop, dp = dental papilla. Scale bar in A = 200 μm (same scale in B-D).

been shown to lead to invasion of the tooth germ by the bone; therefore, we predicted that an increase in osteoclasts would lead to an expansion of the TBI. Addition of RANKL at 5 ng/mL to tooth slices at E14.5 led to a significant increase in the number of TRAP-positive cells that surrounded the developing tooth germ in our cultures (Figs. 3B, 3D, 3E), without causing an increase in cell death (Appendix Fig. 1). The increased number of osteoclasts observed in the cultures was presumably derived from progenitor cells residing in the developing slice. In those cultures with large numbers of TRAP-positive cells around the developing tooth, the TBI between the tooth and bone was wider than in control cultures, indicating enhanced resorption of the bone (Figs. 3A, 3C).

Surrounding Tissues Constrain the Growth of the Tooth Germ

Since the tooth germ develops surrounded by a hard case of bone, the size of the tooth might be restricted by the presence of this hard tissue. To understand the impact of the surrounding tissues and alveolar bone on tooth development, we cultured tooth germs in isolation or within the surrounding tissue and bone. Tooth germs from one side of a slice were dissected out, while tooth germs from the contralateral side were left intact (Figs. 4A, 4B). Tooth germs isolated from the surrounding tissue appeared to grow much larger than their reciprocal tooth germs surrounded by jaw tissue (Figs. 4C, 4D, Appendix Fig. 2). When the increase in surface area of the tooth germs was calculated, the larger size of the isolated tooth germs was shown to be highly statistically significant (Fig. 4E). When the volumes of fixed cultures were assessed, the isolated tooth germs were already larger than the encapsulated tooth germs after 2 days in culture, with this difference increasing after 3 days (Fig. 4F). Analysis of the number of nuclei in a set area showed that the size difference was not due to a reduced cell density in the isolated tooth germs (Fig. 4G). However, the mitotic index was significantly increased in the isolated tooth germs compared with the encapsulated contralateral side after 2 days (Figs. 4H, 4I, 4K). In contrast, this difference was no longer evident after 3 days in culture, indicating that the increase in proliferation occurred during a limited time-window (Figs. 4H, 4J, 4L). Analysis of the mitotic index in the enamel organ alone gave equivalent results, with a statistically significant increase observed after 2 days in isolated cultures (6.54% compared with 2.88%) but not after 3 days (3.41% compared with 2.73%). When the experiments were repeated with dissected whole molar placodes rather than slices, a similar increase in volume was detected after 3 days in culture in those placodes where the tooth germ had been cropped from the surrounding bone and tissue (Appendix Fig. 3).

It might be expected that a similar expansion of the tooth germ would occur after the addition of RANKL because of increased bone resorption freeing up space for the tooth germ to grow. To test this, we analyzed the increase in surface area after the addition of RANKL. Although in many of the cultures the tooth germs appeared to grow larger than control treated cultures (see Appendix Figs. 1D, 1E), large variations in size were observed, and the results were not statistically significant (data not shown).

DISCUSSION

Our results illustrate the close relationship of the tooth and bone during development. *In vivo* and in culture, the alveolar bone appears to form as an extension of the dentary bone. In our DiI labeling experiments, we show that cells at the margin of the dentary bone do indeed end up surrounding the tooth as part of the developing alveolar bone. This movement appears aided by the downgrowth of the tooth germ toward the dentary bone. Previous labeling experiments have shown that cells within the dental follicle can contribute to the developing alveolar bone (Diekwisch, 2002; Diep *et al.*, 2009). It would appear, therefore,
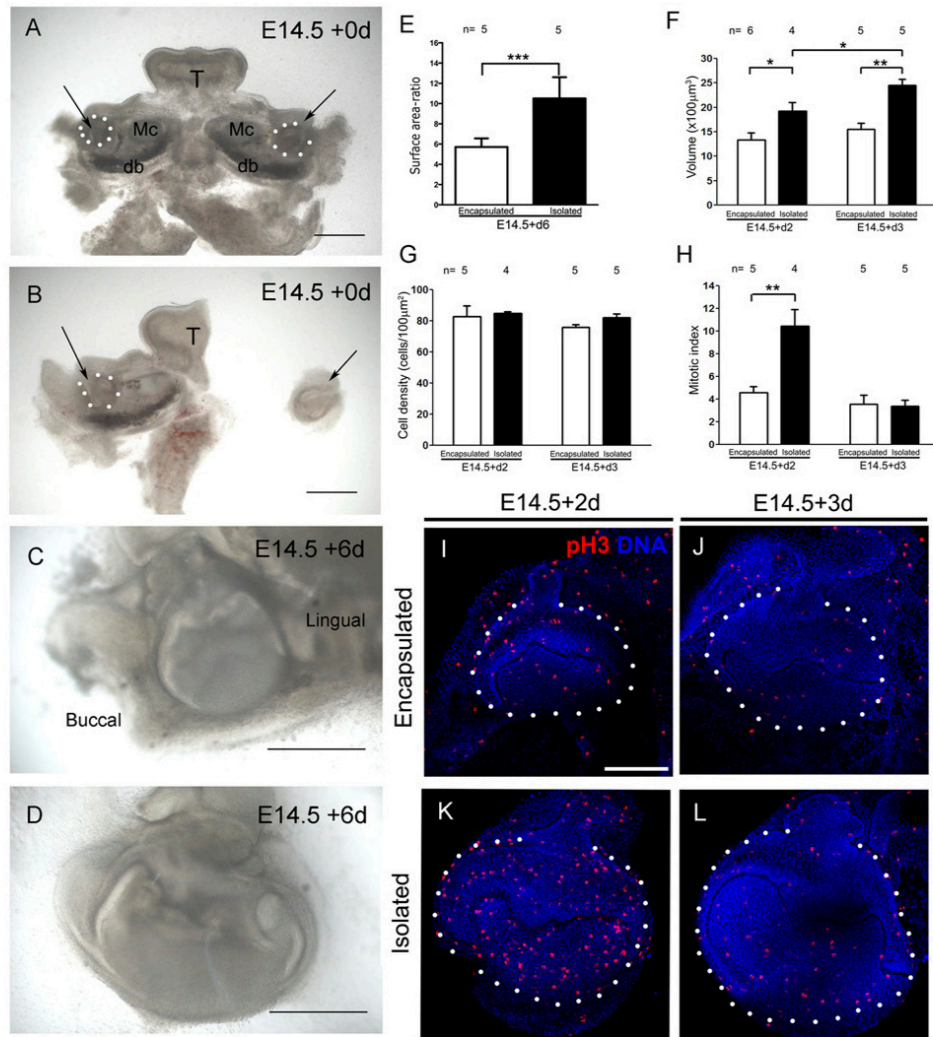
Bone-Tooth Interactions during Development

Figure 4. The surrounding tissue constrains tooth growth. **(A-D, I-L)** Cultured tooth germs. (A,B) E14.5 tooth slices, day 0. (A) Intact representative slice with cap-stage molars highlighted by arrows and outlined with white dots. (B) Hemi-sected slice with isolation of the molar tooth germ on one side. Arrows indicate molar tooth germs. (C,D) Explants after 6 days in culture. (C) Encapsulated molar. (D) Isolated molar. **(E)** Surface areas were used to calculate the ratio of growth in surface area (based on a ratio of surface area at the last day of culture divided by the surface area at the first day of culture). Graph showing statistically significant difference in surface area between tooth germs cultured with or without the surrounding tissue after 6 days in culture. **(F)** Volumes calculated from confocal images of cultured tissue after 2 and 3 days in culture. **(G)** Cell density after 2 and 3 days in culture. **(H)** Mitotic index after 2 and 3 days in culture. (I-L) Confocal images of tooth germs incubated with Phosphohistone H3 antibody for assessment of the mitotic index. (I) Two-day culture, encapsulated. (J) Three-day culture, encapsulated. (K) Two-day culture, isolated. More positive cells are observed compared with I. (L) Three-day culture, isolated. Similar numbers of positive cells are observed compared with J. One (*), 2 (**), and 3 (***) asterisks correspond to $p < .05$, $p < .01$, and $p < .001$, respectively. T = tongue, db = dentary bone, Mc = Meckel's cartilage. Scale bar in A-D = 500 μm. Scale bar in I = 200 μm (same scale in J-L).

that 2 distinct mechanisms form the alveolar bone, both a differentiation of dental follicle cells around the tooth and, concurrently, a recruitment of bone cells from the margins of the dentary.

It has previously been proposed that osteoclasts play a role in protecting the tooth germ from invasion by bone. Here we show that osteoclasts line the bone along the TBI from the very earliest stages of tooth development, as soon as bone is deposited. Enhancement of osteoclastogenesis leads to a widening of the TBI, just as previous experiments have shown that a reduction in osteoclasts leads to tooth germ invasion, and therefore loss of the TBI (Ida-Yonemochi *et al.*, 2002; Kitahara *et al.*, 2002). The number of osteoclasts is therefore very important for maintaining the size of the TBI during development. How this number is controlled during normal development is unclear, but it seems likely that a signal from the tooth germ controls this process.

Our isolation experiments indicate that the growth of the tooth germ is constrained by the surrounding tissues. This may represent a physical restriction by the enveloping alveolar bone or, equally, it may indicate the presence of inhibitory signaling molecules in the surrounding tissue. From 3D reconstructions of the developing mandible, it has been suggested that spatial impediment by the developing bone might be a factor in controlling the morphogenesis of the developing tooth from the bell stage onward (Radlanski *et al.*, 1998). Inhibitory signals in the tooth mesenchyme have been proposed to control the number of tooth germs that develop, as trimmed incisor explants develop supernumerary incisors (Munne *et al.*, 2009). Here we show that removal of the surrounding mesenchyme and bone leads to a significant increase in size of the molar tooth germ, led by a significant increase in proliferation. The increased proliferation was evident after 2 days in culture, matched by an increase in volume, which became more pronounced after 3 days in culture. After 3 days, however, proliferation levels dropped to those of the control cultures, indicating that the later size differences might all be driven by the earlier increase in proliferation. Since the size and proliferation change occurred relatively early in tooth development, before complete encapsulation of the tooth germ by bone, this may indicate that size differences were not solely due to physical constraint by the bone and that inhibitory influences from non-osseous tissue are involved.

Interestingly, when RANK was overexpressed in the macrophage lineage, leading to more TRAP-positive cells in the alveolar bone, accelerated root elongation was observed at postnatal stages (Castaneda *et al.*, 2011). This was shown to be due to an increase in proliferation in the HERS cells of the tooth. However, no change was found in final root length. A similar situation may be occurring in our studies, whereby isolation of the tooth germ leads to an initial acceleration in growth that might be caught up by the encapsulated tooth after a longer period in culture. This may explain the lack of any obvious tooth expansion in OPG knockout adult mice, despite reduction in the alveolar bone (Sheng *et al.*, 2010), with these mice perhaps showing a size phenotype earlier in development. Given the above, removal of bone by RANKL to enhance osteoclastogenesis might be expected to lead to an expansion of the tooth germs. However, our results in culture varied. This may be due

to the fact that the RANKL signaling pathway affects not only osteoclastogenesis but also tooth development, affecting early morphogenesis and tooth mineralization (Ohazama *et al.*, 2004; Sheng *et al.*, 2010). The number of osteoclast progenitors found in each slice prior to culture might also differ, leading to variable findings.

Further understanding of the potential mechanical role of the alveolar bone and surrounding tissue on tooth development, combined with an understanding of the signals that lead to coordinated development of the tooth and bone, will help us understand how defects such as ankylosis occur and can be avoided or treated more efficiently.

ACKNOWLEDGMENTS

REFERENCES

Albers DD (1986). Ankylosis of teeth in the developing dentition. *Quintessence Int* 17:303-308.

Castaneda B, Simon Y, Jacques J, Hess E, Choi YW, Blin-Wakkach C, *et al.* (2011). Bone resorption control of tooth eruption and root morphogenesis: involvement of the receptor activator of NF-kappaB (RANK). *J Cell Physiol* 226:74-85.

Chai Y, Jiang X, Ito Y, Bringas P Jr, Han J, Rowitch DH, *et al.* (2000). Fate of the mammalian cranial neural crest during tooth and mandibular morphogenesis. *Development* 127:1671-1679.

Cho MI, Garant PR (2000). Development and general structure of the periodontium. *Periodontol* 2000 24:9-27.

Diekwisch TG (2002). Pathways and fate of migratory cells during late tooth organogenesis. *Connect Tissue Res* 43:245-256.

Diep L, Matalova E, Mitsiadis TA, Tucker AS (2009). Contribution of the tooth bud mesenchyme to alveolar bone. *J Exp Zool B Mol Dev Evol* 312B:510-517.

Fleischmannova J, Matalova E, Sharpe PT, Misek I, Radlanski RJ (2010). Formation of the tooth-bone interface. *J Dent Res* 89:108-115.

Frazier-Bowers SA, Puranik CP, Mahaney MC (2010). The etiology of eruption disorders – further evidence of a 'genetic paradigm'. *Semin Orthod* 16:180-185.

Hayman AR, Bune AJ, Bradley JR, Rashbass J, Cox TM (2000). Osteoclastic tartrate-resistant acid phosphatase (Acp 5): its localization to dendritic cells and diverse murine tissues. *J Histochem Cytochem* 48:219-228.

Helfrich MH (2005). Osteoclast diseases and dental abnormalities. *Arch Oral Biol* 50:115-122.

Ida-Yonemochi H, Noda T, Shimokawa H, Saku T (2002). Disturbed tooth eruption in osteopetrotic (op/op) mice: histopathogenesis of tooth malformation and odontomas. *J Oral Pathol Med* 31:361-373.

Kaku M, Komatsu Y, Mochida Y, Yamauchi M, Mishina Y, Ko CC (2012). Identification and characterization of neural crest-derived cells in adult periodontal ligament of mice. *Arch Oral Biol* 57:1668-1675.

Kim JY, Cho SW, Hwang HJ, Lee MJ, Lee JM, Cai J, *et al.* (2007). Evidence for expansion-based temporal BMP4/NOGGIN interactions in specifying periodontium morphogenesis. *Cell Tissue Res* 330:123-132.

Kitahara Y, Suda N, Kuroda T, Beck F, Hammond VE, Takano Y (2002). Disturbed tooth development in parathyroid hormone-related protein (PTHrP)-gene knockout mice. *Bone* 30:48-56.

Lekic P, McCulloch CA (1996). Periodontal ligament cell population: the central role of fibroblasts in creating a unique tissue. *Anat Rec* 245:327-341.

Li J, Sarosi I, Yan XQ, Morony S, Capparelli C, Tan HL, *et al.* (2000). RANK is the intrinsic hematopoietic cell surface receptor that controls osteoclastogenesis and regulation of bone mass and calcium metabolism. *Proc Natl Acad Sci USA* 97:1566-1571.

Liu JG, Tabata MJ, Fujii T, Ohmori T, Abe M, Ohsaki Y, *et al.* (2000). Parathyroid hormone-related peptide is involved in protection against invasion of tooth germs by bone via promoting the differentiation of osteoclasts during tooth development. *Mech Dev* 95:189-200.

Mekaapiruk K, Suda N, Hammond VE, Beck F, Kuroda T, Takano Y, *et al.* (2002). The influence of parathyroid hormone-related protein (PTHrP) on tooth-germ development and osteoclastogenesis in alveolar bone of PTHrP-knock out and wild-type mice in vitro. *Arch Oral Biol* 47:665-672.

Munne PM, Tummers M, Jarvinen E, Thesleff I, Jernvall J (2009). Tinkering with the inductive mesenchyme: Sostdc1 uncovers the role of dental mesenchyme in limiting tooth induction. *Development* 136:393-402.

Ohazama A, Courtney JM, Sharpe PT (2004). *Opg, Rank*, and *Rankl* in tooth development: co-ordination of odontogenesis and osteogenesis. *J Dent Res* 83:241-244.

Radlanski RJ, Mocker E, Rahlfs D (1998). Computer-aided graphical reconstructions of the development of murine dental primordia and surrounding structures from day 12 until birth. *Eur J Oral Sci* 106(Suppl 1):71-79.

Ramaesh T, Bard JB (2003). The growth and morphogenesis of the early mouse mandible: a quantitative analysis. *J Anat* 203:213-222.

Rothova M, Thompson H, Lickert H, Tucker AS (2012). Lineage tracing of the endoderm during oral development. *Dev Dyn* 241:1183-1191.

Sheng ZF, Ye W, Wang J, Li CH, Liu JH, Liang QC, *et al.* (2010). OPG knockout mouse teeth display reduced alveolar bone mass and hypermineralization in enamel and dentin. *Arch Oral Biol* 55:288-293.

Sodek J, McKee MD (2000). Molecular and cellular biology of alveolar bone. *Periodontol* 2000 24:99-126.

Suzuki T, Suda N, Ohyama K (2004). Osteoclastogenesis during mouse tooth germ development is mediated by receptor activator of NFKappa-B ligand (RANKL). *J Bone Miner Metab* 22:185-191.

Wise GE, King GJ (2008). Mechanisms of tooth eruption and orthodontic tooth movement. *J Dent Res* 87:414-434.

S.A. Alfaqeeh[1,2], M. Gaete[1,3], and A.S. Tucker[1]*

[1]Department of Craniofacial Development and Stem Cell Biology, Department of Orthodontics, King's College London, London, UK, SE1 9RT; [2]Department of Pediatric Dentistry and Orthodontics, College of Dentistry, King Saud University, Riyadh, Kingdom of Saudi Arabia; and [3]Department of Anatomy, Faculty of Medicine, Pontificia Universidad Católica de Chile, Santiago, Chile; *corresponding author, abigail.tucker@kcl.ac.uk

Interactions of the Tooth and Bone during Development

APPENDIX

METHODS

Slice Culture

Mandibles were dissected from E14.5 mouse embryos in culture medium (DMEM/F12 supplemented with 1% penicillin/streptomycin and 1% Glutamax; Gibco, Life Technologies, Carlsbad, CA, USA). Mandibles were frontally sliced at 250 µm. Tissue slices containing the central region of the first molars (M1) were selected for culture. These were identified by the presence of the enamel knot (EK) as a bulge in the inner enamel epithelium within the slice. For the comparison of isolated and encapsulated tooth germs, slices were divided into left and right, one side cultured as a whole slice, while the molar tooth germ was dissected out of the other side by means of a sharpened tungsten needle. Both pieces (encapsulated and isolated tooth germ) were cultured on the same filter paper, so that the culture conditions would be as standard as possible. Similar cultures were performed containing encapsulated and isolated dissected placodes from unsliced mandibles. Explants were cultured in DMEM/F12 supplemented with 1% penicillin/streptomycin and 1% Glutamax and incubated in a humidified atmosphere of 5% CO_2 at 37°C.

Immunofluorescence

Fixed samples were permeabilized in PBS 0.5% Triton X-100 (PBS-Tr), blocked in PBS-Tr, 10% goat serum, and incubated in rabbit polyclonal anti-phospho-Histone H3 (Upstate 06-570; Millipore, Billerica, MA, USA) 1:300 overnight at 4°C. Samples were then washed in PBS-Tr, incubated for 2 hrs in AlexaFluor® 568 (Life Technologies, Carlsbad, CA, USA) goat anti-rabbit containing DAPI 1:1,000 in PBS-Tr 10% BSA, washed again, and mounted in Vectashield® (Vector Labs, Burlingame, CA, USA). This method labels all cells in the M phase but may miss cells that are at other stages of the cell cycle.

Confocal Imaging and Analysis

Confocal optical sections (Leica SP5 laser scanning confocal microscope) from complete z-stacks were used and quantified for tooth germ volume measurement with Volocity Software (Perkin Elmer). The cervical-loop-containing section was used to quantify cell density (number of nuclei/area) and mitotic index (pH3+ cells/100 nuclei) in the enamel organ and dental papilla, with Volocity. Results were plotted and analyzed by paired *t* test with Graph Pad Prism 5 software®.

To calculate the two-dimensional surface areas, we analyzed an image of the tooth germs using Fiji software (http://fiji.sc/Fiji). The epithelial and mesenchymal portions of the first molar tooth germ were outlined and measurements were performed using the set scale option with a pre-defined known distance in µm per pixel.

Numbers for morphometric analysis: N = 5 encapsulated and 5 isolated tooth germs at 3 time points (2, 3, and 6 days in culture).

Whole-placode Culture Analysis

In whole-placode cultured samples, volume estimation was performed on stratified measures of serial sections as described (Hepworth *et al.*, 1989).

Tartrate-resistant Acid Phosphatase (TRAP) Staining

Tissues were fixed in 4% paraformaldehyde (PFA) in PBS and processed for wax embedding. The slides were placed within the TRAP staining solution (see below) in a Coplin jar incubated at 37°C for 30 to 40 min.

TRAP staining solution, consisting of 1 mg naphthol-AS-TR-phosphate (Sigma®, St. Louis, MO, USA), was added *per* mL actetate buffer (pH 5.2) [10.5 mL Glacial acetic acid: 0.2 M + 39.5 mL sodium acetate (Sigma-Aldrich®), 0.2 M, brought to 100 mL with H_2O]. A 1-µL quantity of N-N-dimethylformamide, 23 mg sodium tartrate (Sigma®), and 1 mg Fast Red TR Salt (Sigma®) were added *per* mL of staining solution.

DS1

For histology, alternate slides were stained with Sirius red, Alcian blue, and Hematoxylin (trichrome) or Hematoxylin and Eosin.

To assess the number of osteoclasts, we counted all multinucleated red stained cells within a set field on a slide and performed a Student's *t* test.

Cell Death Assay

Analysis of cell death after RANKL treatment was performed by the incubation of cultures for 30 min in LysoTracker® red (Invitrogen, Carlsbad, CA, USA). Cultures were then fixed and incubated in Alexa Fluor® 488 Phalloidin (Invitrogen) 1:150 for 3 hrs at RT, washed- mounted as described for immunofluorescence and scanned confocally.

Dose Response to RANKL

To assess which dose to use for our RANKL experiments, we initially chose 3 concentrations of RANKL (5 ng/mL, 25 ng/mL, and 50 ng/mL). Cultures were fixed after 6 days and then processed for wax embedding. All multinucleated red stained cells within a set field on a slide were counted and compared with untreated controls.

N = 3 molar slices for each concentration, the average of counts from several fields for each slice.

APPENDIX REFERENCES

Hepworth WB, Carter MW, Seegmiller RE (1989). Technique for estimating fetal mouse thoracic volumes through image analysis of histological sections. *Anat Rec* 225:176-179.

Matalova E, Svandova E, Tucker AS (2012). Apoptotic signaling in mouse odontogenesis. *Omics* 16:60-70.

Appendix Figure 1. A 5-ng/mL quantity of RANKL leads to an increase in TRAP-positive cells in culture but does not induce cell death. (A-B) Confocal image of molar tooth cultures cultured for 2 days. Cell death (red spots); Phalloidin (green) outlines the cells to show morphology. **(A)** Control molar slice culture. **(B)** Slice treated with 5 ng/mL RANKL. **(A'B')** Same images as A and B, showing LysoTracker®-positive cells only (white spots). Yellow dots outline tooth germ. Apoptosis is low in the tooth germ but high in the surrounding tissue where bone remodeling is taking place in both sets of cultures (Matalova *et al.*, 2012). Scale bar in A = 50 μm. dp = dental papilla. **(C)** Dose response to rising concentrations of RANKL as indicated by the average number of TRAP-positive cells counted within a cultured tooth germ. High levels of RANKL (50 ng/mL) have negative effects on enhancement of osteoclastogenesis compared with lower concentrations. **(D, E)** Molar tooth after 6 days in culture. (D) Control medium. (E) RANKL, 5 ng/mL. Dental epithelium outlined with white dots.

Appendix Figure 2. Increased size of isolated molar tooth germs in slice culture. (A-H) Cultured E14.5 tooth germs in slice culture. (A, E) E14.5 tooth slices, day 0. The tooth germ (dotted lines in **A'**) was left intact, while the tooth germ in **E** was dissected out of the surrounding tissue (along dotted lines in **E'**). (B, F) Same slices as above after 1 day in culture. (C, G) Same slices as above after 3 days in culture. (D, H) Same slices as above after 6 days in culture. (**A'-H'**) High-power view of boxed regions in A-H. Scale bar in A = 500 μm (same scale in B-H).
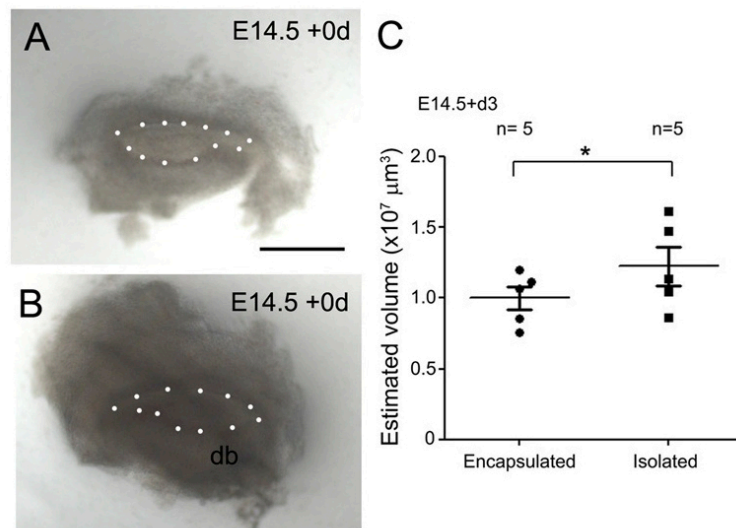
Appendix Figure 3. Increased size of isolated molar tooth germs after whole-placode culture. **(A,B)** Dissected molar placodes, E14.5, day 0. (A) Placode with majority of underlying mesenchyme removed. (B) Placode plus condensing bone (db) and Meckel's cartilage. Molar placode outlined with white dots. **(C)** Volume of final tooth germs after 3 days in culture. The cultures with less mesenchymal tissue resulted in a significantly larger tooth germ. Scale bar in A = 500 μm (same scale in B).

Appendix *ii*

Published abstracts from PhD

Alfaqeeh, S., McDonald, F. and Tucker, A.S. (2012) 'Maintenance of the tooth-bone interface during development', *Journal of Dental Research* 91((Spec Iss B)): 21.

Start | Browse by Day | Author Index | Keyword Index

21 Maintenance of the Tooth-Bone Interface during Development

Wednesday, June 20, 2012: 9 a.m. - 10:30 a.m.
Location: Iguacu Room (Mabu Hotel)
Presentation Type: Oral Session

*S. ALFAQEEH, F. MCDONALD, and **A.S. TUCKER**, Craniofacial Development and Orthodontics, King's College London, London, United Kingdom*
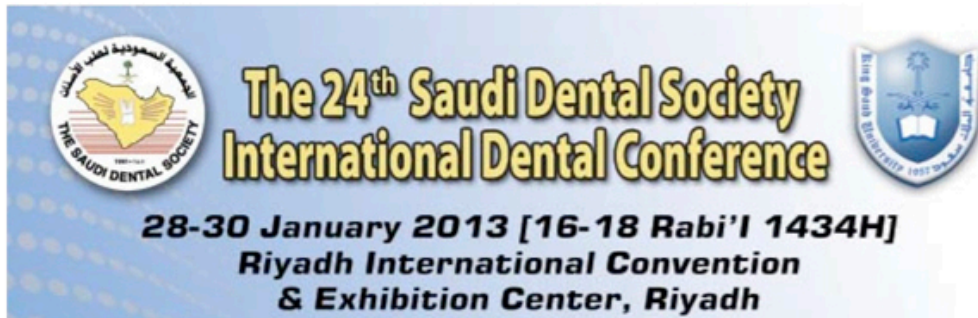
Objective:

The tooth forms a functional complex with the surrounding alveolar bone cushioned by the soft tissues of the periodontium. The ability of the tooth and its associated periodontium to undergo rapid remodelling during the process of mastication, tooth movement, and the progression of periodontal diseases is crucial to understand. During development a space is created between the developing tooth and bone, allowing the tooth to grow and periodontal ligament to form. We have called this region the tooth-bone interface (TBI). Defects in the TBI lead to ankylosis of the tooth. When isolated in culture the cells of the TBI differentiate into osteoblasts and form bone. During normal development both bone formation in the TBI and encroachment of the alveolar bone into the TBI must be prevented. We have started to characterise the mechanisms that protect the TBI utilising murine tooth slice explants, which allow for the developing tooth, bone and TBI to be visualised in culture.

Method:

Signalling molecules hypothesised to play a role in creation of the TBI were added to the cultures and analysed by TRAP assays, *in situ* hybridisation and histology.

Result:

Osteoclasts were shown to line the alveolar bone at the border of the TBI during development. Addition of RANKL and OPG to developing tooth germs in culture altered the number of osteoclasts, leading to changes in the size and shape of the TBI and encroachment of the bone into the tooth germ. A change in fate of the TBI was observed after altering the level of BMP signalling in culture, indicating that this molecule plays an important role in controlling the size of the TBI.

Conclusion:

We intend to clarify these results and further investigate the interactions between the tooth and bone during development, looking at the roles of Noggin, Runx2, Twist, and Periostin.

Keywords: Bone, Growth & development, Periodontium-gingiva, RANKL and Teeth

Alfaqeeh, S., McDonald, F. and Tucker, A.S. (2012) 'Constraints on tooth growth by the developing alveolar bone', *Genetics Research* 94(06): 353-360.

353

Abstracts of papers presented at the 23rd Genetics Society's Mammalian Genetics and Development Workshop held at the Institute of Child Health, University College London on 22nd November 2012

Edited by: NICHOLAS D. E. GREENE AND ANDREW J. COPP
UCL Institute of Child Health, 30 Guilford Street, London WC1N 1EH

Constraints on tooth growth by the developing alveolar bone

SARAH ALFAQEEH, FRASER MCDONALD and ABIGAIL TUCKER
Department of Craniofacial Development and Stem Cell Biology & Orthodontics, Dental Institute at Guy's, King's College and St. Thomas' Hospitals, London, UK

The growth of the tooth and alveolar bone is co-ordinated so that a studied distance always separates the two. We have called this distance, the tooth-bone interface (TBI). Lack of mineralization, a crucial feature of the TBI, creates the space for the developing tooth to grow and the soft tissues of the periodontium to develop. No studies have been done to understand the signals that maintain the bone-free TBI, or the influence of the TBI on tooth development. We have investigated the impact of the developing alveolar bone on the size and development of the mouse first molar (M1). We evaluated the growth and osteoclasts distribution of the M1 in explant cultures using two methods, isolation of the M1 from the surrounding alveolar bone, and enhancement of osteoclastogenesis through RANK-RANKL signalling after treatment with RANKL, an osteoclast activator. Both methods showed a significant increase in the size of M1. Our data indicate that alveolar bone and RANKL regulate tooth size without altering development and osteoclasts are indispensable in promoting the formation of the TBI. We intend to further investigate the interactions between the tooth and alveolar bone during development, looking at the roles of other genes involved in TBI formation.

Investigating the role of mitochondrial folate metabolism in neural tube defects

YUN-JIN PAI, KIT-YI LEUNG, DAWN SAVERY, ANDREW J. COPP and NICHOLAS D. E. GREENE
Neural Development Unit, Institute of Child Health, University College London, London, UK

Folate one-carbon metabolism (FOCM) is a network of reactions that provide one-carbon units for processes vital to cell function, such as de novo biosynthesis of purines and thymidylate for DNA replication and methionine for methylation. FOCM has long been associated with a common group of congenital disorders: neural tube defects (NTDs), in which the neural tube, the embryonic precursor of the brain and spinal cord, fails to close. Evidence from clinical trials and mice models have hinted at the potential roles that FOCM play during neurulation, but the multifactorial nature of NTDs and complexity of FOCM pathways has hampered elucidation of precise causal relationships between the two. We focused on the glycine cleavage system (GCS), a mitochondrial component of the FOCM mediated by four enzymes: *GLDC*, *AMT*, *GCSH* and *DLD*. Collectively, these enzymes cleave glycine to supply one-carbon units to FOCM reactions occurring in the cytoplasm. Deficiencies in the GCS result in non-ketotic hyperglycinemia, but recent evidence has emerged suggesting that they also predispose to neural tube defects. The aim of this project is to study the effects of GCS deficiency on folate metabolism and the developmental mechanisms underlying NTDs found in *Gldc* and *Amt* mice models.

Appendix *iii*

Meeting abstracts from PhD

King's College London Dental Institute

14th Annual Postgraduate Research Day

Floor 18 Tower Wing, Guy's Campus

Tuesday 3rd April 2012

Session 3: Development of the head

3D. SARAH A. ALFAQEEH

Maintenance of the Tooth-bone Interface during Development

Craniofacial Development and Orthodontics

Dr. Abigail Tucker and Prof. Fraser McDonald

The tooth forms a functional complex with the surrounding alveolar bone cushioned by the soft tissues of the periodontium. During development, a space is created between the developing tooth and bone, allowing the tooth to grow and periodontal ligament to form. We have called this region the tooth-bone interface (TBI). Defects in the TBI lead to ankylosis of the tooth. When isolated in culture, cells of the TBI differentiate into osteoblasts and form bone. During normal development, therefore, bone formation in the TBI must be prevented. We have started to characterise the mechanisms that protect the TBI utilising murine tooth slice explants. Signalling molecules hypothesised to play a role in creation of the TBI were added to the cultures, which were analysed by TRAP assays, *in situ* hybridisation and histology. Osteoclasts were shown to line the alveolar bone at the border of the TBI during development. Addition of RANKL and OPG to developing tooth germs in culture altered the number of osteoclasts, leading to changes in the size and shape of the TBI and encroachment of bone into the tooth germ. We intend to clarify these results and further investigate the interactions between the tooth and bone during development.

Abstract no. 543: Maintenance of the Tooth-bone Interface during Development

Authors: S. Alfaqeeh, A.S. Tucker, and F. Mcdonald
Craniofacial Development and Orthodontics, King's College London

Abstract: The tooth forms a functional complex with the surrounding alveolar bone cushioned by the soft tissues of the periodontium. The ability of the tooth and its associated periodontium to undergo rapid remodelling during the process of mastication, tooth movement, and the progression of periodontal diseases is crucial to understand. During development a space is created between the developing tooth and bone, allowing the tooth to grow and periodontal ligament to form. We have called this region the tooth-bone interface (TBI). Defects in the TBI lead to ankylosis of the tooth. When isolated in culture the cells of the TBI differentiate into osteoblasts and form bone. During normal development, therefore, both bone formation in the TBI and encroachment of the alveolar bone into the TBI must be prevented. We have started to characterise the mechanisms that protect the TBI utilising murine tooth slice explants. Such explants allow for the developing tooth, bone and TBI to be visualised in culture. Signalling molecules hypothesised to play a role in creation of the TBI were added to the cultures, which were analysed by TRAP assays, in situ hybridisation and histology. Osteoclasts were shown to line the alveolar bone at the border of the TBI during development. Addition of RANKL and OPG to developing tooth germs in culture altered the number of osteoclasts, leading to changes in the size and shape of the TBI and encroachment of the bone into the tooth germ. A change in fate of the TBI was observed after altering the level of BMP signalling in culture, indicating that this signalling molecule plays an important role in controlling the size of the TBI. We intend to clarify these results and further investigate the interactions between the tooth and bone during development, looking at the roles of Noggin, Runx2, Twist, and Periostin.

Constraints on Tooth Growth by the Developing Alveolar Bone

Sarah A. Alfaqeeh[1,2], Dr. Abigail S. Tucker[1] and Prof. Fraser McDonald[1]

[1]*Department of Craniofacial Development and Stem Cell Biology, and Department of Orthodontics, Dental Institute at Guy's, King's College and St Thomas' Hospitals, London, UK*
[2]*Department of Pediatric Dentistry and Orthodontics, College of Dentistry, King Saud University, Riyadh, KSA*

Teeth must grow in the right positions relative to the forming jaw-bones, attaching to alveolar bone via periodontal ligaments (PDL). The growth of tooth and alveolar bone is co-ordinated so that a distance always keeps the two apart. We have called this distance, the tooth-bone interface (TBI). In adults, the TBI accommodates the shock-absorbing properties of the PDL and distribute the mechanical stress generated during mastication, tooth movement and rapid teeth remodelling. During development, lack of mineralization, a crucial feature of the TBI, creates the space for the developing tooth to grow and forms a gap between the tooth and bone in which soft tissues of the periodontium can develop. The TBI protects the tooth from any defective fusion with the alveolar bone, which would result in ankylosis. No studies have been done to understand the signals that maintain the bone free TBI, or to understand the influence of the TBI on tooth development. This study has investigated the impact of the developing alveolar bone on the size and development of the mouse first molar (M1). The growth of the mandibular M1 and distribution of osteoclasts were evaluated *in vivo* and in tissue explant cultures. The role of the surrounding bone was investigated using isolation of the M1 from the surrounding alveolar bone and enhancement of osteoclastogenesis through RANK-RANKL signaling. The M1 showed a significant increase in size when cultured without alveolar bone compared to controls with the alveolar bone. Similar results were obtained after treatment with RANKL, an osteoclast activator. Both, RANKL treatment and removal of the alveolar bone in culture had the same effect on M1 size. These data indicate that alveolar bone and RANKL regulate tooth size without altering development. These suggest that osteoclasts in the alveolar bone are indispensable in promoting the formation of the TBI required to accommodate tooth development. We intend to clarify these results and further investigate the interactions between the tooth and alveolar bone during development, looking at the roles of other genes involved in TBI formation.

7th Annual Meeting Scientific Program
February 18-21, 2013
Riyadh, Saudi Arabia

Constraints on Tooth Growth by the Developing Alveolar Bone

Sarah A. Alfaqeeh[1,2], Dr. Abigail S. Tucker[1] and Prof. Fraser McDonald[1]

[1]*Department of Craniofacial Development and Stem Cell Biology, and Department of Orthodontics, Dental Institute at Guy's, King's College and St Thomas' Hospitals, London, UK*
[2]*Department of Pediatric Dentistry and Orthodontics, College of Dentistry, King Saud University, Riyadh, KSA*

The growth of the tooth and the alveolar bone is co-ordinated so that a studied distance always separates the two. We have called this distance, the tooth-bone interface (TBI). In adults the TBI accommodates the shock-absorbing properties of the PDL and distribute the mechanical stress generated during mastication, tooth movement and rapid remodelling of teeth. During development, lack of mineralization, a crucial feature of the TBI, creates the space needed for the developing tooth to grow and forms a gap between the tooth and bone in which the soft tissues of the periodontium can develop. The TBI protects the tooth from any defective fusion with the alveolar bone, which would result in ankylosis. No studies have been done to understand the signals that maintain the bone free TBI, or to understand the influence of the TBI on tooth development. We have investigated the impact of the developing alveolar bone on the size and development of the mouse first molar (M1). We evaluated the growth of the M1 and the distribution of the osteoclasts *in vivo* and in explant cultures using two methods, isolation of the M1 from the surrounding alveolar bone, and enhancement of osteoclastogenesis through RANK-RANKL signalling after treatment with RANKL, an osteoclast activator. The M1 showed a significant increase in size when cultured without alveolar bone compared to controls. Similar results were obtained after treatment with RANKL, the RANKL activity was confirmed by an increase in the number of TRAP-positive osteoclasts. Our data indicate that both alveolar bone and RANKL regulate tooth size without altering development and that osteoclasts are indispensable in promoting the formation of the TBI. We intend to further investigate the interactions between the tooth and alveolar bone during development, looking at the roles of *BMP*, *Runx2*, *Twist*, and *Periostin* genes involved in TBI formation.

King's College London Dental Institute

15th Annual Postgraduate Research Day

Floor 18 Tower Wing, Guy's Campus

Wednesday, 13 March 2013

Session 6: Craniofacial Anomalies: Development & Disease II

6C. SARAH A. ALFAQEEH

Constraints on Tooth Growth by the Developing Alveolar Bone

Department of Craniofacial Development and Stem Cell Biology, and Department of Orthodontics

Dr. Abigail S. Tucker and Prof. Fraser McDonald

The growth of the tooth and alveolar bone is co-ordinated so that a studied distance always separates the two. We have called this distance, the tooth-bone interface (TBI). Lack of mineralization, a crucial feature of the TBI, creates the space for the developing tooth to grow and the soft tissues of the periodontium to develop. No studies have been done to understand the signals that maintain the bone-free TBI, or the influence of the TBI on tooth development. We have investigated the impact of the developing alveolar bone on the size and development of the mouse first molar (M1). We evaluated the growth and osteoclasts distribution of the M1 in explant cultures using two methods, isolation of the M1 from the surrounding alveolar bone, and enhancement of osteoclastogenesis through RANK-RANKL signalling after treatment with RANKL, an osteoclast activator. Both methods showed a significant increase in the size of M1. Our data indicate that alveolar bone and RANKL regulate tooth size without altering development and osteoclasts are indispensable in promoting the formation of the TBI. We intend to further investigate the interactions between the tooth and alveolar bone during development, looking at the roles of other genes involved in TBI formation.

The Nature of Ankylosis

Sarah Alfaqeeh[1-2*], Agamemnon E Grigoriadis[1], Fraser McDonald[1], Abigail S. Tucker[1]

[1]*Craniofacial Development and Stem Cell Biology, and Department Orthodontics, Guy's Hospital, King's College London, UK;* [2]*Department of Pediatric Dentistry and Orthodontics, College of Dentistry, King Saud University, Riyadh, KSA*

* presenting author: sarah.alfaqeeh@kcl.ac.uk

BACKGROUND: The growth of the tooth and alveolar bone is coordinated so that a specific defined distance keeps the two apart. We have called this distance, the tooth-bone interface (TBI). In adults, the TBI accommodates the shock-absorbing properties of the PDL and distributes the mechanical stress generated during mastication, tooth movement, and rapid remodelling of teeth. During development the TBI creates the space for the developing tooth to grow, and forms a gap between the tooth and bone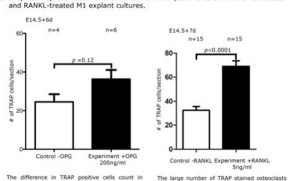 in which the soft tissues of the periodontium can develop [1]. Ossification of the TBI results in ankylosis of the tooth to the bone. The prevalence of ankylosed teeth can reach up to 40 % depending on the population [2]. During development ankylosis can to be caused by ossification of the cells in the TBI or by encroachment of bone into the TBI. We propose that signaling factors produced by the tooth may be instrumental in preventing the cells within the TBI from differentiating into osteoblasts, while the osteoclasts will play a role in preventing encroachment of the alveolar bone into the space around the tooth.

METHODOLOGY: The relative movement of the bone and tooth during development was followed in slice culture using the lineage label DiI. The role of osteoclasts in preventing encroachment of bone was investigated in c-Fos knockout mice. Homozygous mutants have a cell-autonomous block in osteoclast differentiation and the teeth fail to erupt [3]. We evaluated the growth of c-Fos knockout (KO) and heterozygous (+/-) first molars (M1) and the distribution of osteoclasts *in vivo* and in tissue explant cultures.

PRINCIPAL FINDINGS: During normal development osteoclasts were found to line the TBI along the alveolar bone from E14.5. DiI labeling of the alveolar bone showed that the tooth moves
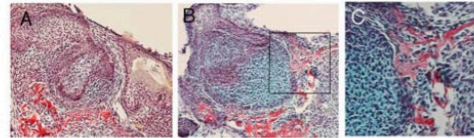
Legend. Histological sections showing signs of bone invasion into the TBI of a c-Fos (+/-) M1 after 5 days in culture. (A) A bone-free TBI is shown in the M1 at the cap stage. (B,C) As the tooth expands it meets the bone, which starts to invade into the pulp.

towards the bone as it grows but a TBI was always maintained. In c-Fos knockouts no TRAP positive cells were observed at birth and the bone started to invade into the TBI encroaching on the tooth. This invasion could be followed in culture as the tooth expanded from the cap to the bell stages. Encroachment of the bone towards the dental papilla was also evident in c-Fos heterozygous mandibles in culture.

DISCUSSION and CONCLUSIONS: Osteoclasts in the alveolar bone play an essential role in promoting the maintenance of the TBI, removing bone as the tooth advances and providing the space required to accommodate the developing tooth. Defects in this process will lead to ankylosis and may restrict the growth of the tooth.

REFERENCES: [1] Fleischmannova *et al*. Journal of Dental Research (2010); [2] Helpin and Duncan ASDC Journal of Dentistry for Children (1986); [3] Grigoriadis *et al*. Science (1994).

Appendix *iv*

Printed posters from PhD

Presented at the 6th Saudi Scientific International Conference, Brunel University, London, United Kingdom, 11-14 October 2012.

Constraints on Tooth Growth by the Developing Alveolar Bone

KING'S *College* **LONDON**
University of London

Sarah A. Alfaqeeh[1-2], Abigail S. Tucker[1], and Fraser McDonald[1]
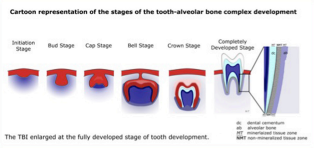
[1]Craniofacial Development and Orthodontics, Dental Institute at Guy's, King's College and St Thomas' Hospitals, London, UK

[2]Department of Pediatric Dentistry and Orthodontics, College of Dentistry, King Saud University, Riyadh, KSA

sarah.alfaqeeh@kcl.ac.uk

Keywords: Bone, Growth & development, Periodontium-gingiva, RANKL and Teeth

Introduction

Teeth must grow in the right positions relative to the forming jaw-bone, attaching to the tooth-associated bone, alveolar bone, via the periodontal ligament (PDL).
The growth of the tooth and alveolar bone is coordinated so that a studied distance always keeps the two apart. We have called this distance, **the tooth-bone interface (TBI)**. It is the space between the cementum of the tooth and the alveolar bone. Little is known about the development of this region.

In adults, the **TBI** accomodates the shock-absorbing properties of the PDL and distributes the mechanical stress generated during mastication, tooth movement, and rapid remodelling of teeth.

During development, lack of mineralization, a crucial feature of the **TBI**, creates the space for the developing tooth to grow, and forms a gap between the tooth and bone in which the soft tissues of the periodontium can develop. The TBI protects the tooth from any defective fusion with the alveolar bone, which would result in ankylosis.

The prevalence of ankylosed teeth can reach upto 40 % depending on the population (Helpin and Duncan, 1986). Osteointegration of dental implants, which can be considered as a functional form of ankylosis, is a major challenge in nowadays dentistry (Schroeder *et al*, 1981).

Ankylosis can be casued by two ways. The first one is, **a.**, the actual **TBI** tissue transformation into bone while the second one is, **b.**, bone encroachment into the **TBI**.

We hypothesize that one or more cellular mechanisms may be responsible for the prevention of bone formation at the **TBI**. We propose that signalling factors produced by the tooth may be instrumental in preventing the cells within the **TBI** from differentiating into osteoblasts, while osteoclasts play a role in preventing encroachment of the alveolar bone into the space around the tooth.

Goal

We aim to investigate the impact of the developing alveolar bone on the size and development of the mouse mandibular first molar (M1).

Materials and Methods

We evaluated the growth of the M1 and distribution of the osteoclasts *in vivo* and in tissue explant cultures.

We investigated the role of the surrounding bone using 2 methods:
1. Isolation of the M1 from the surrounding alveolar bone
2. Enhancement of osteoclastogenesis through RANK-RANKL signalling
   by the addition of RANKL, an osteoclast activator.

Results

1. Histological sections showing the development of TBI during embryonic stages (from E13.5 up to E17.5) of the M1.
Localization of TRAP-positive osteoclastic cells in M1 regions, respectively.

Strongly TRAP positive cells are shown to be present in the region that surrounds the gap between the developing tooth germ and the alveolar bone from E14.5 onwards. These TRAP positive cells are likely to be osteoclasts as they are closely associated with the developing alveolar bone. TRAP positive cells were not observed in the TBI but were restricted along the margins of the alveolar bone that surrounds it.

2. Development of M1 in an encapsulated explant culture technique.

Cultures of M1 explants were followed from E14.5. On day 2, (C) the alveolar bone approached the tooth and on day 3 (D), it started differentiating around the tooth.

3. Development of M1 explants cultured in isolation from surrounding alveolar bone, isolated, and within surrounding alveolar bone, encapsulated.

a. The Isolated M1s (H) grew to a larger extent than the encapsulated M1s (D).

b. A graph comparing the ratio of M1 surface area development in encapsulation and isolation.

The statistical significant increase in the ratio of M1 surface area when cultured without surrounding alveolar bone is evident.

c. A whole mount BrdU immunostaining showing the proliferating cells in the cervical region, as we anticipate the difference in the rate of cells proliferation to be the reason behind the ratio of M1 surface area statistical significance difference when cultured in encapsulation and isolation of the surrounding tissues.

4. Manipulation of RANK-RANKL signalling pathway. Enhancement of osteoclastogenesis by the addition of RANKL.

a. M1 development in explant cultures treated with RANKL.

RANKL-treated M1 explants (D) were found to be more developed, larger in size in comparison to controls (B).

b. TRAP assay of RANKL-treated M1 explants.

A large number of TRAP positive stained cells were observed in RANKL-treated M1 explant cultures (B) compared to the untreated ones (A).

c. Graphical representation of the number of TRAP positive cells in the RANKL-treated M1 explant cultures.

The large number of TRAP positively stained osteoclasts observed in the RANKL-treated M1 explant cultures was statistically significant as compared to controls.

5. The encapsulated RANKL-treated M1s growth was enhanced and reached the size of similar isolated Non-RANKL-treated M1s.

a. Graphical representation of the ratio of encapsulated and isolated RANKL-treated M1 surface area.

No statistical significant difference is found between the two groups.

b. Graphical representation of the ratio of encapsulated RANKL-treated M1 surface area compared to isolated Non-RANKL-treated M1s.

No statistical significant difference is found between the two groups.

Conclusions

Both RANKL treatment and removal of the alveolar bone in culture had the same effect on M1 size.

The net increase in noticed M1 growth is the same despite the difference in the experimental factor investigated.

- Alveolar bone and RANKL regulate tooth size without altering development.
- Osteoclasts in the alveolar bone play a role in promoting the formation of the TBI required to accomodate tooth development.
- We intend to clarify these results and further inverstigate the interactions between the tooth and alveolar bone during development, looking at the roles of *BMP, Runx2, Twist*, and *Periostin*, genes involved in TBI formation.

References

Castaneda, B., Y. Simon, et al. (2011). "Bone resorption control of tooth eruption and root morphogenesis: Involvement of the receptor activator of NF-kappaB (RANK)." Journal of Cellular Physiology 226(1): 74-85.
Helpin, M. L. and W. K. Duncan (1986). "Ankylosis in monozygotic twins." American Society of Dentistry for Children Journal of Dentistry for Children 53(2): 135-139.
Kim, J. Y., S. W. Cho, et al. (2007). "Evidence for expansion-based temporal BMP4/NOGGIN interactions in specifying periodontium morphogenesis." Cell and tissue research 330(1): 123-132.
Schroeder, A., E. van der Zypen, et al. (1981). "The reactions of bone, connective tissue, and epithelium to endosteal implants with titanium-sprayed surfaces." Journal of Maxillofacial Surgery 9(1): 15-25.

Presented at the 24th Saudi Dental Society International Dental Conference, Riyadh International Convention & Exhibition Center, Riyadh, Kingdom of Saudi Arabia, 28-30 January 2013.